

DIAGNOZA - GENEZA - PROGNOZA => PODSTAWA KAŻDEJ DECYZJI



afiliowane przy

Wydziale Nauk
Technicznych
Polskiej Akademii Nauk

Diagnostyka

ISSN 641-6414



Nr 4(44)/2007

RADA PROGRAMOWA / PROGRAM COUNCIL

PRZEWODNICZĄCY / CHAIRMAN:

prof. dr hab. dr h.c. mult. **Czesław CEMPEL** *Politechnika Poznańska*

REDAKTOR NACZELNY / CHIEF EDITOR:

prof. dr hab. inż. **Ryszard MICHALSKI** *UWM w Olsztynie*

CZŁONKOWIE / MEMBERS:

prof. dr hab. inż. **Jan ADAMCZYK**
AGH w Krakowie

prof. dr. **Ioannis ANTONIADIS**
National Technical University Of Athens – Grecja

dr inż. **Roman BARCZEWSKI**
Politechnika Poznańska

prof. dr hab. inż. **Walter BARTELMUS**
Politechnika Wroclawska

prof. dr hab. inż. **Wojciech BATKO**
AGH w Krakowie

prof. dr hab. inż. **Lesław BĘDKOWSKI**
WAT Warszawa

prof. dr hab. inż. **Adam CHARCHALIS**
Akademia Morska w Gdyni

prof. dr hab. inż. **Wojciech CHOLEWA**
Politechnika Śląska

prof. dr hab. inż. **Zbigniew DĄBROWSKI**
Politechnika Warszawska

prof. dr hab. inż. **Marian DOBRY**
Politechnika Poznańska

prof. **Wiktor FRID**
Royal Institute of Technology in Stockholm – Szwecja

dr inż. **Tomasz GAŁKA**
Instytut Energetyki w Warszawie

prof. dr hab. inż. **Jan KICIŃSKI**
IMP w Gdańsku

prof. dr hab. inż. **Jerzy KISIŁOWSKI**
Politechnika Warszawska

prof. dr hab. inż. **Daniel KUJAWSKI**
Western Michigan University – USA

prof. dr hab. **Wojciech MOCZULSKI**
Politechnika Śląska

prof. dr hab. inż. **Stanisław NIZIŃSKI**
UWM w Olsztynie

prof. **Vasyl OSADCHUK**
Politechnika Lwowska – Ukraina

prof. dr hab. inż. **Stanisław RADKOWSKI**
Politechnika Warszawska

prof. **Bob RANDALL**
University of South Wales – Australia

prof. dr **Raj B. K. N. RAO**
President COMADEM International – Anglia

prof. **Vasily S. SHEVCHENKO**
BSSR Academy of Sciences Mińsk – Białoruś

prof. **Menad SIDAHMED**
University of Technology Compiègne – Francja

prof. dr hab. inż. **Tadeusz UHL**
AGH w Krakowie

prof. **Vitalijus VOLKOVAS**
Kaunas University – Litwa

prof. dr hab. inż. **Andrzej WILK**
Politechnika Śląska

dr **Gajraj Singh YADAVA**
Indian Institute of Technology – Indie

prof. **Alexandr YAVLENSKY**
J/S company "Vologda Bearing Factory" – Rosja

prof. dr hab. inż. **Bogdan ŻÓŁTOWSKI**
UTP w Bydgoszczy

Wszystkie opublikowane prace uzyskały pozytywne recenzje wykonane przez dwóch niezależnych recenzentów. Obszar zainteresowania czasopisma to problemy diagnostyki, identyfikacji stanu technicznego i bezpieczeństwa maszyn, urządzeń, systemów i procesów w nich zachodzących. Drukujemy oryginalne prace teoretyczne, aplikacyjne, przeglądowe z badań, innowacji i kształcenia w tych zagadnieniach.

WYDAWCA:

Polskie Towarzystwo Diagnostyki Technicznej
02-981 Warszawa
ul. Augustówka 5

REDAKTOR NACZELNY:

prof. dr hab. inż. **Ryszard MICHALSKI**

SEKRETARZ REDAKCJI:

dr inż. **Sławomir WIERZBICKI**

CZŁONKOWIE KOMITETU REDAKCYJNEGO:

dr inż. **Krzysztof LIGIER**

dr inż. **Paweł MIKOŁAJCZAK**

ADRES REDAKCJI:

Uniwersytet Warmińsko – Mazurski w Olsztynie
Katedra Budowy, Eksploatacji Pojazdów i Maszyn
10-736 Olsztyn, ul. Oczapowskiego 11
tel.: 089-523-48-11, fax: 089-523-34-63
www.uwm.edu.pl/wnt/diagnostyka
e-mail: diagnostyka@uwm.edu.pl

KONTO PTDT:

Bank Przemysłowo Handlowy S.A.
II O/ Warszawa
nr konta: 40 1060 0076 0000 3200 0046 1123

NAKLAD: 250 egzemplarzy

Wydanie dofinansowane przez Ministra Nauki i Szkolnictwa Wyższego

Spis treści

Andrzej GRZĄDZIELA – AMW Gdynia	5
<i>Dynamic Problems Of Shaftlines</i>	
<i>Problemy dynamiki linii wałów okrętowych</i>	
Bogusław ŁAZARZ, Grzegorz WOJNAR, Tomasz FIGLUS – Politechnika Śląska	11
<i>Comparison Of The Efficiency Of Selected Vibration Measures Used In The Diagnosis Of Complex Cases Of Tooth Gear Damage</i>	
<i>Porównanie skuteczności wybranych miar drganiowych stosowanych w diagnozowaniu złożonych przypadków uszkodzeń przekładni</i>	
Grzegorz WOJNAR, Bogusław ŁAZARZ – Politechnika Śląska	19
<i>Averaging Of The Vibration Signal With The Synchronizing Impulse Location Correction In Tooth Gear Diagnostics</i>	
<i>Wykorzystanie uśredniania sygnału drganiowego z korekcją położenia impulsu synchronizującego w diagnostyce przekładni zębatych</i>	
Marek FLEKIEWICZ, Henryk MADEJ – Politechnika Śląska	25
<i>Recovery Of Impact Signatures In Diesel Engine Using Wavelet Packet Transform (WPT)</i>	
<i>Wykrywanie wymuszeń impulsowych w silniku zs za pomocą pakietów falkowych (WPT)</i>	
Dariusz GRZYBEK, Andrzej JURKIEWICZ, Piotr MICEK, Marcin APOSTOŁ – AGH Kraków	31
<i>Synchronization System Of The Hydraulic Cylinders Motion In The Research Of The Bridge Prestressing Systems</i>	
<i>Układ synchronizacji ruchu siłowników hydraulicznych w badaniach mostowych ustrojów sprężających</i>	
Andrzej JURKIEWICZ, Piotr MICEK, Marcin APOSTOŁ, Dariusz GRZYBEK – AGH Kraków	37
<i>Safety Assurance At The Design Stage Of The New Pump On The Basis Of Eu Directives</i>	
<i>Zapewnienie bezpieczeństwa na etapie projektowania nowej pompy w oparciu o Dyrektywę UE</i>	
Anna PIĄTKOWSKA – Instytutu Technologii Materiałów Elektronicznych w Warszawie, Tadeusz PIĄTKOWSKI – WAT Warszawa	43
<i>Measurement And Analysis Of Acoustic Emission In The Tribological System Ball-On-Disc</i>	
<i>Pomiary i analiza parametrów tribologicznych oraz emisji akustycznej zarejestrowanych w układzie trącym kula - powierzchnia płaska</i>	
Wojciech MANAJ – Materials Engineers Group Sp. z o.o., Krzysztof SIKORSKI, Krzysztof KURZYDŁOWSKI – Politechnika Warszawska	49
<i>Application Of Ultrasonic Techniques For The Evaluation Of The Properties Of Prestressed Concrete Structures</i>	
<i>Zastosowanie ultradźwiękowych technik pomiarowych w ocenie stanu konstrukcji sprężonych</i>	
Grzegorz KLEKOT – Politechnika Warszawska	53
<i>Selected Diagnostic Aspects Of Propagation Of Vibroacoustic Energy</i>	
<i>Wybrane aspekty diagnostyczne propagacji energii wibroakustycznej</i>	
Andrzej JURKIEWICZ, Piotr MICEK, Marcin APOSTOŁ, Dariusz GRZYBEK – AGH Kraków	57
<i>Modelling And Simulation Of The Dynamic Structure Of The Vibration Forcing System Of The Prestressing System</i>	
<i>Modelowanie i symulacja struktury dynamicznej układu wymuszania drgań ustroju sprężającego</i>	
Wojciech BATKO, Leszek MAJKUT – AGH Kraków	63
<i>Damage Identification In Prestressed Structures Using Phase Trajectories</i>	
<i>Identyfikacja uszkodzeń konstrukcji sprężonych z wykorzystaniem obserwacji trajektorii fazowych</i>	
Wojciech BATKO – AGH Kraków	69
<i>Stability In Technical Diagnostics</i>	
<i>Stateczność w diagnostyce technicznej</i>	

Bogna MRÓWCZYŃSKA – Politechnika Śląska.....	73
<i>Optimal Distribution Of Sub-Assemblies In Stores Of Factory By Evolutionary Algorithms</i> <i>Optymalizacja rozkładu podzespołów w magazynach fabryki przy pomocy algorytmów ewolucyjnych</i>	
Tadeusz UHL, Mariusz SZWEDO – AGH Kraków	77
<i>Active Thermography And It's Application For Damage Detection In Mechanical Structure</i> <i>Aktywna termografia i jej wykorzystanie do detekcji uszkodzeń struktur mechanicznych</i>	
Andrzej KLEPKA, Tadeusz UHL – AGH Kraków.....	85
<i>MATLAB® Flutter Toolbox</i> <i>MATLAB® Flutter Toolbox</i>	
Tomasz BARSZCZ – AGH Kraków	91
<i>Application of Virtual Power Plant for Condition Monitoring of Power Generation Unit</i> <i>Zastosowanie wirtualnej elektrowni do diagnostyki bloku energetycznego</i>	
Grzegorz KARPIEL, Maciej PETKO, Tadeusz UHL – AGH Kraków.....	99
<i>Mechatronic Approach Towards Flight Flutter Testing</i> <i>Mechatroniczne podejście do badania marginesu flatteru samolotów</i>	
Stanisław RADKOWSKI, Adam GAŁĘZIA, Jędrzej MĄCZAK, Krzysztof SZCZUROWSKI – Politechnika Warszawska	105
<i>Structural Condition Evaluation Of Prestressed Concrete Structures Based On Vibroacoustic Monitoring</i> <i>Ocena stanu technicznego betonowych konstrukcji sprężonych na podstawie monitoringu wibroakustycznego</i>	
Janusz ZACHWIEJA – UTP w Bydgoszczy.....	113
<i>The Role Of Vibroisolators In Damping An Radial Fan's Vibrations</i> <i>Rola wibroizolatorów w tłumieniu drgań wentylatora promieniowego</i>	
Tomasz KORBIEL, Piotr KRZYWORZEKA – AGH Kraków	119
<i>An Application Of Splines In Synchronous Analysis Of Nonstationary Machine Run</i> <i>Wykorzystanie funkcji sklepanych w analizie synchronicznej niestacjonarnego biegu maszyn</i>	
Witold CIOCH, Piotr KRZYWORZEKA – AGH Kraków.....	125
<i>Analysis Of Running-Up Vibrations Of Turbine Engine GTD-350</i> <i>Badanie drgań rozruchowych silnika turbinowego GTD-350</i>	
Wojciech BATKO, Witold CIOCH, Ernest JAMRO – AGH Kraków.....	131
<i>Monitoring System For Diagnosing Machines In Non-Stationary States</i> <i>System monitoringu maszyn w niestacjonarnych stanach pracy</i>	
XIII Konferencja Naukowa Wibroakustyki i Wibrotechniki i VIII Ogólnopolskie Seminarium Wibroakustyka w Systemach Technicznych „WibroTech 2007”	137

DYNAMIC PROBLEMS OF SHAFTLINES

Andrzej GRZĄDZIELA

Naval University of Gdynia, Mechanical – Electrical Faculty
ul. Śmidowicza 69, 81-103 Gdynia, Poland, e-mail: agrza@amw.gdynia.pl

Summary

Ships' propulsion plant usually works in a hard environment caused by static forces and permanent dynamic loads. Elastic strains from machine vibration can cause resonance of plastic strain of shell plating and foundation of shafting elements. Exceeding of tolerated values of shaft alignments causes a damage of radial and thrust bearings in relative short time. The alignment deviations in the construction of ships propulsion shaft line has been an effect of tensile forces, compressive forces, bending moments and transverse vibration from disturbances of rotation movement. Modeling of dynamical reactions could bring information to the project data base for recognizing the level of hazard for propulsion system of the naval vessels. Recorded signals were recognized within sensitive symptoms of two models: model of propulsion system and model of underwater explosion.

Keywords: ship shaft lines, technical diagnostics, modelling, vibrations, underwater explosion.

PROBLEMY DYNAMIKI LINII WAŁÓW OKRĘTOWYCH

Streszczenie

W artykule przedstawiono propozycję identyfikacji stopnia zagrożenia od obciążenia impulsowego wywołanego przez wybuch podwodny na okrętową linię wałów. Dokonano analizy teoretycznej wpływu zmian współosiowości wałów na prędkości krytyczne drugiego rodzaju wynikające z odkształceń sprężystych kadłuba w rejonie fundamentów łożysk nośnych. Przedstawiono wyniki pilotażowych badań na poligonie morskim z wykorzystaniem eksplozji podwodnej. Zaproponowano wstępny model matematyczny opisu eksplozji podwodnej uwzględniający masę ładunku oraz odległość od obiektu. We wnioskach przedstawiono sposób identyfikacji zagrożenia dla linii wałów przy wykorzystaniu analizy widmowej przebiegów czasowych sygnałów drganiowych rejestrowanych na łożyskach nośnych.

Słowa kluczowe: linia wałów okrętowych, diagnostyka techniczna, modelowanie, drgania, wybuch podwodny.

1. INTRODUCTION

Ship propulsion systems are subjected to specific sea loads due to waving and dynamical impacts associated with mission of a given ship. Sea waving can be sufficiently exactly modeled by means of statistical methods. Much more problems arise from modeling impacts due to underwater explosion. In operation of contemporary technical objects including naval ships greater and greater attention is paid to such notions as : time of serviceability, repair time, maintenance and diagnosing costs [1]. Diagnosing process has become now a standard procedure performed during every technical maintenance. Out of the above mentioned, the notions of time of serviceability and maintenance costs seem to be crucial for the diagnosing process of ship power plant. Knowledge of a character of impulse loading which affects ship shaft line, can make it possible to identify potential failures by means of on-line vibration measuring systems.

2. ANALYSIS OF FORCES ACTING ON SHAFT-LINE BEARINGS

Ship shaft lines are subjected to loads in the form of forces and moments which generate bending, torsional and axial vibrations. In most cases strength calculations of driving shafts are carried out by using a static method as required by majority of ship classification institutions. Moreover they require calculations of torsional vibrations which have to comply with permissible values, to be performed. Calculation procedures of ship shaft lines generally amount to determination of reduced stresses and safety factor related to tensile yield strength of material – Fig. 1.

The above mentioned methods do not model real conditions of shaft-line operation, which is confirmed by the character of ship hull response, i.e. its deformations under dynamic loads. Much more reliable would be to relate results of the calculations to fatigue strength of material instead of its yield strength [5].

In static calculation procedures no analysis of dynamic excitations, except torsional vibrations, is taken into consideration. In certain circumstances the adoption of static load criterion may be disastrous especially in the case of resonance between natural vibration frequencies and those of external forces due to dynamic impacts.

To analyze the dynamic interaction a simplified model of shaft line is presented below, Fig. 2.

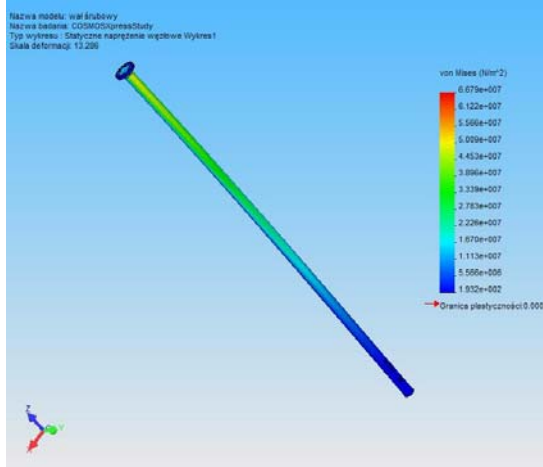


Fig. 1. Simulated static bending stresses in propeller shaft due to weight of propeller

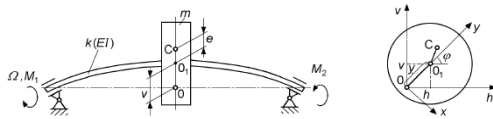


Fig. 2. A simplified shaft-line model for critical speed calculation [4]

Let us note : M_1 - torque, M_2 - anti-torque. The system can be represented by the following set of equations:

$$\begin{aligned} m\ddot{h} + kh &= me(\ddot{\varphi} \sin \varphi + \dot{\varphi}^2 \cos \varphi), \\ m\ddot{v} + kh &= me(-\ddot{\varphi} \cos \varphi + \dot{\varphi}^2 \sin \varphi), \\ (J + me^2)\ddot{\varphi} &= me(\ddot{h} \sin \varphi - \ddot{v} \cos \varphi) + M_1 - M_2 \end{aligned} \quad (1)$$

The presented form of the equations is non-linear. Considering the third of the equations (1) one can observe that the variables h , v and φ are mutually coupled. It means that any bending vibration would disturb rotational motion of the shaft. The third of the equations (1) can be written also in the equivalent form as follows:

$$J\ddot{\varphi} = ke(v \cos \varphi - h \sin \varphi) + M_1 - M_2 \quad (2)$$

To obtain the shaft angular speed Ω_w constant to use time-variable torque is necessary:

$$M = M_1 - M_2 = ke(h \sin \varphi - v \cos \varphi) \quad (3)$$

Theoretical analysis indicates that shaft bending deformation continuously accumulates a part of shaft torque. However the quantity of torque non-uniformity is rather low since shaft-line eccentricity is low; it results from manufacturing tolerance, non-homogeneity of material, propeller weight and permissible assembling clearances of bearing foundations.

For ship propulsion system the torque pulsation expressed by means of Fourier series is much more complex. It additionally contains components resulting from number of propeller blades, kinematical features of reduction gear as well as disturbances from main engine and neighbouring devices. In general case occurrence of only one harmonic does not change reasoning logic.

For long shaft lines of ships the influence of gravity forces on critical speeds should be taken into consideration [7]. According to Eq. (4) the generated vibrations will be then performed respective to static deflection axis of the shaft.

$$\begin{aligned} m\ddot{h} + kh &= me\Omega^2 \cos \varphi \\ m\ddot{v} + kv &= me\Omega^2 \sin \varphi \\ \ddot{\varphi} &= 0 \end{aligned} \quad (4)$$

Hence the equations obtain the following form:

$$\begin{aligned} \ddot{h} + \omega_0^2 h &= e \cdot \Omega^2 \cos \varphi \\ \ddot{v} + \omega_0^2 v &= e \cdot \Omega^2 \sin \varphi - mg, \\ J\ddot{\varphi} &= -mge \cos \varphi. \end{aligned} \quad (5)$$

Since in the third equation of the set (1), i.e. that for Ω_{3KR} , appears the exciting torque of the frequency/angular speed ratio $\beta=1$ it means that one has to do with the critical state of 2nd kind for $\beta=1$, namely:

$$\Omega_{KR(2)} = \frac{1}{2} \omega_0 \quad (6)$$

Occurrence of such kind vibrations is conditioned by non-zero value of e , which – in the case of ship shaft line – appear just after dislocation of a weight along ship, a change of ship displacement or even due to sunshine operation on one of ship sides. A similar situation will happen when e varies due to dynamic excitations resulting from e.g. sea waving or explosion. In this case the critical speed will vary depending on instantaneous value of e and damping.

Theoretical analysis of operational conditions of intermediate and propeller shafts indicates that static and dynamic loads appear. In a more detailed analysis of dynamic excitations of all kinds the following factors should be additionally taken into consideration:

– disturbances coming from ship propeller (torsional, bending and compressive stresses);

- disturbances from propulsion engine (torsional and compressive stresses);
- disturbances from reduction gear (torsional stresses);
- disturbances from other sources characteristic for a given propulsion system or ship mission.

3. PROBLEM OF UNDERWATER EXPLOSION

Information on potential hazard resulting from underwater explosion is crucial not only for ship's commander during warfare but also for ship structure designers. Knowledge of loads determined during simulative explosions is helpful in dimensioning ship's hull scantlings [3]. Another issue is possible quantification of explosion energy as well as current potential hazard to whole ship and its moving system.

From the point of view of shock wave impact on shaft line, underwater and over-water explosions should be considered in two situations:

- when shock wave (or its component) impacts screw propeller axially,
- when shock wave (or its component) impacts screw propeller perpendicularly to its rotation axis.

The axial shock-wave component affects thrust bearing and due to its stepwise character it may completely damage sliding thrust bearing. Rolling thrust bearings are more resistant to stepwise loading hence they are commonly used on naval ships [3]. The shock wave component perpendicular to shaft rotation axis is much more endangering.

Shock wave can cause: damage of stern tube, brittle cracks in bearing covers and tracks, plastic displacement of shaft supporting elements including transmission gear and main engine, and even permanent deformation of propeller shaft.

The problem of influence of sea mine explosion on hull structure is complex and belongs to more difficult issues of ship dynamics. Underwater explosion is meant as a violent upset of balance of a given system due to detonation of explosives in water environment. The process is accompanied with emission of large quantity of energy within a short time, fast running chemical and physical reactions, emission of heat and gas products. The influence of underwater explosion does not constitute a single impulse but a few (2 to 4) large energy pulsations of gas bubbles [2, 8, 9].

The pulsation process is repeated several times till the instant when the gas bubble surfaces. Hence the number of pulsations depends a.o. on immersion depth of the explosive charge. The character of changes of pressure values in a motionless point of the considered area is shown in Fig. 3.

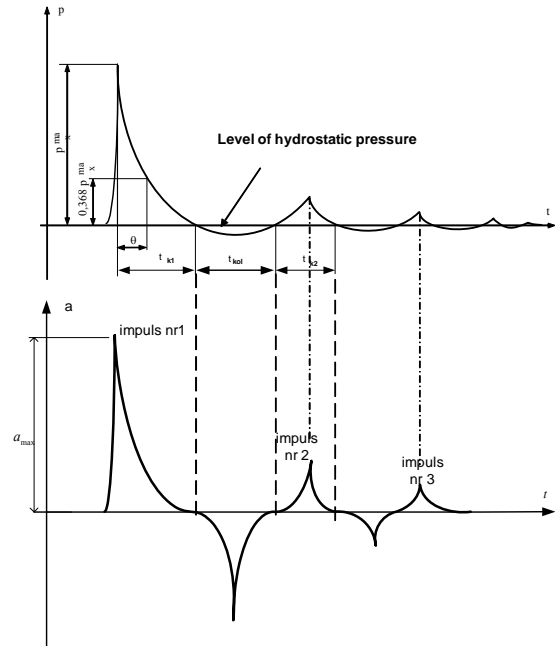


Fig. 3. Run of changes of shock wave pressure and ship hull acceleration measured on hull surface during underwater explosion

In the subject-matter literature can be found many formulae for determining maximum pressure value, based on results of experiments, however data on a character of pulsation and its impact on ship structures are lacking. To identify underwater explosion parameters a pilotage test was performed with the use of the explosive charge having the mass $m = 37,5$ kg. The schematic diagram of the experiment is shown in Fig. 4.

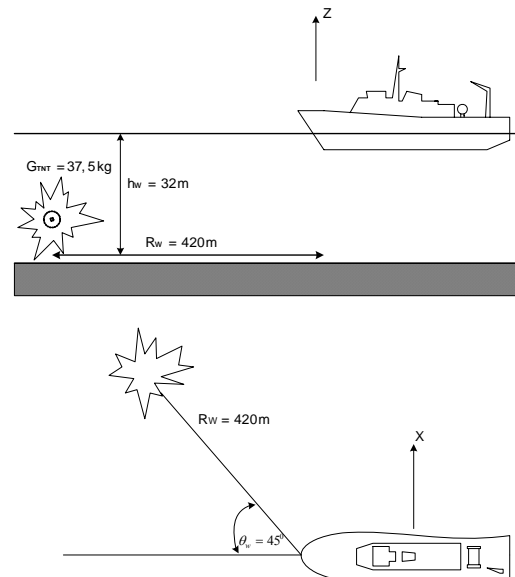


Fig. 4. Schematic diagram of the performed experimental test

During the test were measured vibration accelerations of casings of intermediate and thrust bearings in the thrust direction and that perpendicular to shaft rotation axis. The ship course angle relative to the explosion epicentre was 45° and the shaft line rotated with the speed $n_{LW} = 500$ rpm. Ship's distance from the mine and its immersion depth was determined by using a hydro-location station and ROV underwater vehicle – figure 5. The vibration gauges were fixed over the reduction gear bearing as well as on the intermediate shaft bearing.



Fig. 5. ROV vehicle with TNT charge

The measurement directions (X and Z axes) are presented in Fig. 6 as well.

The time lag of the recorded signals was the same in all measurement points, as shown in Fig. 6 and 7.

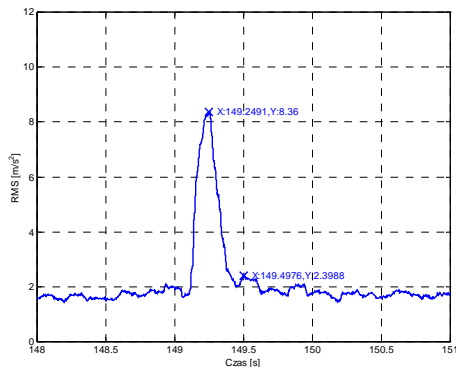


Fig. 6. Explosion, Port side (LB), Thrust bearing, X axis

The performed test was aimed at achieving information dealing with :

- character of shock wave impact on shaft-line bearings, in the form of recorded vibration parameters;
- assessment of time-run of vibration accelerations with taking into account dynamic features of the signals in set measurement points;
- assessment of possible identification of influence of pulsation of successive gas bubbles during the time-run of vibration accelerations;

- identification of features of the signals by means of spectral analysis.

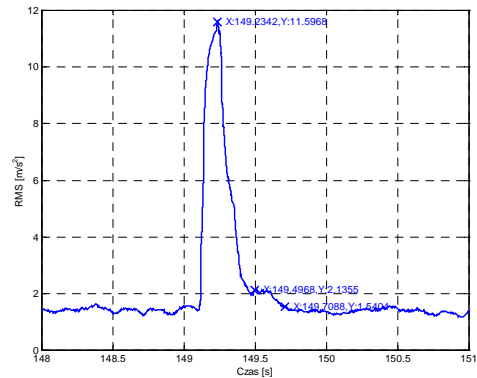


Fig. 7. Explosion, Starboard (PB), Intermediate bearing, Z axis

Since the mass of the explosive charge was small, to reliably identify the effect of only first and second pulsation was possible during the test.

4. MODELS OF EXCITATION DUE TO UNDERWATER EXPLOSION

Analysis of dynamic impacts including impulse ones should take into account basic parameters which influence character of time-run of a given signal as well as its spectrum. The basic parameters which identify impulse impact resulting from explosion, are the following:

- form of impulse which identifies kind of impulse;
- impulse duration time t_i at the ratio A/t_i maintained constant, which identifies explosive charge power (time of propagation of gas bubble);
- influence of damping on spectrum form, which identifies distance from explosion and - simultaneously - epicentre depth
- number of excitation impulses, which informs on distance from explosion, combined with explosive charge mass;
- time between successive impulses, which characterizes explosive charge mass;

The possible recording of measured shock wave pressure and accelerations on intermediate and propeller shaft bearings enables to identify some explosion parameters hence also hazards to power transmission system. Analysing the run of underwater shock wave pressure one is able to assume its time-dependent function (Fig. 8 and 9).

$$A = at^{kb} \cdot e^{kct} \quad (7)$$

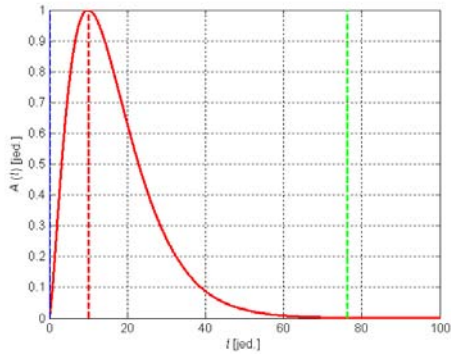


Fig. 8. Example of the function form for $b=1,5$; $c=-0,15$ and $k=1$

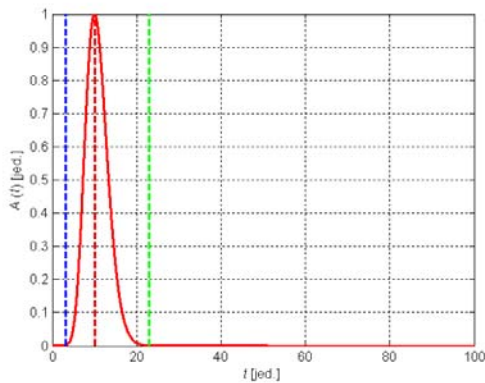


Fig. 9. Example of the function form for $b=1,5$; $c=-0,15$ and $k=10$

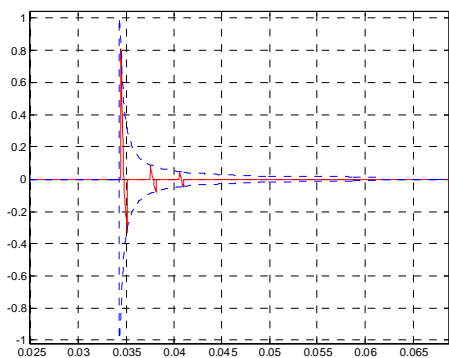


Fig. 10. Run of the assumed vibration acceleration model

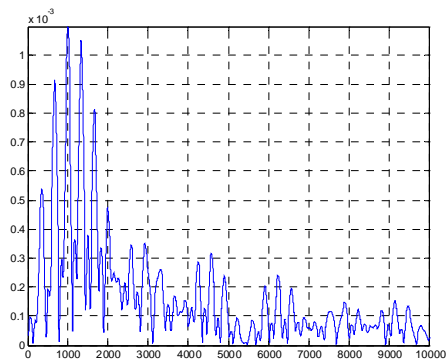


Fig. 11. Spectrum of the assumed vibration acceleration model

For the assumed mathematical model of the first shock wave impulse the run of vibration accelerations recorded on ship hull - for the example function given in Fig. 8 - can be presented as shown in Fig. 10 and 11.

5. FINAL CONCLUSIONS

- It's common knowledge that failure frequency is the most hazardous factor in marine industry, just after aeronautics. Dynamic reactions which occur on ships in service at sea are rarely able to produce wear sufficient to cause a failure.
- The possible application of an on-line monitoring system of vibration parameters of the propulsion system of mine hunter makes it possible to perform the typical technical diagnostic tests of torque transmission system and to identify possible plastic deformations of hull plating as a result of underwater explosion.
- The modelling of impulse impact form and next its identification makes it possible additionally: to identify explosion power by using an analysis of the first vibration impulse amplitude and its duration time, to identify distance from explosion epicentre (hence a degree of hazard) by analysing signal's damping, to identify a kind of explosion and even characteristic features of type of used mine, to select dynamic characteristics of a measuring system which has to comply with requirements for typical technical diagnostics and for a hazard identification system, to identify elastic or plastic deformation of shaft line by using spectral assessment of its characteristic features from before and after underwater explosion.
- The presented results of modelling related to the performed experimental test do not make it possible - due to strongly non-linear character of interactions occurring in sea environment - to assign unambiguously the modelled signal features to those of the recorded ones during the real test.
- Successive experimental tests will make it possible to verify features of the signals assumed for the analysis, to be able to build reliable models.
- The wide range of stochastic dynamic loads acting on ships during its life-time makes that in the nearest future the application of on-line diagnostic techniques to ship propulsion systems, based on analysing vibration signals, will constitute an obvious tactical and technical necessity.

BIBLIOGRAPHY

- [1] Cempel Cz., Tomaszewski F. (Ed.): *Diagnostics of machines*. General principles. Examples of applications (in Polish), Publ. MCNEM, Radom 1992.
- [2] Cole R. H.: *Underwater Explosions*. Princeton University Press, Princeton 1948.
- [3] Cudny K., Powierża Z.: *Selected problems of shock resistance of ships* (in Polish) Publ. Polish Naval University, Gdynia 1987.
- [4] Dąbrowski Z.: *Machine shafts* (in Polish), State Scientific Publishing House (PWN), Warszawa 1999.
- [5] Dietrych I., Kocańda S., Korewa W.: *Essentials of machine building* (in Polish). Scientific Technical Publishing House (WNT), Warszawa 1974.



Dr inż. **Andrzej GRZĄDZIELA** jest Kierownikiem Zakładu Napędów Okrętowych w Instytucie Konstrukcji i Eksploatacji Okrętów Wydziału Mechaniczno – Elektrycznego Akademii

Marynarki Wojennej w Gdyni. W swojej działalności zawodowej zajmuje się problemami oceny niewyważenia i oceny współosiowości w okrętowych układach napędowych a także projektowaniem okrętów i doбором układów napędowych. Członek Polskiego Towarzystwa Diagnostyki Technicznej oraz Polskiego Towarzystwa Naukowego Silników Spalinowych

COMPARISON OF THE EFFICIENCY OF SELECTED VIBRATION MEASURES USED IN THE DIAGNOSIS OF COMPLEX CASES OF TOOTH GEAR DAMAGE

Bogusław ŁAZARZ, Grzegorz WOJNAR, Tomasz FIGLUS

The Silesian University of Technology, Faculty of Transport
8 Krasińskiego Street, 40-019 Katowice, tel: (032) 603 43 23,
e-mail: Boguslaw.Lazarz@polsl.pl, Grzegorz.Wojnar@polsl.pl, Tomasz.Figus@polsl.pl

Summary

The diagnostics of tooth gears is a vital scientific issue for its utilitarian and cognitive aspects. An essential part of this process is the ability to differentiate the impact of various effects on the vibration signal of a tooth gear both working in the correct mode, including meshing of the tooth gear, and possible damage to it.

The papers of authors present various diagnostic measures applied in the detection of tooth gear damage. They are based on specially processed and filtered vibration signals. This paper presents an attempt to compare the sensitivity of selected diagnostic measures to the studied types of tooth gear damage in the work of tooth gears with bearings of various technical conditions.

Keywords: diagnostics, tooth gear damage, complex cases, efficiency of measures.

PORÓWNANIE SKUTECZNOŚCI WYBRANYCH MIAR DRGANIOWYCH STOSOWANYCH W DIAGNOZOWANIU ZŁOŻONYCH PRZYPADKÓW USZKODZEŃ PRZEKŁADNI

Streszczenie

Ze względów użytkowych i poznawczych diagnozowanie przekładni zębatych jest ważnym zagadnieniem naukowym. W procesie tym istotna jest umiejętność rozróżnienia oddziaływania na sygnał drganiowy przekładni różnych zjawisk związanych zarówno z normalną pracą przekładni, a w tym zazębaniem się kół, jak i uszkodzeniami, które mogą w niej wystąpić.

W publikacjach autorów do wykrywania uszkodzeń przekładni zębatych przedstawione są różne miary diagnostyczne. Bazują one na odpowiednio przetworzonych i filtrowanych sygnałach drganiowych. W niniejszej pracy przedstawiono próbę porównania wrażliwości niektórych miar diagnostycznych na badane rodzaje uszkodzeń kół zębatych w przypadku pracy przekładni z łożyskami w różnym stanie technicznym.

Słowa kluczowe: diagnostyka, uszkodzenia kół zębatych, wrażliwość miar.

1. INTRODUCTION

The diagnostics of tooth gears is a vital scientific issue for its utilitarian and cognitive aspects. An essential part of this process is the ability to differentiate the impact of various effects on the vibration signal of a tooth gear both working in the correct mode, including meshing of the tooth gear, and possible damage to it.

The methods described in literature concerning the detection of tooth gear damage have been developed providing that the damages do not coincide. The precise specification of gear tooth condition is considerably hindered when damage to other elements of the tooth gear, e.g. bearings, occurs simultaneously. In such cases the vibration signal generated by the tooth gear contains additional modulations resulting from the concurrent damage of tooth gears and bearings.

The papers of different authors present various diagnostic measures applied in the detection of tooth gear damage. They are based on e.g. Wigner-Ville distribution, continuous wavelet analysis, and the envelope spectrum of appropriately processed and filtered vibration signals. This paper presents an attempt to compare the sensitivity of selected diagnostic measures on the studied types of tooth gear damage in the work of tooth gears with bearings in various technical conditions.

2. EXPERIMENTAL STUDIES

The experimental studies applied a unit working in a power circulating system. During the studies the tooth gear worked as a reducer. The acceleration and vibration velocity for selected locations of the tooth gear casing, and the vibration velocity of its transverse shafts were measured. Apart from that,

synchronic reference signals corresponding to the shaft rotations were recorded [3, 17].

The experimental studies concerned wheels with two different hardness factors, depending on the performed experiment:

- 60-62 HRC (carbon coated) – diagnostics of tooth top crushing and tooth base cracking, - 37-40 HRC (carbon coated and tempered) – diagnostics of wear of tooth working surface.

While modelling the tooth crushing at subsequent stages of an active experiment, the height of the head of one wheel tooth was lowered by grinding off the appropriate quantity of material: 0.75, 1.5 and 2.0 mm. This operation resulted in the shortening of the contact line of the tooth and a decrease in the local contact ratio CR (Table 1).

Table 1. Influence of lowered height of the head of a wheel tooth on local contact ratio

Lowered height of the head of tooth head [mm]	Local contact ratio CR [-]
0	1.32
0.75	1.18
1.5	1.03
2.0	0.93

Measurements of tooth gear vibration aimed at the specification of the influence of the wear of the tooth's working surface on the diagnostic signal were performed in four phases which corresponded with the different phases of the wear of the tooth's surface (Fig. 1).

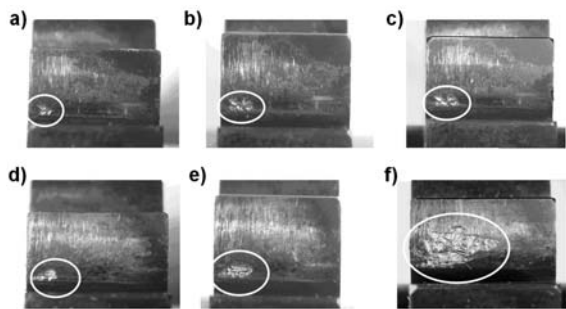


Fig. 1. Subsequent phases of the wear of the tooth's working surface: a) - c) tooth 1, d) - f) tooth 2

The shafts of the power circulating unit were supported by ordinary ball bearings. The experimental study applied bearings in good technical condition, with modelled damage of bearing raceway, and raceway worn out in long-term use (Fig. 2).

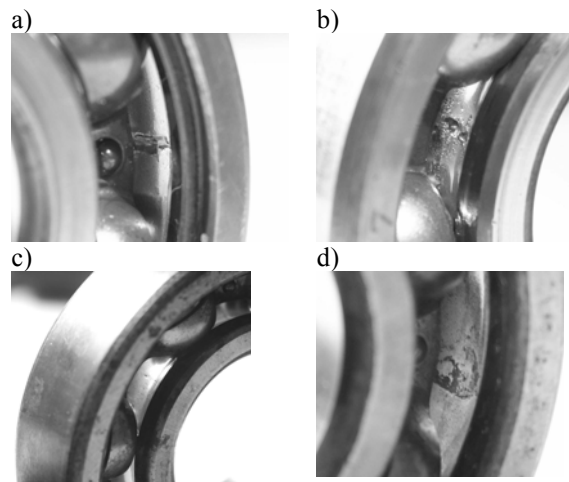


Fig. 2. Damage (wear) of ball bearing raceways: a) damage to outer raceway; b) damage to inner raceway; c)-d) usual wear

3. SIMULATION STUDY

One of the most common types of damage to tooth gears is cracking at the base. An initial study carried out by the authors of this paper demonstrated that fast tooth cracking progress [18, 13, 14, 8, 10, 17, 3] disables the possibility of the recording and comparison of the same phase of cracking in the case of bearing shafts with different experimentally established degrees of damage. For that reason it was necessary to carry out simulation studies and their experimental verification by the performance of several short series of studies on a working unit. For the simulation of the tooth base cracking this study employed a dynamic model of a tooth gear in a drive unit developed at the Faculty of Transport of the Silesian University of Technology and performed in the Matlab-Simulink environment [5, 4]. The application of this model in the diagnostics of local damage, dynamic analysis or designing requires the identification of the parameters of this model. Within the framework of the study [4] the identification of the friction factor in meshing was carried out and the values of the meshing attenuation factor were specified by the comparison of the values of effective accelerations of the torsional vibration of the wheel, which were measured and obtained by simulation. One of the significant factors determining the compliance of obtained results with the experiment was the identification of attenuation for bearing nodes [6, 17].

4. SIGNAL FILTERING

The separation of components containing information on wheel damage is possible, in accordance with papers [12, 9, 8, 17, 3], by residual filtering, also named differentiation filtering [8, 9, 17, 3].

The diagnosis of tooth gear condition is considerably hindered in the case of concurrent damage in its other element, e.g. a bearing. In such

a case the vibration signal of the tooth gear contains an additional component resulting from bearing damage. Therefore, it is suggested that direct comb filtering for diagnostic purposes is used. To identify the damage to tooth gears by this method filters are used which transmit frequency bands connected with a wide-bandwidth signal modulation $k f_u$, where: f_u – rotational frequency of a damaged wheel, and $k \in C^+$. Two options for the performance of the direct comb filter were assumed: the first option provides that information concerning tooth gear damage is only contained in harmonic bands of rotational frequency of a pinion (filter I) or a wheel (filter II), and in the second option information concerning damage is contained in harmonic bands of rotational frequency of the pinion and wheel (filter III). Based on such prepared signals the diagnostic measures demonstrated in part 5 were determined.

5. DIAGNOSTIC MEASURES

Measure M_{wWV} (2) was proposed for the diagnosis of local wheel damage, and was determined based on the signal obtained as a result of the summation of the discrete values of the Wigner-Ville distribution [7] denominated $SWWV$ (1).

$$SWWV(i) = \sum_{j=1}^K WV(i, j) \quad (1)$$

where:

$WV(i, j)$ – discrete values of Wigner-Ville distribution,

$i = 1, 2, \dots, N$,

N – number of line of $WV(i, j)$ distribution corresponding with a 360° turn of a wheel,

K – number of column of $WV(i, j)$ distribution corresponding with the top frequency limit

$$M_{wWV} = \frac{SWWV_{UMAX} - \overline{SWWV}}{SWWV_b} \quad (2)$$

where:

$SWWV_{UMAX}$ – maximum value of $SWWV$,

\overline{SWWV} – mean value of $SWWV$,

$SWWV_b$ – mean value of baseline signal $SWWV(i)$ determined in the case of meshing and bearing mounting in good conditions.

Measure M_{wCWT} (4), similar to M_{wWV} (2), was used to diagnose local wheel damage. It is determined based on the signal obtained as a result of the summation of the discrete values of continuous wavelet transform [2] denominated $SWCWT$ (3).

$$SWCWT(i) = \sum_{j=A_{CWT}}^{B_{CWT}} C_{ab}(j, i), \quad (3)$$

where:

$C_{ab}(j, i)$ – discrete values of continuous wavelet transform CWT ,

$i = 1, 2, \dots, N$,

N – number of column of $C_{ab}(j, i)$ distribution corresponding with a 360° turn of a wheel,

A_{CWT} – number of line of $C_{ab}(j, i)$ distribution corresponding with the bottom limit of scale range (frequency),

B_{CWT} – number of line of $C_{ab}(j, i)$ distribution corresponding with the top limit of scale range (frequency),

$$M_{wCWT} = \frac{SWCWT_{UMAX} - \overline{SWCWT}}{SWCWT_b} \quad (4)$$

where:

$SWCWT_{UMAX}$ – maximum value of $SWCWT$,

\overline{SWCWT} – mean value of $SWCWT$,

$SWCWT_b$ – mean value of baseline signal $SWCWT(i)$ determined in the case of meshing and bearing mounting in good condition.

Vibroacoustic diagnostics often applies an envelope spectrum, whose utility in the diagnosis of wheel meshing was demonstrated in papers [1, 15, 11]. To define changes in the envelope spectrum the $SWWO$ measure defined by the correlation (9.5) was proposed:

$$SWWO = \sum_{i=1}^K |X(f_i)|, \quad (5)$$

where:

$X(f_i)$ – amplitude of i -th component of envelope spectrum,

f_i – frequency of i -th component of spectrum,

i – number of spectrum component,

K – number of discrete spectrum components.

To diagnose local damage in a tooth gear a discrete wavelet transform [2] was also used with the incorporation of the Daubechies 2 wavelet.

Owing to the specific nature of signal changes caused by the tooth base cracking further calculations applied the measure M_{wDWT} , determined according to the correlations (6, 7), based on the signal reconstructed at the subsequent stages of decomposition. Apart from that, the summarized measure SD1-5, i.e. the sum of the values of M_{wDWT} measures for details 1 to 5, was applied.

$$M_{wDWT(Di)} = \frac{D_{iUMAX} - D_i}{D_{ib}} \quad (6)$$

or

$$M_{wDWT(Ai)} = \frac{A_{iUMAX} - A_i}{A_{ib}}, \quad (7)$$

where:

D_{iUMAX}, A_{iUMAX} – maximum value of a detail or approximation,

$\overline{D}_i, \overline{A}_i$ – mean value of a detail or approximation,

$\overline{D}_{ib}, \overline{A}_{ib}$ – baseline mean value of a detail or approximation calculated for meshing and bearing mounting in good condition,

i – number of a detail or approximation.

As in paper [16] the measure of the wear of tooth surface was determined as the sum of the discrete values of the Wigner-Ville distribution:

$$SWV = \sum_{i=1}^N \sum_{j=1}^K WV(i, j), \quad (8)$$

where:

$WV(i, j)$ – discrete values of Wigner-Ville distribution,

N – number of line of $WV(i, j)$ distribution corresponding with a 360° turn of a wheel,

K – number of column of $WV(i, j)$ distribution corresponding with the top frequency limit.

The measure describing the wear of tooth working surface calculated based on continuous wavelet transform applied the $SCWT$ parameter calculated from the correlation (9):

$$SCWT = \sum_{i=1}^N \sum_{j=A_{CWT}}^{B_{CWT}} C_{ab}(j, i) \quad (9)$$

where:

$Cab(j, i)$ – discrete values of continuous wavelet transform CWT ,

N – number of column of $Cab(j, i)$ distribution corresponding with a 360° turn of a wheel,

A_{CWT} – number of line of $Cab(j, i)$ distribution corresponding with the bottom limit of scale range (frequency),

B_{CWT} – number of line of $Cab(j, i)$ distribution corresponding with the top limit of scale range (frequency).

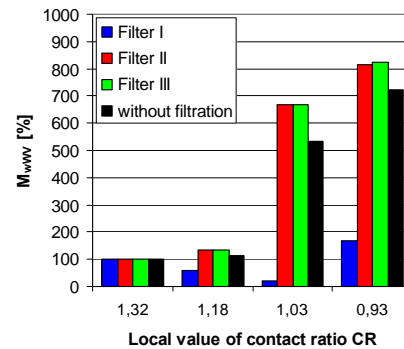
Discrete wavelet analysis was also used to identify the wear of tooth working surface. As in the detection of tooth gear crushing, the stages of signal decomposition were identified, for which the largest energetic changes were observed. Based on initial studies the $coif 1$ wavelet was selected and the condition imposed that the analysis of the signal should be performed at 5 stages of decomposition. For the analysis of vibration signal, including signals obtained from details and approximation, the calculation of root-mean-square (RMS) and central moment of 4th degree ($M4$) was proposed.

More information concerning the presented measures is contained in [7].

6. ESTIMATION OF MEASURES EFFICIENCY

This section presents a comparison of the sensitivity of the studied diagnostic measures to the studied types of tooth gear damage in the work of a tooth gear with bearings in various technical conditions. However, this will be introduced by the sensitivity of the M_{wWV} measure to the changes of the value of the local contact ratio for various types of direct comb filtering in the case of the work of a tooth gear with good bearings (Fig. 3). The demonstrated results of the analysis indicate that within the harmonic rotational frequencies of a pinion and gear only the harmonics of the wheel with a damaged tooth contain information on crushing presence.

a)



b)

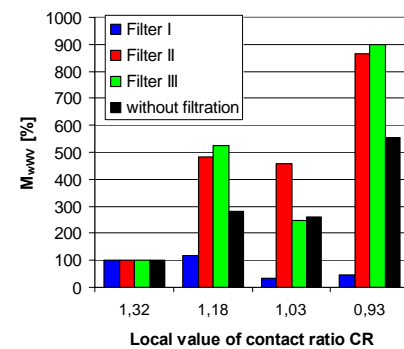


Fig. 3. Percentage value of M_{wWV} depending on the type of direct comb filtering and local contact ratio:

- a) measurements of shaft vibrations,
b) measurements of casing vibrations

In the case of tooth top crushing resulting in the decrease of local contact ratio to 1.18, the increase of M_{wWV} measure expressed in percent was greater when the measure was calculated based on the signal of accelerated vibrations of the tooth gear casing (Fig. 3b) than when it was based on the shaft vibration velocity signal (Fig. 3a). However, a continued increase of the simulated tooth crushing, resulting in the decrease of the local contact ratio to 1.03, no longer resulted in the increase of the M_{wWV} measure (even decreasing it) when it was calculated based on the signal of accelerated vibrations of the

tooth gear casing (Fig. 3b). This increase occurred, however, when the measure in question was calculated based on the shaft vibration velocity (Fig. 3a), both in the case of used filter II and filter III.

Figure 4 demonstrates the changes in *SWV* value depending on the type of direct comb filtering and the phase of wear of tooth working surface. As in the already discussed part, the results refer to the work of a tooth gear with efficient bearings. It can be stated based on the obtained results that the application of direct comb filtering does not deteriorate the sensitivity of measures considerably, and in the diagnostics of a tooth gear with damaged bearings enables the inclusion in the analysis of only the signal components containing information on tooth gear damage. This enables us to ignore highly energetic signal components connected with bearing damage and the diagnostics of the tooth gear in the case of concurrent bearing damage.

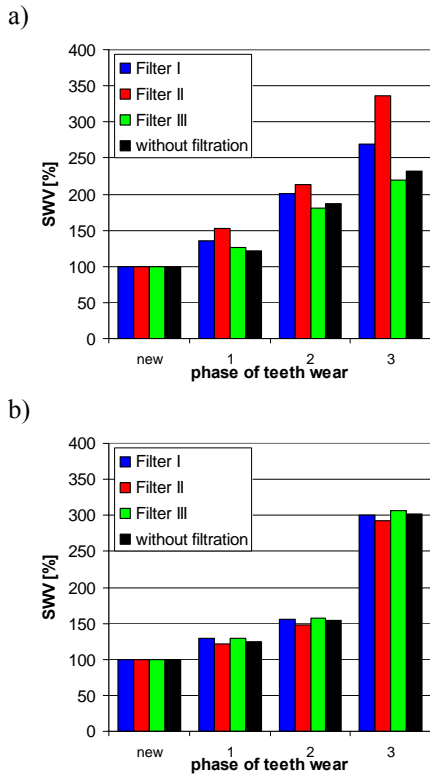


Fig. 4. Percentage *SWV* value depending on the type of direct comb filtering and the phase of wear of tooth working surface: a) measurements of shaft vibrations, b) measurements of casing vibrations

In the first and second phases of the wear of the tooth working surface the *SWV* measure, calculated based on the signal of shaft vibration velocity, increases more considerably than for *SWV* calculated based on the signal of accelerated vibrations of the tooth gear casing (Fig. 4).

The results demonstrated in Figures 3 and 4 suggest that an appropriate direct comb filtering, especially with respect to tooth gear shaft vibrations, results in a greater increase in damage and wear measures than in the case of their calculation based on non-filtered signals. Additionally, as previously

mentioned, it enables us in most cases to ignore the frequencies connected with ball bearing damage.

While comparing the sensitivity of measures (Fig. 5, 6) on tooth top crushing in the work of a tooth gear with bearings in various technical conditions it can be stated that the highest increase expressed in percent is typical for measures based on the Wigner-Ville distribution and wavelet transform.

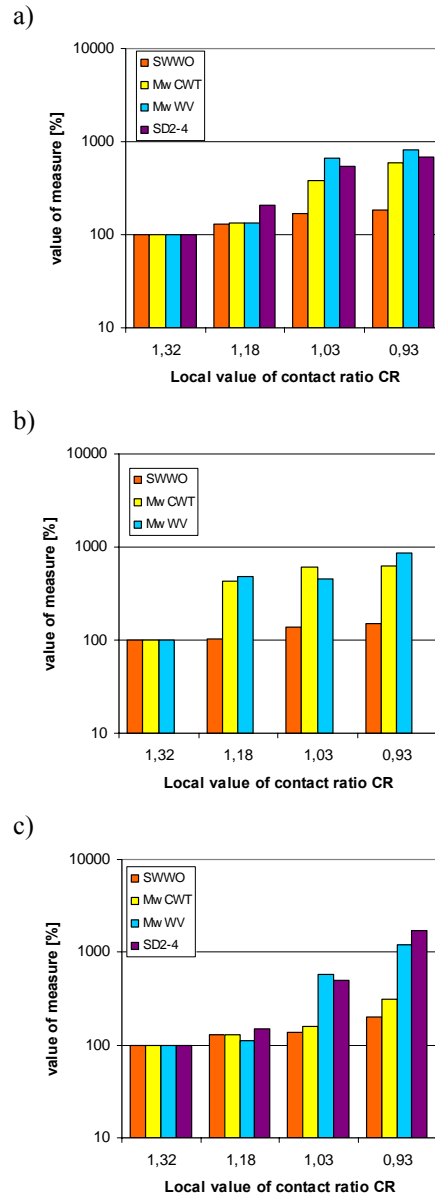


Fig. 5. Change in percent value of selected measures depending on the value of local contact ratio – tooth gear load $Q=3.85\text{MPa}$: a) good bearings - measurements of shaft vibrations, b) good bearings – measurements of casing vibrations, c) damage to inner raceway - measurements of shaft vibrations

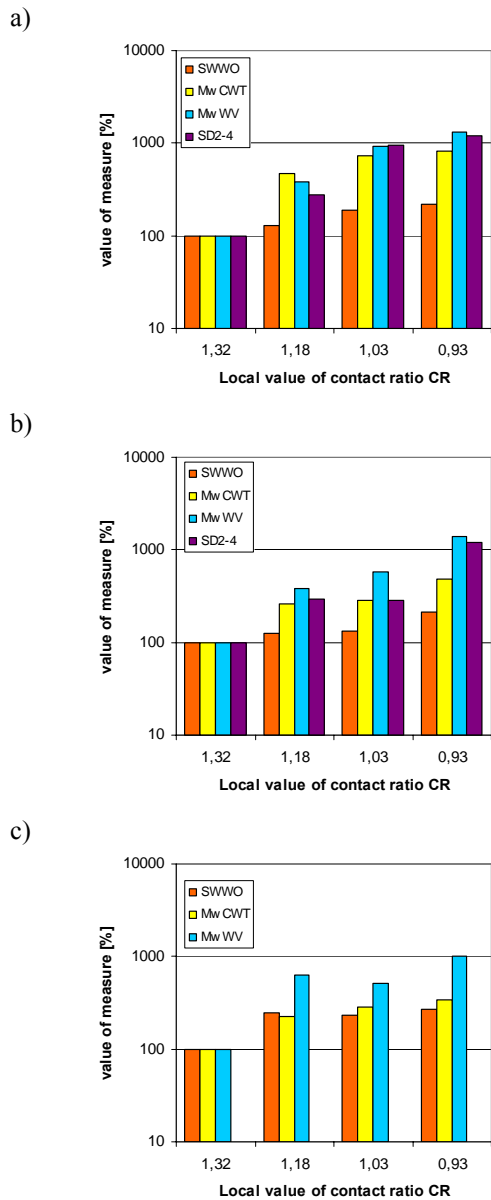


Fig. 6. Change in percent value of selected measures depending on the value of local contact ratio – tooth gear load $Q=3.85\text{MPa}$: a) damage to outer raceway - measurements of casing vibrations, b) damage to inner raceway - measurements of shaft vibrations c) damage to inner raceway - measurements of casing vibrations

The measure based on the central moment of the fourth degree proved to be very sensitive for the wear of the tooth working surface, the same as for the measure based on the Wigner-Ville distribution. The values of the measures presented in Figures 7 and 8 were calculated based on appropriately filtered vibration signals (filter III).

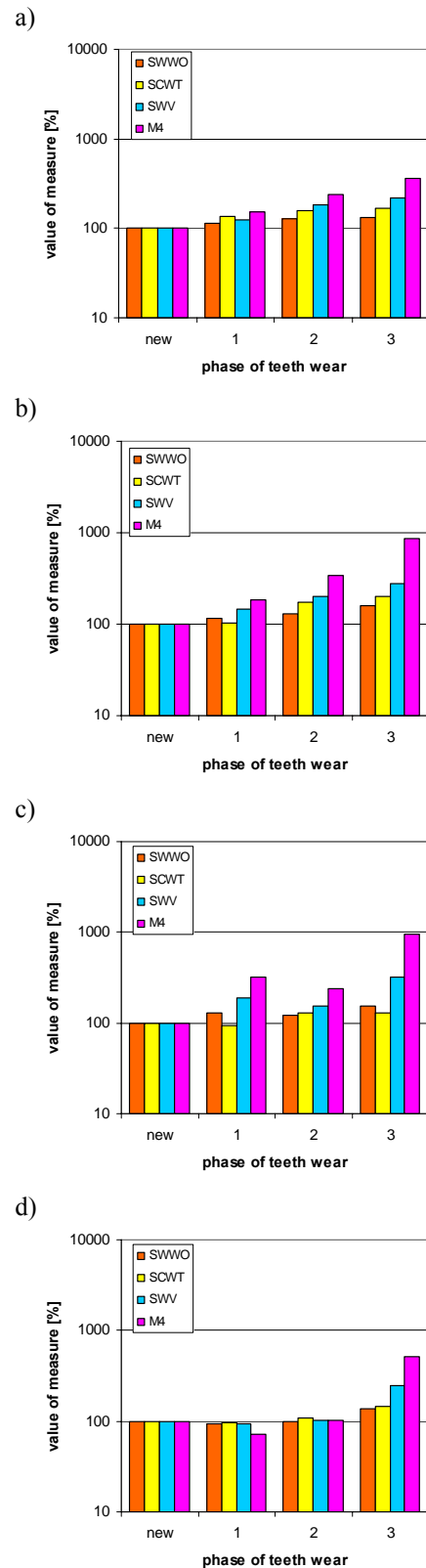


Fig. 7. Change in percent value of selected measures depending on the phase of tooth wear – shaft vibration measurement at tooth gear load $Q=3.1\text{MPa}$: a) good bearings, b) damage to outer raceway, c) damage to inner raceway, d) usual wear of bearings

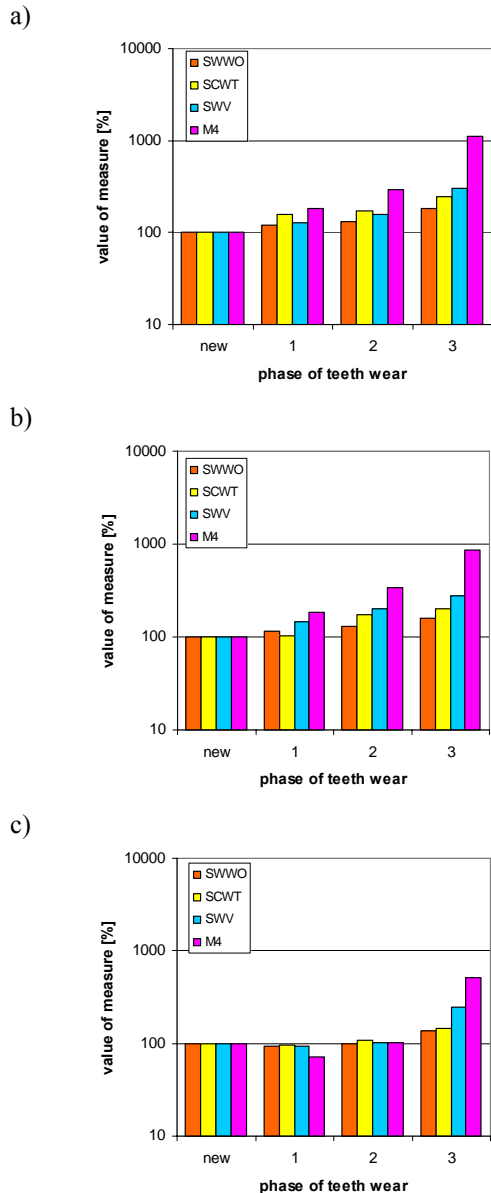


Fig. 8. Change in percent value of selected measures depending on the phase of tooth wear – casing vibration measurement at tooth gear load $Q=3.1\text{MPa}$: a) good bearings, b) damage to outer raceway, c) usual wear of bearings

In tooth base cracking, as in tooth top crushing, the suggested measures calculated based on appropriately filtered vibration signals are sensitive to this local damage (Fig. 9).

7. CONCLUSIONS

The results enable us to state that the application of direct comb filtering does not deteriorate the sensitivity of measures considerably. In the diagnostics of tooth gears with damaged bearings it is advisable to include in the analysis only those signal components containing information on tooth gear damage. This enables us to ignore highly energetic signal components

connected with bearing damage and to diagnose the tooth gear in the case of concurrent bearing damage.

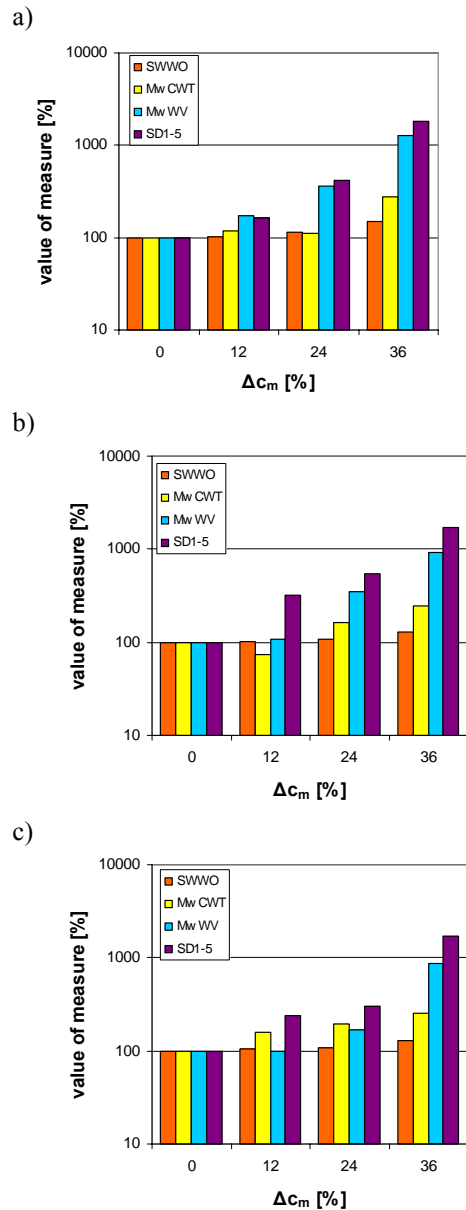


Fig. 9. Change in percent value of selected measures depending on the decrease in the achieved meshing rigidity Δc_m resulting from the cracking of the wheel tooth and the decrease in rigidity in the bearing nod resulting from damage to: a) outer bearing raceway equal to 10% ($\Delta f/f=0.1$), b) outer bearing raceway equal to 20% ($\Delta f/f=0.1$), c) inner bearing raceway equal to 10% ($\Delta f/f=0.1$)

However, it is relatively difficult to unambiguously define the diagnostic measure most sensitive to all the studied types of tooth gear damage. In the opinion of the authors of this paper the developed methods should be used as complementary methods so as to increase the confidence of diagnostic results.

REFERENCES

- [1] Bartelmus W., Zimroz R.: *Cepstrum, widmo obwiedni i bispectrum w diagnostyce wielostopniowych przekładni zębatych*, Diagnostyka vol. 30 tom 1 2004r. 39-44.
- [2] Batko W., Ziółko M.: *Zastosowanie teorii falek w diagnostyce technicznej*. Problemy Inżynierii Mechanicznej i Robotyki – AGH, Kraków 2002.
- [3] Figlus T.: *Metoda drganiowa diagnozowania stanu kół zębatych w przypadkach zużycia i uszkodzeń łożysk tocznych przekładni*. Rozprawa doktorska, Politechnika Śląska 2005 r.
- [4] Łazarz B.: *Zidentyfikowany model dynamiczny przekładni zębatej w układzie napędowym jako podstawa projektowania*. Wydawnictwo i Zakład Poligrafii Instytutu Technologii Eksploatacji w Radomiu, K-ce-Radom 2001.
- [5] Łazarz B., Wojnar G.: *Model dynamiczny układu napędowego z przekładnią zębatą*. XVII Ogólnopolska Konferencja Przekładnie Zębate, Węgierska Górka 09.10 ÷ 11.10.2000r., s. 101÷108.
- [6] Łazarz B., Wojnar G.: *Modelowanie lokalnych uszkodzeń łożysk tocznych w przekładni zębatej do celów diagnostycznych*. Materiały V Krajowej Konferencji "Diagnostyka Techniczna Urządzeń i Systemów" DIAG' 2003, 13÷17.10.2003.
- [7] Łazarz B., Madej H., Wilk A., Figlus T., Wojnar G.: *Diagnozowanie złożonych przypadków uszkodzeń przekładni zębatych*. Wydawnictwo i Zakład Poligrafii Instytutu Technologii Eksploatacji w Radomiu, Kielce-Radom 2006.
- [8] Madej H.: *Wykorzystanie sygnału resztkowego drgań w diagnostyce przekładni zębatych*. Diagnostyka vol. 26, 2002.
- [9] McClintic, Lebold M., Maynard K., Byington C., Cambell R.: *Residual and difference feature analysis with transitional gearbox data*. 54th Meeting of the Society for Machinery Failure Prevention Technology, Virginia Beach, 2000.
- [10] Radkowski S., Zawisza M.: *Napężeniowo-drganiowe modele diagnostyczne zmęczeniowych uszkodzeń kół zębatych*. Diagnostyka vol. 30 tom 2 2004r., s. 85-88.
- [11] Radkowski S., Zawisza M.: *Obwiednia sygnału wibroakustycznego jako parametr diagnostyczny zmęczeniowego uszkodzenia podstawy zęba w przekładni zębatej*. XXIX Ogólnopolskie Sympozjum Diagnostyka Maszyn, Węgierska Górka 2002, s. 331-338.
- [12] Stewart R. M.: *Some Useful Data Analysis Techniques for Gearbox Diagnostics*, Report MHM/R/10/77, Machine Health Monitoring Group, Institute of Sound and Vibration Research, University of Southampton 1977.
- [13] Wang W.: *Early detection of gear tooth cracking using the resonance demodulation technique*. Mechanical Systems and Signal Processing (2001) 15(5), s. 887-903.
- [14] Wilk A., Łazarz B., Madej H.: *The Application of Time-Frequency Analysis in Diagnostics of Local Damages of Toothed Gears*. 6th International Conference on Rotor Dynamics. IFToMM. Sydney, 2002, s. 706-713.
- [15] Wilk A., Łazarz B., Madej H.: *Diagnozowanie przemysłowych przekładni obiegowych metodami drganiowymi*. Przegląd Mechaniczny. 2000, s. 24-28.
- [16] Wilk A., Łazarz B., Madej H., Wojnar G.: *Metody wczesnego wykrywania lokalnych uszkodzeń kół zębatych*. XXIX Ogólnopolskie Sympozjum Diagnostyka Maszyn, Węgierska Górka 2002, s. 345-355.
- [17] Wojnar G.: *Wykrywanie uszkodzeń kół zębatych wybranymi metodami przetwarzania sygnałów drganiowych*. Rozprawa doktorska, Politechnika Śląska 2004 r.
- [18] Zakrajsek J., Townsend D., Lewicki D., Decker H., Handshuh R.: *Transmission diagnostic research at NASA*. Lewis Research Center. Report Documentation Page NASA, TM-106901, 1995.



DSc. Eng. **Bogusław ŁAZARZ** professor of The Silesian University of Technology. Scientific interest: modelling of dynamic processes, diagnostics of tooth gear, machine design and processing vibroacoustic signal. Member of Machines Construction Committee.



PhD. Eng. **Grzegorz WOJNAR** adjunct of The Silesian University of Technology. Scientific interest: modelling of dynamic processes, diagnostics of tooth gear, machine design and processing vibroacoustical signal.



PhD. Eng. **Tomasz FIGLUS** adjunct of The Silesian University of Technology. Scientific interest: processing vibroacoustical signal and finite element method.

AVERAGING OF THE VIBRATION SIGNAL WITH THE SYNCHRONIZING IMPULSE LOCATION CORRECTION IN TOOTH GEAR DIAGNOSTICS

Grzegorz WOJNAR, Bogusław LAZARZ

The Silesian University of Technology, Faculty of Transport
8 Krasińskiego Street, 40-019 Katowice
tel: (032) 603 41 93, e-mail: Grzegorz.Wojnar@polsl.pl, Boguslaw.Lazarz@polsl.pl

Summary

One of the methods applied to detect pinion or gear wheel damage is an analysis of a signal synchronously averaged by the rotation period of a pinion shaft or gear shaft, respectively. For technical reasons, it is often impossible to record the reference signal directly connected with the diagnosed wheel in industrial conditions. The signal is then connected with a rotating element available outside the gear. As a result of torsional vibration in a system of shafts or gear casing vibration in a place where the shaft's angular position sensor is fixed, or in consequence of a too slowly rising reference signal edge, a synchronizing impulse occurs at wheel's angular positions varying by an insignificant value. This paper presents the usefulness of time-delay estimation methods in the process of vibration signals' synchronous averaging.

Keywords: signal averaging, time-delay estimation, diagnostics, toothed gear.

WYKORZYSTANIE UŚREDNIANIA SYGNAŁU DRGANIOWEGO Z KOREKCJĄ POŁOŻENIA IMPULSU SYNCHRONIZUJĄCEGO W DIAGNOSTYCE PRZEKŁADNI ZĘBATYCH

Streszczenie

Jednym ze sposobów wykrywania uszkodzeń zębника lub koła jest analiza sygnału uśrednionego synchronicznie odpowiednio okresem obrotu wału zębника lub koła. W warunkach przemysłowych ze względów technicznych często nie jest możliwe rejestrowanie sygnału odniesienia związanego bezpośrednio z diagnozowanym kołem. Wtedy sygnał ten wiąże się z dostępnym na zewnątrz przekładni elementem wirującym. Na skutek drgań skrętnych w układzie wałów, drgań korpusu przekładni w miejscu mocowania czujnika położenia kąowego wału i często zbyt wolno narastającego zbrocza sygnału referencyjnego impuls synchronizujący występuje przy położeniach kąowych koła różniących się o niewielką wartość. W niniejszym artykule przedstawiono przydatność metod estymacji przesunięcia czasowego w procesie uśredniania synchronicznego sygnałów drganiowych.

Słowa kluczowe: uśrednianie synchroniczne, estymacja opóźnienia czasowego, diagnostyka.

1. INTRODUCTION

In rotor machines, some processes repeat in cycles. For toothed gears with permanent axles, the processes are: the period of entering into contact by the same teeth couple, the pinion or wheel shaft rotation period, and the meshing period connected with the frequency of meshing. In the diagnostics of machinery and appliances containing rotating components, synchronous averaging is applied to improve the signal-to-noise ratio and eliminate constituents not connected with the rotation period of a selected element [1, 4, 5]. Attempts are often made to detect damage of selected elements of the diagnosed object. In such case, it is necessary to determine the diagnosed element's rotation period as well as the period in which the damage will generate disturbance of the measured vibration signal.

Application of synchronous averaging in the right period will reduce in that case the impact of disturbance not connected with the damage. Drawing conclusions about the occurrence of damage based on the averaged signal will be thereby more effective. However, one should bear in mind that by applying synchronous averaging connected with the pinion shaft rotation period, e.g. in a toothed gear with permanent axles, the information connected with the wheel shaft rotation period gets lost, and vice versa, except for a case where the gear ratio equals 1.

In industrial toothed gears, for constructional reasons, the reference signal used in the averaging process connected with the rotating element can be most easily recorded on the shaft running outside the gear. A remote distance of the signal recording place from the diagnosed wheel, torsional vibration in the

gear shaft system, as well as a too slowly rising synchronizing signal edge, make the synchronizing impulse occur at wheel's angular positions varying by an insignificant value. The differences are particularly important for constituents of a high frequency signal and when diagnosing local damage of wheels generating impulse disturbance, whose duration is comparable to the synchronizing impulse deviation.

2. EXPERIMENTAL RESEARCH

Experimental research was conducted, whose aim was to detect local chipping of a pinion or gear's tooth. The damage was modelled by shortening the tooth tip [6, 8]. Both the vibration accelerations of selected points of the gear casing and the velocity of its shafts' transverse vibration were measured. The reference signals corresponding to the shafts' rotation were also synchronously recorded. During testing, the gear was loaded with the moment $M_h=207$ Nm, with the pinion's rotational speed amounting to 2700 rpm.

3. SYNCHRONOUS AVERAGING OF VIBRATION SIGNALS

Any deviations in the workmanship of gear components, in particular toothed wheels, make it difficult to detect gear damage [8], since a tooth couple with a considerable resultant deviation of pitch, when coming into contact, generates a force impulse similar to that generated during the wheels' interaction with the damaged tooth. The impulse maximum value is influenced by both the damage scale and the deviations in the workmanship of the interacting teeth. Therefore, the course of the vibration recorded when the pinion enters into contact with a damaged wheel tooth, where the total deviation in the workmanship of such couple is relatively small, differs from the vibration course where the deviation is greater. Figure 1 presents the course of pinion shaft's transverse vibration velocity averaged with the teeth couples' repetition period in the case of considerable chipping of a wheel tooth to a depth of 3 mm. As a result of chipping, the contact ratio CR for the damaged tooth reduced locally from 1.33 to 0.71. Two local increases in the vibration amplitude are visible here, caused by chipping of a tooth in a wheel interacting with different pinion's teeth, varying in amplitude and duration.

In diagnosing, the acceleration of selected points of gear casing is measured most often. The differences between changes in the signal, caused by local damage, may be even greater. In such case, detection of damage will be much easier when based on an analysis of a signal synchronously averaged by the wheel revolution period.

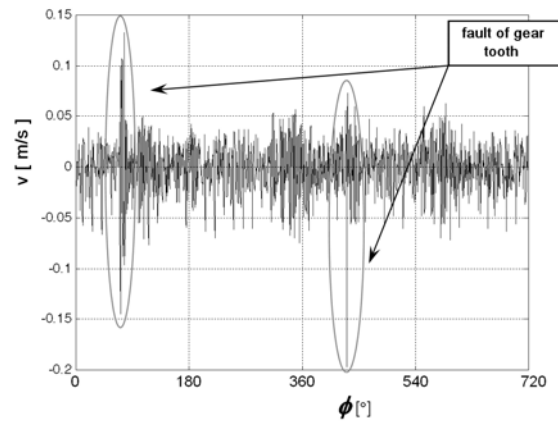


Fig. 1. Pinion shaft vibration velocity signal averaged by the repetition period of teeth couples presented as a function of the wheel rotation angle

As a result of torsional vibration in a system of shafts or gear casing vibration in a place where the shaft's angular position sensor is fixed, some shifts of the synchronizing impulse take place in relation to the wheel. The shifts may increase as the distance between the reference signal recording place and the investigated wheel grows. For technical reasons, it is often impossible to record the reference signal directly connected with the diagnosed wheel in industrial conditions. The signal is then connected with a rotating element available outside the gear.

By analyzing the overlapping averaged time signals of pinion shaft's transverse vibration (Fig. 2) when the synchronizing impulse location was not initially corrected, it was found that the impulse location deviation equaled ± 2 sampling periods, i.e. ca. $\pm 1^\circ$ of shaft's revolution. To minimize the impact of the deviation, a computational correction of the synchronizing impulse location was made by utilizing time-delay estimation between the successive recorded periods of averaged time signals. It was significant, since the duration of impulse coming from a damaged tooth amounted to $0.12 \div 0.16 \cdot 10^{-3}$ [s], i.e. $3 \div 4$ of the sampling periods with the sampling frequency applied. For this reason, the averaging synchronization impulse should be very accurately correlated with the wheel's angular position, since any deviation in its position may lead to removal of the information about the appearing damage from the averaged signal.

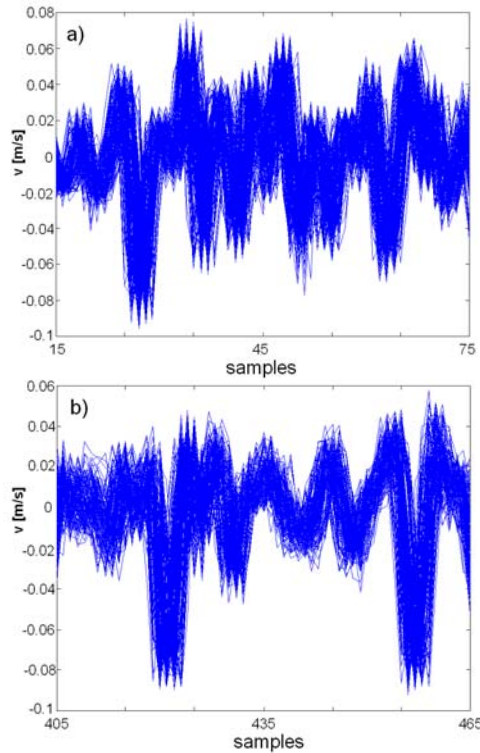


Fig. 2. Overlapping of averaged time signals of pinion shaft's transverse vibration velocity – uncorrected location of synchronizing impulse, a) signal fragment from 15th to 75th sample, b) signal fragment from 405th to 465th sample, pinion's rotation period – 572 samples

Before applying time-shift estimation, a fragment was selected of the vibration time signal, equal to the averaging period in relation to which the time-shift was determined. It was the time signal fragment best correlated with the other periods. Usefulness of the time-shift methods available in the Matlab system [7] was checked. First, the time delay was determined using a method based on the third-order cumulants (TDE). The method will be presented using an example with the signals: x and y .

$$x(t) = s(t) + \varpi_x(t), \quad (1)$$

$$y(t) = A_m \cdot s(t - D_t) + \varpi_y(t). \quad (2)$$

The signals can be also presented in a form useful for a digital analysis:

$$x(n) = s(n) + \varpi_x(n), \quad (3)$$

$$y(n) = A_m \cdot s(n - D) + \varpi_y(n), \quad (4)$$

where:

- s - stationary process,
- A_m - relative amplitude multiplier,
- D_t - signal y shift in relation to signal x ,
- D - signal y shift in relation to signal x , expressed in sampling periods,
- ϖ_x and ϖ_y - noise.

The third-order cumulants of signal $s(t)$ according to [2] are described by the dependence:

$$C_{sss}(\tau_1, \tau_2) = E\{s(t)s(t + \tau_1)s(t + \tau_2)\} = \frac{1}{T} \int_0^T s(t)s(t + \tau_1)s(t + \tau_2) dt, \quad (5)$$

where:

T – observation time of signal $s(t)$.

The third-order cumulants in a form useful for a digital analysis are described by the dependencies [7]:

$$C_{xxx}(q, \rho) = E\{x(n)x(n+q)x(n+\rho)\}, \quad (6)$$

$$C_{yxx}(q, \rho) = E\{y(n)x(n+q)x(n+\rho)\}. \quad (7)$$

If signal $s(t)$ is not a Gaussian signal and noises $\varpi_x(t)$ and $\varpi_y(t)$ are non-Gaussian noises, the third-order cumulants can be used even where the noises are correlated. If P is the maximum expected shift and assuming that shift D is an integer, we obtain [7].

$$y(n) = \sum_{i=-P}^P a(i)x(n-i) + \varpi(n), \quad (8)$$

where:

$$a(n) = 0, n \neq D, i a(D) = A.$$

By utilizing (8) and (7), we obtain:

$$C_{yxx}(q, \rho) = \sum_{i=-P}^P a(i)C_{xxx}(q+i, \rho+i). \quad (9)$$

By applying this equation for different values of ρ and q , we will obtain a system of linear equations $a(i)$:

$$C_{xxx} \mathbf{a} = \mathbf{c}_{yxx}. \quad (10)$$

The estimated delay is marked with index n , at which $|a(n)|$ reaches its maximum.

It is important that the allowable signal shift P cannot be too large. In particular, P must always be smaller than the number of samples falling on a shaft's rotation by one meshing pitch, otherwise, the signals may get completely desynchronized.

In order to obtain the best results, the following numbers of samples were used to calculate the third-order cumulants: $n_{\text{samp}} = 256, 128, 64, 32, 16$. The best results were obtained where $n_{\text{samp}} = 32$ samples (Fig. 3). Compared to Fig. 2, improvement was visible.

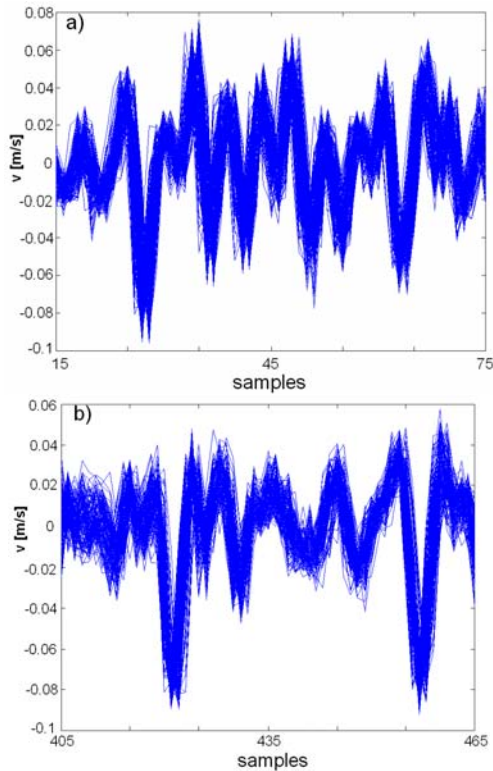


Fig. 3. Overlapping of averaged time signals of pinion shaft's transverse vibration velocity – location of synchronizing impulse corrected by means of the TDE method, $n_{\text{samp}} = 32$, a) signal fragment from 15th to 75th sample, b) signal fragment from 405th to 465th sample

The next method applied was the time-delay estimation using cross-bispectrum (TDEB). The auto- and cross-bispectra are defined as follows [7]:

$$B_{xxx}(f_{B1}, f_{B2}) = E\{X(f_{B1}) X(f_{B2}) X^*(f_{B1} + f_{B2})\}, \quad (11)$$

$$B_{xyx}(f_{B1}, f_{B2}) = E\{X(f_{B1}) Y(f_{B2}) X^*(f_{B1} + f_{B2})\}. \quad (12)$$

The absolute value $h(\tau)$ determined from dependence [7]:

$$h(\tau) = \int df_{B1} \int df_{B2} \exp(j2\pi f_{B2} \tau) \frac{B_{xyx}(f_{B1}, f_{B2})}{B_{xxx}(f_{B1}, f_{B2})}, \quad (13)$$

reaches its maximum at τ equal to the real shift D_t of signal y in relation to signal x .

Fig. 4 shows the overlapping of signals where the location of synchronizing impulse was corrected by means of the TDEB method and where the number of samples FFT (n_{FFT}) equalled the number of samples corresponding to the pinion rotation period. The calculation time was then much longer than where the TDE method was applied.

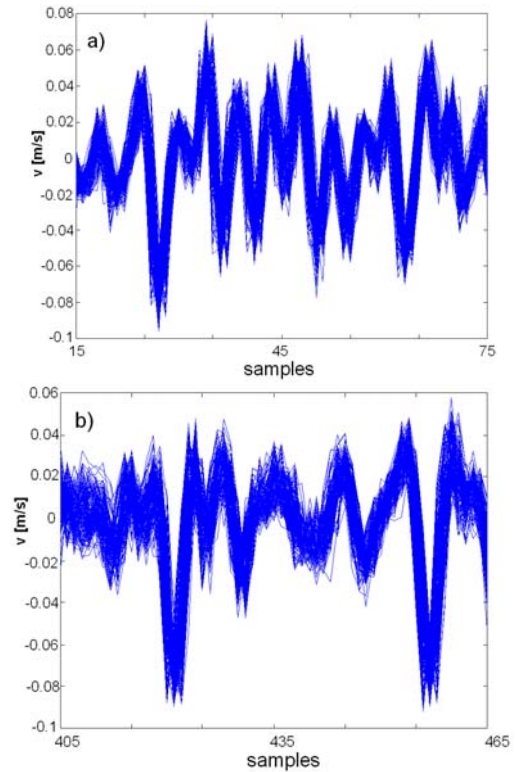


Fig. 4. Overlapping of averaged time signals of pinion shaft's transverse vibration velocity – location of synchronizing impulse corrected by means of the TDEB method: a) signal fragment from 15th to 75th sample, b) signal fragment from 405th to 465th sample

Fig. 5a presents the pinion shaft's vibration velocity signal averaged by the pinion's rotation period, obtained by applying a correction of the synchronizing impulse location. The arrow shows the local maximum coming from the damaged pinion tooth; also, the time intervals are marked, in which the overlapping time signals were presented before averaging – Fig. 2÷4.

Fig. 5b shows the pinion shaft's transverse vibration velocity signal averaged by the pinion's rotation period, where the location of synchronizing impulse was not corrected. When compared to the signal presented in Fig. 5, a reduction of the signal amplitude is visible.

In the spectra of those signals, as shown in Fig. 6, differences in the values of constituent amplitudes are also visible. The differences grow as the frequency increases.

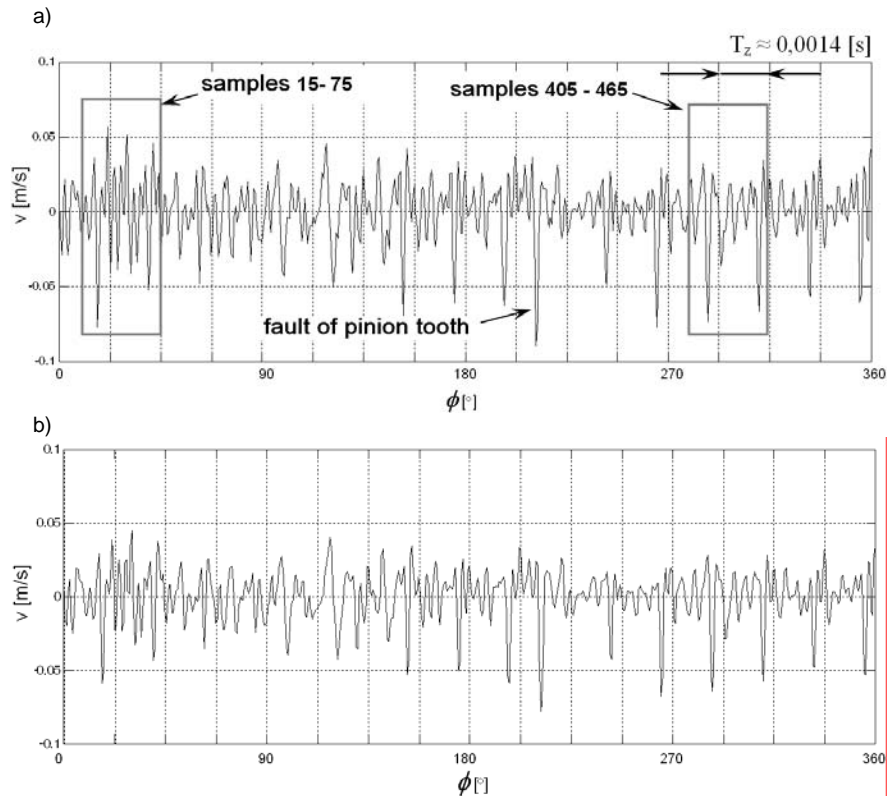


Fig. 5. Course of the pinion shaft's transverse vibration velocity averaged by the pinion's rotation period - chipping of pinion tooth to 3 mm, corresponding to $CR = 0.96$: a) the synchronizing impulse location was corrected, b) the synchronizing impulse location was not corrected

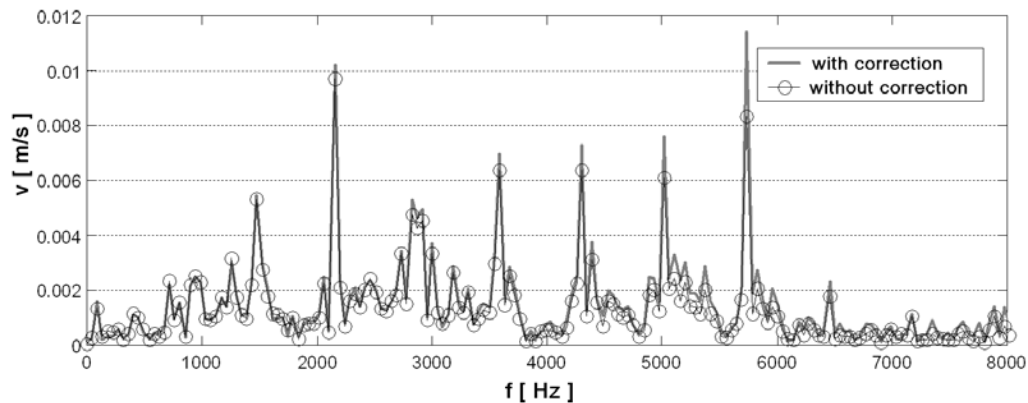


Fig. 6. Averaged signal spectrum before and after correction of the synchronizing impulse location

4. CONCLUSIONS

Based on the research conducted it can be concluded that:

- In the case of averaging the vibration signal when diagnosing toothed gears, it is purposeful to apply correlation of the synchronizing impulse location.
- The time-delay estimation using cross-bispectrum (TDEB) proved to be the best method to determine the correction of the synchronizing signal location for a toothed gear shaft's vibration velocity signal.

- It seems useful to apply this method for averaging the time signals when diagnosing other components of machinery and appliances.

REFERENCES

- [1] Adamczyk J., Krzyworzeka P., Łopacz H.: *Systemy synchronicznego przetwarzania sygnałów diagnostycznych*. Collegium Columbinum Kraków 1999 r.
- [2] Cempel Cz.: *Podstawy wibroakustycznej diagnostyki maszyn*. WNT Warszawa 1982 r.
- [3] Dąbrowski Z., Radkowski S., Wilk A.: *Dynamika przekładni zębatach*. Warszawa-Katowice-Radom 2000.

- [4] Krzyworzeka P.: *Synchroniczne wspomaganie odwzorowań diagnostycznych*. Uczelniane Wydawnictwa Naukowo-Dydaktyczne, Kraków 2001 r.
- [5] Krzyworzeka P.: *Synchronizm niezamierzony w maszynach*. Diagnostyka, Vol. 28, 2003, s. 37÷46 (in Polish).
- [6] Łazarz B., Wojnar G.: *Detection of early stages of pinion tooth chipping in transmission gear*. Machine Dynamics Problems 2003, Vol. 27.
- [7] Swami A., Mendel J. M., Nikias Ch. L.: *Higher-Order Spectral Analysis Toolbox*. Copyright by The Math Works, Inc, third printing 1998.
- [8] Wojnar G.: *Wykrywanie uszkodzeń kół zęba-tych wybranymi metodami przetwarzania sygnałów drganiowych*. Rozprawa doktorska, Politechnika Śląska 2004 r.
-



PhD. Eng. **Grzegorz WOJNAR** adjunct of The Silesian University of Technology. Scientific interest: modelling of dynamic processes, diagnostics of tooth gear, machine design and processing of vibroacoustic signals.



DSc. Eng. **Bogusław ŁAZARZ** professor of The Silesian University of Technology. Scientific interests: modeling of dynamic processes, diagnostics of tooth gear, machine design and processing of vibroacoustic signals. Member of Machines

Construction Committee.

RECOVERY OF IMPACT SIGNATURES IN DIESEL ENGINE USING WAVELET PACKET TRANSFORM (WPT)

Marek FLEKIEWICZ, Henryk MADEJ

Silesian University of Technology, Department of Automotive Vehicle Construction
marek.flekiewicz@polsl.pl; henryk.madej@polsl.pl

Summary

A fault diagnosis technique for internal combustion engines using time-scale representations of vibration signal is presented in this paper. Engine block vibration results as a sum of many excitations mainly connected with engine speed and their intensity increases with the appearance of a fault or in case of higher engine elements wearing. In this paper an application of acceleration signals for the estimation of the influence of piston skirt clearance on diesel engine block vibrations has been described. Engine body accelerations registered for three simulated cases representing piston skirt clearance variations were an object of preliminary analysis. The presented procedures were applied to vibration and pressure signals acquired for a 0.5 dm³ Ruggerini, air cooled diesel engine. Reciprocating machines are difficult to diagnose using traditional frequency domain techniques because of generate transient vibration. In conducted experiments WPT has been chosen as the decomposition tool for feature extraction as a tool providing a flexible time-frequency resolution and a rich library of redundant wavelet bases.

Keywords: fault diagnosis, engine vibration, WPT.

WYKRYWANIE WYMUSZEŃ IMPULSOWYCH W SILNIKU ZS ZA POMOCĄ PAKIETÓW FALKOWYCH (WPT)

Streszczenie

W artykule przedstawiono wyniki badań diagnostycznych silnika ZS za pomocą analizy czasowo-częstotliwościowej. Drgania bloku i głowicy badanego silnika są spowodowane wieloma wymuszeniami związanymi z jego prędkością obrotową a ich intensywność wzrasta wraz z pojawianiem się uszkodzeń mechanicznych, zużycia eksploatacyjnego oraz występowania anomalii w procesie spalania. Sygnały przyspieszeń drgań wykorzystano do określenia wpływu stanu symulowanego luzu w złożeniu tłok cylinder.

W ramach badań silnika ZS, chłodzonego powietrzem o pojemności 0,5 dm³ firmy Ruggerini zasymulowano trzy wartości luzu. Ze względu na fakt, że silniki spalinowe są złożonymi obiektami diagnozowania wykorzystanie tradycyjnych metod analizy częstotliwościowej nie zapewnia precyzyjnej identyfikacji charakterystycznych wymuszeń. W prowadzonych badaniach przeprowadzono dekompozycję sygnału drganiowego za pomocą pakietów falkowych (WPT).

Słowa kluczowe: diagnostyka uszkodzeń, silniki spalinowe, drgania, WPT.

1. INTRODUCTION

Identification of engine vibration sources is most important for making noise reduction strategies and engine diagnosis. An IC engine noise signal is composed of many components from different sources. To identify the requirement of noise signal analysis it is necessary to begin a discussion on the noise signal components. The combustion noise is produced by a rapid rate of in-cylinder pressure rise, which besides being a source of engine structural vibrations [3, 9, 17, 18]. The contribution of the combustion to the whole noise signal is some transient components. In a normal condition, the combustion noise is usually in a frequency range above a few 100 Hz as the combustion energy below

this range is mostly transformed into useful work by pushing pistons forward. In the case of abnormal conditions, degradation in the combustion quality may produce some low frequency content in the combustion noise. A rise in the cylinder pressure pushes the piston from the top dead center – TDC, advancing to the bottom dead center - BDC. In this movement, the clearance between the piston and the cylinder or damage to piston rings can cause the piston to impact with the cylinder, the phenomenon of piston slap, which is another major source of engine noises. As the piston slap is caused by both the combustion and the clearance, the noise level reflects the combustion quality and changes in the clearance. The impacts will add transient components to the engine noise signal [15, 17, 18,

19]. As piston slap happens on the way from the TDC to the BDC, it can be identified by referring to the time axis. An important feature of IC engines is that they have both reciprocating and rotating parts. Different type of parts will produce different signal components. Rotating parts, such as the flywheel and front pulley, can excite harmonic components to the noise.

Decided by the engine speed, these harmonic components mainly distribute in the low-frequency range. An increase in the amplitude of the harmonic components indicates condition variations of these rotating parts. Contributions of different rotating parts to the noise can be identified with reference to their speeds. Injectors and valves are reciprocating moving parts. They produce impacts to the engine structure and hence contribute transient components to the noise. In an injector, the needle is held onto its seat by a high rate spring. This spring also serves to control the injection pressure and regulate the injection time. A decrease in the stiffness of the spring will bring forward the injection time. As a consequence, the combustion quality will be degraded. An engine has many inlet valves and exhaust valves. A valve is opened by a camshaft and pushed back to its seat by a valve spring. Any problems with valve seats, tappets, and mechanisms can cause a change to the transient vibrations produced during opening and closing, and thus the corresponding transient components of the noise signal. These valves open and close at different times, and so the contribution of different valves to the noise can be identified from the times of events. Fluid-induced noise, such as exhaust and inlet noise, is also an important part of the noise. Along with the sudden release of gas into the exhaust system or the rush of a sharp pulse of fresh air into the cylinder, oscillation of the air volume in the cylinder and the exhaust system is excited and hence noise is produced. When inlet and exhaust valves close, noises will also be generated for a change in the fluid field. The fluid-induced noise contributes transient components to the whole noise. Some early research shows that fluid-induced noise usually has high frequencies. With modern fluid passage designs, the level of fluid-induced noise is normally very low. Damage or problems with the exhaust and inlet system will increase the magnitude of the fluid-induced noise.

A noise signal can be mathematically described as:

$$x(t) = \sum A_i \cos(\omega_i t + \varphi_i) + \sum \sum B_{ij}(t) u(t - t_j) \cos(\omega_j t + \varphi_j) \quad (1)$$

where:

- A_i and $B_{ij}(t)$ denote amplitude of signal component,
- ω_i and ω_j represent the frequency,
- $u(t)$ is the function step,
- t_j is the instant at which an event occurs,
- φ_i and φ_j are phases of signal components.

The sample of engine noise signal is presented on figure 1.

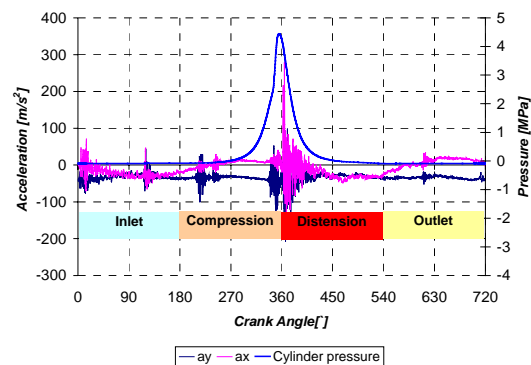


Fig. 1. Engine block vibration vs. crank angle for one cycle

2. SIGNAL PROCESSING PROCEDURE

2.1. Joint time frequency analysis

A basic requirement on a signal processing technique is that it should at least reveal information on the amplitude, the time, and the frequency content of an event. To satisfy the requirement, a signal processing technique should be two-dimensional, in the time-frequency domain [1, 6, 8, 11, 13, 14].

It is possible to get the information about main noise sources using JTFA (Joint time frequency analyses) based on few methods, i.e.:

- Gabor Spectrogram,
- Wigner Ville distribution,
- Choi-Williams distribution,
- Cone Shape distribution,
- Adaptative Spectrogram,
- STFT Spectrogram.

Each quadratic JTFA method has its own advantages and disadvantages. The STFT spectrogram is faster than all the other methods, but it has the worst joint time-frequency resolution. Based on the specific application a suitable JTFA method must be selected and a compromise must be chosen between the resolution, the cross-term interference and computation speed. Possibility to analyze a signal in the time-frequency domain simultaneously enables better process a particular signal. Especially this analysis allows observing how power spectrum of signal changes over time.

2.2. Wavelet decomposition of engine block vibration signals

The Wavelet Transform provides a more flexible way of time –frequency representation of a signal by allowing the use of variable sized windows. WT gives precise frequency information at low frequencies and precise time information at high frequencies. This makes the WT suitable for the analysis of irregular data pattern, such as impact signatures in IC engines. Wavelet function is

composed of a family of basis functions that are capable of describing signal in a localized time and frequency (or scale) domain. The Continuous Wavelet Transform of a time varying signal $x(t)$ consists of coefficient that are the convolution of the signal $x(t)$ with a family of wavelets $\{\psi_{a,b}\} \in L^2(R)$ with finite duration in time and finite frequency:

$$W_x(a, b) = \int_{-\infty}^{+\infty} x(t) \psi_{a,b}^*(t) dt \quad (2)$$

where:

$$\psi_{a,b}(t) = \frac{1}{\sqrt{|a|}} \psi\left(\frac{t-b}{a}\right), \quad a, b \in R, a \neq 0 \quad (3)$$

where the (*) symbol denotes complex conjugation. The continuous wavelet transform (2) depends on the choice of the wavelet function. CWT creates redundant information. A discrete set of translation and dilation parameters are often sufficient for most tasks. The wavelet packet transform (WPT) is an extension of the WT which provides a complete level by level decomposition of signal /fig. 2/ Wavelet packets consist of a set of linearly combined usual wavelet function [2, 5].

The wavelet packet is a function where integers indices i, j and k are the modulation, scale and translation parameters:

$$\psi_{j,k}^i(t) = 2^{j/2} \psi^i(2^j t - k) \quad (4)$$

The wavelet function can be obtained from the following recursive relationships:

$$\psi^{2j}(t) = \sqrt{2} \sum_{k=-\infty}^{\infty} h(k) \psi^i(2t - k) \quad (5)$$

$$\psi^{2j+1}(t) = \sqrt{2} \sum_{k=-\infty}^{\infty} g(k) \psi^i(2t - k) \quad (6)$$

The discrete filters $h(k)$ and $g(k)$ are the quadrature mirror filters associated with the scaling function and wavelet function. The WPT contains a complete decomposition at every level and hence can achieve a higher resolution in the high frequency bands The recursive relations between the j th and the $(j+1)$ th level components are following:

$$x_j^i(t) = x_{j+1}^{2i-1}(t) + x_{j+1}^{2i}(t) \quad (7)$$

$$x_{j+1}^{2i-1}(t) = Hx_j^i(t) \quad (8)$$

$$x_{j+1}^{2i}(t) = Gx_j^i(t) \quad (9)$$

where: H and G are the filtering decimation operators related to the discrete filters $h(k)$ and $g(k)$.

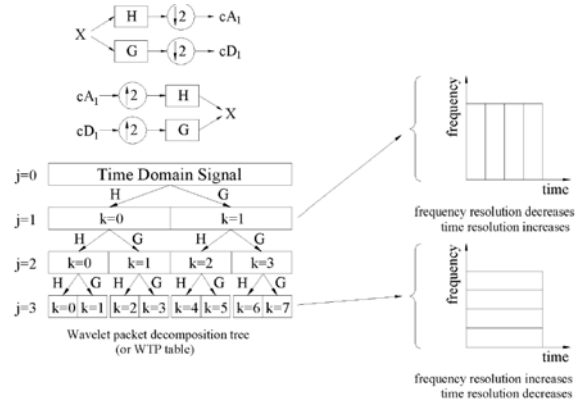


Fig. 2. Decomposition tree of time varying signal using wavelet packet transform

The basis step of a fast wavelet algorithm is presented in fig. 2 which can be implemented in two opposite directions, decomposition and reconstruction. In the decomposition step, the discrete signal x is convolved with a low-pass filter H and a high-pass filter G , resulting in two vectors cA_1 and cD_1 . The elements of the vector cA_1 are called approximation coefficients, and the elements of vector cD_1 are called detailed coefficients. The symbol $\downarrow 2$ denotes down sampling.

3. EXPERIMENTAL SETUP

The experimental setup developed consisted of one cylinder, The procedures presented in this paper were applied to vibration and pressure signals from an 0,5 dm³ Ruggerini, air cooled diesel engine (Fig. 3). Technical details describing the test object are listed in the table 1.

Table 1
 Technical features of the engine

Parameters	Manufacturer data
Displacement [cm ³]	477
Stroke [mm]	75
Bore [mm]	90
Maximum power [kW]	6,0
rpm for max power [min ⁻¹]	3000
Max torque [Nm]	21
rpm for max torque [min ⁻¹]	2500

Test program provided sampling of the following data:

- in-cylinder pressure,
- vibration signal of engine head and wall, for two directions: x and y (Fig. 3),
- crankshaft revolution, together with TDC recognition,
- engine torque,
- manifold pressure.

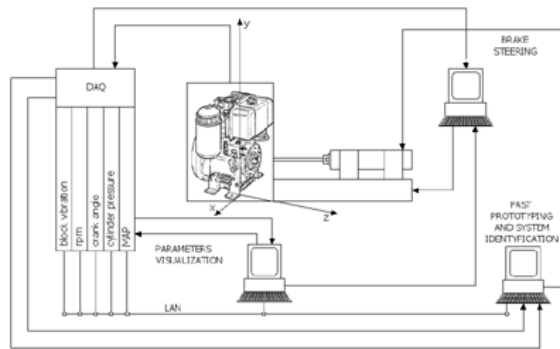


Fig. 3. Schematic diagram of experimental setup

In-cylinder pressure was measured with the use of piezoelectric pressure transducer type 6121 by KISTLER, coupled with charge amplifier model 5011. Crankshaft position and TDC recognition was done with the use of KISTLER 2613B transducer. Engine body vibrations were measured with ICP sensors by PCB interfacing with PA3000 signal conditioner manufactured by Roga Instruments.

Acceleration transducers were installed on engine body and engine head using thread connections. Signals were acquired with the use of eight channel data acquisition card NI PCI-6143, running under LabView 7.1 environment, where a dedicated program has been implemented. Sampling rate for all channels was set up to 50 kHz.

Research program was realized for engine running on idle, at higher rpm of 1500 min^{-1} without load and for rpm range from $1000 - 1500 \text{ min}^{-1}$ with load not exceeding 10 Nm. Tests were carried on for three different setups of engine piston skirt clearances: nominal, 2 times bigger than nominal, 4 times bigger in respect to the nominal. For the purposes of simulation tests, at the selected clearance values the compression pressure was left at the same level. An example of in-cylinder pressure, and vibration signal traces is presented on figures 1 In-cylinder pressure and engine body vibration signals were registered for 18 engine operation points, each covering 150 engine cycles.

4. ANALYSIS RESULTS

Figures 4, 5, 6 present engine body acceleration traces and its time-frequency representation for three different simulated clearance values. Trace obtained for nominal clearance are presented on figure 4, meanwhile figure 5 presents results for 2 times bigger clearance and figure 6 for the 4 times bigger clearance. With the increase of clearance, an important raise of vibration signal level together with trace properties variations and increased engine body response time for excitation are observed. Changes in signal traces due to bigger clearance may also be noticed in time frequency plane. The distribution of vibration energy with scale is different for the normal clearance and 2xN and 4x N.

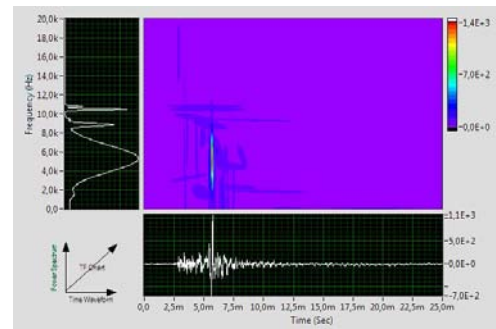


Fig. 4. Time-frequency representation of engine acceleration for nominal skirt piston clearance

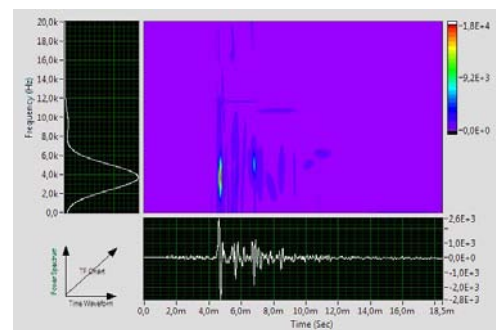


Fig. 5. Time-frequency representation of engine head acceleration for 2 times bigger skirt piston clearance

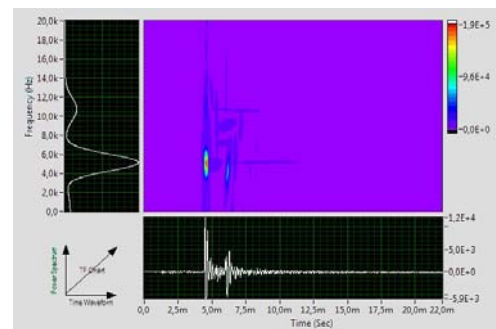


Fig. 6. Time-frequency representation of engine acceleration for 4 times bigger skirt piston clearance

Figures 7, 8 and 9 present results of vibration signal analysis using wavelet packet decomposition. The acceleration signal was decomposed into 4 levels for each transform. With the signal being decomposed into a number of sub-bands, features can be extracted from the wavelet packet coefficient in each sub-bands to provide information on the condition of IC engine being monitored. The energy content of acceleration signal can be calculated, based on the coefficient of the signals transform. Since the energy content of signal after decomposition /fig. 7, 8, 9/ is directly related to the simulated clearance it can be used as an effective indicator of the IC engine condition.

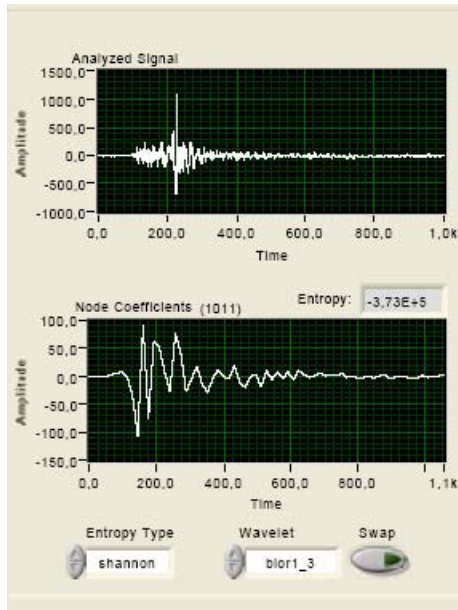


Fig. 7. WPT result of engine acceleration by nominal clearance for crankshaft angle range 372 – 420°

Figures 7, 8 and 9 present results of vibration signal analysis using wavelet packet decomposition. The acceleration signal was decomposed into 4 levels for each transform. With the signal being decomposed into a number of sub-bands, features can be extracted from the wavelet packet coefficient in each sub-bands to provide information on the condition of IC engine being monitored. The energy content of acceleration signal can be calculated, based on the coefficient of the signals transform.

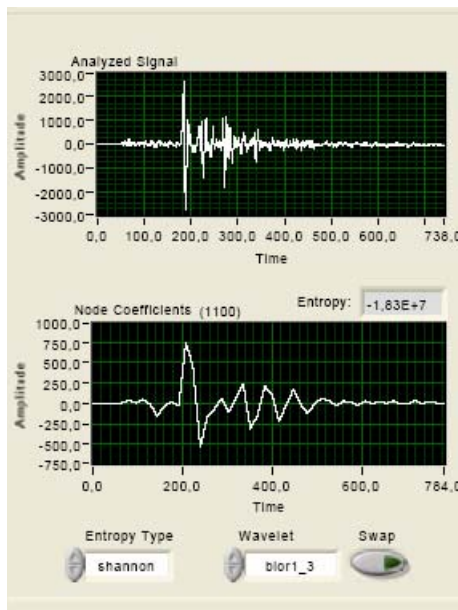


Fig. 8. WPT result of engine acceleration by 2 times bigger clearance for crankshaft angle range 372 – 420°

Since the energy content of signal after decomposition /fig. 7, 8, 9/ is directly related to the simulated clearance it can be used as an effective indicator of the IC engine condition.

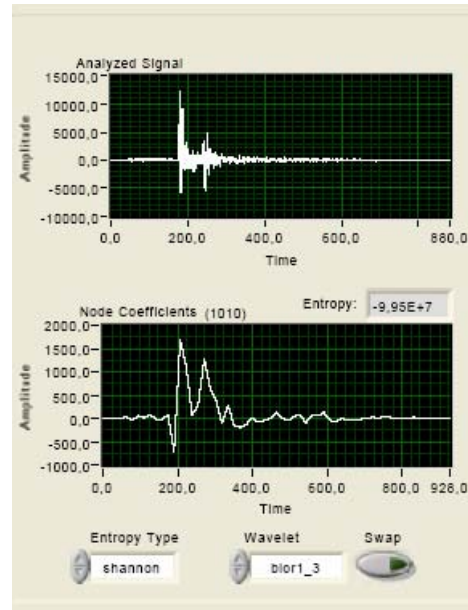


Fig. 9. WPT result of engine acceleration by 4 times bigger clearance for crankshaft angle range 372 – 420°

5. CONCLUSION

The WPT is powerful tool for on-line monitoring and diagnostic of combustion process. The WPT decomposes a vibration signal into different components in different time windows and frequency bands.

It can recover important features of the vibration signal that are sensitive to the change of IC engine condition.

By using the WPT, accurate and reliable on-line monitoring decisions can be made.

LITERATURA

- [1] Batko W., Ziółko M.: *Zastosowanie teorii falek w diagnostyce technicznej*. Problemy Inżynierii Mechanicznej i Robotyki. Monografia nr 7. WIMiR, AGH, Kraków 2002.
- [2] Białasiewicz J.: *Falki i aproksymacje*. WNT, Warszawa 2000.
- [3] Flekiewicz M., Madej H.: *Influence of combustion noise on engine block vibration in IC engine fueled by LPG*. VAFSEP 2006 DCU Dublin.
- [4] Flekiewicz M., Madej H., Wojnar G.: *Dekompozycja sygnału przyspieszeń drgań korpusu silnika ZI*. XII Konferencja Naukowa Wibrotechniki i Wibroakustyki WIBROTECH. Kraków 2006.

- [5] Zieliński T. P.: *Od teorii do cyfrowego przetwarzania sygnałów*. WEAIiE, AGH, Kraków 2002.
- [6] Zhang S., Mathew J., Ma L., Sun Y.: *Best basis-based intelligent machine fault diagnosis*. Mechanical Systems and Signal Processing. 19 (2005), p. 357-370.
- [7] Gelle G., Colas M., Serviere C.: *Blind separation: a tool for rotating machine monitoring by vibration analysis*. J. Sound and Vibration 2001; 248: 865-885.
- [8] Shibata K., Takahashi A., Shirai T.: *Fault diagnosis of rotating machinery through visualization sound signals*. Mech. Syst. Signal Process 2000. 14: 229-241.
- [9] Geng Z., Chen J., Hull B.: *Analysis of engine vibration and design o fan applicable diagnostic approach*. Int. J. Mech. Sci. 2003: 1391-1410.
- [10] Wang W. Q. Ismail F. Golnarghi F.: *Assessment of gear damage monitoring techniques using vibration measurements*. Mech. Sys. Signal Process. 2003. 15(5): 905-1022.
- [11] Zheng H., Li Z., Chen X.: *Gear fault diagnosis based on continuous wavelet transform*. Mech. Syst. Signal Process. 2002, 16; 447-557.
- [12] Bai M. R., Jeng J., Chen C.: *Adaptative order tracking technique using recursive last-square algorithm*. Trans. ASME J. Sound Vibr. 2004. 124: 502-511.
- [13] Tse P. W., Yang W. X., Tan H. Y.: *Machine fault diagnosis trough an effective exact wavelet analysis*. J. Sound Vib. 2004, 227; 1005-1024.
- [14] Lin J., Qu L.: *Feature extraction based on Morlet wavelet and its application for mechanical fault diagnosis*. J. Sound Vib. 2000, 234(1); 135-148.
- [15] Jang S., Cho J.: *Effect of skirt profiles on the piston secondary movements by the lubrication behaviors*. Int. Journal Aut. Technology. 2004, Vol 5; 23-31.
- [16] Antoni J., Daniere J., Guillet F.: *Effective vibration analysis of IC engines using cyclostationarity*. Part I – A methodology for condition monitoring. Journal of Sound and Vibration, 257(5), pp. 815-837, 2002
- [17] Geng Z., Chen J.: *Investigation into piston-slap-induced vibration for engine condition simulation and monitoring*. Journal of Sound and Vibration, 282, pp. 731-751, 2004.
- [18] Zheng H., Liu G. R., Tao J. S., Lam K. Y.: *FEM/BEM analysis of diesel piston slap induced ship hull vibration and underwater noise*. Applied Acoustics, vol.62, pp. 341-358, 2001.
- [19] Inagaki M., Kawamoto T., Yamamoto K.: *Prediction of structural and kinematics coupled vibration on Internal Combustion engine*. R&D Review of Toyota CRDL, Vol 37, No. 2.



Marek FLEKIEWICZ, Ph.D. Eng. is an assistant professor at the Department of Automotive Vehicle Construction Silesian University of Technology in Katowice. His research interest include vehicle dynamics and diagnostics.

He also deals with application of alternative fuels for internal combustion engines and alternative powertrains. Member of SAE International.



Henryk MADEJ, Ph.D., D.Sc. Eng. work as a professor in the Department of Automotive Vehicle Construction Silesian University of Technology in Katowice. He deals with IC engines and powertrains diagnostics with the application of

vibroacustical signal analysis, also with minimization of machine vibroactivity. Autor over 140 publication including 6 monographies. Member of Polish Society of Technical Diagnostics.

SYNCHRONIZATION SYSTEM OF THE HYDRAULIC CYLINDERS MOTION IN THE RESEARCH OF THE BRIDGE PRESTRESSING SYSTEMS

Dariusz GRZYBEK, Andrzej JURKIEWICZ, Piotr MICEK, Marcin APOSTOL

AGH University of Science and Technology
Department of Process Control
Al. Mickiewicza 30, 30-059 Kraków
dariusz.grzybek@agh.edu.pl

Summary

The safety of the peoples using with the bridges which are made in the prestressing concrete technology, is dependent on the quality of the elements of the applying prestressing system. Thus the research of the bridge prestressing system, particularly static research, are conducted in the conditions which simulate the real loads affecting on the each elements. Such defined conditions of the conducting of the prestressing systems research need the building of the adequate research stand. The article presents the system conception of the hydraulic cylinders motion synchronization, which will be used in the prestressing systems research. The mathematical model was presented also with the results of the simulation researches.

Keywords: prestressing concrete, static research, synchronization of motion.

UKŁAD SYNCHRONIZACJI RUCHU SIŁOWNIKÓW HYDRAULICZNYCH W BADANIACH MOSTOWYCH USTROJÓW SPRĘŻAJĄCYCH

Streszczenie

Bezpieczeństwo ludzi korzystających z mostów wykonanych w technologii betonów sprężonych zależy w bardzo dużym stopniu od jakości elementów zastosowanego ustroju sprężającego. Stąd badania mostowych ustrojów sprężających, a w szczególności badania statyczne są przeprowadzane w warunkach, które symulują rzeczywiste obciążenia działające na poszczególne elementy. Jednak tak zdefiniowane warunki przeprowadzania badań ustrojów sprężających wymagają budowy odpowiedniego stanowiska badawczego. Artykuł prezentuje koncepcję układu synchronizacji ruchu siłowników hydraulicznych, który to układ zostanie wykorzystany w badaniach ustrojów sprężających. Przedstawiono również model matematyczny układu wraz z wynikami badań symulacyjnych.

Słowa kluczowe: betony sprężane, badania statyczne, synchronizacja ruchu.

1. INTRODUCTION

The safety of the peoples using with the bridges which are made in the prestressing concrete technology, is dependent on the quality of the elements of the applying prestressing system. Thus the research of the bridge prestressing system, particularly static research, are conducted in the conditions which simulate the real loads affecting on the each elements. The ETAG 013 norm defines the conditions, in which the research have to be conducted. The research procedure contains following stages:

- tension of the strings is realized by the stressing devices which are used in the building of the prestressing structure. The force of tension should be increased with the constant speed of 100 MPa per minute,
- transfer of the tension force from the stressing devices to body of laboratory stand after reach

the level of 80 % of the characteristic strength of the strings by the tension force,

- the tension force is kept at the level of 80 % of the characteristic strength during 1 hour,
- the increasing of tension force with the maximal speed of the strain increase of 0,002 per minute until the failure of the one or more strings¹.

Such defined conditions of the conducting of the prestressing systems research require the building of the adequate research stand. Taking into consideration that the characteristic strength of the strings applying in the prestressing bridge building amount to 279 kN, the value of the necessary force increase with the increase of the strings number in the anchoring block. The obtainment of such force value is possibility by the using of hydraulic

¹ ETAG 013 Guideline for European Technical Approval of Post-tensioning Kits for Prestressing of Structure, June 2002

cylinders system. The cylinders motion synchronization in such system is difficulty by the randomness of the hydraulic cylinders load resulting among other from slip in the jaws.

2. LABORATORY STAND FOR THE PRE- AND POST-TENSIONED RESEARCH

2.1. The building of laboratory stand

The laboratory stand to the static research consists of three following main parts: body, movable disc and four cylinders system (fig. 1).

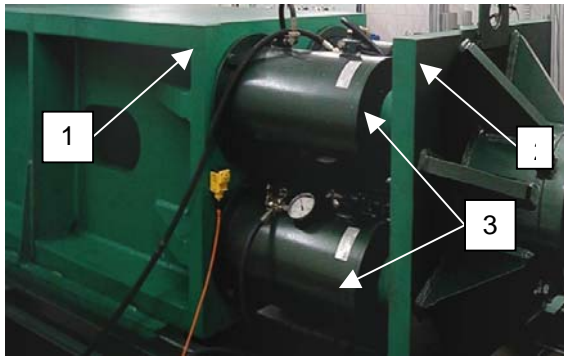


Fig. 1. View of the laboratory stand:
1-body of the stand, 2-movable disc, 3- four cylinders system

The system of four cylinders has the following tasks:

- load increase of the movable disc with the maximal speed of displacement increment of 0,002 per minute until one or more string scarifying,
- load decrease of the movable disc after 1 or more string scarifying (the rest of strings still carry the load).

2.2. The characteristics of the synchronization process

The general characteristics are following:

- maximal speed of the cylinders motion approximates 0,000641 [m/s],
- external forces $P_1(t), \dots, P_4(t)$ (fig. 2) are randomly changeable,
- range of the value changes of external forces approximates from 0 to 2162 [kN].

The maximal speed results from the ETAG 013 requirements according to which the maximal speed of the displacements increase in the stretched strings can't be bigger than 0,002 per minute. It results from the length of the tensioned strings which amount to 6 m for described laboratory. The load of the movable disc depends from the researched anchored block (fig. 3).

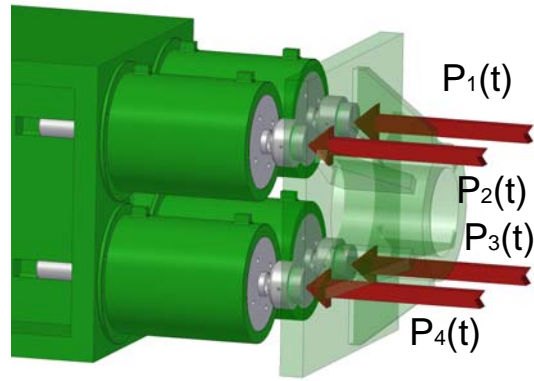


Fig. 2. Force distribution on the cylinder piston

Thus, the number of the strings can range from 1 to 32 and needed force also increases (tab. 1).

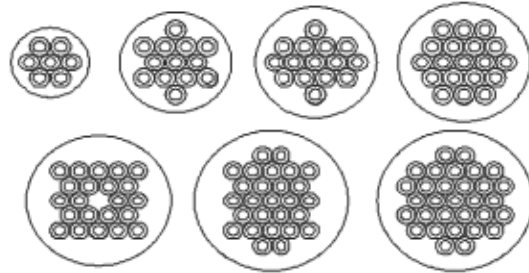


Fig. 3. Kinds of the anchored blocks

Table. 1. The needed forces values

Number of the strings	7	12	13	15	19	31
The force value[kN]	1953	3348	3627	4185	5301	8649

The values of the external forces $P_1(t), \dots, P_4(t)$ change from the point of view of occurrence of the following phenomena:

- slides of the strings in the jaws,
- displacements of the jaw in anchored block (fig. 4),
- friction between the movable disc and body of the laboratory stand.

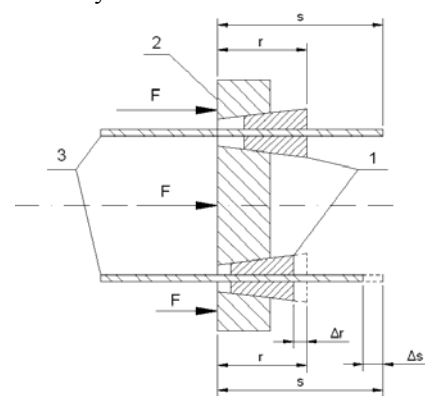


Fig. 4. Asymmetry of displacements of the jaw in the anchored block: 1-jaws, 2- anchored block, 3 – strings

2.3. Hydraulic structure of the synchronization system

The hydraulic structure of the synchronization system (fig. 6) was based of the basic hydraulic elements like throttle valves. The achievement of the required accuracy of synchronization will be realized by adequate control algorithm.

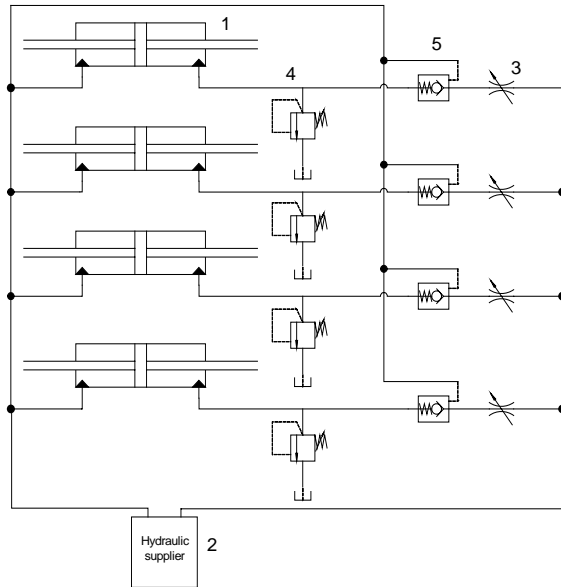


Fig. 5. Hydraulic structure of the synchronization system

Fig. 5 presents the hydraulic structure of the cylinders motion synchronization system. The system consists of the four hydraulic cylinder (1), control hydraulic supplier (2), four throttle valves (3) which are controllable by the corresponding stepping motors, four relief valves (4), four hydraulic locks (5). The presented system work in the open-loop of control. This way of control doesn't enable to eliminate the displacement cylinders differences which are caused by the compressibility of the working fluid with the high external load changes. Obviously, the hydraulic structure could be other by the application other hydraulic elements such as a flow synchronizer. The view of this system is presented in fig. 6.



Fig. 6. The view of synchronization system

3. MATHEMATICAL MODELLING OF THE SYNCHRONIZATION SYSTEM

3.1. The basic assumptions of the system work

The main assumption, apart from the elimination of the synchronization mistakes, is the minimization of the energy losses in this system. It can be achieved by the minimization of the energy losses in the maximal valve. Thus, the following condition must be granted:

$$p_1(t) < p_{max}(t) \quad (1)$$

where: $p_1(t)$ - the pressure in the common input lines (fig. 7)

$p_{max}(t)$ - the pressure set in maximal valve

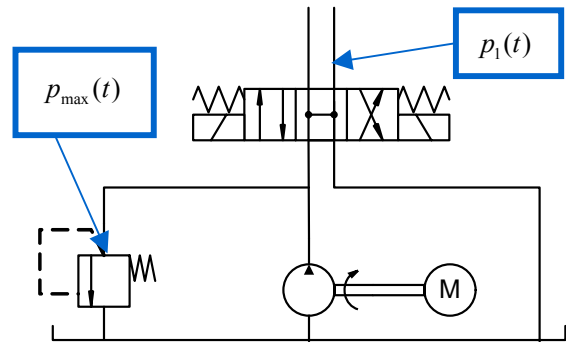


Fig. 7. Structure of the hydraulic supplier

However, the fulfilment of condition (1) leads to the multivariable structures of control system (fig. 8) and generates difficulties with the choice of leading cylinders.

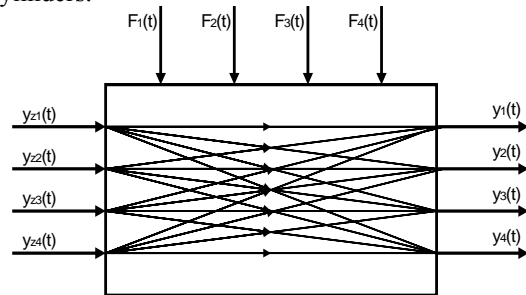


Fig. 8. Signal flow in the control system
 $y_i(t)$ - displacement of the piston of cylinder,
 $y_{zi}(t)$ - displacement of the moving pin of throttle valve,
 $F_i(t)$ - unknown external load

3.2. The basic assumptions to the mathematical modelling

The basic assumption to the building of the mathematical model:

- parameters of the elements are concentrated;
- surfaces and masses of every pistons and pin of throttle valve are identical;
- there is laminar flow in all the local elements;
- there is turbulent flow in all the linear elements;
- fluid temperature is constant;
- stream of fluid is continuous;

- connecting conduits are short and rigid (pressure losses in this conduits are negligible);
- dry friction doesn't occur in the surfaces of the carry-out elements.

3.3. The mathematical model

The calculated schema is presented in fig. 9.

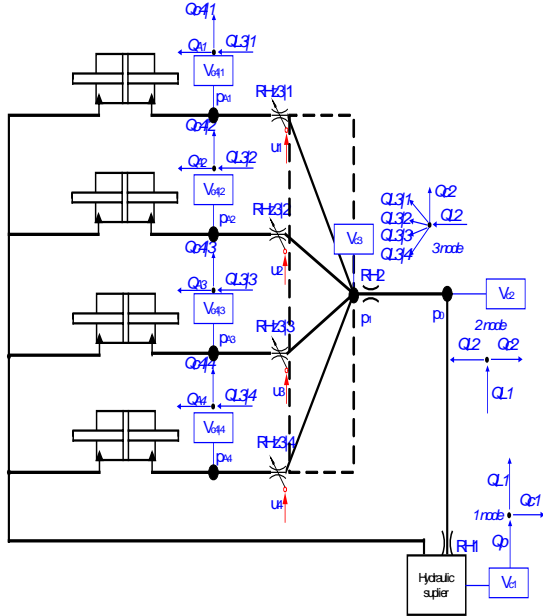


Fig. 9. The calculated schema of four hydraulic cylinder synchronization system

The basic equations are following:

$$\frac{d^2 y_i(t)}{dt^2} = \frac{1}{m_{zs}} [A p_{Ai}(t) - F_i(t) - F_{ii} \left(\frac{dy_i(t)}{dt} \right) + -k_{sc} ((\text{sgn}(y_i(t) + l_c) + 1)(y_i(t) + l_c) + (\text{sgn}(y_i(t)) + 1)y_i(t))] \quad (2)$$

$$\frac{dp_{Ai}(t)}{dt} = \frac{E_c}{V_0 + A y_i(t)} \left[Q_{Ai}(t) - A \frac{dy_i(t)}{dt} - k_p p_{Ai}(t) \right] \quad (3)$$

$$\frac{d^2 y_{zi}(t)}{dt^2} = \frac{1}{m_z} \left(k_u u_i(t) - f_{iz} \frac{dy_{zi}(t)}{dt} - \frac{\rho}{m d} \cos \varepsilon Q_{zi}^2(t) y_{zi}(t) \right) \quad (4)$$

$$\frac{dQ_{Ai}(t)}{dt} = \frac{A_{pi}}{\rho l_{pi}} [p_1(t) - p_{Ai}(t) - (0.5 \lambda_i \frac{l_{ii} \rho}{2 d_{ii} A_{ii}^2} + 0.5 \lambda_i \frac{l_{Ai} \rho}{2 d_{Ai} A_{Ai}^2} + \frac{\rho}{2 C_d^2 f_{di} (y_{zi})^2} + \frac{\rho}{2 C_d^2 A_{sh}^2}) Q_{Ai}(t)^2] \quad (5)$$

$$\frac{dp_1(t)}{dt} = \frac{E}{V_1} (Q_p - Q_{A1}(t) - Q_{A2}(t) - Q_{A3}(t) - Q_{A4}(t) - Q_{An}(t)) \quad (6)$$

where:

$$F_{ii} \left(\frac{dy_i(t)}{dt} \right) = f_i \frac{dy_i(t)}{dt} - F_{ik} \text{sgn} \left(\frac{dy_i(t)}{dt} \right) - F_{iv} \exp \left(- \frac{dy_i(t)}{v_k} \right) \frac{dy_i(t)}{dt} \text{sgn} \left(\frac{dy_i(t)}{dt} \right)$$

$$f_{di}(y_{zi}) = \text{tg} \frac{\alpha}{2} (y_{z0} + y_{zi}(t))^2$$

$y_i(t)$ – displacement of the piston of cylinder, $p_{Ai}(t)$ – pressure in the A chamber of cylinder, $F_i(t)$ – unknown external load $F_{ii} \left(\frac{dy_{zi}(t)}{dt} \right)$ - friction force

$Q_{Ai}(t)$ – flow between throttle valves and A chamber of cylinder $y_{zi}(t)$ – displacement of the moving pin of throttle valve, $p_1(t)$ – the pressure in the common input branch, $u_i(t)$ – the control signal from the

stepping motor, m_{zs} – reduced mass of the cylinder, A – surface of pistons, k_{sc} – coefficient of the elasticity of cylinder, E_c – modulus of elasticity of the fluid, V_0 – initial volume of the cylinder chamber k_p – coefficient of the leaks, k_u – coefficient of the stepping motor, f_{iz} – coefficient of viscous friction in the throttle valves, ρ – density of the fluid, A_{pi} – surface of the conduits, l_{pi} – length of the conduits, m_z – reduced mass of the moving pin of throttle valve, C_d – coefficient of the flow through the throttle valve, α – the angle which depends on the construction of throttle valve, Q_p – flow from the supplier.

The schema of the signal flow is presented in fig. 10.

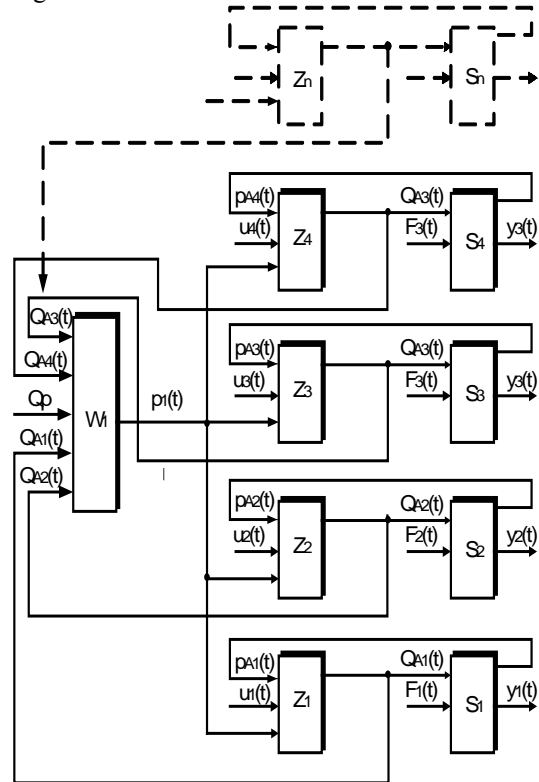


Fig. 10. The schema of the signal flow
W₁ – input conduit, Z_i – throttle valves,
S_i – cylinders

Presented over mathematical model of four hydraulic cylinders can describe in states space:

$$\begin{bmatrix} \dot{x}_{1n} \\ \vdots \\ \dot{x}_{2n} \\ \vdots \\ \dot{x}_{3n} \\ \vdots \\ \dot{x}_{4n} \end{bmatrix} + \begin{bmatrix} A_1 & A_s & A_s & A_s \\ A_s & A_2 & A_s & A_s \\ A_s & A_s & A_3 & A_s \\ A_s & A_s & A_s & A_4 \end{bmatrix} \begin{bmatrix} x_1 \\ x_2 \\ x_3 \\ x_4 \end{bmatrix} + \begin{bmatrix} B_1 & 0 & 0 & 0 \\ 0 & B_2 & 0 & 0 \\ 0 & 0 & B_3 & 0 \\ 0 & 0 & 0 & B_4 \end{bmatrix} \begin{bmatrix} u_1 \\ u_2 \\ u_3 \\ u_4 \end{bmatrix}$$

where: A_i – state matrix for each throttle valve-cylinder systems;

B_i – control matrix for each throttle valve-cylinder systems;

A_s – feedback matrix between throttle valve-cylinder systems.

3.4. The simulation experiment

Presented mathematical model was implemented to the Matlab Simulink program. Simulation diagram for equations is shown in figure 11.

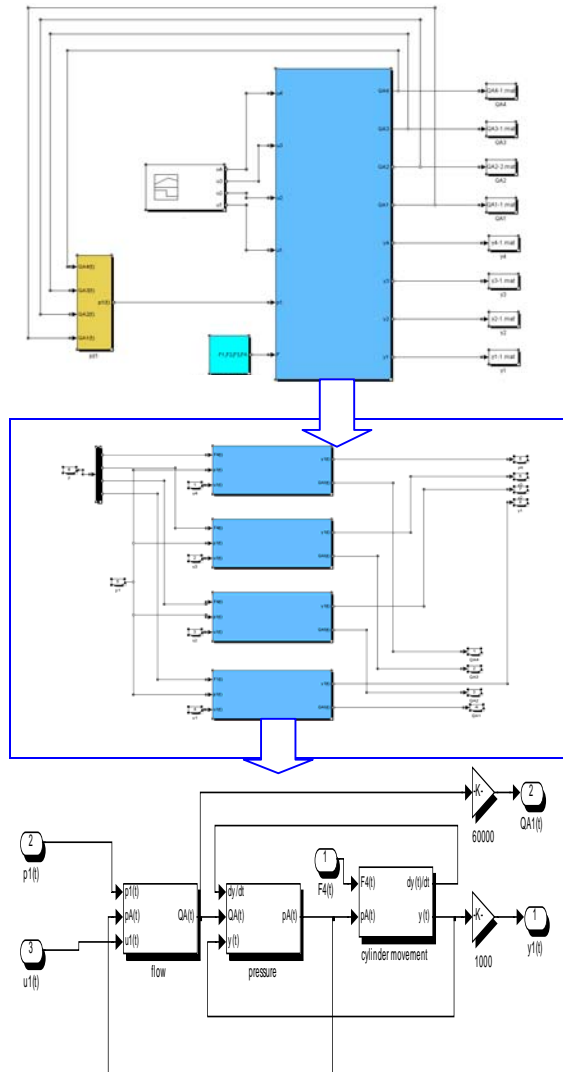


Fig. 11. Simulation diagram for synchronization system

Simulations was conducted for the parameters, which are presented in tab 2. The value of parameters was determined according to the construction conditions of the laboratory stand.

Table 2. The value of parameters

Q_z	A	E_C	k_p	m_{zs}
m^3/s	m^2	MPa	m^2/Ns	kg
$6,6 \cdot 10^{-5}$	0,065	$1,4 \cdot 10^3$	10^{-12}	10
V_0	f_{Tz}	C_d	k_{sc}	A_{pj}
m^3	Ns/m	-	N/m	m^2
$2 \cdot 10^{-5}$	300	0,6	$1 \cdot 10^{10}$	$3,1 \cdot 10^{-6}$

In the simulation model, a change of the external load acting one 1 cylinder was established in order to determination of the effect among particular throttle valve - cylinder system. The course of basic characteristics are presented in fig. 12.

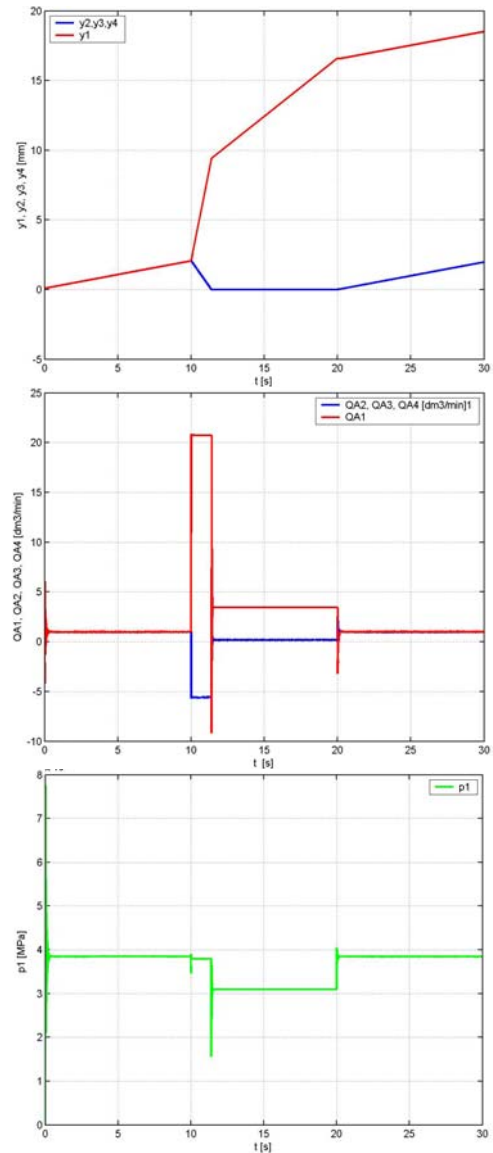


Fig. 12. Characteristics for the change of the force effecting on 1 cylinder

In the second simulation test, the change of the setting of throttle valve was established in order to definition of the interactions among particular control signal $u_1(t)$. The course of basic characteristics are presented in fig. 13.

Taking into consideration that the pressure in the input conduit is changeable, the change of external load acting on 1 cylinder have the effect on the motion of other cylinders. Hence, the application of control system based a super-ordinated cylinder, which the piston displacement is a input signal for other cylinders is only possible in the situation when the super-ordinated cylinder is the most loaded. However, the cylinder load s changeable, hence super-ordinated cylinder will have to be change.

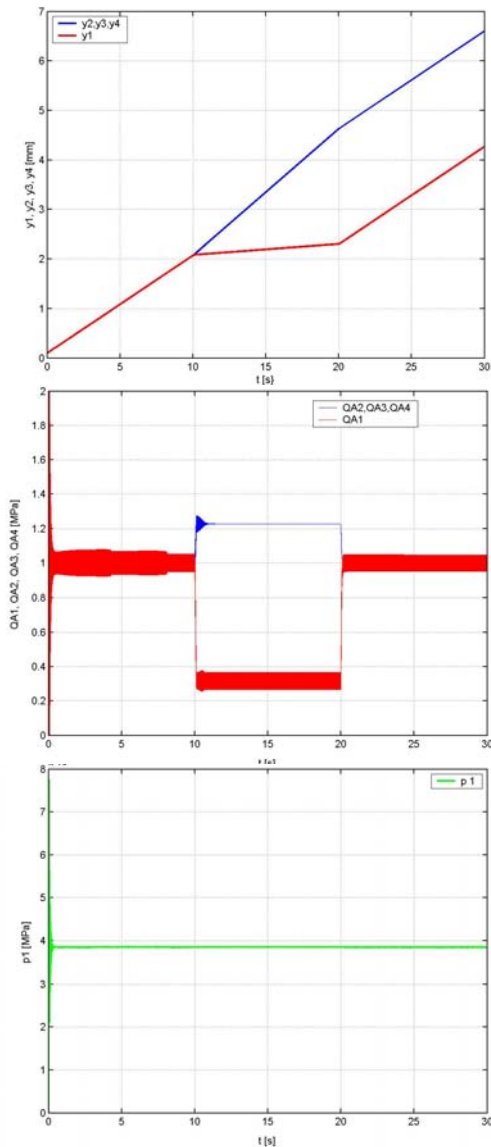


Fig. 13. Characteristics for the change of the throttling surface in 1 throttle valve

4. CONCLUSIONS

1. The research requirements resulted from adequate norms demand the using of the big forces, which are possible to get by the application of the set consisting of several cylinders.
2. The long-tasking of the research causes the large energy losses, which can be decreased by the using of the system with changeable value of the input pressure.
3. The application of such system causes the necessity of elaboration of the control system algorithm because the system with super-ordinated cylinder can be used.

REFERENCES

- [1] Grzybek D.: *Mathematical modeling of electrohydraulic system of four hydraulic cylinders velocity control*. ICCC. Ostrava 2006, pp. 157-160.
- [2] Jurkiewicz A., Grzybek D., Micek P.: *Control system of string scarifying at the research stand of prestressing structure*. ICCC. Ostrava 2006, pp. 217-220.
- [3] Jurkiewicz A.: *Laboratory stand for asim type anchor blocks research for prestressed post-tensioned concrete technolgy, legal with eurocodes and euronorm*. International Carpathian Control Conference ICCC'2001, Krynica 22-25.05.2001, s.519-524.
- [4] Dindorf R.: *Modelowanie i symulacja nieliniowych elementów i układów regulacji napędów płynowych*. Wydawnictwo Politechniki Świętokrzyskiej. Kielce 2004.

SAFETY ASSURANCE AT THE DESIGN STAGE OF THE NEW PUMP ON THE BASIS OF EU DIRECTIVES

Andrzej JURKIEWICZ, Piotr MICEK, Marcin APOSTOŁ, Dariusz GRZYBEK

Department of Process Control, University of Science and Technology
Kraków, Poland, tel/fax: 0048 12 617 30 80, e-mail: jurkand@agh.edu.pl

Summary

The creation of the new construction solution of the device is a complicated process, in which the correct choice of the device conception has the main meaning. The chosen conception should fulfil the customer requirements as well as the obligatory law requirements on the market, on which the designed device will be admitted to the trade. These requirements began to apply in Poland, which are on the EU market, when Poland became the EU member. This article presents the effect of this requirements with particular attention on the effect of the safety principles on the new device creation process. This effect was shown on the example of the new construction solution of the pump. The concurrent design process was applied in this process, which allowed the time shortening of the project conduct. The creation of the solid models of the elements and components and the simulation research were conducted in the same time. It allowed the correction of the geometrical parameters as well as straight parameters of the created models. The conducted simulation research static, kinematical and dynamic pairs allow the approximation of the modeled phenomena with the particular meaning for the device reliability. This is important for the assurance of the device durability, the long time of operating as well as the fulfilment of the high safety requirements.

Keywords: safety, design, pump.

ZAPEWNIENIE BEZPIECZEŃSTWA NA ETAPIE PROJEKTOWANIA NOWEJ POMPY W OPARCIU O DYREKTYWY UE

Streszczenie

Tworzenie nowego rozwiązania konstrukcyjnego urządzenia jest złożonym procesem, w którym istotną rolę odgrywa prawidłowy wybór koncepcji urządzenia. Wybrana koncepcja powinna spełniać zarówno wymagania zamawiającego jak również wymagania prawne obowiązujące na rynku, na którym projektowane urządzenie ma być dopuszczone do obrotu handlowego.

W związku z wejściem Polski do Unii Europejskiej, w Polsce zaczęły obowiązywać wymagania istniejące na rynku UE. W artykule przedstawiono wpływ tych wymagań ze szczególnym uwzględnieniem zasad bezpieczeństwa na proces tworzenia nowego urządzenia na przykładzie projektowanego, nowego rozwiązania konstrukcyjnego pompy. W procesie tym zastosowano system projektowania współbieżnego co pozwoliło przede wszystkim na znaczne skrócenie czasu trwania projektu. Równorzędnie z tworzeniem modeli bryłowych części i zespołów prowadzone były badania symulacje co umożliwiło na bieżąco korygowanie parametrów geometrycznych jak również wytrzymałościowych tworzonych modeli. Przeprowadzone badania symulacyjne par statycznych, kinematycznych i dynamicznych pozwoliły na przybliżenie modelowanych zjawisk o szczególnym znaczeniu dla niezawodności urządzenia do zjawisk rzeczywistych. Jest to ważne ze względu na zapewnienie trwałości urządzenia, długiego czasu bezawaryjnej eksploatacji oraz spełnienia wysokich wymagań bezpieczeństwa.

Słowa kluczowe: bezpieczeństwo, projektowanie, pompa.

1. INTRODUCTION

Creating a new construction solution of a device is a complex process, in which the correct choice of the device concept plays a significant role. The chosen concept should meet both requirements of

the party ordering the device as well as the legal requirements in force in the market where the designed device is to be admitted to trading and use. When Poland joined the European Union, the requirements existing in the EU market started becoming effective in Poland. The paper presents

the effect of these requirements on the process of creating a new device, with the example of the designed, new construction solution of the pump.

2. EU DIRECTIVES IN THE NEW PUMP CREATION PROCESS

The determination of directives, which the requirements have to be fulfilled, is the duty of a producer. The following directives are obliged in the pump creation:

- directive 98/37/EC of the European Parliament and of the Council of 22 June 1998 on the approximation of the laws of the Member States relating to machinery;
- directive 94/9/EC of the European Parliament and the Council;
- of 23 March 1994 on the approximation of the laws of the Member States concerning equipment and protective systems intended for use in potentially explosive atmospheres;
- directive 89/336/EEC of 3 May 1989 on the approximation of the laws of the Member States relating to electromagnetic compatibility.

The main aim of 98/37/EC directive requirements is the minimization of the threats which result from the mechanical construction.

Taking into account the pump work in the potentially explosive atmospheres, one of most important requirements are in directive 94/9/EC. On the basis of the conducted threats analysis, the new pump was classified to the M1 category in the 1 group. The following main requirements have to fulfil by the devices from this group:

- necessity of the dustproof housing application;
- surface temperature should be lower than the temperature ignition of the explosive mixture;
- special measurement and control elements should be designed for the elimination of the forceful equalization of the pressure.

The determination of harmonized European norm (EN) is the next stage of the design process. The detailed technical requirements are in this norm. The harmonized norms can divide on three groups:

1. General norms (A) applied to the different groups of product (EN 292).
2. Sector norms (B) contain the detailed requirements for the chosen safety aspect (EN 982, EN 953).
3. Detailed norms (C) contain the detailed requirements for the group of products (EN 809).

3. CONSTRUCTION OF THE PUMP

The pump (Fig. 1) is dedicated for pumping oil and water emulsion with 3 to 5% of oil contents. The basic requirements required by the ordering party for this pump are:

- nominal pressure at the outlet: 40 MPa,
- flow capacity: 320 dm³/min,
- motor power output: 250 kW.

The proposed solution is a new construction solution of a radial piston pump. Its main working elements are seven pistons spaced radially around the shaft axle. The pistons move in the pump body in plane and return motion forced by the properly shaped cam set on the shaft pin. Lift spaces are connected with the inlet and outlet (pumping) pipes from the outside of the immovable cylinder block. Valve timing is used as the element controlling the flow of the liquid.

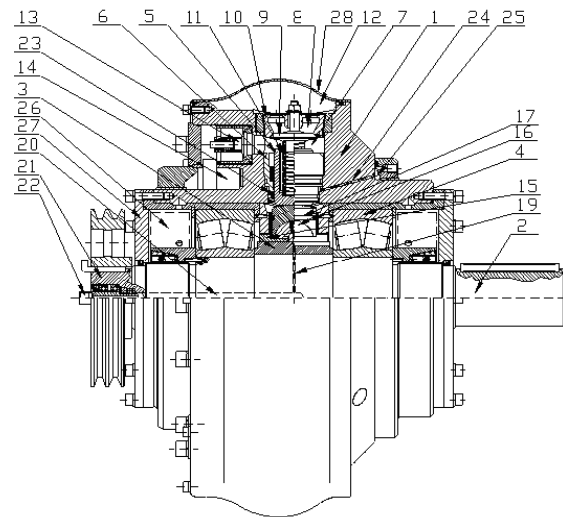


Fig. 1. Construction of the pump
 1 – pump body, 2 – shaft, 3 – eccentric pin, 4 – rolling bearings, 5 – small piston, 6 – small cylinder, 7 – lift chamber, 8 – inflow valve, 9 – inflow valve head, 10 – inflow valve seat, 11 – inflow valve spring, 12 – inflow collecting pipe, 13 – pumping valve head, 14 – pumping collecting pipe, 15 – bearing foot, 16 – ball-shaped pin, 17 – lifter, 18 – non-return valve, 19 – radial duct, 20 – axial duct, 21 – peripheral drive pin, 22 – rotating oil line, 23 – additional sealing, 24 – oil duct, 25 – oil collecting pipe, 26 – counterweights, 27 – cover, 28 – inflow collecting pipe casing



Fig. 2. View of the pump

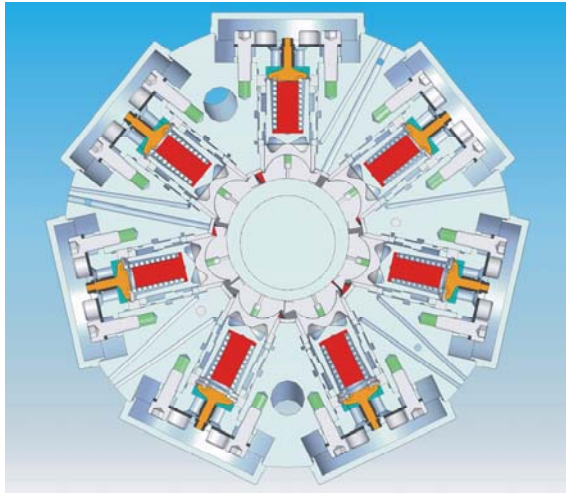


Fig. 3. Building of the pump

4. TECHNICAL HARMONISATION IN THE EUROPEAN UNION

Since 1985, the so-called “new approach” to technical harmonisation is used in EU. This approach is based on harmonisation of legislation in the scope of the basic technical requirements, significant to ensure safety, health, protection of the environment and public interest. The basic requirements are included in legal acts called directives.

The directives of the new approach have common structure, which includes the articles defining their scope of effectiveness, the conditions of marketing products and admitting them for use, the rules for free flow and presumption of compliance, the procedures for assessment of compliance and marking with the CE sign, the requirements for the notifying units. Appendixes are enclosed with the directives, which specify, among others, the basic requirements related to health and safety, the contents of the EC declaration of compliance, the rules of EC testing. The technical specification of products which meet the basic requirements of a specific directive, is to be found in the standards harmonised with the requirements of the appropriate directive. One has to note that products produced in accordance with harmonised standards are considered to meet the basic requirements of the appropriate directive.

In order to ensure coherent assessment of compliance of products with the basic requirements of the appropriate directives, in 1989, common policy as regards certification and tests was set forth, which was called the global approach. Breaking down the assessment of compliance into modules, including the design and production stages, is significant from the point of view of developing pump elements in this approach. In order to document compliance of the product with the appropriate directives, it must be provided with the

CE sign. Only the products, which meet the basic requirements of the appropriate directives, may be freely admitted to trading in the internal EU market and released for use.

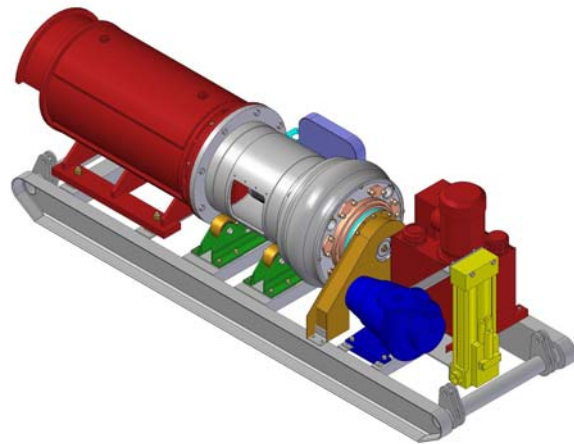


Fig. 4. View of the pump unit

5. EU DIRECTIVES COVERING THE DESIGNED PUMP

Defining the directives to cover the device is one of the duties of the producer. Only the devices, which meet the requirements of all the directives referring to them, may be introduced in commercial trading in the EU area.

The pump as a machine is first of all subject to the requirements in the 98/37/WE directive on harmonising regulations of member countries in reference to machines (the so-called machine directive). The main objective of this directive is to reduce threats resulting mostly from the mechanical structure of machines. The basic requirements set forth in Appendix I to this directive refer to threats.

Considering that the pump will work in a mine, that is in the possibly explosive atmosphere, it should also meet the basic requirements of the 94/9/WE directive on protection devices and systems dedicated for use in spaces with explosion hazard. Appendix I to this directive sets forth the classification of devices into groups and categories. On the basis of the conducted identification of threats, it has been determined that the pump is in category M1 in group I. The M1 category includes devices dedicated for work in mine underground areas and on the surface, where explosion of methane or coal dust is probable. This group includes machines fitted with additional anti-explosion protection measures. The equipment in this group should maintain very high degree of safety even in case of damages to one of the protection measures or in case when two independent damages occur in the machine). On the basis of the requirements for the M1 category (apart from the requirements for all the groups), additional requirements for the designed pump have been set forth:

- the necessity of using a dust-proof casing,
- surface temperature should be significantly lower than flash point of the surrounding explosive mixtures,
- the possibility of opening a part of the pump, which may cause ignition, may only occur when the power supply is off and under spark-safe conditions,
- the pump should have appropriate elements preventing accumulation of static electricity capable of causing hazardous discharges,
- random or leak currents should be prevented in the conductive parts of the pump, which are conducive to corrosion, overheating the surface and causing sparks.

A special measuring device should be designed for control and setting up, to prevent violent balancing of pressures in the hydraulic system. The above requirements along with the basic requirements of the 98/37/WE directive and the basic requirements of the 94/9/WE directive referring to all the groups of equipment constitutes the premises adopted for developing the construction solution concept of the pump.

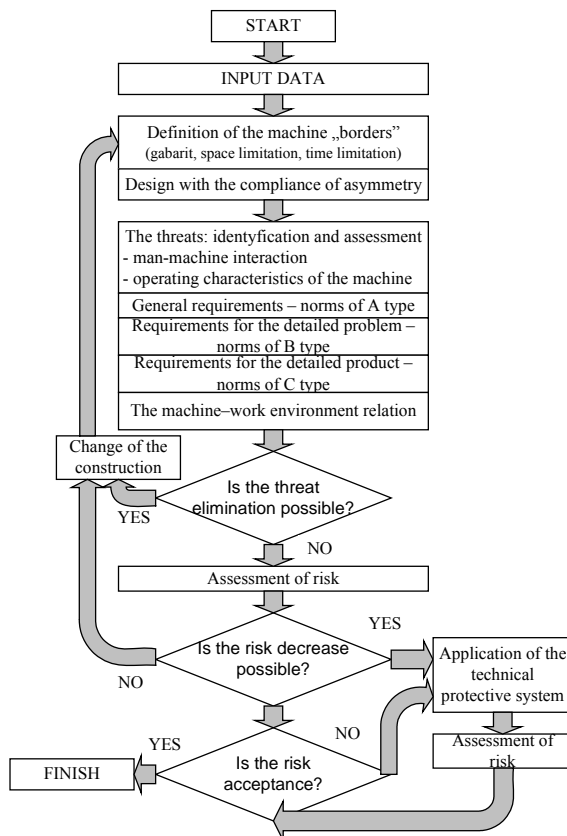


Fig. 5. Diagram of the design proces according with the basic requirements of EU directions

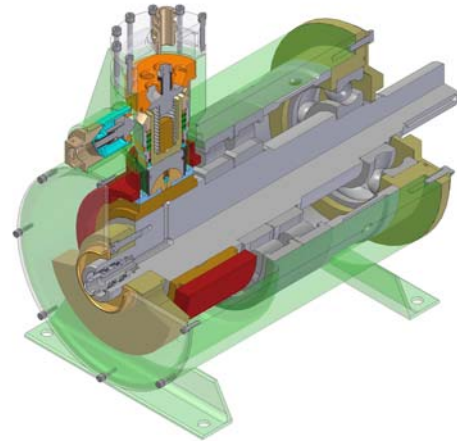


Fig. 6. Stand to the pump research

6. HARMONISED STANDARDS IN THE PROCESS OF DEVELOPING THE PUMP

The next stage after defining the directives related to the pump was to specify the detailed technical requirements which allow meeting the basic requirements of the directives. The detailed technical requirements are included in the harmonised standards. A harmonised standard does not need to include all the basic requirements of the directive. Therefore, the producer must use a supplementary technical specification.

Harmonised standards may be broken down into 3 groups:

1. General standards (A): used for many groups of products, e.g. EN 292 *General principles for design*.
2. Industry standards (B): these include detailed requirements in the selected scope, significant from the view point of safety, e.g. EN 952 *Guards*.
3. Detailed standards (C): addressing a specific group of products, e.g. EN 809 *Pumps and pump units for liquids. Common safety requirements*.

In order to meet the basic requirements of the machine directive in the scope of protection against mechanical hazards (Appendix I to the 98/37/WE directive, clause 1.3), the detailed technical requirements are used, which are included in the harmonised standards:

- 1) EN 809 *Pumps and pump units for liquids. Common safety requirements*.
- 2) EN 982 *Safety of machinery. Safety requirements for fluid power systems and their components. Hydraulics*.
- 3) EN 953 *Safety of machinery. Guards. General requirements for the design and construction of fixed and movable guards*.

On the basis of the above standards, technical requirements have been set forth, which allow meeting the basic requirements of the machinery directive only in the scope of protection against mechanical hazards:

- covered moving parts, such as clutch units, which may pose hazard, should be secured with guards (according to EN 953 Safety of machinery. Guards. General requirements for the design and construction of fixed and movable guards);
- rotating shafts with protruding elements, which can cause wounds, should be guarded;
- the clutch transferring drive force and its mounting should be capable of withstanding constant maximum load of the torque generated by the motor under all expected conditions of operation;
- the guard may be only removed with a dedicated tool, and the casing in the open position should be fixed to the pump;
- access should be provided for sealing the shaft in order to check its operation;
- open elements or elements accessible at a certain stage of assembly / repair should have blunt or machined edges and feathers removed;
- the elements of the hydraulic system should be easily accessible and safe in regulation and maintenance;
- all parts of the system should be so designed or secured in any other way that the pressure not exceeding the maximum working pressure of the system or any of its parts or the nominal pressure of each specified element could not cause damages to them;
- the pump should be fitted with sealing appropriate for the liquid used and for the threat from the possible leakage of this liquid;
- the producer should specify the allowed values of force and moments at the inlet and outlet pipes;
- percussive pressure and counterpressure should not pose hazard;
- leakage (internal or external) should not pose hazard;
- the paths for removing internal leakage should be located and installed so as to prevent air-locking of the system and should be selected for dimensions and location so as not to generate excess high counterpressure;
- high pressure vents should be located so as not to pose hazard for employees;
- temperature of liquid should not exceed the defined limiting values, at which it may be safely operated, or the defined range of operating temperature for particular elements of the system;
- the pump or pump unit should not lose stability during transport and assembly at tilts of up to 10°;
- the installed pump should be stable with the used clamping screws.

7. CONCLUSIONS

Based on the experience acquired during the process of creating a new solution for the pump, the following conclusions come to mind:

1. Selection of the solution concept for the device largely depends on the basic requirements included in the EU directives for the given device. The basic requirements of the directives had effect on the shape of the pump concept in the scope of:
 - selection of materials and peripheral elements,
 - control,
 - mechanical structure,
 - construction and principles of operation,
 - maintenance of operation,
2. As assessment of compliance in the global approach applies to both the production and designing stages, the designing process must be conducted based on the appropriate harmonised standards.

Identification of threats and their assessment constitute the basis for the process of reaching compliance with the basic requirements of the directives.

REFERENCES

- [1] Dyrektywa 98/37/WE Parlamentu Europejskiego i Rady z 22 czerwca 1998 r. w sprawie zbliżenia ustawodawstwa Państw członkowskich dotyczące maszyn.
- [2] Dyrektywa 94/9/WE Parlamentu Europejskiego i Rady z 23 marca 1994 r. w sprawie zbliżenia ustawodawstw Państw członkowskich dotyczących urządzeń i systemów ochronnych przeznaczonych do użytku w przestrzeniach zagrożonych wybuchem.
- [3] Nurnikowy agregat pompowy nowej generacji o parametrach technicznych nie gorszych od określonych przez Zamawiającego, Sprawozdanie wykonawcy z I etapu pracy naukowo-badawczej pod red. A. Jurkiewicz, Kraków 2003.

MEASUREMENT AND ANALYSIS OF ACOUSTIC EMISSION IN THE TRIBOLOGICAL SYSTEM BALL-ON-DISC

Anna PIĄTKOWSKA¹, Tadeusz PIĄTKOWSKI²

¹Institute of Electronic Material Technology, Wólczyńska 133, 01-191 Warsaw
e-mail: Anna.Piatkowska@itme.edu.pl

²Institute of Optoelectronics, Military University of Technology, Kaliskiego 2, 00-908 Warsaw

Summary

In the present work the following results of tribological measurements are presented: changes of the friction coefficient, instantaneous values of friction force F_t , topography of worn surfaces (SEM) and detected vibroacoustic and acoustic emission signals. The measurements were performed on flat Si substrates covered with thin films of Cr and Au with thickness of 1 and 2 μm , respectively. Two types of tribological tests were done: one with a single-pass sliding of the ceramic ball with 0.5 mm in diameter and at sliding speed of $v_{s1}=0.025$ mm/s, and the other one with a cyclic reciprocating motion of the ball at $v_{s2}=0.21$ mm/s. Registration of the vibroacoustic and acoustic emission signals was in the 60 s periods in the same way for all tests. On the basis of our study one can conclude that the set-up used allowed us to detect and register vibroacoustic and acoustic emission signals related to microfriction. Various kinds of abrasive wear were determined.

Keywords: Wear mechanism, Abrasion, Friction, Acoustic emission, FFT-time.

POMIARY I ANALIZA PARAMETRÓW TRIBOLOGICZNYCH ORAZ EMISJI AKUSTYCZNEJ ZAREJESTROWANYCH W UKŁADZIE TRĄCYM KULA – POWIERZCHNIA PŁASKA

Streszczenie

W pracy przedstawione zostały wyniki badań tribologicznych: zmiany współczynnika tarcia μ oraz chwilowe wartości siły tarcia F_t , topografia śladów zużycia (SEM) i otrzymane sygnały wibroakustyczne i EA. Do pomiarów użyte zostały płaskie próbki z cienkimi warstwami chromu, o grubości 1 μm i złota, o grubości 2 μm naniesione na podłoże z płytki Si.

Pomiary tarciove wykonane zostały w dwóch rodzajach testów: z pojedynczym przesuwem kulki (przeciwpróbki) ceramicznej o średnicy 0.5mm z prędkością poślizgu $v_{s1}=0.025$ mm/s oraz cykliczne, kulka przemieszczała się wielokrotnie ruchem postępowo-zwrotnym z prędkością poślizgu $v_{s2}=0.21$ mm/s. Rejestracja sygnałów wibroakustycznych i EA odbywała się w określonych, jednakowych dla wszystkich testów 60-cio sekundowych odcinkach czasu, na początku, podczas i na koniec testu. Na podstawie przeprowadzonych badań można przyjąć, że w zaproponowanym stanowisku pomiarowym możliwa jest detekcja i rejestracja sygnałów wibroakustycznych i emisji akustycznej związanej z mikrotarciem. Określone zostały różne rodzaje zużycia abrazyjnego

Słowa kluczowe: mechanizmy zużycia, ścieranie, tarcie, emisja akustyczna, FFT-time.

1. INTRODUCTION

Tribological studies of wear elements play important role in determination of mechanical properties and functional parameters of new materials designed for numerous applications from biomedicine to electronics. Vibroacoustic and acoustic emission signals being emitted during friction contain information about different processes occurring during friction such as deformation, surface damages, phase transformations, chemical reactions and micro-collisions, e.g., of single asperities [1, 2]. This relation is used to detect the initiation and

propagation of cracks and other damages processes, as well as for determination of the wear resistance, times of life for rolling bearings and tools for metal cutting, durability of head-disc interface [3-6]. This technique is used also in numerous industries: refineries, pipelines, power generation, aircraft, paper mills.

Most papers [2, 3] [7-9] describe the biggest damages of elements upon cyclic, intense loading or in extreme conditions (load, speed, environment), where the information about wear is quite general. However, it is supposed to find relationships between the AE parameters and different wear mechanisms proceeded during the

friction in any tribosystem. The development of AE sensors and data acquisition methods is promising for very precise description of tribological properties of different materials.

The aim of this study is the development of a set-up for the measurements of vibroacoustic and acoustic emission signals, as well as elaboration of a method for their detection and for analysis of the phenomena occurring during sliding friction in the ball-on-disc system at the reciprocating motion of the friction elements.

2. EXPERIMENTAL DETAILS

2.1. Specimen

The material used in this work was Si-wafer 2" and 3" in diameter with thickness of 1.5 mm, covered with thin Cr and Au-coating.

The coatings parameters are listed in Table 1.

Table 1. Description of specimens

Substrat	Si-wafer	2" in diameter fine polished	3" in diameter polished
Au-coating by galvanic deposition		Thickness of – 1 μm	Thickness of – 1 μm
Cr-coating by cathode sputtering deposition		Thickness of – 2 μm	Thickness of – 2 μm

2.2. Tribological apparatus and test conditions

All tests were carried out on "the ball-on-disc" tribometer at the reciprocating motion of the friction elements. Two kinds of tribological test were done: simple-pass and multi-pass. Experiments were designed to generate various, simple wear mechanisms during dry sliding contact. The conditions of the tests are presented in Table 2.

Table 2. Summary of the dry sliding tests conditions

	Multi-pass	Single-pass
Ball	Ceramic 0.5 mm of diameter	
Load [N]	1.6	1.6 and 2.4
Sliding velocity [mm/s]	0.21	0.025
Test duration [s/cycles]	650(550)/73(61)	160/1
Wear trace length [mm]	1.9	4

During the friction test the coefficient of friction was registered on-line .

2.3. Vibroacoustic and AE signals measurement set-up

Registration of the vibroacoustic and acoustic emission signals was in the 60 s periods in the same way for all tests. Limitation of the measurement time was related to technical parameters of the control unit (PC) and to data transmission.

A block diagram of the set-up for the measurements of acoustic emission signals is shown in Fig. 1.

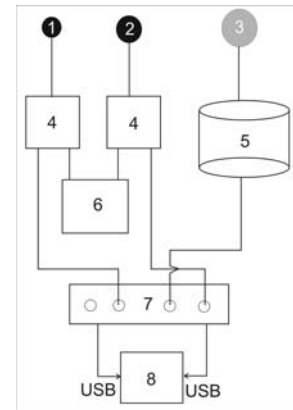


Fig. 1. Schematic diagram of the set-up for measurement of acoustic emission signals:

- 1 – AE Sensor freq. range: 400 – 750 kHz;
- 2 – AE Sensor freq. Range: 60-1950 kHz;
- 3 – Accelerometer freq. Range: 5 – 60 kHz;
- 4 – AE Preamplifier;
- 5 – Signal Conditioner;
- 6 – Power;
- 7 – Data Acquisition Card;
- 8 – Control Unit (PC).

Two AE-sensors were pressed at the specimen surface by two separate holders, accelerometer was fixed with cyanocrylate glue, of them were placed in distance about 10 mm to wear track.

2.5. Wear measurements

After tests, wear tracks were observed by optical microscope with Nomarsky contrast and by Scanning Electron Microscope (SEM). Cross sections of wear tracks were determined by high sensitivity profiler.

3. RESULTS AND DISCUSSION

Figure 2 shows variations of friction coefficient and AE signal, obtained from AE sensor no. 2 (Fig. 1) saved during tribological multi-pass test on Au-coating specimens.

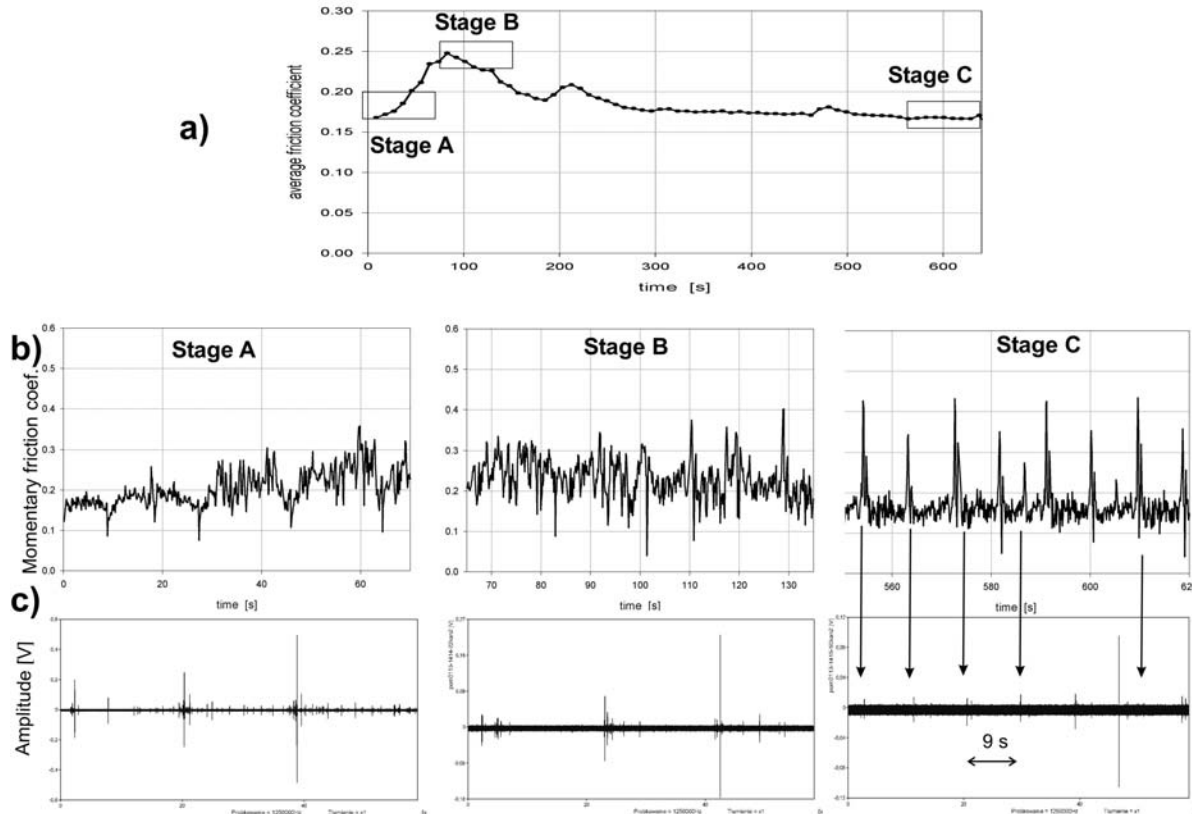


Fig. 2. The test results from multi-pass sliding test: a) average friction coefficient for the whole test, b) momentary friction coefficient, c) AE time signals

The most important stages are marked by rectangle in Fig. 2a: A – start of friction, B- coefficient increase, C-coefficient stabilization. Fig. 2b shows the momentary friction coefficient for these three stages of friction, respectively, and below, in Fig. 2c the appropriate AE time signals are presented.

Shortly after beginning of the test, when changes of momentary friction coefficient are too small to be analysed (Fig. 2b) first transient AE signals appear (Fig. 2c). Stage B is characterized by visible changes of friction coefficient but the amplitude of AE signals and number of peaks is lower. Results for stage C of the test did not show severe perturbations neither in the momentary friction coefficient nor in AE signals registered. The arrows mark AE peaks relative to change of motion direction of with time-period similar to one-cycle time (approximately 9 s).

The amplitude of AE signal noise was comparable to that found in the non-loading test. The diagrams of FFT-time calculated for the AE measurements described above, Fig. 3, show small differences in increase of amplification of frequencies in the range of: 240-300 kHz, for A and B stages. At the FFT-time for stage C, values were uniform for the whole range. The level of signal amplitudes is higher than for stage A and B.

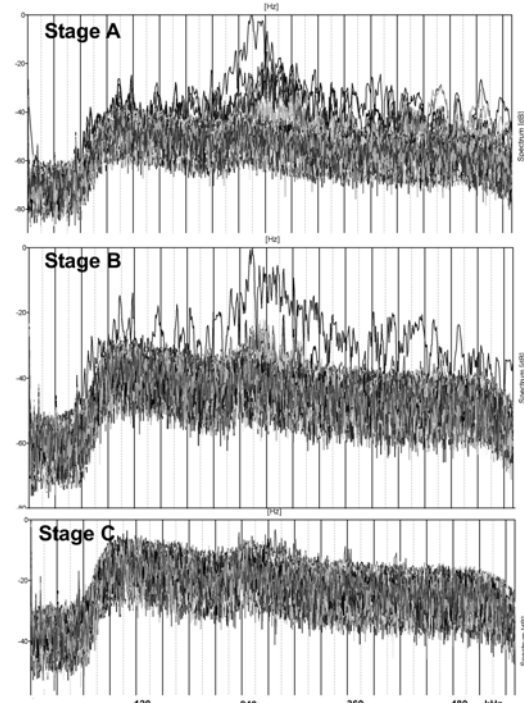


Fig. 3. FFT-time diagrams for A, B, C friction stages

SEM-image of this described wear track is presented in Fig. 4.

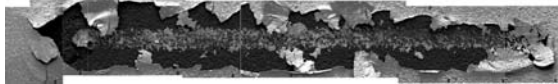


Fig. 4. Wear track after multi-pass friction test on Au-coating surface

As a consequence of the described friction test the Au-coating was totally delaminated. Analyse of the results allows us to specify the following stages of friction test:

- A- first micro-cracks with their propagation during second and next passes;
- B – transfer of Au-coating, delamination and agglomeration of debris on extremities of wear track;

C – uniform friction on Si-substrate without new visible damages.

Friction on Au-coating sample with very small speed $v_{s2}=0.025$ mm/s did not generate any AE burst signal. Continuous type AE signals were associated with plastic deformation in ductile material of coating.

Optical and SEM images inform about predominate wear mechanisms, which is abrasion manifested by plastic deformation and polishing. It is presented on Fig. 5.

The same tests simple- and multi-pass were repeated on Cr-coating sample. These results are shown in Fig. 6.

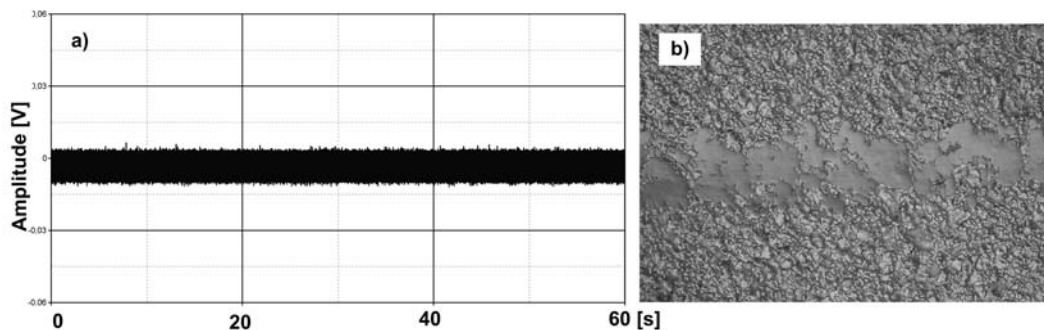


Fig. 5. Dry sliding with very slow speed, simple-pass test on Au-coating surface, a) AE time signal, b) optical image of wear trace

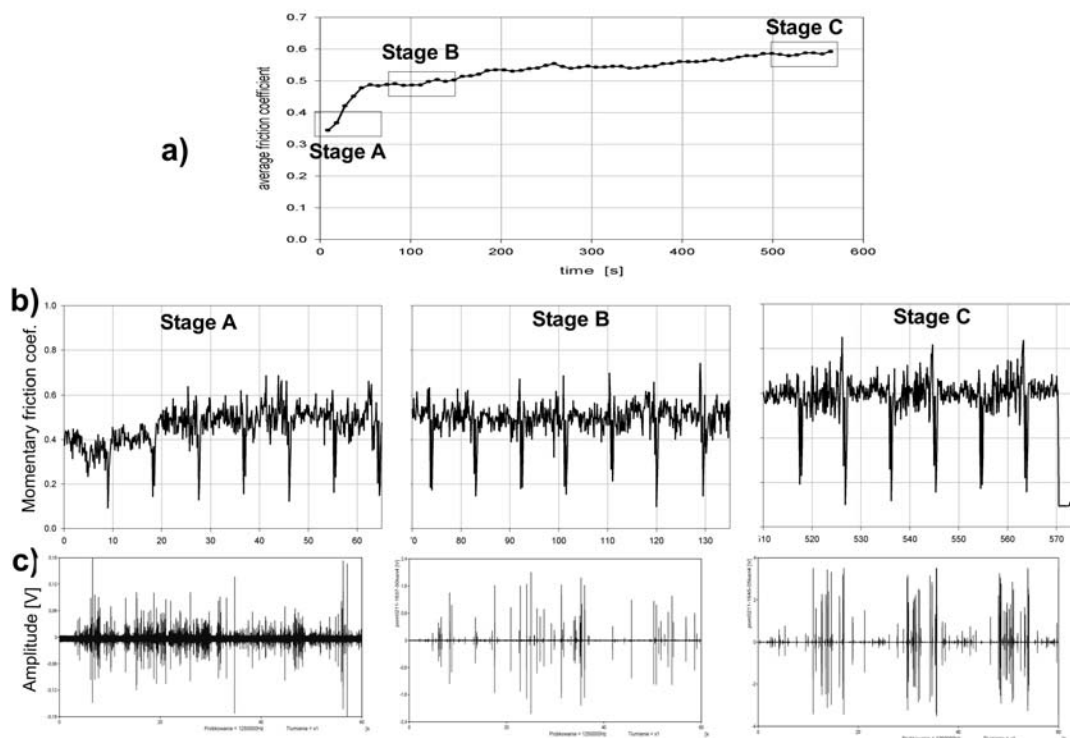


Fig. 6. The test results from multi-pass sliding test: a) average friction coefficient f or the whole test, b) momentary friction coefficient, c) AE time signals

As before, three stages (A – start friction, B – development of friction and C – stabilisation of friction) were monitored simultaneously by the friction coefficient, vibroacoustic and AE signals.

It seems that at first cycle of friction micro-cracks and extraction of particles were produced. The amplitude of AE signals was various: higher values were generated at both extremities of wear trace than during movement. Probably this observation indicates the formation of significant quantity of wear debris and their intensive accumulation on ends of wear trace. During the stage B, number of AE signals peaks was reduced but their amplitude was approximately ten times higher. Next stage C was characterised by non-important perturbations of momentary friction coefficient, average values were relatively low, whereas the amplitudes AE burst signals increased up to 4V (max. range). It's value was up to 20 times higher than generated in A stage (at the beginning of the test). Moreover, a dependence between the rise time of the AE burst signals and the friction stage was observed. Development of friction generated long rise time and multi-burst signal in clusters.

Fig. 7 shows optical image of the wear trace, where the abrasion by micro-scratching and spalling of Cr-particles was the predominant wear mechanism. Comparing AE signal and wear evolution it can be seen that the amplitude AE signals increases with the progress of damages on the surface.

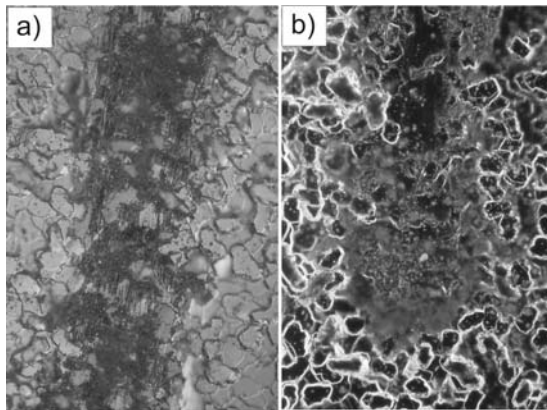


Fig. 7. SEM/optical image of wear trace on Cr-coated sample, magnification x 50: a) middle, b) extremity of trace

FFT-time spectra calculated for three stages were similar and indicated many peaks in the range of 60-600 kHz superimposed onto a background signal (Fig. 8).

For stage A signal amplitudes for frequencies over 75kHz are included in the range from -60dB to 0dB. For stage C the amplitudes are included in range from -40dB to -10dB. It is result from series of singular, short pulses in the AE signal.

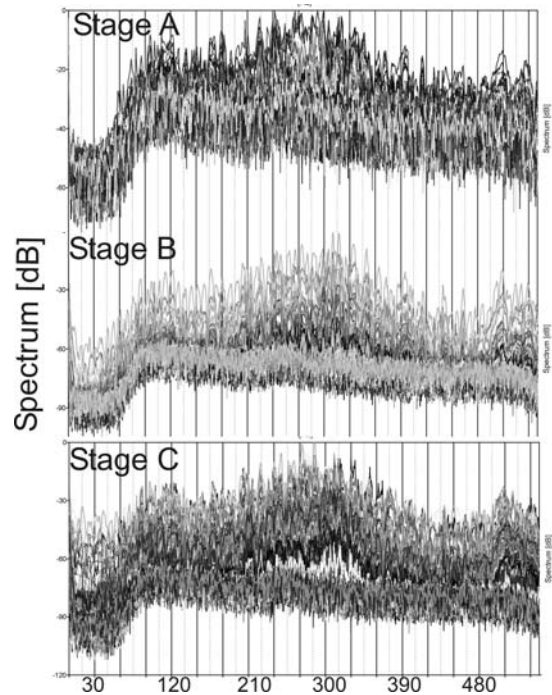


Fig. 8. FFT-time diagrams for A, B, C friction stage on Cr-coating surface

Vibroacoustic time-signals registered for all stages of tribological test demonstrated only a constant background noise signal. Few peaks, related to AE-burst signals were occurred during multi-pass friction on Au-coating specimen.

4. CONCLUSIONS

Proposed set-up for the measurements of vibroacoustic and acoustic emission signals enable the detection and monitoring AE signals with frequencies higher than 90 kHz. The signals below 60 kHz, measured by accelerometer, were observed only in multi-pass friction on Au-coating sample. Tribological multi-pass tests with higher speed were characterized by generation of irregular AE burst signals. The amplitude, number of peaks and AE pulse multi-clusters and range of signal frequencies permit for the analyse and evaluation of the dominating wear process. The tests with very small sliding speed, simple-pass ball movement, generated measurable AE signals only in the case of Cr-coating sample and with the dominating abrasive wear in the form of spallation of coating grain (spalling).

Conclusions are as follows:

1. After dry sliding tests the following surface damages were observed: delamination, spallation, polishing.
2. The wear-life of Au and Cr-coating can be determined.
3. The AE signals are more sensitive to the local failure of coating.

4. For various wear processes: delamination, spalling, polishing different AE signals were registered.
5. Difference in AE signals are manifested in:
 - AE time signal – the amplitude and number of pulses;
 - Frequency spectrum – FFT-time.

ACKNOWLEDGEMENTS

The study was performed under Grant No.1661/T07/2005/29 from the Polish Ministry of Science and Higher Education.

REFERENCES

- [1] Miettinen J., Pataniitty P.: *Acoustic Emission in Monitoring Extremely Slowly Rotating Rolling Bearing*. www.acustest.fi/docs/PAPER_C.PDF.
- [2] Chung-Woo Cho, Youn-Ze Lee: *Wear-life evaluation of CrN-coated steels using acoustic emission signals*. *Surface and Coatings Technology* (2000) 127, 59-65.
- [3] Jun Sun, Wood R. J. K., Wang L., Care I. Powrie H. E. G.: *Wear monitoring of bearing steel using electrostatic and acoustic emission techniques*. *Wear* (2005) 259, 1482-1489.
- [4] Dolinsek S., Kopac J.: *Acoustic emission signals for tool wear identification*. *Wear* (1999) 255-229, 295-303.
- [5] Kum-Hwan Cha, Sung-Chang Lee, Dong-Kuk Han, Sang-Min Lee, Dae-Eun Kim: *Experimental investigation of AE and friction signals related to the durability of head/disk interface*. *Tribology* (1999) 32, 399-405.
- [6] Mathews P. G., Shunmugam M. S.: *Condition monitoring in reaming through acoustic emission signals*. *Material Processing Technology* (1999) 86, 81-86.
- [7] Manes L., De Monicault J. M., Gras R.: *Monitoring damage by acoustic emission in bearing steels in cryogenic environment*. *Tribology* (2001) 34, 247-253.
- [8] Marczak M.: *Emisja akustyczna procesu tribologicznego, rozprawa doktorska* (2001) WITPIS, Sulejów.
- [9] Von Stebut J., Lapostolle F., Bucsa M., Vallen H.: *Acoustic emission monitoring of single cracking events and associated damage mechanism analysis in indentation and scratch testing*, (1999) 116-119 160-171.



Anna PIĄTKOWSKA is a specialist in the micro- and nano-tribological research. She obtained a doctoral degree (Ph.D) from the Institute of Electronic Materials Technology, where she is an assistant professor. Her principal research subjects are: ion implantation, micro-, nano-mechanical and structural properties of implanted materials. Dr Piątkowska is a member of Polish Society of Tribology.



Tadeusz PIĄTKOWSKI graduated from the Faculty of Precision Engineering (1981) and Faculty of Electronics of Warsaw University of Technology (1984). He received his PhD from Military University of Technology in 2003. He is now an assistant professor at the Institute of Optoelectronics of Military University of Technology. His research area is mainly in fusion sensors systems, remote temperature measurements. He took part in 19 research projects and he is an author and co-author of 30 publications.

APPLICATION OF ULTRASONIC TECHNIQUES FOR THE EVALUATION OF THE PROPERTIES OF PRESTRESSED CONCRETE STRUCTURES

Wojciech MANAJ*, Krzysztof SIKORSKI, Krzysztof KURZYDŁOWSKI

*Materials Engineers Group Sp. z o.o.

Ul. Wołoska 141, 02-507 Warszawa, fax:(22) 234 81 08, w.manaj@megroup.home.pl

Politechnika Warszawska, Wydział Inżynierii Materiałowej

Ul. Wołoska 141, 02-507 Warszawa, fax: (22) 234 87 50, kjk@inmat.pw.edu.pl

Summary

During service concrete structures undergo degradation caused by the applied stresses, the temperature and the working environment. This degradation causes a decrease in the mechanical properties and limits the safe working life of concrete components.

In order to reduce costs of the removal of concrete structures, special methods to control the material degradation are sought. In particular, non-destructive testing methods which enable the properties to be determined without physical interference of the elements integrity.

The paper focuses on the possible ultrasonic methods that can be applied to examine concrete structures. The effectiveness of these methods was assessed on prestressed concrete structures, widely used in civil engineering. The resulting measurements of ultrasonic velocity and the made ultrasonic wave analysis from tests on concrete structures are described and analyzed.

Keywords: prestressed concrete, ultrasonic.

ZASTOSOWANIE ULTRADŹWIĘKOWYCH TECHNIK POMIAROWYCH W OCENIE STANU KONSTRUKCJI SPRĘŻONYCH

Streszczenie

Konstrukcje betonowe ulegają degradacji pod wpływem naprężeń, temperatury i środowiska pracy. Powoduje to obniżenie właściwości mechanicznych konstrukcji i ograniczenie jej dalszego bezpiecznego czasu eksploatacji.

Ze względu na ekonomiczne konsekwencje wyłączenia konstrukcji z eksploatacji uzasadnione są działania mające na celu kontrolę stopnia degradacji. W szczególności stosowane są metody nieniszczące, nie wymagające wycinania próbek z badanego materiału.

W artykule przedstawiono wyniki badań ultradźwiękowych elementów betonowych podlegających degradacji. Zastosowana metoda była badana na przykładzie betonów sprężonych, szeroko stosowanych w konstrukcjach cywilnych. Zaprezentowano wyniki pomiarów ultradźwiękowych oraz analizę sygnału ultradźwiękowego materiału konstrukcji betonowych.

Słowa kluczowe: beton sprężony, ultradźwięki.

1. INTRODUCTION

Concrete constructions, prestressed concrete constructions included, are often used in civil engineering. Because of their wide application and use by the public, the economical consequences of their destruction, or temporary closure, may be high. For this reason, the degree of degradation of the properties of the material needs to be monitored. Ensuring safety, from the point of view of endangering users, as well as impact on the natural environment, call for systematic control of the most highly stressed elements. Contemporary testing techniques allow for the monitoring and evaluation of the materials degradation, in a way which does not influence the properties or the use of the structure. This type of examination, by non-

destructive testing can be performed. Ultrasonic measurements are used to evaluate the general condition of the material, as well as for locating material discontinuities.

Ultrasonic waves are frequently applied for the non-destructive testing of concrete structures. Strength, porosity and damage cause changes of ultrasonic parameters [1]. Because of the significant non-homogeneity of concrete, which is composed of results obtained are usually interpreted using empirically established data without a deeper insight into the structure of the material. Therefore, to evaluate the technical condition of the structure it is necessary to perform laboratory tests to build up an experimental database, which will supply the information necessary to interpret the results obtained under operational conditions.

Because of considerable attenuation of the ultrasonic waves in concrete, it has been established that the most meaningful measurements are, performed using ultrasonic heads with a frequency in the range 50 kHz to 1 MHz.

A characteristic of ultrasound waves related to the material's property is the speed of the waves, which is dependent on the density of the material examined, the elastic properties, temperature and stress [2].

The results of the ultrasonic wave speed measurements obtained and the ultrasonic signal analyses in relation to the degree of the concrete prestress are presented in this paper.

2. EXPERIMENTAL PROCEDURE

2.1. Test methodology and equipment

The transmitter–receiver method was used in the study. It is performed with two ultrasonic heads, one being a transmitter and the other as the receiver of the ultrasonic waves. The principles of the system are shown schematically in Figure. 1.

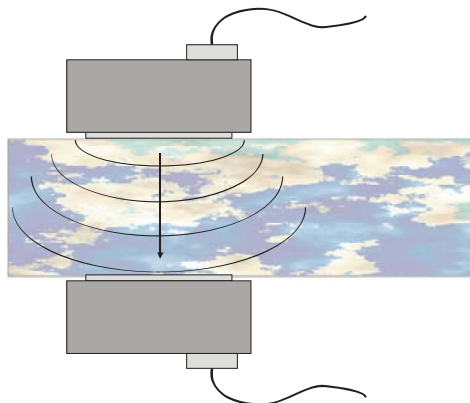


Fig. 1. Principles of the transmitter-receiver method of testing

Because of considerable attenuation of the ultrasonic wave in concrete, longitudinal waves were chosen for the testing. Ultrasonic heads with 100 kHz frequency were selected. This ensured the quality of the ultrasonic signal detected. During testing of each specimen, 3 measurements of the longitudinal wave speed were made. The average values were determined and the results obtained were compared to the degree of the pre-stress in the material.

Ultrasonic measurements were conducted using a Panametrics-NDT Epoch 4 flaw detector. Because of considerable attenuation of the ultrasonic wave, ultrasonic transducer probes of 50 mm diameter were employed.

The selection of the test parameters such as gain and voltage were set experimentally taking into account the quality of the detected signal and noise level.

During the measurements, a special gel was used as the coupling agent between the head and the structure being examined.

The measurements of ultrasonic wave speed were carried out together with digital recording of the spectra (Figure 2). EpochData software was used to perform these measurements. The results obtained were analysed using Fourier transforms allowing for decomposition of the spectra into its frequency components [3]. In the analysis, the focus was the dominant frequency of the ultrasound signal spectra.

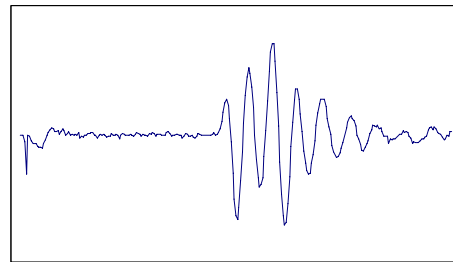


Fig. 2. Frequency spectra of the ultrasonic wave

Because of the construction of the element tested and the distribution of the prestressing elements, the tests were performed in such a way that the ultrasonic wave was not reflected by the prestressing elements.

2.2. Specimens

The tested structures were concrete beams with different degrees of prestress. The stress was achieved by straining 4 symmetrically distributed, internal strings. Measurements were performed on 9 beams with the stress ranging from 20 to 100 kN. The dimensions of the beam were 110x140x1300 mm (Figure 3).

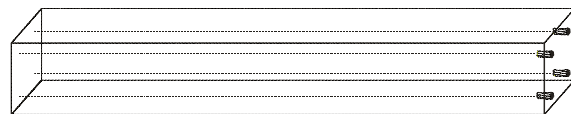


Fig. 3. The schematic exploration of the examined elements showing the distribution of the prestressing strings

3. EXPERIMENTAL RESULTS

The ultrasonic studies, concentrated on measuring the speed of the longitudinal waves in structures and the analysis of the spectra of the ultrasonic waves. Analysis of the spectra consisted of determination of the dominant frequency,

In both cases, the results were related to the degree of the beam prestress as shown in figure 4. The results of the measurements of the dominant frequency in the spectra of the ultrasonic waves related to the prestress in the beam are shown in Figure 5.

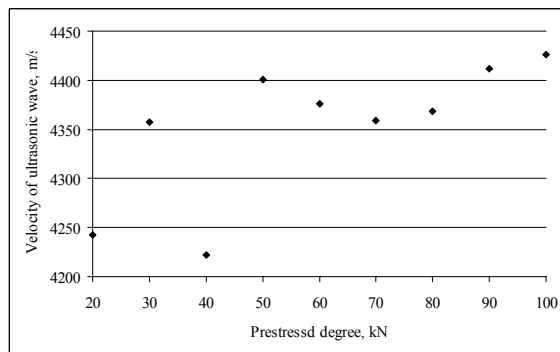


Fig. 4. The results of the measurements of the speed of the ultrasonic waves related to the degree of the beam prestress

The test results show the rise in the speed of the ultrasonic waves with the increase in the level of the prestress of the beams from 20 to 100 kN. It is worth noting, that a method dependent on the measurements of the speed of the ultrasonic waves may be of a little value with only small differences in the amount of prestress. Differences of prestress in the concrete up to 40 kN display only small changes of the recorded parameters.

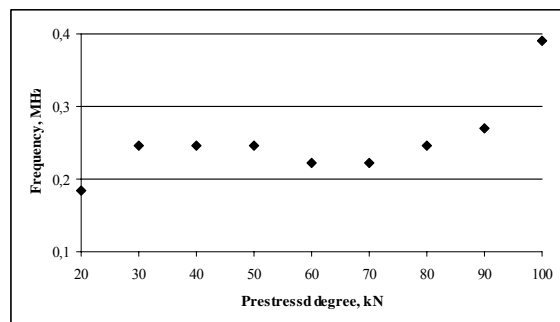


Fig. 5. Analysis of the dominant frequency in the spectra of the ultrasonic waves related to the degree of the beam prestress

The results of the analyse of the dominant frequency in the spectra of the ultrasonic wave show the rise of the dominant frequency with a considerable increase in the level of prestress in the beams from 20 to 100 kN. Similarly, as in the case of measurements of the speed of the ultrasonic waves, a method relying on the determination of the

dominant frequency spectra may be of a very little help withonly small differences of prestress level in the suture. Difference in the prestress level up to 50 kN displays only small changes of the measured parameter.

4. CONCLUSIONS

In this paper, the ease of use and effectiveness of the ultrasonic transmitter receiver method of evaluation of the degree of prestress in the concrete beams has been confirmed. In the case of the measurements of the speed of the longitudinal waves, as well as in the case of analysis of the dominant frequency in the spectra of the ultrasonic waves, evaluation of changes in the level of prestress is possible when it has risen to about 80 kN. The results presented indicate the possibility of making errors where evaluation of changes in the level of prestress when this prestress is relatively low

ACKNOWLEDGEMENT

This work was supported by the Polish Committee for Scientific Research as research project 134/E-365/SPB/COST/KG/DWM 66/2005-2007.

REFERENCES

- [1] Philipipidis T. P, Aggelis D. G.: *Experimental study of wale dispersion and attenuation in concrete*, Ultrasonic 43,584-595.
- [2] Deputat J.: *Badania nieniszczące wyrobów i półwyrobów hutniczych*. Badania ultradźwiękowe. Wydawnictwo IMŻ Gliwice, 1979.
- [3] Proakis J. G., Monolakis D. G.: *„Digital Signal Processing”*; Prentice Hall, New Jersey 1996, third edition.

Dr inż. **Wojciech MANAJ** jest kierownikiem Laboratorium Badań Materiałowych spółki Materials Engineers Group Sp. z o.o.

SELECTED DIAGNOSTIC ASPECTS OF PROPAGATION OF VIBROACOUSTIC ENERGY¹

Grzegorz KLEKOT

Warsaw University of Technology, Institute of Machinery Design Fundamentals
02-524 Warszawa, Narbutta 84, fax 022 234 8622, email gkl@simr.pw.edu.pl

Summary

Methods based on diffusion of vibroacoustic energy play a particular role in solving practical engineering tasks, including evaluation of the object's state, improvement of user's comfort, and shaping the acoustic atmosphere. The way of propagation of noise and vibration often determines the functional advantages of a technical object.

One of the reasons why the detectable changes in vibroacoustic signal appear can be modification of ways of propagation caused by damages or exploitation wearing. Studies on these problems comprise also search for the measures susceptible to the changes of the object's state, based on analysis of propagation of vibroacoustic energy. The discussion is illustrated by two cases.

Keywords: noise, vibrations, vehicle.

WYBRANE ASPEKTY DIAGNOSTYCZNE PROPAGACJI ENERGII WIBROAKUSTYCZNEJ

Streszczenie

Metody bazujące na rozprzestrzenianiu energii wibroakustycznej odgrywają szczególną rolę w rozwiązywaniu praktycznych zadań inżynierskich między innymi dotyczących oceny stanu, poprawy komfortu użytkownika, oraz kształtowania klimatu akustycznego. Sposób propagacji drgań i hałasu często decyduje o walorach funkcjonalnych obiektu technicznego.

Jednym z powodów rozróżnialnych zmian sygnału wibroakustycznego może być modyfikacja dróg propagacji bezpośrednio spowodowana uszkodzeniem bądź zużyciem eksploatacyjnym. Badania tych aspektów obejmują poszukiwania miar wrażliwych na zmiany stanu obiektu bazujące na analizie propagacji energii wibroakustycznej. Rozważania zilustrowano dwoma przykładami.

Słowa kluczowe: hałas, drgania, pojazd.

1. INTRODUCTION

Studies of propagation of vibroacoustic energy play a particular role in solving practical engineering tasks, including evaluation of the object's state, improvement of user's comfort, and shaping the acoustic atmosphere. Actually, it is propagation of vibroacoustic energy that often determines (in a very broad meaning) the functional advantages of a technical object.

The model analysis form an important part of all the studies aiming at optimization of the exploitation process of machines and units. The relations between diagnostic symptoms and technical state have been searched using numeric simulation, without costly and laborious experimental studies. However, it has been found that the results of simulation calculations cannot be directly translate

into practical applications: they require the empirical verification as well as the adaptation to technical realities. It concerns also the question of modeling of generation and propagation of vibroacoustic signals: the level of complexity of the phenomena shaping these signals makes unreal any attempt to construct a model fully describing the reality.

The dynamic models of one or several degrees of freedom are often good enough to analyze construction or characteristics of machines and units. The important setbacks start when a non-linear component appears; however, it is in non-linear way that the technical state of objects change [1].

The disturbances in propagation of vibroacoustic energy considered in relation to diagnostic reasoning are also result of non-linearity. A relationship between the damping qualities of the object's structure and the surrounding environment has been

¹ The work financed from the budget for scientific development in 2006-2009 as a research grant

observed. Therefore, the search for methods that in a relatively easy way could take into account the elements mentioned above seems quite logical.

2. MODELING OF PROPAGATION

Forecasting the frequency structure of vibroacoustic signal received in particular point requires an analysis of input characteristics and ways of propagation of vibroacoustic energy. Assuming that there is a dominating source, the signal received by the observer, treated as a response in the domain of frequency can be written as the following equation [2]:

$$Y(f) = X(f) \cdot H(f) \cdot \Phi^*(f) \cdot \Psi^*(f) \quad (1)$$

In the relationship $Y(f)$ is Fourier's transform of the received output signal $y(t)$, $X(f)$ - the Fourier's transform of the input process $x(t)$, $H(f)$ - transmittance of the propagation way, $\Phi^*(f)$ - an attempt to describe the non-linearity as a product in the identification process, and $\Psi^*(f)$ reflects the influence of external disturbances (noise).

Both sides of the equation (1) can be transformed by operator that transforms the scale into the logarithmic one (decibel). Then the task described by the relationship can be brought to the equation of level decrease:

$$L(f) = L_s(f) + \Delta L_h(f) + \Delta \Phi^*(f) + \Delta \Psi^*(f) \quad (2)$$

$L(f)$ is the input level, $L_s(f)$ - level of dominating source (input), $\Delta L_h(f)$ - decrease (increase) of level resulting from transmittance of the system, $\Delta \Phi^*(f)$ - change of the output level provoked by non-linear disturbances and defined by identification, $\Delta \Psi^*(f)$ - change of level provoked by contingent disturbances, impossible to forecast: this is description error.

The description presented above can be applied under the condition of elaborating it for a particular object and identifying parameters of the model. However, a relatively simple form of the equation (2) reflects certain philosophy that can help developing the efficient reasoning leading to the solution of particular engineering tasks. The following paragraphs present two examples of application. The first case illustrate possibilities of reproducing development of damage using measures susceptible to disturbances of propagation of vibration. The second one reflects the need of deeper analysis of propagation of vibroacoustic energy in construction of noiseless machinery.

3. EVALUATION OF DAMAGE DEVELOPMENT

The discussion is based on the results of testing vibrations forced in truss beams made of compressed concrete in different stages of degradation [3]. The time courses registered with the force processor ($F(t)$, input) and accelerometers ($a(t)$, response) have been used for calculating value of the measures of propagation of vibration energy H_a :

$$H_a = \frac{\int_0^T (a(t))^2 dt}{\int_0^T (F(t))^2 dt} \quad (3)$$

The formula were discussed in [4], where also the questions of focusing the susceptibility of measure on particular failure by proper choosing the positions of accelerometers and the input excitation points were presented. There was an obvious relationship between the propagation of vibroacoustic energy by the structure of the objects under scrutiny and a failure resulting from overloading.

Synthesis of the results of research on changes of efficiency measures of vibration propagation in function of static loading of two beams are shown in the graph below (fig. 1). The values have been calculated as the average of five changes courses for vibration accelerations in the fixing points of accelerometers and the impulse input processed according to the relationship (3).

If we compare the graph's characteristics with the deflection and the observed stage of brake development, we can see their obvious interrelationship. There was visible increase of deflection [5], under the load of about 35 kN, while high bending stress resulted in the initiation of breaking process. These load values are accompanied by visible in the graph, local trend disturbance in changes of measures of propagation of vibration.

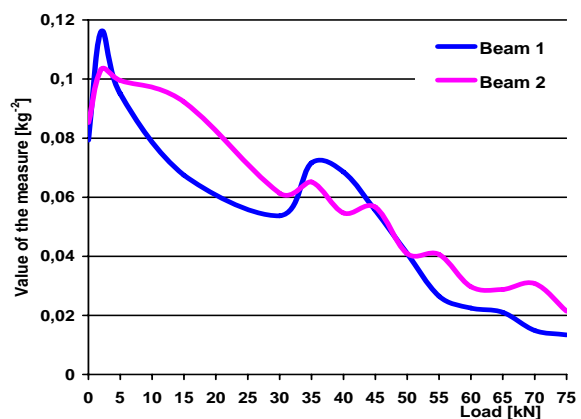


Fig. 1. Changes in measures of propagation of vibration energy in function of load

It seems to be the effect of change in vibration form resulting from non-linearity of structure that modifies the ways of propagation of vibroacoustic energy. Susceptibility of the measures of vibroacoustic energy propagation to structural non-linearity illustrated in the graph is related to the direction of input force which in this case is perpendicular to the direction of load and the breaking surface. The localization of accelerometers makes the wave spreading in the structure after the impulse input pass the particularly damage-prone

zone. Different input direction or another location of accelerometers result in lower diagnostic susceptibility of the measures set according to the formula (3) to a particular damage. Therefore, for the diagnostic usefulness of measures in the context of their susceptibility for structural non-linearity in the most damage-prone zones it becomes crucial to relate the localization of vibroacoustic signal transducers with the spot and input direction.

4. MINIMIZATION OF VIBRATIONS AND NOISE

The approach has been applied in improving the prototype solutions of power transmission unit of an atypical environment-friendly vehicle. The innovative construction idea and lack of previous experience with similar machines made it necessary to determine main noise sources in the cabin, as well as the ways of propagation of vibroacoustic energy in order to establish noiseless conditions.

Extensive studies applying highly developed measurement techniques, backed with the professional scientific software allowed analysis that let us identify causes of excessive noisiness. As a result, several modifications were suggested, which improved the exploitation conditions of the vehicle.

The key tests of vibrations and noise in the vehicle were carried out in form of passive road experiment on the real object. The attention was put on guaranteeing comparable measurement conditions (mainly velocity). Further stages of testing, designed to verify and improve the methodology include also some active experiments at the laboratory test-bed. They concern basically separate units of the vehicle.

In the experiment the vibrations of selected points on the body of power unit were recorded, as well as the noise in two places within the cabin (near the heads of the driver and of the passenger) during acceleration, with constant speed of 60 km/h and during breaking with the power unit. The set of two accelerators and two microphones collaborating with a portable computer via the measurement module by National Instruments, the computer being programmed in the environment LabView. Time courses were sampled in frequency of 50 kHz. The main elements of the set used in the tests are shown in the diagram in the Figure 2.



Fig. 2. The measurement equipment

While analyzing the results an outstanding propagation of vibroacoustic energy between the power unit and the cabin of vehicle became visible. The interrelationship between the vibrations generated by the main power units (the engine and the two-step belt toothed gear) and noise in the cabin resulted in a detailed identification of the ways of transmission of noise and vibrations.

The main construction element of the vehicle in question consists of closed aluminium profile (load-supporting beam) joined with the power unit using a self-aligning joint. The tests have shown that the construction solution applied determines transmission of vibrations of the whole power unit onto the load-supporting profile. Flat surfaces of the profile become secondary sound sources in the cabin and induce the body vibrations. In this case “cutting” this way of propagation of vibroacoustic energy seems to be necessary (in the spot marked with the red arrow in the diagram below – see Figure 3).

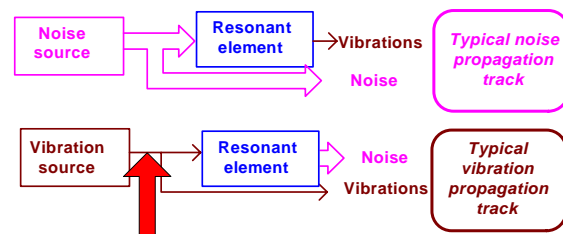


Fig. 3. Diagram of vibrations and noise propagation

The self-aligning joint of the power unit with the main construction element of vehicle should allow rotation in a minor angle range and at the same time stabilize the unit in relation to the two remaining axis. This is what substantially limits the area of possible solutions of minimizing the vibrations transmission. However, it is clear that proper damping elements should be used.

For minimizing the transmission of vibrations from the power unit to the load bearing beam two axially symmetrical elements made of rubber and metal were used, fixed on pins stiffly joined with the body of power unit. The rubber was 75 degrees Shore hard. Having applied the modification the resultant sound level in the cabin dropped (comparable experiment conditions) by more than 6 dB(A) which means more than two times lower amplitude of acoustic pressure.

The applied solution eliminates the main way of propagation of vibroacoustic energy between the power unit and the driver’s cabin. However, it does not influence the noise transmitted directly by the air in form of sound wave. To reduce the negative influences in this area we should “cut” the typical way of sound propagation using close soundproof barriers.

5. CONCLUSIONS

The work described in the article is a part of a project aiming at elaborating the methodology of using information contained in the vibroacoustic signal for monitoring vehicles and reducing their noisiness. The results seem to confirm usefulness of the measures of propagation of vibroacoustic energy as parameters applicable for evaluating the object's state. At the same time we can see that an extensive analysis, backed by both modeling and experimental research on mechanisms of transmitting vibrations is a proper tool for efficient minimization of vibroacoustic nuisance of machinery.

In spite of complexity of the problems outlined in this article it can be already said that the direction of studies and research has been positively verified. The cases confirm that consistent strategy realized according to the outlined philosophy lead to technical application of assumed parameters.

LITERATURA

- [1] Dąbrowski Z.: *Modeling and identification of nonlinear system for technical diagnostics*. The 8th International Congress on Sound and Vibration, Hong Kong, China, 2001, pp. 1083÷1090.
- [2] Dąbrowski Z., Radkowski S., Dziurdź J., Dybała J., Mączak J., Tomaszek S.: *Kształtowanie właściwości wibroakustycznych elementów i zespołów maszyn (uwagi*

metodyczne), Warszawa 2000 (ISBN 83-912190-4-6).

- [3] Radkowski S., Szczurowski K.: *The Influence of Stress in a Reinforced and Pre-stressed Beam on the Natural Frequency*, Workshop of COST on NTD assessment and new systems in pre-stressed concrete structures, COST Action 534 New materials and systems for pre-stressed concrete structures. Kielce 19-21.09.2005, 160-170.
- [4] Klekot G.: *Globalne miary wibroakustyczne jako narzędzie oceny stanu na przykładzie zmiennego stopnia uszkodzenia sprężonej belki betonowej*, Przegląd Mechaniczny nr 12/06, Warszawa 2006, strony 11-14.
- [5] Dziurdź J.: *Wpływ obciążenia belki betonowej sprężonej na jej drgania po wymuszeniu impulsowym*, Diagnostyka, Vol. 36 (2005), Warszawa 2005, strony 67-72.



Dr eng. **Grzegorz KLEKOT**, assistant professor at the Institute of Machine Design Fundamentals, Faculty of Automobiles and Heavy Machinery Engineering, Warsaw University of Technology, member of the Polish Society of Technical Diagnostics.

MODELLING AND SIMULATION OF THE DYNAMIC STRUCTURE OF THE VIBRATION FORCING SYSTEM OF THE PRESTRESSING SYSTEM

Andrzej JURKIEWICZ, Piotr MICEK, Marcin APOSTOŁ, Dariusz GRZYBEK

Department of Process Control, AGH University of Science and Technology
Kraków, Poland, , Tel/fax: 0048 12 617 30 80
e-mail: jurkand@agh.edu.pl

Summary

The intensive researches, which are conducted at the KAP AGH, led to a creation of the prestressing system. This system consists of among other the tensioning and transporting devices and the series of types of the anchoring block cooperating with the devices. The next stage of the development of this technology was the building of laboratory stand which enables to conduct the static and fatigue researches of the prestressing system elements. This stand consist of body with actuators system, hydraulic pulsator, universal station for plunger supplier, crosshead – connecting-rod system, cooling system, Spider-Hottinger measuring and control system. A definition of work parameters of the vibration forcing system and their effect on the obtained characteristics of the real system vibrations at high safety requirements calls for expensive experiments. The mathematical model of the vibration forcing system was built with the purpose of the minimization of this costs. This mathematical model was implemented in the Matlab Simulink program. The article presents the mathematical model and the results of simulation and operating research.

Keywords: vibration, prestressing, simulation.

MODELOWANIE I SYMULACJA STRUKTURY DYNAMICZNEJ UKŁADU WYMUSZANIA DRGAŃ USTROJU SPRĘŻAJĄCEGO

Streszczenie

Dzięki współpracy z przemysłem w AGH powstało Laboratorium Badań i Analiz Maszyn i Budowli wyposażone w stanowisko do badań statycznych i dynamicznych pras, bloków kotwiących, zakotwień oraz ustrojów sprężających. Stanowisko to składa się z ramy nośnej, układu siłowników oraz hydraulicznego, nurnikowego wzbudnika drgań. Zostało zaprojektowano zgodnie z wymogami Eurokodów i Euronorm, które zakładają uzyskanie wysokich parametrów niezawodnościowych w fazie projektowej oraz w fazie badań weryfikacyjnych ustrojów sprężających. Określenie parametrów pracy układu wymuszania drgań oraz ich wpływ na uzyskiwane przebiegi drgań rzeczywistego badanego obiektu przy wysokich wymaganiach bezpieczeństwa całego systemu wymaga wykonania szeregu kosztownych badań. Aby zminimalizować te koszty zbudowano matematyczny model układu wymuszania drgań, który zaimplementowano w środowisku Matlab Simulink. W artykule zaprezentowano budowę modelu matematycznego oraz wyniki badań symulacyjnych i eksploatacyjnych.

Słowa kluczowe: drgania, sprężanie, symulacja, badania.

1. INTRODUCTION

This article presents a results of researches, which were conducted in order to a definition of the influence of the constructional, hydraulic and electric parameters on the vibration characteristics in a real prestressing system. Because of the high cost of the real system research, the simulation research was conducted. For this purpose the mathematical model of the vibration forcing system was built. The elaborated model was implemented in Matlab Simulink program.

The laboratory stand to the strength research consists of the following components (fig. 1):

- frame (1),
- cylinders set of tensioning of prestressing system (2),
- operating elements of the hydraulic pulsator (3),
- hydraulic pulsator (4),
- electro-hydraulic set controlling the set of tensioning of prestressing system,
- cooling system (5),

- measurement and control system.

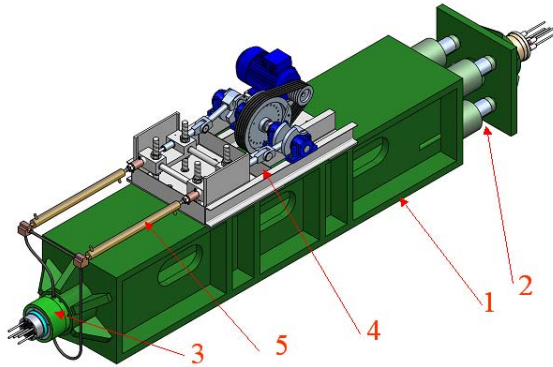


Fig. 1. View of the research stand

The hydraulic pulsator (fig. 2) consist of the frame (1), asynchronous motor (2), belt transmission (3), connecting rod (4), crosshead system (5), plungers and slides set (6), cooling system (7), operating element of the plunger hydraulic vibration generator (8).

The hydraulic pulsator is realized through two plungers system droved by crankshaft-crosshead system with pulsation frequency of 4-8 Hz. The supplier construction allow the vibration generator working control by the amplitude and hydraulic impulse shape changing. The schematic diagram of the stand construction is shown in fig. 1.

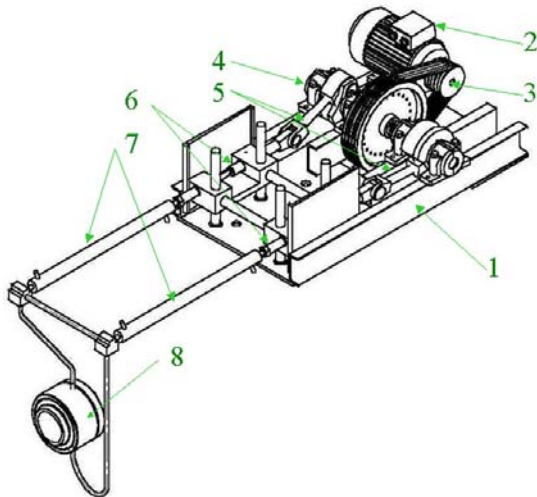


Fig. 2. View of the hydraulic pulsator

The operating element – hydraulic vibration generator is presented in fig. 3 i 4. The structure of this element enables the replacement of main seals without the interruption of research cycle. This assumption was basic in the design process of hydraulic pulsator.

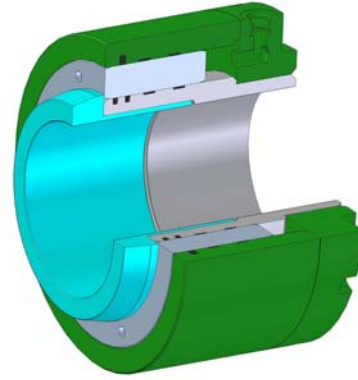


Fig. 3. The view of the vibration generator

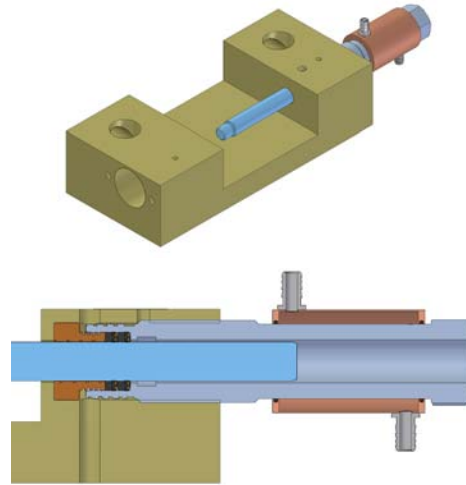


Fig. 4. The view and intersection of plunger block (piston)

2. ASSUMPTIONS OF THE MATHEMATICAL MODEL

Before beginning of studies simplifying assumptions for mathematical model were established.

1. Working medium temperature is constant, so that their properties are unchangeable.
2. String elastic forces are linear.
3. Elastic forces and moving elements friction resistances can be described by linear equations.
4. Losses caused by working medium leakage don't appear.
5. Till reaching maximum value of the pressure unit is supplying by constant efficiency source.
6. In all local elements there is turbulent flow.

These assumptions should be compared every time with calculations results.

3. MATHEMATICAL MODEL

After taking into consideration above model simplifying assumptions, the calculation scheme, which is shown in fig. 5, were constructed. Medium flow intensities in the analyzed unit and the elements

influence on pressure and load balance are shown on those scheme. In case of limited length of this paper only hydraulic part of the model is presented.

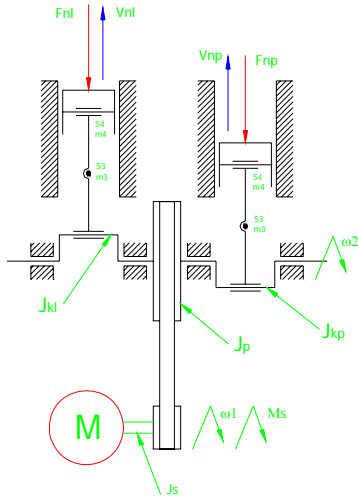


Fig. 5a. Calculation scheme of the drive part

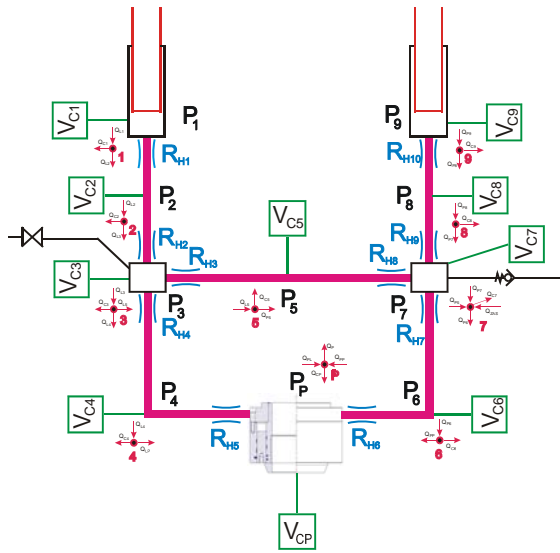


Fig. 5b. Calculation scheme the hydraulic part

The mathematical model of the plunger supplying hydraulic system consists of the following basic equations:

- dynamic equation of the hydraulic pulsator working elements motion
- flow intensity balance equation for the hydraulic system specific nodes.

The hydraulic pulsator (fig. 6) force balance equation:

$$F_c + F_B + F_m - F_p - F_{op} = 0,$$

hence:

$$m \frac{d^2x}{dt^2} + B \frac{dx}{dt} + k_c x = A_p \cdot P_p + k_{op} \cdot x \quad (1)$$

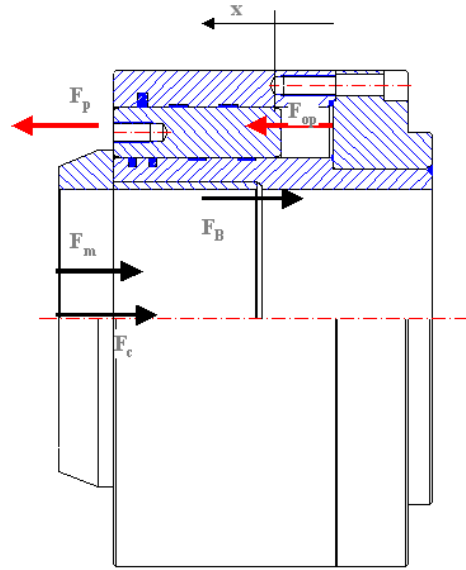
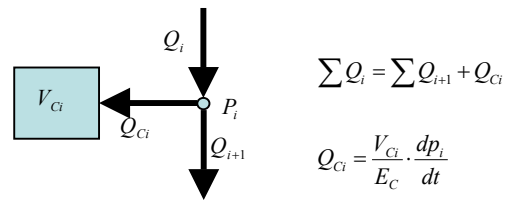


Fig. 6. The force distribution of the hydraulic pulsator

The medium pressure in the specific nodes were calculated from the flow intensity balance $Q_{ci} = \sum Q_i$ after substitution $Q_{ci} = \frac{V_c}{E_c} \cdot \frac{dp_i}{dt}$ and bilateral

integration: $p_i = \frac{E_c}{V_c} \int \sum Q_i \cdot dt$



The flow intensities coming in and out of the node were calculated as a difference of pressures between nodes. The pressure losses in lines and losses caused by medium inertia are situated at some characteristic places of system were assumed. For model simplifying losses were concentrated at elements causing local pressure losses. The equation [1] describes the pressure between the specific nodes:

$$p_i - p_{i-1} = \lambda_i \cdot \rho \cdot \frac{L_i}{2 \cdot D_i \cdot A_i^2} \cdot |Q_i| \cdot Q_i + \xi_i \cdot \frac{8 \cdot \rho}{\pi^2 \cdot D_i^2} \cdot |Q_i| \cdot Q_i + \frac{\rho \cdot L_i}{A_i} \cdot \frac{dQ}{dt} \quad (2)$$

After integration of both sides of the equation:

$$Q_i = \frac{A_i}{\rho \cdot L_i} \int \left(p_i - p_{i-1} - \lambda_i \cdot \rho \cdot \frac{L_i}{2 \cdot D_i \cdot A_i^2} \cdot |Q_i| \cdot Q_i - \xi_i \cdot \frac{8 \cdot \rho}{\pi^2 \cdot D_i^2} \cdot |Q_i| \cdot Q_i \right) dt \quad (3)$$

Above equations were used to all nodes in system, however flow intensity produced by plungers and hydraulic pulsator movement is written as:

$$Q_{Ai} = A_i \cdot \frac{dx_i}{dt} \quad (4)$$

4. SIMULATION RESEARCH

The mathematical model was elaborated on the basis of the taken assumptions and the computational scheme. It consist of several basic elements: hydraulic cylinder model (hydraulic pulsator), mechanical and hydraulic supplying system as well as the model of the asynchronous motor.

A lot of the simulation research of the generator was conducted. The verified laboratory research of the vibration generator was also conducted. The measurement scheme is shown in fig. 7. The exemplary results of the laboratory research are shown in fig. 11-16.

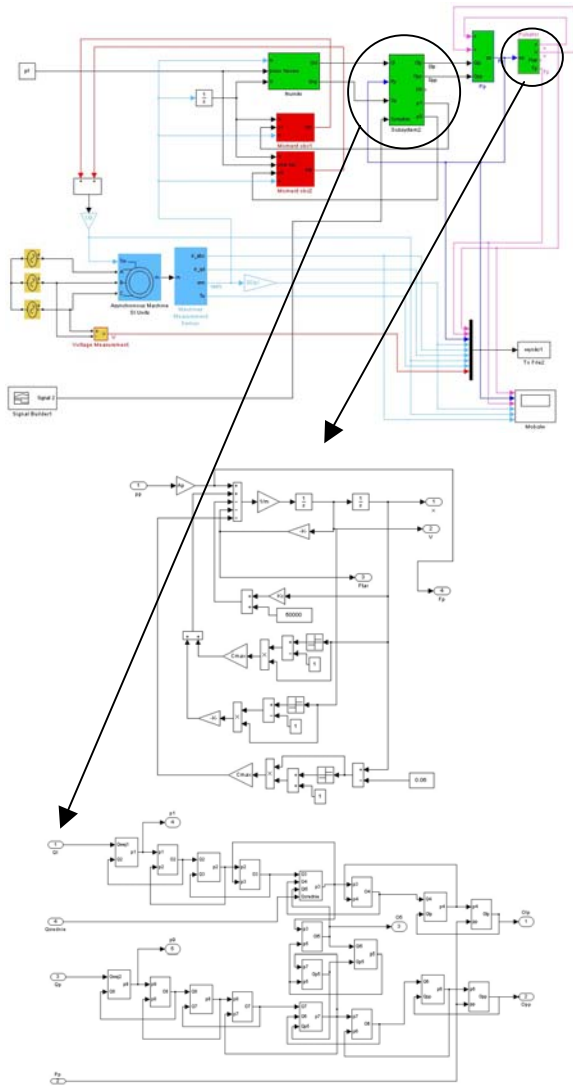


Fig. 7. Simulation diagram for the hydraulic pulsator

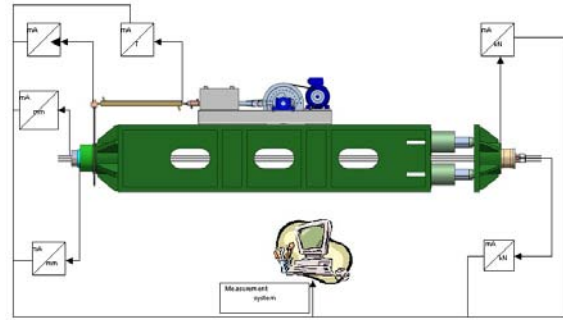


Fig. 8. Schema of the measurement system in the laboratory stand



Fig. 9. View of the fasten of force sensors



Fig. 10. View of the SPIDER 8 measurement system

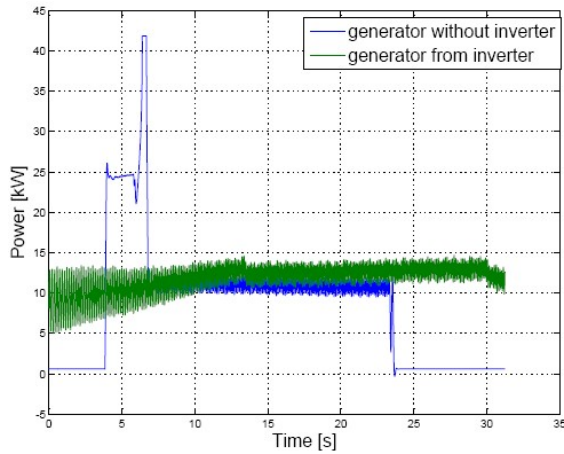


Fig. 11. The comparison of the useful power of generator for the motor feeding from electrical system and from frequency inverter

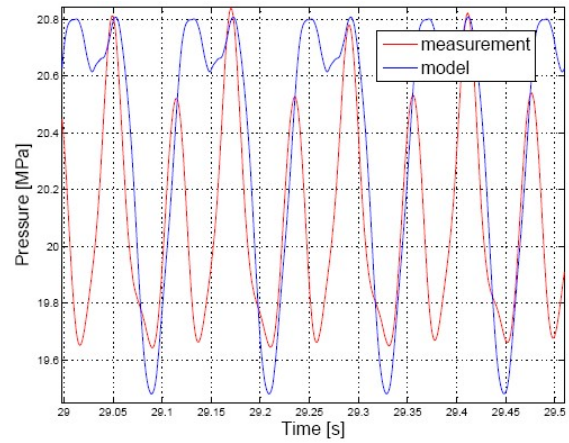


Fig. 14. The verification of the generator pressure for the angle of 15° phase shift of the split pulley

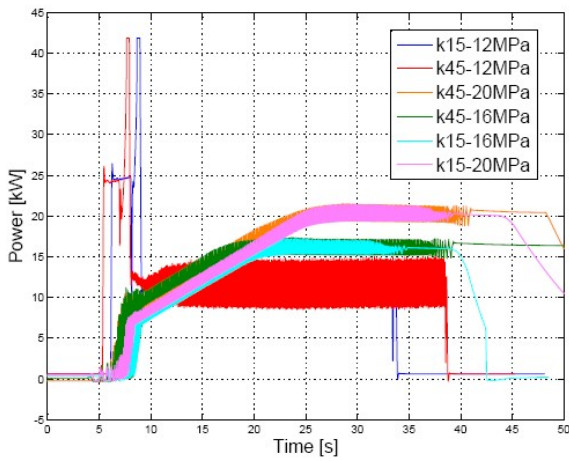


Fig. 12. The comparison of the useful power of generator for the different angles of the phase shift of split pulley and different supplying pressure

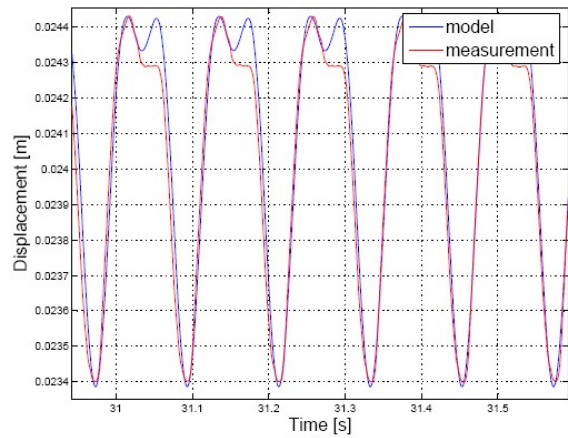


Fig. 15. The verification of the piston displacement of the pulsator for the angle of 15° phase shift of the split pulley

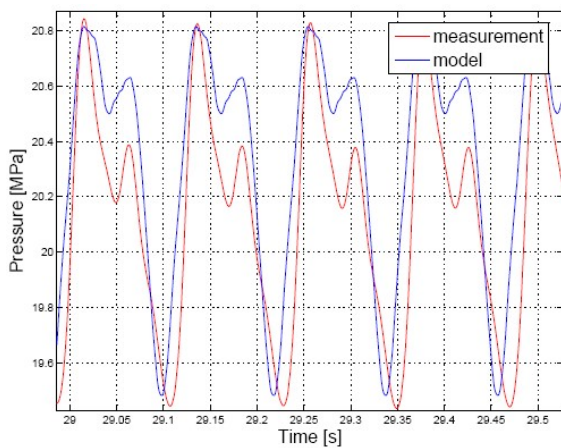


Fig. 13. The verification of the generator pressure for the angle of 45° phase shift of the split pulley

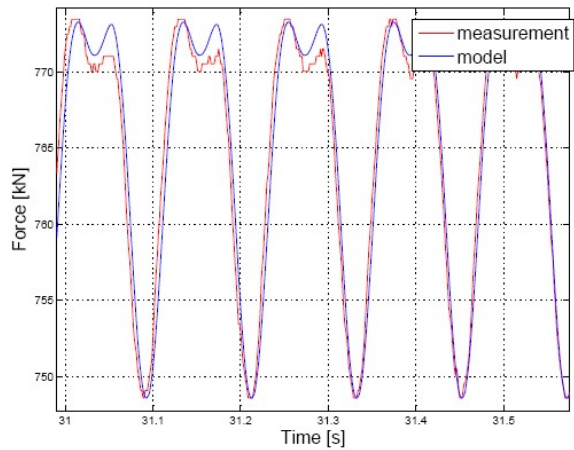


Fig. 16. The verification of the generator force for the angle of 15° phase shift of the split pulley

5. CONCLUSIONS

The presented above model of the vibration forcing system enables:

- research and testing of different structure. Due to it the correction of the research parameters like temperature, energy consumption and dynamic parameters is possible,
- analysis of the effect of crank and phase shift of the split pulley on the energy parameters,
- analysis of the effect of eccentric shift on the correction of amplitude, the energy and dynamic
- research of the different control algorithms of research parameters particularly maximal pressure value (medium),
- analysis of the other solution of the operating elements which can give energy recovery (parallel cylinder, disc with springs).

The results of the conducted simulation in Matlab Simulink program as well as the laboratory experiments confirm the correctness of elaborated mathematical model. The simulation tests give the knowledge about the interactions between hydraulic, geometric and energetic parameters in the system and become the contribution to the stand construction optimization.

REFERENCES

- [1] Stryczek S.: *Napęd hydrostatyczny*, WNT, Warszawa, 1990.
- [2] Jurkiewicz A., Apostoł M., Cygankiewicz T.: *Technology of individual tensioning of strings in pre-stressed constructions - development and the implementation work*, Acta Montanistica Slovaca, 1/1998, s. 37-42.
- [3] Jurkiewicz A., Apostoł M., Kot A.: *Simulation researches and laboratory tests of anchor plates for post-tensioned prestressed concrete technology*, ICC, Slovak Rep. 2000.
- [4] Apostoł M., Cygankiewicz T., Jurkiewicz A.: *Laboratory stand for ASIM type anchor blocks research for prestressed post-tensioned concrete technology, legal with Eurocodes and Euronorm*, ICC, Krynica 2001.

DAMAGE IDENTIFICATION IN PRESTRESSED STRUCTURES USING PHASE TRAJECTORIES

Wojciech BATKO, Leszek MAJKUT

Department of Mechanics and Vibroacoustics
AGH University of Science and Technology
batko@agh.edu.pl, majkut@agh.edu.pl

Summary

The work deals with the utilization of the diagnostics of prestressed structures. Considered in work damage were: change (the decrease) the tension force as well as the crack in the prestressed element. Phase trajectories were determined by simulation on analytical Bernoulli-Euler model of beam. In order to compare the sensitivity proposed method of diagnosis (changes in phase trajectories) the other vibro-based damage detection symptoms are shown (the first natural frequency).

Keywords: prestressed structures, diagnostics, crack, phase trajectories.

IDENTYFIKACJA USZKODZEŃ KONSTRUKCJI SPRĘŻONYCH Z WYKORZYSTANIEM OBSERWACJI TRAJEKTORII FAZOWYCH

Streszczenie

Praca dotyczy wykorzystania trajektorii fazowych do diagnostyki struktur sprężonych. Analizowanymi w pracy uszkodzeniami były: zmiana (obniżenie) siły sprężającej oraz pęknięcie elementu sprężonego. Trajektorie fazowe wyznaczone zostały za pomocą symulacji na modelu Bernoulli-Eulera belki. Pęknięcie zamodelowano w oparciu o mechanikę pęknięcia i twierdzenie Castigliano. W celu porównania wrażliwości proponowanej metody diagnostyki (obserwacja zmian trajektorii fazowych) porównano ją ze zmianami częstości drgań własnych uszkodzonego elementu sprężonego.

Słowa kluczowe: struktury sprężone, diagnostyka, pęknięcie, trajektorie fazowe.

1. INTRODUCTION

The detection of damages in concrete prestressed elements of building constructions determines the serious challenge for present technique. The used at present non-destructive procedures of diagnosis the damages, it means the method: visual observations, ultrasonic, radiographical, or magnetical analysis, possess the many essential limitations. The most often to effective their utilization, it is necessary to carry out many of additional actions connected with correctness of diagnosis process, as well as the a priori knowledge about the place of potential damage. From here using these methods in places with difficult access, and on early stage of damage evolution is limited and burdened with large uncertainty.

Mentioned above conditions required research on finding the new methods of damage detection, the global one, which based on changes of dynamic response of constructions, would permit to estimate degree of damage. This approach was checked out with the changes of different useful measures of wave propagation in prestressed constructions (eigenfrequency, eigenvectors, damping factor, amplitudes of forced vibration), going out with

assumption, that they are the function of physical properties of diagnosed construction (mainly the stiffness) connected with the current state of the system. They are the object numerous publications [3, 4]. But in processes of diagnosis connected with these methods the essential difficulty is the matters connected with nonstationarity of measuring conditions, or the changes of construction conditions (temperature, humidity, unknown loads of diagnosed construction) could cause the change of dynamic properties. It imposes the necessity of use a complicated algorithms and the techniques of the measured signals processing, dedicated the processes of symptoms separation.

Helpful information in building such diagnostic of damage detection system could be found by computer simulations. Computer models are based on accepted models of defects and could lead to new observational premises.

The content of present article with this direction of investigations is connected. Going out with methodology of investigation of technical stability [2] and conception of it connection with tasks of diagnostics [1], we seek on the numeric experiments of prestressed beam, the relationships of type "defect - symptom", which could be helpful

for process of damage detection of studied constructional elements.

2. PRINCIPLE OF PRESTRESS

Principle of prestress is shown in fig. 1

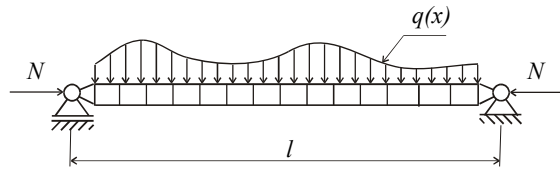


Fig. 1. Principle of prestress

If a set of separate elements was subjected by a compressive force, it can carry its own weight as well as possible external transverse load - $q(x)$. These loads lead to appearing of a tension zone in transverse section. Shown in fig. 1 set of elements does not possess any tensile strength, but it gains this strength thanks to compressive force N .

In fig. 2 the distribution of stresses was showed in the most loaded section of prestressed element. The distribution of reduced stress depends on point where the compressive force is applied.

In the first case the force is applied in beam axis therefore the stress (from compression) has solid value. In the second case the compressive force is applied in $1/3$ height of beam, what causes to create the complex state of stress - the bending with the tension - therefore linear distribution of stress.

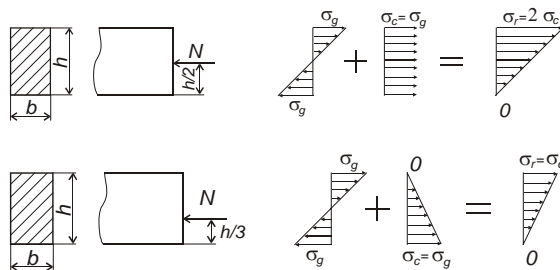


Fig. 2. Stress distribution

In both cases of compression, in no phase of element work, in no fibre of transverse section the tensile stress will not appear. Only larger or smaller compressive stress will appear.

In dependence however on the point of the compressive force applying to obtain the same effect it is necessary, in first case (the force in centre of the beam height), to apply the twice larger force N , and also the maximum compressive stress is twice larger than in the second case. In case of eccentric compression it is possible to apply material about twice-smaller ultimate compressive stress k_c so, it is more economical solution.

Assuming, that the force is applied in $1/3$ height of beam we can define the maximal value of the compressive force:

$$N_{\max} = b \cdot h \cdot k_c$$

where:

b, h – the dimensions of the beam cross section,
 k_c – the ultimate compressive strength.

3. DESCRIPTION OF THE PROBLEM

Analysed beam model in fig. 3 is shown

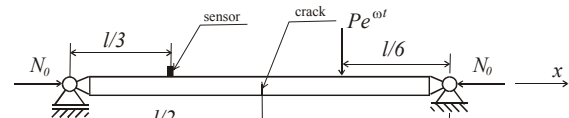


Fig. 3. Model of analysed beam

The equation of motion of the beam can be written as

$$X^{(4)}(x) + \beta X''(x) - \lambda^4 X(x) = 0 \quad (1)$$

where: $\beta = \frac{N}{EI}$; $\lambda^4 = \frac{\rho A}{EI}$; ρ - mass density of the beam, $A = b \times h$ - the cross-sectional area, EI - bending stiffness, N - compressive force.

The solution of equation (1) has form:

$$X(x) = P \cosh \kappa_1 x + Q \sinh \kappa_1 x + R \cos \kappa_2 x + S \sin \kappa_2 x \quad (2)$$

where:

$$\kappa_1 = \sqrt{\frac{-\beta + \sqrt{\beta^2 + 4\lambda^4}}{2}}; \quad \kappa_2 = \sqrt{\frac{\beta + \sqrt{\beta^2 + 4\lambda^4}}{2}}$$

Integral constants P, Q, R, S depends on boundary conditions.

In work, two kinds of prestressed element damage were considered: the loss of prestress, that is the decrease the force N_0 and a crack in the element (without the loss in prestress).

As a damage symptoms the change of phase trajectories were used. The trajectories are determined in section with co-ordinate $x = l/3$ (sensor in fig. 3).

As excitation a harmonic force with amplitude P and frequency ω was accepted. About frequency was assumed that it has been smaller than the first natural frequency of the beam.

Proposed method sensibility has been compared with sensibility of method based on measurement the first natural frequency.

4. LOSS IN PRESTRESS

The compressive force is most often introduced by tensioning of a prestressed concentrate wire either before hardening of concentrate - prestressing, or after hardening - posttensioning.

Every prestressed element may lose some of its prestress force due to creep and relaxation from a long period of service under design or overloaded vehicles.

Fig. 4a shows the changes of phase trajectories, and fig. 4b shows the first natural frequency change for the prestressed beam with force $N_0 = 0.7 N_{\max}$.

An analysed damage was the change (percentage decrease) of the prestressed force.

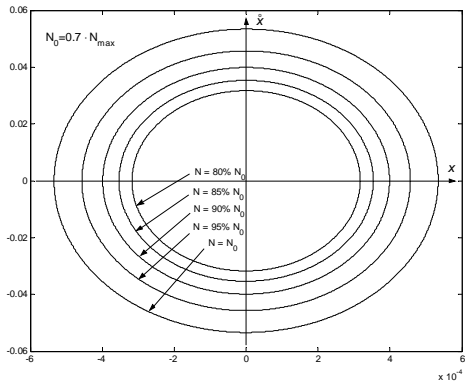


Fig. 4a. Damaged beam phase trajectories

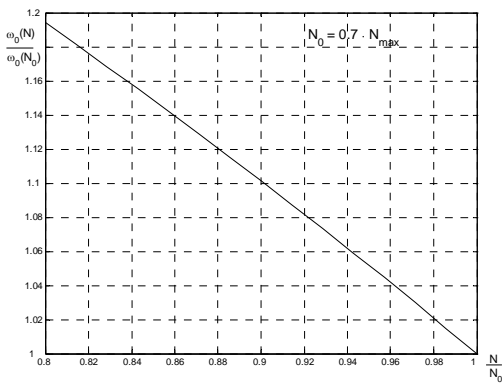


Fig. 4b. Natural frequency changing

Fig. 5a shows the changes of phase trajectories, and fig. 5b the first natural frequency change for the beam with prestress force $N_0 = 0.5 N_{max}$

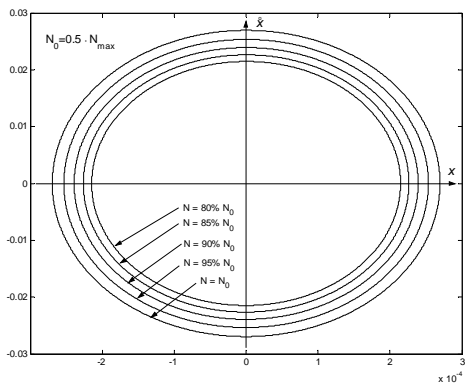


Fig. 5a. Damaged beam phase trajectories

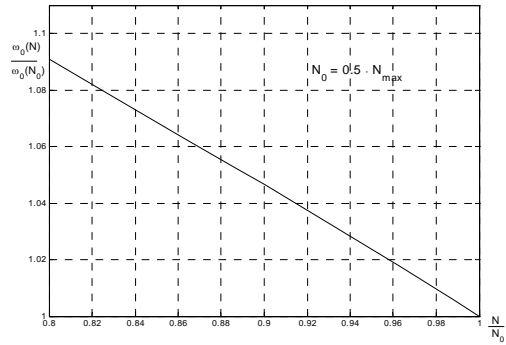


Fig. 5b. Natural frequency changing

Fig. 6a shows the changes of phase trajectories, and fig. 6b the first natural frequency change, for the beam with force $N_0 = 0.3 N_{max}$

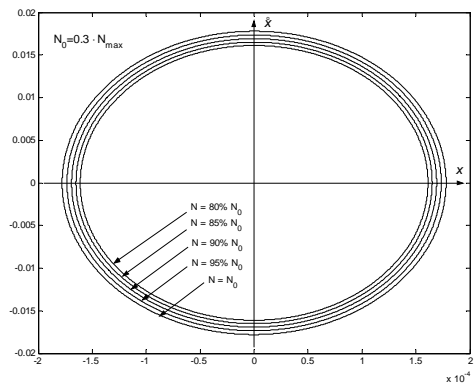


Fig. 6a. Damaged beam phase trajectories

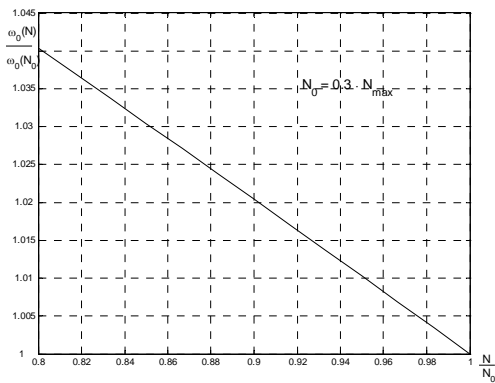


Fig. 6b. Natural frequency changing

Analysis of curves showed in figs 4, 5 and 6 leads to conclusion that the observation of phase trajectories permits to detect the smaller change in compressing force than the first natural frequency change. Therefore the proposed method of diagnostics is more sensitive than the most often used method based on the eigenfrequency change method.

5. CRACK MODEL IN PRESTRESSED BEAM

The model of crack is based on fracture mechanics laws and Castigliano theorem [9, 10].

The fracture mechanics studies allows finding relations between global quantity G - Energy Release Rate determining the increase in elastic strain energy for infinitesimal crack surface increase [11]:

$$G = \frac{\partial U}{\partial A_p}$$

and local quantity K - Stress Intensity Factor (SIF), which is function of crack depth a :

$$G = \frac{1-\nu^2}{E} \cdot K_I^2$$

where:

- G - energy release rate represents the elastic energy per unit crack surface area,
- A_p - area of crack,
- ν - Poisson ratio,
- E - Young modulus,
- K_I - Stress Intensity Factor (SIF) of mode I .

In case of prestressed element one have to take under consideration fact that the normal stress come from both bending moment and the longitudinal (prestressed) force, that is

$$K_I = K_{I_g} + K_{I_w}$$

K_{I_g} - Stress Intensity Factor of mode I for bending moment M_g ,

$$K_{I_g} = \sigma_g \cdot \sqrt{\pi \cdot a} \cdot F_{I_g} \left(\frac{a}{h} \right)$$

where:

- σ_g - normal stress from bending moment,
- a - depth of crack,
- F_{I_g} - correction function [6],

K_{I_w} - SIF of mode I for axial force N_0 ,

$$K_{I_w} = \sigma_w \cdot \sqrt{\pi \cdot a} \cdot F_{I_w} \left(\frac{a}{h} \right),$$

where:

- σ_w - normal stress from axial force,
- F_{I_w} - correction function [6].

Total increase the elastic strain energy due to the crack has form

$$U = \int_{A_p} G dA_p.$$

The above designations demonstrate that elastic strain energy will depend on: square of bending moment $M_g(x_p)$, square of longitudinal (prestressed) force N_0 and product of both $M_g(x_p)$ and N_0 .

Hence, the crack has been modelled as [2x2] flexibility matrix containing c_g and c_w coefficients on the main diagonal, and flexibility coefficients c_{gw} and c_{wg} outside the diagonal. Relation between displacements (longitudinal $u(x)$ and lateral $y(x)$) from the right and left hand side of the cross-section with crack and longitudinal force N_0 and bending moment $M_g(x_p)$ in this cross-section is given by matrix relation [9, 10]:

$$\begin{bmatrix} c_g & c_{gw} \\ c_{wg} & c_w \end{bmatrix} \begin{bmatrix} M_g(x_p) \\ N_0 \end{bmatrix} = \begin{bmatrix} y'(x_p^+) - y'(x_p^-) \\ u(x_p^+) - u(x_p^-) \end{bmatrix}$$

Individual flexibilities included in the flexibility matrix can be calculated using the Castigliano theorem:

$$c_g = \frac{\partial^2 U}{\partial M_g^2(x_p)} \quad c_w = \frac{\partial^2 U}{\partial P_w^2(x_p)}$$

$$c_{gw} = \frac{\partial^2 U}{\partial M_g(x_p) \partial P_w(x_p)}$$

$$c_{wg} = \frac{\partial^2 U}{\partial P_w(x_p) \partial M_g(x_p)}$$

According to the Schwarz's theorem the sequence of differentiation has no effect on the final result, which means that $c_{gw} = c_{wg}$.

6. DIAGNOSTICS OF CRACKS IN PRESTRESSED ELEMENT

Described in section 5 model of crack was used to analysis of changes of phase trajectories as well as first frequency the prestressed beam. As it is showed in fig. 3 crack is in beam centre ($x_p = l/2$).

Fig. 7a shows the changes in phase trajectories, and fig. 7b the change in first natural frequency for the beam with prestress force $N_0 = 0.7 N_{max}$. An analysed damage was the change (increase) the relative crack depth - $\alpha = a/h$.

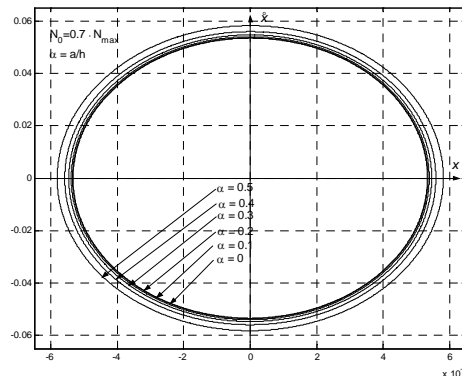


Fig. 7a. Damaged beam phase trajectories

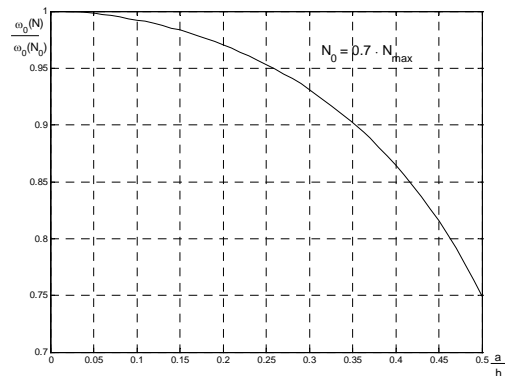


Fig. 7b. Natural frequency changing

Fig. 8a shows the phase trajectories changes and fig. 8b the change in the first natural frequency for the beam with prestress force $N_0 = 0.5 N_{max}$.

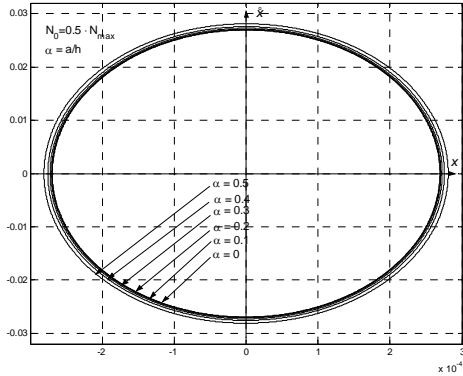


Fig. 8a. Damaged beam phase trajectories

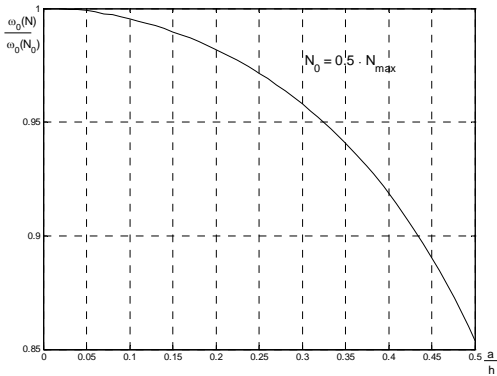


Fig. 8b. Natural frequency changing

Fig. 9a shows the phase trajectories changes and fig. 9b the change of the first natural frequency for the beam with prestress force $N_0 = 0.3 N_{max}$.

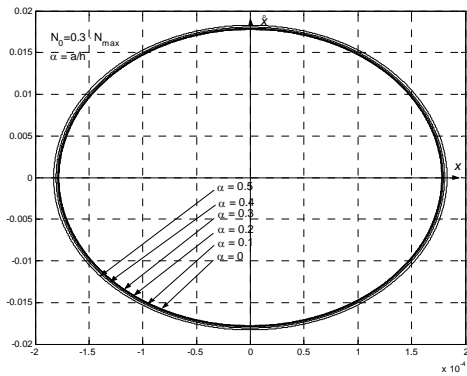


Fig. 9a. Damaged beam phase trajectories

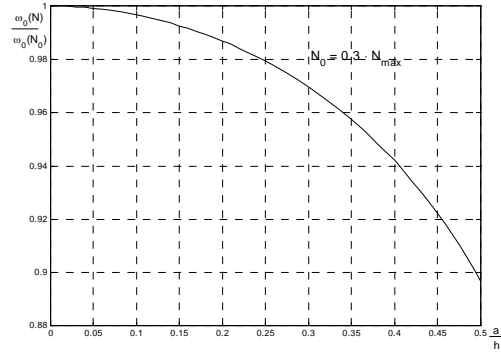


Fig. 9b. Natural frequency changing

The change of trajectories showed in figs 7, 8 and 9 leads to conclusion that the observation of phase trajectories permits to detect the crack the prestressed element.

7. SUMMARY

Analysis of the diagrams showed in figs 4-9 leads to conclusion that the observation of phase trajectories permits to detect the damage of prestressed element. The comparison of the trajectory changes (figs "a") and first natural frequency (figs "b") permits to affirm that the proposed method of diagnostics is more sensitive.

The observation of crack element trajectories (figs 7-9) could lead to wrong conclusion that this method of diagnostics is not suitable to detect this kind of damages. The change of phase trajectories strongly depend on this, how "far" the frequency of excitation is from the beam natural frequency. For example if we want to monitor crack in beam with prestress force $N_0 = 0.3 N_{max}$, we may "better" choose the frequency of excitation in diagnostic experiment. Results in such case were showed in fig. 10.

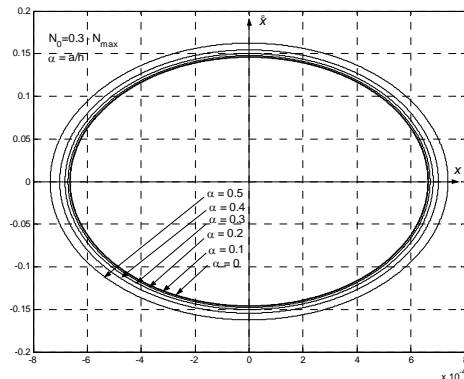


Fig. 10. Damaged beam phase trajectories

LITERATURE

- [1] Batko W.: *Stateczność techniczna – nowa perspektywa modelowa dla budowy rozwiązań systemów monitorujących zmiany stanu maszyn*. Mat.XXXIV Ogólnopolskiego Sympozjum Diagnostyka Maszyn. Wyd. Wydz.Transportu Politechnika Śląska CD-Węgierska Górka 2007.
- [2] Bogusz W.: *Stateczność techniczna*, PWN, Warszawa 1972.
- [3] Carpinteri A., Spagnoli A., Vantadori S.: *Mechanical damage of ordinary or prestressed reinforced concrete beams under cyclic bending*. Engineering Fracture Mechanics 72(2005) pp. 1313-1328.
- [4] Hamed E., Frosting Y.: *Free vibrations of cracked prestressed concrete beams*. Engineering Structures 26(2004) pp. 1611-1621.
- [5] Kaufman S., Olszak W., Eimer Cz.: *Budownictwo betonowe*, tom III Konstrukcje sprężone, Arkady, warszawa 1965.
- [6] Murakami Y.: *Stress Intensity Factors Handbook*, Pergamon Press Oxford, 1987.
- [7] Majkut L.: *Identyfikacja pęknięcia w belkach na podstawie pomiaru częstości własnych kwartalnik* AGH Mechanika 24 (2005).
- [8] Majkut L.: *Identyfikacja pęknięcia w belkach o znanych warunkach brzegowych*. Diagnostyka, 2004, 32 str. 107-116.
- [9] Majkut L.: *Modelowanie pęknięcia w wibroakustycznej diagnostyce według modelu*. Diagnostyka, 34 (2005), str. 15-22.
- [10] Majkut L.: *Wibroakustyczne symptomy pęknięcia belki*, Zagadnienia Eksploatacji Maszyn, 40 z.4, str. 165-181.
- [11] Neimitz A.: *Mechanika pęknięcia*, Warszawa PWN 1998.
- [12] Olszak W.: *Konstrukcje wstępnie sprężone*. Tom 1, PWN Warszawa 1955.



Prof. dr hab. inż. **Wojciech BATKO**, prof. zw. AGH ur. 1949. Kierownik Katedry Mechaniki i Wibroakustyki AGH, autor i współautor ponad 230 publikacji, w tym 12 książkowych. Zajmuje się zagadnieniami dynamiki i wibroakustyki maszyn oraz zagadnieniami diagnostyki technicznej.



Dr inż. **Leszek MAJKUT** (ur. 1970), absolwent Wydziału Elektroniki, Automatyki, Informatyki i Elektrotechniki AGH (1995). Pracę doktorską dotyczącą wpływu lokalnej zmiany sztywności na amplitudę drgań i widmo częstości obronił w 1999 na Wydziale Inżynierii Mechanicznej i Robotyki AGH w Krakowie. Obecnie prace badawcze dotyczące diagnostyki wibroakustycznej, problemów związanych z odwracaniem modeli diagnostycznych oraz szeroko pojętej teorii drgań (drgania, wibroizolacja, hałas), ze szczególnym uwzględnieniem układów ciągłych i dyskretno-ciągłych prowadzi w Katedrze Mechaniki i Wibroakustyki AGH.

This work was done as a part of research project
N 504 042 32/3443.

STABILITY IN TECHNICAL DIAGNOSTICS

Wojciech BATKO

Department of Mechanics and Vibroacoustics
AGH – University of Science and Technology
Al. Mickiewicza 30, 30-059 Kraków, fax: +48 (12) 633-23-14, email: batko@agh.edu.pl

Summary

The aim of the paper is the presentation of new methodological approach in the machine state monitoring system building process. It is related to the attempt of state change monitoring task affiliation to the behavior (dynamics) testing task after some time from certain starting point. The work draws attention to the solutions of technical stability theory, which might be useful tool of machine state recognition algorithm building. It describes its relation to the tasks defining monitoring system building that is: possible exploitative deviations with the dynamic behavior of the monitored object, the problem of diagnostic symptoms choice and the quantification levels choice allowing making the diagnostic decisions. It also covers possible methods of their implementation. It points to the purposefulness of phase image change of the diagnostic signals control, assigning to them the value of useful tool of process identification of origin and development of faults in the monitored object.

Keywords: stability, monitoring, dynamic behaviour, damage identification.

STATECZNOŚĆ W DIAGNOSTYCE TECHNICZNEJ

Streszczenie

Celem pracy jest prezentacja nowego podejścia metodologicznego w procesie budowy systemów monitorujących stan maszyn. Wiąże się on z próbą powiązania zadania monitorowania zmian stanu kontrolowanego obiektu, z zadaniem badania jego zachowań (dynamiki) po upływie pewnego czasu od wybranego punktu startowego. Praca kieruje uwagę na rozwiązania teorii stateczności technicznej, które mogą być użytecznym narzędziem budowy algorytmów rozpoznawania zmian stanu monitorowanej maszyny. Opisuje jej powiązanie z określającymi budowę systemu monitorującego zadaniami tj.: badaniami możliwych zaburzeń eksploatacyjnych z zmianami zachowań dynamicznych monitorowanego obiektu, problemem wyboru symptomów diagnostycznych oraz doбором poziomów ich kwantyfikacji, umożliwiającą podejmowanie decyzji diagnostycznych. Omawia możliwe metody dla ich realizacji. Wskazuje na celowość kontroli zmian obrazów fazowych kontrolowanych sygnałów diagnostycznych, przypisując im walor użytecznego narzędzia identyfikacji procesu powstawania i rozwoju uszkodzeń monitorowanego obiektu.

Słowa kluczowe: stateczność techniczna, monitorowanie, zachowania dynamiczne, identyfikacja uszkodzeń.

1. INTRODUCTION

The function analysis of the monitored object heavily depends on its construction parameters and its exploitation conditions determining its dynamic behavior. Given such conditions monitored object's behavior might be foreseen by theoretical means, as for mechanical object and the deviation from the planned movement estimated thus assessing their acceptability from the exploitative point of view. The defining procedures might bring a new dimension to the monitoring process, bringing it down to simple analysis.

Lets assume that the monitored object is defined by the differential equations:

$$x_1 = f_1(x_1, \dots, x_n, t) \quad (1)$$

$$x_n = f_n(x_1, \dots, x_n, t)$$

where:

$$x^i = \frac{d x_i}{d t}; i = 1, \dots, n$$

$f: \mathbf{W} \rightarrow \mathbf{R}$ is some open subset of $\mathbf{R}^n \times \mathbf{R}$.

Its behavior is given by the equation set (1) solution and its differentiable function $\Phi_t = (\Phi_{t1}, \dots, \Phi_{tm})$ defined in the range $I \subset \mathbf{R}$, for which $(\Phi_t, t) \in U$, for each $t \in I$ fulfilling the condition:

$$\dot{\Phi}(t) / dt = f(\Phi(t), t) \text{ for each } t \in I \quad (2)$$

The projections (1) and (2) describe each point of phase space, their dynamics and location and also the behavior of the tested system for each coordinate. The describing solution of the monitored dynamic system (1) is given by function $\Phi_t(x(0))$, where $x(0) = (x_1(0), x_2(0), \dots, x_n(0))$ is the initial condition.

Its form $\Phi_t(x(0))$ assigns in any moment t , the position of the initial point $x(0)$ after time t in phase space and its trajectory reflects the evolution of the tested system.

So the dynamic behavior analysis of the tested object might be reduced to its trajectory analysis and related to them change assessment task as a response to initial condition change or acting driving forces

2. THE RELATIONSHIPS OF TECHNICAL STABILITY PROBLEM TO THE CONTROLLED OBJECT'S STATE CHANGE MONITORING PROCESS

From the controlled object's state change monitoring point of view there are important questions of assessment of possible behavior of the trajectories in the span of observation time. They relate to the question if the trajectories reflecting the technical state of the tested object, starting from any point of the surroundings of $x(0)$ after time t , will appear again in proximity of this point. It might be formed as a question of trajectory attraction area, that is the neighborhood U of set $A \subset W$ where for each $x(0) \in U$ the trajectory $\Phi_t(x(0))$ remains in $U(A)$ and tends to A , when $t \rightarrow \infty$.

The answers to those questions might be related to the stability testing of the state space points and their trajectories. A good testing criteria to solve a number of tasks appearing in the monitoring process of the machine state change might a criteria of technical stability [6], deciding about the resistance of the controlled object to the deviations appearing during the exploitation time. It decides about the limitations of the dynamic system movement solutions with existing deviations influencing the system during the exploitation time caused by initial conditions change or the acting forces. The result of small deviations from the stable state is widely assumed to be a stability criteria.

For such assessment it is necessary to make some assumptions:

- acceptable deviation of movement trajectory from its stationary state (from the point of view of safe exploitation of the analyzed object);
- acceptable range of changes for initial conditions;

- predicted level of external and internal disturbances constantly influencing the controlled object during its exploitation.

The question of stability of the analyzed technical object with forces $f(x, x, t)$ and disturbances $R(x, x, t)$ acting on it, and its movement described by the equation:

$$\ddot{x} = f(\dot{x}, x, t) + R(\dot{x}, x, t) \quad (3)$$

demands analysis of its solution and answering the questions:

- Does the system have zero-solution and what is the course of the solution in the neighborhood of the zero-solution?
- What are the areas of initial conditions, where solutions coming out of them have the same qualitative course?
- What is the influence of perturbations

$R(\dot{x}, x, t)$ of right side of the equation (1) on qualitative course of the solution?

Taking into consideration that requirements, the definition of technical stability for mechanical system described with the differential equations:

$$\dot{x} = f(x, t) + R(x, t) \quad (4)$$

where x, f, R are vectors in the \mathfrak{R}^n space:

$$x = \begin{bmatrix} x_1 \\ x_2 \\ \dots \\ x_n \end{bmatrix} \quad f = \begin{bmatrix} f_1 \\ f_2 \\ \dots \\ f_n \end{bmatrix} \quad R = \begin{bmatrix} R_1 \\ R_2 \\ \dots \\ R_n \end{bmatrix} \quad (5)$$

where functions $f(t, x)$ $R(t, x)$ are defined in a range included in $n+1$ -dimensional space:

$$t \geq 0, (x_1, x_2, \dots, x_n) \in G \subset E_n \quad (6)$$

where: E_n denotes linear normed n -dimensional space and functions $R_i(t, x_1, x_2, \dots, x_n)$ are disturbances acting constantly, with assumption:

$$\|R(t, x_1, \dots, x_n)\| \leq \delta \quad (7)$$

might be phrased as follows.

Let there be two ranges Ω and ω included in G such that Ω is closed, limited and includes origin of coordinates and ω is open and included in Ω .

Let us assume that the solution of the analyzed system (4) is $x(t)$ with the initial condition $x(t_0) = x_0$.

If for each x_0 belonging to ω , $x(t)$ stays in the range Ω for $t \geq t_0$ with disturbance function satisfying inequality (7), then the system (4) is technically stable in terms of range ω , Ω and limited constantly acting disturbances (7). According to this definition of technical stability,

each movement trajectory derived from the range ω is supposed to stay in the range Ω for $t \geq t_0$.

For monitoring systems, allowing monitored signals to momentarily exceed the accepted levels, the term of technical stability might be weakened to the condition where each trajectory exceeding the range ω is supposed to stay in the range Ω for $t_0 \leq t < T_0$, where $T - t_0$ is the duration of the movement. With such a condition we deal with a technical stability in limited time.

3. TECHNICAL STABILITY TESTING AND ITS DIAGNOSTIC RELATIONS

From the point of view of technical diagnostics, including the need of application of the technical stability theory solutions for the monitoring system development [1, 2], there are interesting questions of algorithm building for condition recognition for technical stability loss of the overviewed object. It could be realized by solving the system of differential equations (4) describing dynamic behavior of the monitored object or analyzing the course of their solution with qualitative methods.

The latter method might be tightly connected to the machine state changes monitoring process. It is related to the examination of the phase portraits of the solutions, that is curves $x(t), \dot{x}(t) = y$ on the plane x, \dot{x} called phase plane, which might be the subject of the monitoring. Such methods are usually included to the set of topological methods of solutions testing of differential equations (4). They allow dynamic behavior analysis of the monitored object, with the disturbances constantly acting and non-linear, which are significant for the fault appearing process [7, 9, 12], including their early phases.

Their testing procedures, based on some topological facts, related to the existence of some constants of homomorphic transformations formed as theorems, allow qualitative assessment of dynamic behavior of the analyzed object and related to it conditions of technical stability loss.

The most often used method is Lapunov method [10], where properties are used of properly chosen, for the dynamics description of the controlled object, scalar function $V(x, t)$. Its derivative testing along the solutions (behaviors) of the equation set (4) determines the decision leading to its stability.

The theorem on which it is based states that if there exist a scalar function $V(x, t)$ of the class C^1 , defined for each x and $t \geq 0$ fulfilling requirements:

$$V(x, t) > 0 \text{ for } x \neq 0$$

$$\dot{V}(x, t) \leq 0 \text{ along solutions of (4)}$$

$$\text{for } x \notin G - \omega \quad (6)$$

$$V(x_1, t_1) < V(x_2, t_2)$$

$$\text{for } x_1 \notin \omega \text{ and } x_2 \in G - \Omega; t_1 < t_2$$

then the object described by (4) is technically stable.

Referring results of that theorem to the issue of creating foundation for machinery state monitoring system, the Lapunov function $V(x, t)$ should be built and should be checked by means of measured trajectories x, y of the tested object conditions (6). In building the Lapunov function $V(x, t)$ directions from [3, 8] might be useful, or an effort made to define its form as total energy of the tested object.

Another way of testing the properties of the monitored trajectories from the point of view of the stability assessment of the monitored dynamic system is its testing by means of two functions [4]:

$$\Phi(x, y) = xy + \dot{x} \dot{y}; \Psi(x, y) = x \dot{y} - \dot{x} y \quad (7)$$

Of which the positive or negative definition allow to assess the character of the monitored movement. Their dependent values allow assigning to the points of trajectories a direction characteristic for the point of entry, exit or slip related to the analyzed curve, which helps in determining the ranges G and Ω in the range of the monitored phase space.

The construction foundation for quantifier of the monitored trajectories properties from their stability point of view might also be searched based on the topological retract method – Ważewski method [12]. In that method ranges are built, limited with curves of the points of entry and exit of the equation set (4) solutions, from the ranges accepted as allowable.

As it emerges from the synthetic review of the technical stability testing methods [5] their usage for the monitoring system development is related to two tasks [1]:

1. Creation of the measurement tools providing observation of the phase portraits changes for the dynamic behavior of the monitored node of the system, defined by measurement:

$$x(t), \dot{x}(t) = y$$

2. Building of the quantifier for the monitored courses by implementation of the technical stability testing algorithms, based on the Lapunov function method or two functions $\Phi(x, y)$ and $\psi(x, y)$ method or the retract method.

From the practical realization of the monitoring system point of view, the solution for the task one is not problematic. There are more inconveniences with determining positively or negatively defined Lapunov function for the monitored construction and the differential equation set describing its dynamics. The significant simplification of the task appears when the monitoring system with defined location of the measurement sensors is dedicated to modal parameters change of the controlled object. In case of using the two functions $\Phi(x, y)$ and $\psi(x, y)$ method there may some difficulties appear in solving their functional equations, necessary to

draw their zero-adjustment curves. A significant advantage of the method is fact that both functions for a non-linear system have identical form, which makes the method more universal for different applications. The usage of the retract method in turn forces the necessity of building some curve-limited range on which there are only points of entry or points of exit which might appear as a significant application problem.

4. SUMMARY

Diagnosed object's state change testing – considered as a task of nonlinear dynamic system behavior analysis which state changes with time – creates a new applicational perspective for monitoring system construction. It might be related to the task of technical stability loss conditions testing in the analyzed object. In technical application it means the necessity of phase image testing of the dynamic behavior of the tested object, related to the chosen conditions of the stability loss assessment. It is considered in relation to the assumed range of constantly acting disturbances and the initial condition range. It well defines the process of transition of the object into the state of functional incapacity. It relates fully to the non-linear physics of the phenomenons describing the process. It ties realized recognition with the dynamic state of the monitored object and with its constructional and exploitational parameter changes, which makes it universal.

The practical application of the phase trajectory change control method seems to be very useful tool of fault emerging and development process identification. It might be its main quality factor and is easily adoptable to practical application. It is not filtering non-linear effects and phenomenons of frequency structure change of the monitored diagnostic signals related to the fault development, which might be its very unique advantage.

It might be easily adapted to the task solutions related to the estimation of the time needed for the monitored variables to leave their acceptable range or issues demanding stability loss probability estimation. It also allows monitored object's behavior analysis by random disturbances and to phrase estimations of their infallibility.

LITERATURE

- [1] Batko W.: *Technical stability – a new modeling perspective for building solutions of monitoring systems for machinery state* (sent for printing to ZEM).
- [2] Batko W., Majkut L.: *Damage identification in prestressed structures using phase trajectories*. Diagnostyka 4(44)/2007. s. 63-68.
- [3] Barbasin E. A.: *O postroenii funkcii Lapunova*. Diferencjalnye uravnenija, 4, 12, 1968, 2127-2158.
- [4] Bogusz W.: *A two tensor method for investigation nonlinear systems*. Proceedings of Vibration Problems. Warszawa, 1961 2, No3.
- [5] Bogusz W.: *Technical stability*. PWN Warszawa 1972.
- [6] Bogusz W.: *Stability of the Process in Nonlinear Automatic Control Systems*. Zeszyty Naukowe AGH, Automatyka, nr 3, 1969.
- [7] Dąbrowski Z.: *Problems of nonlinear models identification. In monograph: Modern methods of vibroacoustic process' testing*. Wyd. ITE PIB Series: The library of Exploitation Problems, part 1, p.7-34, 2005.
- [8] Gurel O., Lapidus L.: *A Guide to the generation of Lyapunov function*. J. Ind. and E. Chem. Vol. 61, 3, p.30-41, 1969.
- [9] Kiciński J.: *Conjugate forms of nonlinear vibrations as new tool in crack testing of revolving shafts*. In monograph: Modern methods of vibroacoustic process' testing. Wyd. ITE PIB Series: The library of Exploitation Problems, part 1, p.35-66. 2005.
- [10] Kozin F.: *On Almost Sure Stability of Linear Systems with Random Coefficients*. J.Math and Phys., vol.42, 1, 1968.
- [11] La Sale J. P., Lefschetz S.: *An outline of Lapunow stability theory and his direct method*. PWN Warszawa 1966.
- [12] Radkowski S.: *Vibroacoustical diagnostics of low-energy faults*. Wyd. ITE PIB, Series: The library of Exploitation Problems, Warszawa-Radom, 2002 r.
- [13] Ważewski T.: *Sur un principe topologique de l'examen de l'allure asymptotique de integrals de equations differentieles ordinaries*. Ann. Soc. Polon. Math. No. 20, 1947.



Prof. dr hab. inż.
Wojciech BATKO
Specjalność naukowa:
wibroakustyka, diagno-
styka techniczna. Zainte-
resowania naukowe:
diagnostyka techniczna,
systemy monitorujące,
wibroakustyka, dynamika
maszyn, teoria drgań

OPTIMAL DISTRIBUTION OF SUB-ASSEMBLIES IN STORES OF FACTORY BY EVOLUTIONARY ALGORITHMS

Bogna MRÓWCZYŃSKA

Faculty of Transport, Silesian University of Technology,
 Krasińskiego 8, 40-019 Katowice, e-mail: bogna.mrowczynska@polsl.pl

Summary

The paper deals with an application of evolutionary algorithms for optimisation of sub-assemblies distribution in the stores of factory. Numerical model is presented. The fitness function is expressed as a function of distances between stores and assembly rooms and costs of inner transport. Penalty function is used to include restrictions. The results showed that the applied method is the efficient tool for solving such problems.

Keywords: evolutionary algorithm, optimisation, store.

OPTYMALIZACJA ROZKŁADU PODZESPOŁÓW W MAGAZYNACH FABRYKI PRZY POMOCY ALGORYTMÓW EWOLUCYJNYCH

Streszczenie

W artykule przedstawiono zastosowanie algorytmów ewolucyjnych do optymalizacji rozłożenia podzespołów i materiałów wykorzystywanych w produkcji w magazynach zakładu produkcyjnego. Przedstawiono model numeryczny problemu. Funkcję przystosowania wyrażono jako funkcję odległości pomiędzy magazynami a halami montażowymi i kosztów wewnętrznego transportu między nimi. Ograniczenia na pojemność poszczególnych magazynów uwzględniono stosując funkcję kary. Otrzymane wyniki są optymalne i potwierdzają skuteczność algorytmów ewolucyjnych w rozwiązywaniu tego typu problemów.

Słowa kluczowe: algorytmy ewolucyjne, optymalizacja, magazyn.

1. INTRODUCTION

Storage is one of the most important link of the logistic chain [4]. Functional efficiency of the storage depends on the storage systems [3]. Optimisation of sub-assemblies distribution in stores of factory is one of such elements. The proper allocation of the sub-assemblies influences the costs of inner transport. There are real money paid for fuel, amortisation and costs of employment of operators of fork-lift trucks. As usual, no optimisation is applied.

This paper presents an application of evolutionary algorithm for optimisation of sub-assemblies distribution in the stores of factory.

2. NUMERICAL MODEL

The factory consist of eight assembly rooms and seventeen stores (fig. 1). The problem is, how to place all sub-assemblies in stores to minimise costs of inner transport used to carry sub-assemblies from store to assembly rooms. Every sub-assembly should be put in one store, but in every store can place a few sub-assemblies. Every store has its capacity. The volume of all sub-assemblies in one store couldn't overstep its capacity.

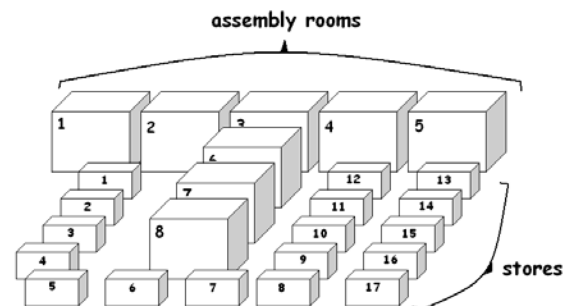


Fig. 1. The factory with assembly rooms and stores

Thus the problem of optimisation consist in finding minimum of the following function:

$$f = \sum_{j=1}^m \sum_{k=1}^l \sum_{i=n_j} C_{jk} \cdot d_{ik} \cdot l_{jk} \quad (1)$$

where

m - number of the sub-assemblies,

l - number of the assembly rooms,

n_j - the ordinal number of the store, in which is placed the i -th sub-assembly

C_{jk} - the costs of transport one unit of the j -th sub-assembly to the k -th assembly room (here $C_{jk} = 1$),

d_{ik} - the length of the road from the i -th store to k -th assembly room (table 1),

Table 1. The length of the road from the i-th store to k-th assembly room

length of the road [m]	assembly rooms								
	1	2	3	4	5	6	7	8	
stores	1	92,1557	102,6025	57,8305	134,316	21,6398	98,8715	89,1709	53,7264
	2	86,1861	96,6329	51,8609	128,3464	15,6702	92,9019	83,2013	47,7568
	3	80,2165	90,6633	45,8913	122,3768	9,7006	86,9323	77,2317	41,7872
	4	74,2469	84,6937	39,9217	116,4072	14,5509	80,9627	71,2621	35,8176
	5	68,2773	78,7241	33,9521	111,1838	20,5205	74,9931	65,6656	30,2211
	6	74,2469	72,7545	27,9825	117,1534	26,4901	69,0235	71,6352	36,1907
	7	80,2165	66,7849	22,0129	123,123	32,4597	63,0539	77,6048	42,1603
	8	86,1861	60,8153	16,0433	129,0926	38,4293	57,0843	83,5744	48,1299
	9	82,8282	54,8457	10,0737	135,0622	44,3989	51,1147	89,544	54,0995
	10	76,8586	48,8761	10,0737	141,0318	50,3685	45,1451	95,5136	60,0691
	11	70,889	42,9065	16,0433	147,0014	56,3381	39,1755	101,4832	66,0387
	12	64,9194	36,9369	22,0129	152,971	62,3077	33,2059	107,4528	72,0083
	13	65,6656	37,6831	27,9825	152,2248	68,2773	27,2363	111,5569	77,9779
	14	71,6352	43,6527	33,9521	146,2552	74,2469	21,2667	117,5265	83,9475
	15	77,6048	49,6223	39,9217	140,2856	80,2165	15,2971	123,4961	89,9171
	16	83,9475	55,965	46,2644	134,316	86,1861	9,3275	129,4657	95,8867
	17	91,4095	63,427	53,7264	128,3464	92,1557	16,7895	135,4353	101,8563

I_{jk} - number of unit j-th sub-assembly transfer to the k-th assembly room (table 2).

The constrains are described as follows:

$$h = \sum_{i=1}^n w_i \sum_{j=1}^m (V_{ij} - V_{gi}) \quad (2)$$

where

V_{ij} - volume of the j-th sub-assembly in the i-th store,

V_{gi} - capacity of the i-th store,

w_i - penalty coefficient.

Table 2. The number of the unit j-th sub-assembly, which were transferred to the k-th assembly room

unit per week	assembly rooms								
	1	2	3	4	5	6	7	8	
sub-assemblies	1	51	85	102	0	68	85	0	68
	2	51	0	102	119	0	0	0	34
	3	68	85	0	119	68	68	0	68
	4	0	0	0	0	0	0	51	51
	5	51	0	0	0	68	0	0	51
	6	0	0	102	0	0	68	0	0
	7	17	51	0	0	68	0	0	17
	8	0	17	0	0	17	0	0	17
	9	0	0	0	0	0	51	0	0

If $\sum_{j=1}^m (V_{ij} - V_{gi}) > 0$ then the i-th store is overloaded and $w_i > 0$.

If $\sum_{j=1}^m (V_{ij} - V_{gi}) \leq 0$ then the i-th store is not overloaded and $w_i = 0$.

Thus the optimisation problem consist in finding minimum of the following function:

$$\tilde{f} = \sum_{j=1}^m \sum_{k=1}^1 \sum_{i=n_j} C_{jk} \cdot d_{ik} \cdot I_{jk} + \sum_{i=1}^n w_i \sum_{j=1}^m (V_{ij} - V_{gi}) \quad (3)$$

3. EVOLUTIONARY OPTIMISATION

The problem of optimisation of the sub-assemblies distribution in the stores of the factory is solved by an evolutionary algorithm. It is one of the methods of artificial intelligence. The evolutionary algorithm is inspired by natural evolution. The algorithm of the evolutionary optimisation is presented in Fig. 2. The algorithm has been described in details elsewhere [1, 2].

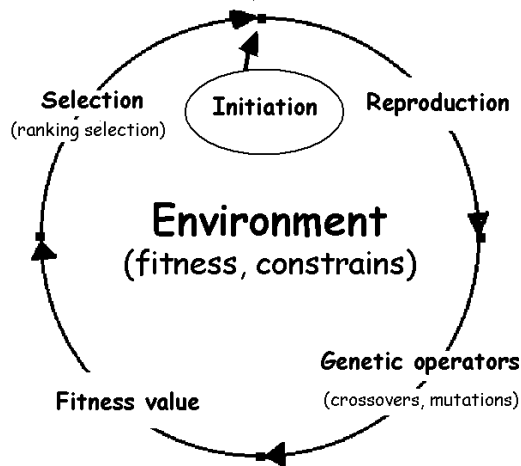


Fig. 2. An algorithm of evolutionary optimisation

Environment

The problem is formulated as follows:

The k-th chromosome from the population, which represents the possible solution is expressed in the form:

$$\mathbf{n}_k = \langle n_{k1}, n_{k2}, \dots, n_{k7} \rangle \quad (4)$$

where:

n_{ki} - i-th gene in the k-th chromosome. It is an ordinal number of the store, in which is placed the i-th sub-assembly.

The population is a set of chromosomes. They will evolve during all process of the artificial evolution.

Fitness function

Because the fitness function should be maximised, it is expressed as follow:

$$\hat{f} = \frac{1}{f} \quad (5)$$

If the value of the fitness function \hat{f} is higher then the solution is better. The optimal solution is obtained by maximising the fitness function with respect to \mathbf{n}_k .

Genetic operators

This evolutionary algorithm uses operators of a crossover (non-uniform crossover, arithmetic crossover, heuristic crossover) and a mutation (uniform mutation, boundary mutation, non-uniform mutation) described in [2]. The genetic operators work with the assumed probabilities. Several number of the tests were calculated in order to tune their proper running.

Selection

This evolutionary algorithm uses operators of the proportional selection in order to select better solutions. Elitist model is used to remember best solution [2].

4. RESULTS

The maximal size of the chromosome population used in the evolutionary computation was 100. The maximal length of the life was 20000. The calculation were repeated 100 times for every set of parameters. The probabilities of the evolutionary operators, the penalty coefficients and the results of the example calculations are presented in tables 3.

The value of the fitness function of the best solution is equal 0,9139. Almost all results fulfil all assumptions and constrains. The constrains were overloaded in the variant 2 and 3, but just this ones on every 100 repeated calculations. It happened for penalty coefficient equal 10. For less penalty coefficient it didn't happen. Thus the results are promising.

The diagram 3 presents the changes of the values of the fitness function trough all generations.

5. CONCLUSIONS

The paper presents the application of evolutionary algorithms for optimisation of the sub-assemblies distribution in the store of the factory to minimise costs of inner transport. The best solutions obtained during the evolutionary optimisation have the highest fitness value and they fulfils all the constrains. The worst results appeared infrequently only for the high value of the penalty coefficient.

The numerical model is simply. Thus the evolutionary algorithm is an efficient tool for solving such discrete optimisation problems.

Table 3. Results of evolutionary optimisation

Variant	Penalty coefficient	Probability of operators:						Value of the best fitness function	overload
		Non-uniform crossover	Arithmetical crossover	Heuristic crossover	Uniform mutation	Boundary mutation	Non-uniform mutation		
1	2	3	4	5	6	7	8	9	overload
1	15	0,9	0,9	0,9	0,1	0,1	0,1	0,8792	0
2	10	0,7	0,7	0,7	0,3	0,3	0,3	0,8763	20,094
3	10	0,8	0,8	0,8	0,2	0,2	0,2	0,8922	20,094
4	5	0,9	0,9	0,9	0,1	0,1	0,1	0,9139	0
5	5	0,8	0,8	0,8	0,2	0,2	0,2	0,9114	0
6	5	0,9	0,8	0,9	0,2	0,1	0,1	0,9131	0
7	5	0,8	0,9	0,9	0,2	0,2	0,1	0,9131	0
8	5	0,9	0,9	0,5	0,2	0,1	0,1	0,9139	0
9	5	0,9	0,8	0,7	0,1	0,2	0,3	0,9030	0
10	5	0,7	0,7	0,7	0,3	0,3	0,3	0,8761	0
11	5	0,9	0,8	0,7	0,3	0,2	0,1	0,9139	0

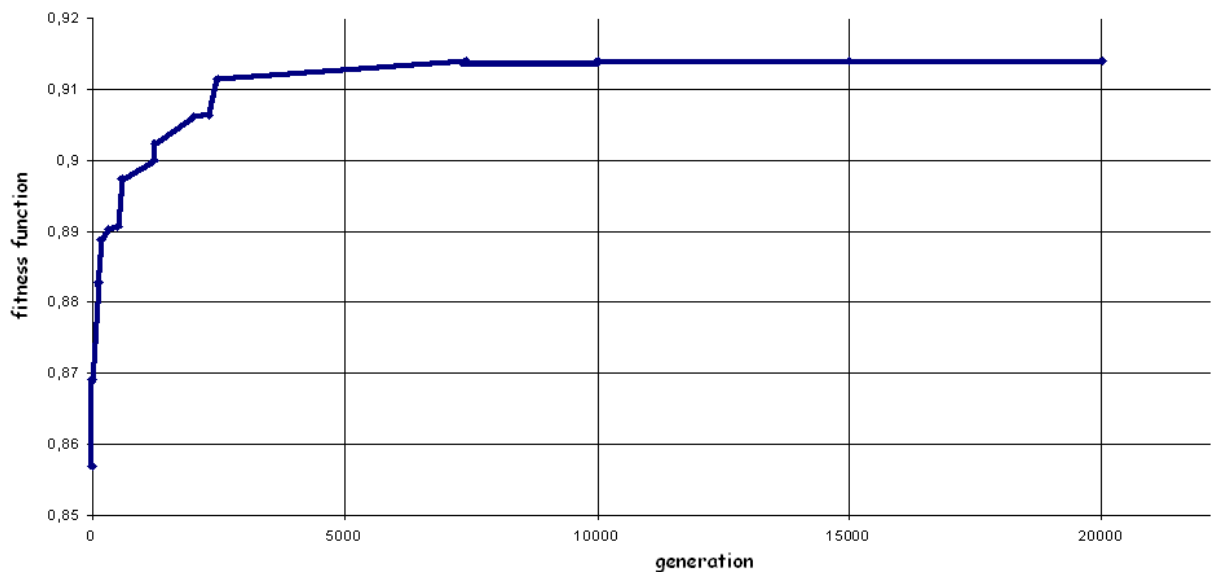


Fig. 3. The diagram of values of fitness function in the best variant

REFERENCES

- [1] Arabas J.: *Wykłady z algorytmów ewolucyjnych*. Wydawnictwo Naukowo – Techniczne, Warszawa 2001.
- [2] Michalewicz Z., *Genetic Algorithms + data Structures = Evolutionary Programs*. Springer-Verlag, Berlin 1996.
- [3] Mrówczyńska B.: *Optimal goods distribution in supermarket's store by evolutionary algorithms*. AI-METH Series, Gliwice, 2007.
- [4] Skowronek C., Sariusz – Wolski Z.: *Logistyka w przedsiębiorstwie*. PWE, Warszawa 2003.

ACTIVE THERMOGRAPHY AND IT'S APPLICATION FOR DAMAGE DETECTION IN MECHANICAL STRUCTURE

Tadeusz UHL, Mariusz SZWEDO

Akademia Górniczo-Hutnicza w Krakowie, Katedra Robotyki i Mechatroniki
Al. Mickiewicza 30, +48 12 634 35 05, tuhl@agh.edu.pl

Summary

Development of measurements techniques helps to apply new more effective tools for damage detection and localization of damage in composite and metal based structure. One of the most intensively developing technology is active thermography which can be directly use for damage detection under operational conditions. The paper presents active thermography techniques, proposed image processing methods and application of vibrothermography for damage (crack) detection in aluminum plate. The experimental results confirm high sensitivity of the methods and its applicability for mechanical structure diagnostics.

Keywords: SHM, NDT, thermography, damage detection, image processing, 2D wavelets analysis.

AKTYWNA TERMOGRAFIA I JEJ WYKORZYSTANIE DO DETEKCJI USZKODZEŃ STRUKTUR MECHANICZNYCH

Streszczenie

Rozwój technik pomiarowych umożliwia zastosowanie nowych, bardziej efektywnych narzędzi do detekcji oraz lokalizacji uszkodzeń w kompozytowych i metalowych strukturach. Jedną z najbardziej intensywnie rozwijających się technologii jest aktywna termografia, która może zostać użyta bezpośrednio do detekcji uszkodzeń w trakcie normalnych warunków pracy urządzenia. W artykule przedstawiono techniki aktywnej termografii, zaproponowano metodę przetwarzania obrazów termograficznych oraz aplikację wykorzystującą wibrotermografię do detekcji uszkodzeń dla płyty aluminiowej. Wyniki przeprowadzonego eksperymentu potwierdzają wysoką czułość metody oraz jej przydatność w diagnostyce.

Słowa kluczowe: SHM, NDT, termografia, detekcja uszkodzeń, przetwarzanie obrazów, dwuwymiarowa analiza falkowa.

1. INTRODUCTION

Nowadays a reliability of the mechanical structures is one of the mostly required feature of many structures like bridges, airplanes, rail vehicles, and many different industrial installations. Indicated below structures due to their responsibility should damage free and should be monitored continuously. The techniques of the assessment of state of operating structures are defined as Structural Health Monitoring (SHM) in the literature [1]. Among many new methods two main classes can be distinguished, passive methods and active methods [1, 2]. In passive methods, the response of the structure, due to any operation excitations (even not measured) is under observation. Based on relation of given signal parameter and its correlation with a state of the structure the damage can be detected, localize and sometimes predicted. In active methods the structure is excited by controlled and measured excitation using external or build in actuators and response is measured. Measured response or estimated based on input and output signals system characteristics can be a measure of system damage. One of the most commonly use in SHM method are

methods based on vibration measurements. Within these methods the symptom based methods and model based methods are in use, now. In the second one the measure of the state of the system are parameters of the model or changes of model parameters [3]. Many methods which are in use for SHM are methods which are directly adopted from the area of Nondestructive Testing (NDT).

Classical NDT methods used during system operation continuously like acoustic emission measurements [1], Lambda waves analysis [2], electromechanical impedance identification [3], are good examples of SHM oriented techniques. The difference between NDT and SHM methods is illustrated in the Fig. 1 and Fig. 2.

In these two solution two different classes of methods can be distinguish; methods with integrated sensors [4] and methods based on contactless measurements [3]. The last one are more and more often use because of lower installation costs and miniaturization of monitored structures.

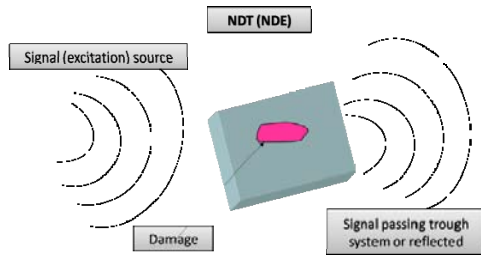


Fig 1 NDT like system

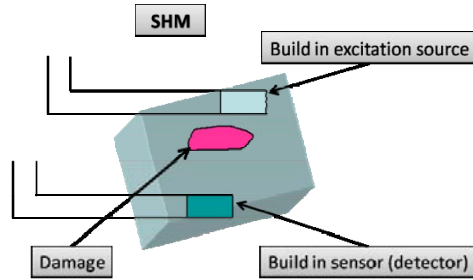


Fig. 2. SHM system

One of the method which can be applied as active and passive method based on contactless measurements is the method based on investigation of thermo-elasticity effect which goes with damage of the structure (lose structural integrity) like cracks in metal structures, delamination or disbonding in composites [5]. The method is under very intensive development, because thermography techniques are significantly developed recently [6]. The paper deals with testing of relation between structural damage and thermo elastic effect. The pattern recognition techniques developed by authors are applied to show sensitivity of the method and its applicability to detect cracks nucleation and propagation in the structure.

2. OVERVIEW OF ACTIVE THERMOGRAPHY TECHNIQUES

Basic theoretical relation employed for dynamic thermography is formula which describe relation between changes of strain, stress and changes of temperature of a body surface [6]:

$$\Delta\varepsilon = \frac{(1-2\nu)\Delta\sigma}{E} + 3\alpha\Delta T \quad (1)$$

where: $\Delta\varepsilon$ - changes of main strains, $\Delta\sigma$ – changes of main stress, ν - Poisson ratio, ΔT – changes of temperature, α – coefficient of thermal expansion, E - Young modulus. Assuming adiabatic transformation (high speed transformation of stress) the following relation between changes of strains $\Delta\varepsilon$ and changes of temperature ΔT is valid:

$$\Delta T = \frac{-3T\alpha K\Delta\varepsilon}{\rho C_v} \quad (2)$$

where: K – compression factor [Pa], C_v heat capacity [J/kg K] at constant volume, ρ – density [kg/m³], T temperature of a body [K].

As the result the formula which approximate relation between changes of temperature and changes of stress is obtained in the form:

$$\Delta T = -\frac{\alpha}{\rho C_p} T \Delta\sigma = K_m T \Delta\sigma \quad (3)$$

where: C_p heat capacity at constant pressure, K_m thermo elastic constant.

As it can be easily notice from formula (3) a change of temperature is proportional to changes of stress. To measure pure stress changes only temperature should be filtered using common signal processing procedure as DC component filtering. DC component filtering can be realized after pattern capture using special pattern processing technique or using dedicated technique for frame capturing using synchronization signal from energy source (thermal excitation).

The method helps to detect changes in stress fields due to damage of structure under active test. The structure should be thermally excited to achieve stress changes which can be measured using thermography. Applying the method the damage can be detected even if have very small dimension immediately after occurring.

To employ the method effectively the following conditions should be fulfilled:

1. The structure is loaded with dynamic load with frequency higher the 3 Hz (all formulas are valid for adiabatic transformation);
2. The DC component of temperature (T) can be filtered;
3. The damage occurred on the surface or very close to surface of a structure
4. Emissivity of the structure is equal or almost equal on the whole surface of a structure.

Listed above assumptions seriously limit classes of structure which can be tested using active thermography in order to detect damages.

Basic assumption in application of active thermography for SHM is that each structure has characteristic response for given excitation. In active thermography several different kind of excitation can be employed; ultrasound waves, vibrations and thermal excitation like infrared or microwaves excitations and other thermal radiation source. The excitation can have character of short impulse or continuous harmonic signal The response of the structure in a form of temperature distribution on surface which changes during system excitation is recorded using thermo camera. In the next step of thermography based SHM procedure the thermographic pattern of the structure in current

state is compared with pattern recorded for healthy system.

Within active thermography four different techniques can be distinguished which differ each other by the way of pattern acquisition or pattern processing.

- 1) Pulsed Thermography – the source of thermal excitation are heat impulses with duration from milliseconds to several seconds. Measurements of the response during cooling of the surface helps to avoid disturbances due to radiation of different heat source in surrounding of structure under the test. Recorded changes of temperature distribution and its comparison with the same temperature distribution for healthy system allows to assess damage location and damage dimension.
- 2) Lock-in Thermography – the source of thermal excitation In his case is harmonic heat flux. Reconstruction of the temperature distribution can be achieved in this method thanks detection of the amplitude and phase of temperature on a surface against excitation signal for given frequency.
- 3) Step-heating Thermography – the source of thermal excitation. In his method are short laser impulses which heat structure locally. The response in a form of a temperature changes (increasing) is recorded and process to find thermal conductivity. The local changes of thermal conductivity for the structure can help to detect damage In the structure.
- 4) Vibrothermography – the source of thermal excitation is vibration in a frequency range between 10 Hz till 20 kHz. The thermal response of the structure due to vibration is heat waves which are recorded using thermo camera The damage in a form of composite delamination or cracking of the structure can be detect based on measured thermal waves propagation disturbances. In the vibrothermography the temperature distribution is measured synchronically with vibration.

Typical scheme of a measurement system for vibrothermography of mechanical structures is shown in Fig. 3.

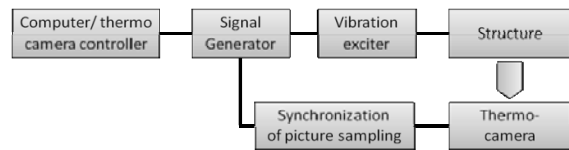


Fig. 3. Measurements set up for vibrothermography of mechanical structures

Due to vibrations the heat is radiated on the surface of a structure under test. This heat is generated on the level of micromechanical phenomena like particle dislocations, friction on a contact surface of cracks or delaminations of damages, local deformations of mode shapes are observed, which can be visualize using thermo camera. Time history of this deformations recorded during vibrothermography test is recorded and analyzed off-line, usually. Heat flux due to structural vibration depends strongly on frequency range [7, 8, 9]. In practical application of vibrothermography for SHM, test of sensitivity of the thermal field on the system surface due to change of excitation frequency should be done, and for the damage detection this frequency interval, in which the sensitivity is biggest has to be chosen. Employing of vibrothermography require external excitation of structural vibration in high frequency range (in higher frequency of vibration, intensity of heat radiation is significantly bigger then for low frequency) that can be done using external electromagnetic exciter or using build in small piezo actuators.

The vibrothermography permits to track changes in stress distribution directly, but classical active thermography in principle allows for testing only changes of thermal conductivity of the structure and cannot be directly applied for SHM like vibrothermography.

Authors experiences in application of the technique indicate that using vibrothermography the defects located deeper under the structure surface can be detected then with application of classical active thermography.

Nowadays many laboratories are intensively investigate possibilities of application of described above technologies for SHM purpose.

3. IMAGE PROCESSING TECHNIQUES APPLIED FOR THERMOGRAPHY BASED DAMAGE DETECTION

For damage detection in mechanical structure using active thermography authors proposed two steps image processing algorithm. Preprocessing image analysis Fig. 4, this step provide normalization of recorded images. Based on thermographic images non defected and defected structure, images differences were computed.

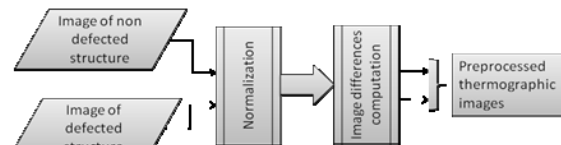


Fig. 4. Preprocessing part of deflection detect procedure

This step preparing data for another step of computation. Normalization image data from thermographic camera is necessary for proper correlation of data acquired for destructed and non destructed structure.

Preprocessed thermographic data let us for detecting areas of changed thermal energy flow (strain field).

Second step Fig. 5 established algorithm are based on wavelet transform for two dimensional signals.

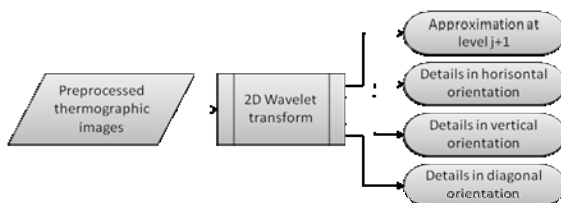


Fig. 5. Wavelet transform of preprocessed thermographic images

Authors picked up multilevel 2D stationary wavelet decomposition: **sym4** Fig. 6 (orthogonal wavelet).

This wavelet type were selected experimentally checking decomposition result for different types of them. Selected wavelet type gives mostly representative and wavelet decomposition results based on this type were best for damaged detection of the mechanical structure algorithms.

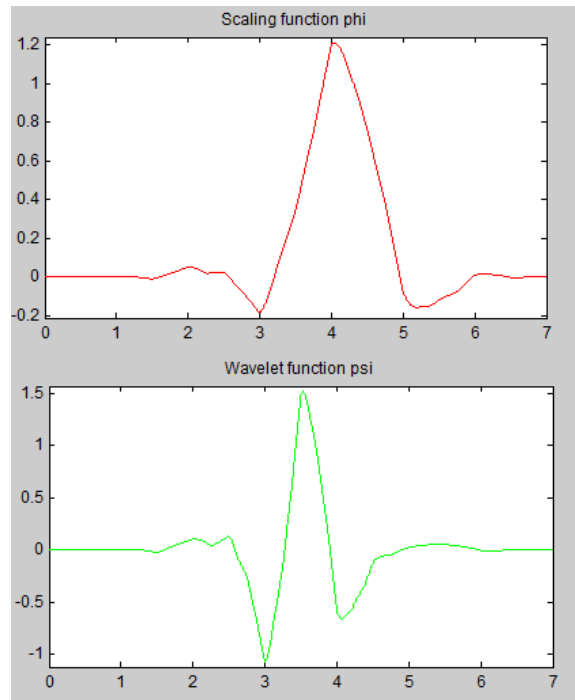


Fig. 6. **Sym4** wavelet selected for decomposition computing

3.1. Improving quality of images

For improving quality resulting image, optical noise computed from first level 2D wavelet are used as background signal subtracted from next levels of wavelet decomposition Fig. 7.

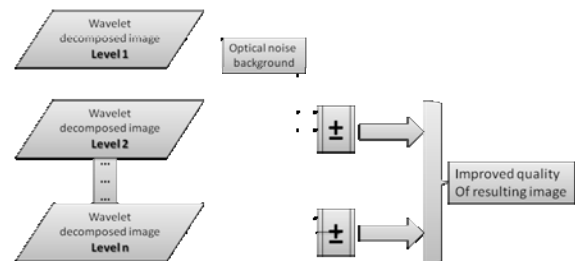


Fig. 7. Improving results quality.

Bad pixel effect are easy for removing in initial part of proposed algorithm. Calibration thermographic camera contain module for bad pixel search. This allow for reject bad pixel from recorded images during preparing data.

4. EXPERIMENTAL VALIDATION OF PROPOSED TECHNIQUE

Proposed algorithm for damage detection in mechanical structure were tested on real data from experiment prepared by authors. Firstly, frequency resonance of tested mechanical structure were setting up during standard modal analysis.

Secondly, active thermography method were used for acquiring thermal image (strain) data with infrared camera.

4.1. Experimental setup

Experiment were lead in laboratory of Department Robotics and Mechatronics – AGH. Experimental setup is shown on Fig. 8, Fig. 9.

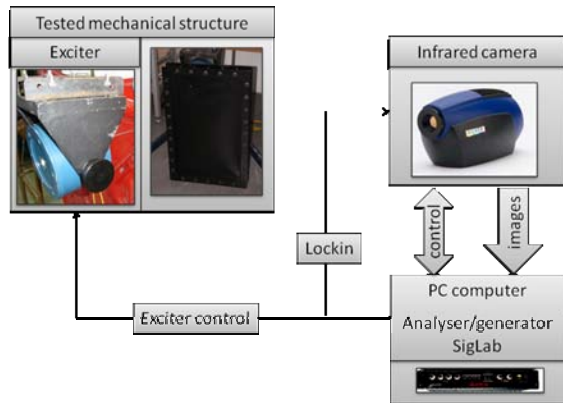


Fig. 8. Experimental setup

Components which are part of the experimental setup:

1. Thermographic measurement:
 - PC computer with CAMLINK interface compatible card;
 - SILVER 480M – advanced IR cooled camera featuring ultra fast temporal analysis, simultaneously with analogue signal recording;
 - Exciter;
2. Initial measurement:
 - Accelerometer;
 - Analyzer SigLab;
 - PC computer with SCSI interface compatible card;
 - Exciter.

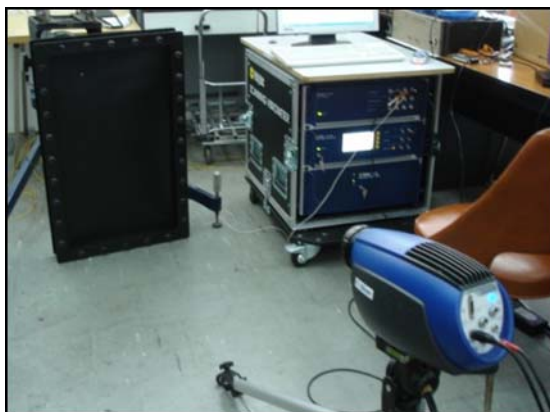


Fig. 9. Experimental setup during measurement

Experiment setup were split in parts. First part were approach for detecting resonance frequency of tested mechanical structure. For this subject white noise signal were set up on control equipment. Accelerometer placed in few points on tested

structure were used to measure time series signal vibrating structure. Modal analysis were used for resonance frequency identification based on time series data from accelerometer based measurement. In second step result of detected resonance frequency were used for control exciter to set up resonance on structure. The same signal were used also as Lockin signal for infrared camera, which allows synchronize frame rate of camera with resonance frequency of the structure.

Measurement were repeated for non defected and defected structure Fig. 10. Recorded by infrared camera images were used as input data for proposed processing algorithm to detect crack place on tested structure using active thermography method.

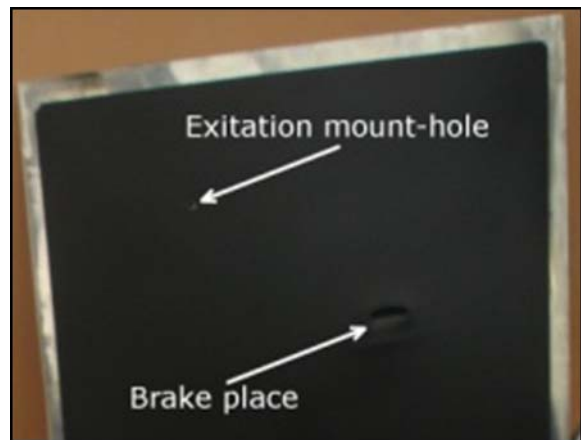


Fig. 10. Defected structure

4.2. Experiment results

After experiment, acquired thermographic images were used for testing proposed by authors algorithm. On Fig. 11 is shown thermographic image acquired by infrared camera for non defected structure. Excitation place is very representative, caused by hi level thermal stresses area.

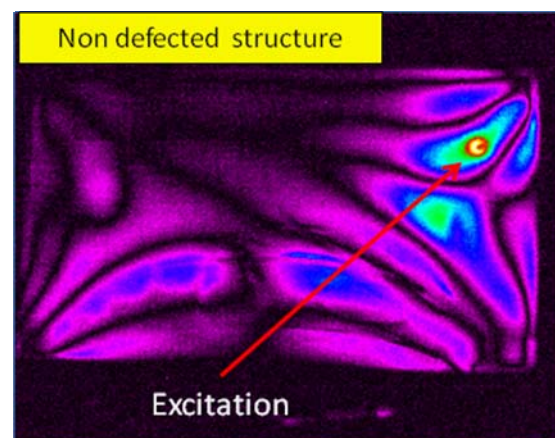


Fig. 11. Thermographic image non defected test structure

Fig. 12 is showing resulting image from acquiring thermographic image for defected structure. Strains (thermal areas) deviation can be seen on this image. Without any a priori knowledge crack place cannot be fined (for different resonance frequencies images can be more noisily).

Defected place were shown on image for better orientation.

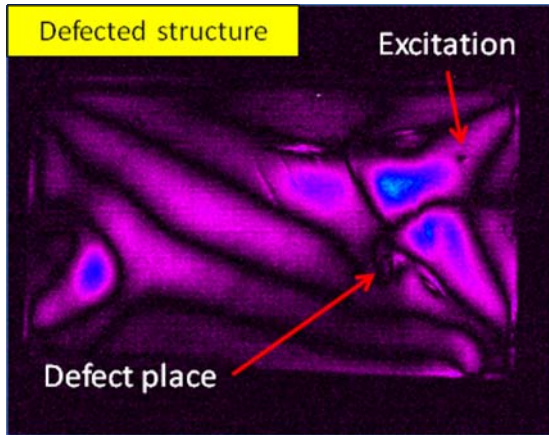


Fig. 12. Thermographic image defected test structure

Presented images were used as starting point data to testing damage detection in mechanical structure algorithm.

4.3. Preprocessing images

Preprocessing image analysis step were approach. Results from this step are shown on Fig. 13. Once, normalization of thermographic images for defected and non defected mechanical structure were computed.

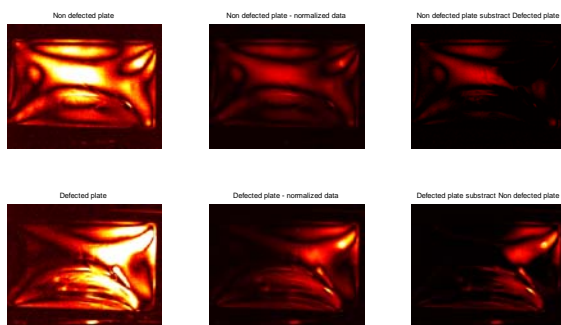


Fig. 13. Preprocessing results. (left – input images; middle – normalized images; right – images differences computation results)

Second, differences between normalized images (defected and non defected) were computed. As can be seen on Fig. 13, differences between thermal energy non defected and defected structure shows dumped values for place where crack were approach. In backwards, defected subtract non defected normalized images, thermal energy areas

were boosted for crack place and excitation neighborhood.

4.4. Separating defect place

Selected **sym4** wavelet type were used for wavelet decomposition computation. Full experiment analysis contained six levels decomposition but level 4th and higher are to blurred and are useless for damage detection purpose Fig. 14 and Fig. 15.

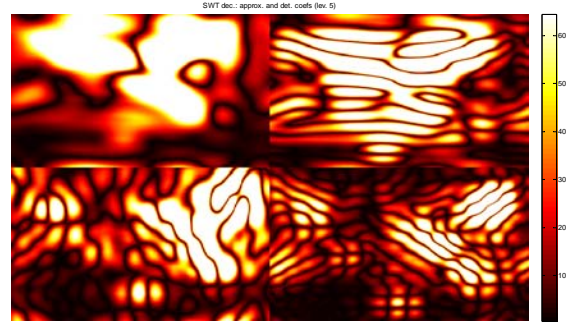


Fig. 14. Fifth level of 2D wavelet decomposition – results useless for damage detection proposed algorithm

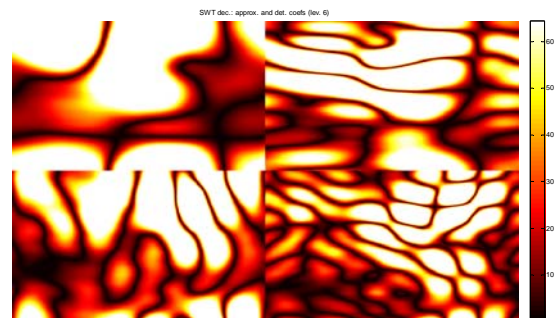


Fig. 15. Sixth level of 2D wavelet decomposition – results useless for damage detection proposed algorithm

First level of wavelet decomposition is shown on Fig. 16. On this level only optical noise and just a little of useful information are shown. This level of wavelet decomposition will be used as background for improving quality for last step defect detection algorithm.

On Fig. 16 approximation at actual level is shown on left-up part. Details coefficient in horizontal (right-up), vertical (left-down) and diagonal (right-down) orientation are displayed.

Bad pixel effect are shown in details coefficients as small single bright dot.

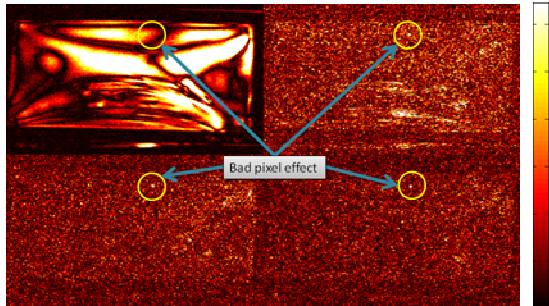


Fig. 16. First level of 2D wavelet decomposition

Second level of decomposition results are shown on Fig. 17. Here can be seen very easily representative areas for each of the interesting points (excitation, defect place, bad pixel effect). Best result gives wavelet decomposition on details coefficient in diagonal orientation (Fig. 17 right-down). On edges images for details coefficient in horizontal and vertical orientation errors from bad boundary conditions (moving structure in-plane with low frequency during measurement).

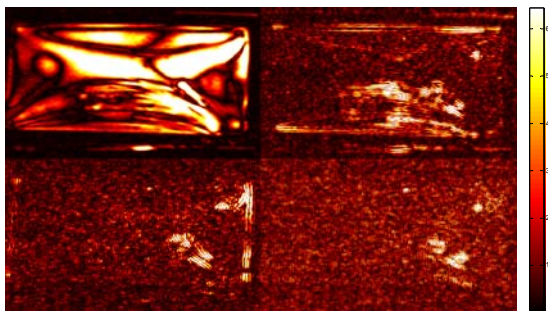


Fig. 17. Second level of 2D wavelet decomposition

Results for third level decomposition are shown in Fig. 18. As can be seen for this decomposition level images are much more blurred and more optical noise effect can be seen.

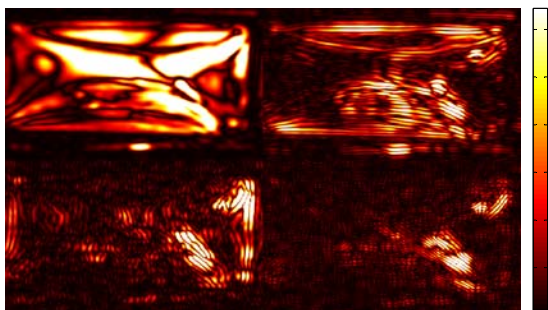


Fig. 18. Third level of 2D wavelet decomposition

For obtain more clearly image as result subtracting of background (first level of wavelet decomposition) from image which gives most accurate results (second level of wavelet decomposition) were obtain. Result of improving quality images processed thermographic data are

shown on Fig. 19. Coefficient in diagonal direction from wavelet decomposition give best result for damage detection for mechanical structure.

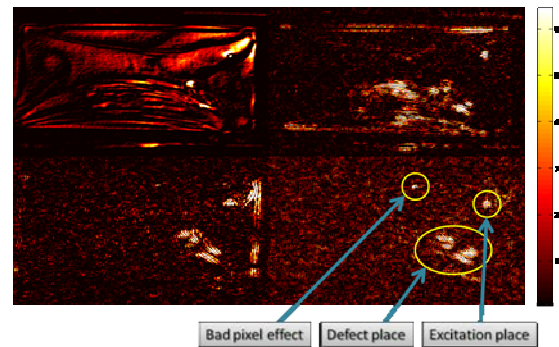


Fig. 19. Result image after background removing for second level of 2D wavelet decomposition

Areas representative for excitation, crack and bad pixel effect were marked on Fig. 19. This information proved proposed by authors algorithm for damage detection based on active thermography images analysis.

5. CONCLUSIONS AND FUTURE RESEARCH

Presented and evaluated SHM techniques gives possibility for detection of even very small damages in vibrating structure. The method is relatively simple in application and can be used for many different plate – like structures of metallic or composite materials. Future investigations, at Robotics and Mechatronics group, in direction of development of vibrothermography technique will go in application for rotating structures using de-rotation techniques.

6. ACKNOWLEDGMENT

The paper has been prepared with financial support of Polish Ministry of Science in the frame of the project no. 0526/T02/2007/02.

BIBLIOGRAPHY

- [1] Balageas D., Fritzen C. P., Guemes A., (Ed.): *Structural Health Monitoring*, ISTE, London, Newport Beach, 2006.,
- [2] Staszewski W., Boller C., Tomlinson G., (Ed.): *Health Monitoring of Aerospace structures, Smart sensors and signal processing*, Wiley & Sons, Chichester, 2003,
- [3] Inman D J, Farrar C. R., Lopes V., Valder S., (Ed.): *Damage Prognosis for aerospace, civil and mechanical systems*, Wiley & Sons, Chichester, 2005.
- [4] Farrar C. R., Worden K.: *An introduction to structural health monitoring*, Philosophical

- Transactions of the Royal Society A, vol. 365, no. 1851, 2007, str. 303- 315.
- [5] Madura H. (red.): *Practical problems In thermovision*. Agenda Wydawnicza PAK, Warszawa, 2004. (in Polish).
- [6] Maladague X. P. V: *Theory and practice of infrared technology for nondestructive testing*, Wiley, & Sons, New York, 2001.
- [7] Tenek L. H, Henneke E. G., Gunzburger M. D.: *Vibration of delaminated composite plate and some applications to non-destructive testing*, Composite Structures, vol.28, no.3, pp.253-262,1993,
- [8] Busse G., Bauer M., Rippel W., Wu D.: *Lockin vibro thermal inspection of polymer composites* Proc. of QIRT – 92 Eurotherm Seminar, vol. 27, pp. 154-159, 1992.
- [9] Bauer M., Guntrum Ch., Ota M., Rippel W., Busse G.: *Thermografic characterization of defects and failure in polymer composites*, of QIRT – 92 Eurotherm Seminar, vol. 27, pp. 141-144, 1992.
- [10] Ritter G. X., Wilson J. N.: *Handbook of Computer Vision Algorithms in Image Algebra*, CRC Press, 1996.
- [11] Tadeusiewicz R., Korohoda P.: *Komputerowa analiza i przetwarzanie obrazów*, Wydawnictwo Fundacji Postępu Telekomunikacji, Kraków 1997.
- [12] Ge M, Zhang GC, Du R, Xu Y.: *Feature extraction from energy distribution of stamping processes using wavelet transform*. J Vib Control 2002;8:1023–32
- [13] Skorpil V., Stastny J.: *Wavelet transform for image analysis*, Control and Communications, 2003. SIBCON 2003. The IEEE-Siberian Conference on 1-2 Oct. 2003 Page(s):50 – 55
- [14] Rioul O. & Vetterli M.: *Wavelets and Signal Processing*, IEEE Signal Processing Mag., 8 October 1991, s. 14-38.



Prof. dr hab. inż. **Tadeusz UHL** jest kierownikiem Katedry Robotyki i Mechatroniki Akademii Górniczo-Hutniczej w Krakowie. W swoich pracach zajmuje się zagadnieniami dynamiki konstrukcji, a zwłaszcza analizą modalną. Jego zainteresowania obejmują także układy aktywnej redukcji drgań, układy sterowania i szeroko pojętą mechatronikę oraz monitorowanie stanu konstrukcji. Jest autorem 15 książek i kilkuset artykułów dotyczących wspomnianych zagadnień.



Mgr inż. **Mariusz SZWEDO** jest doktorantem w Katedrze Robotyki i Mechatroniki Akademii Górniczo – Hutniczej w Krakowie. Jego zainteresowania związane są z przetwarzaniem i analizą obrazów, zastosowaniem technik wizyjnych w robotyce oraz wykorzystaniem wizji maszynowej w zagadnieniach sterowania układami mechatronicznymi. Jest współautorem 7 artykułów dotyczących wspomnianych zagadnień.

MATLAB® FLUTTER TOOLBOX

Andrzej KLEPKA, Tadeusz UHL

Akademia Górniczo-Hutnicza, Wydział Inżynierii Mechanicznej i Robotyki, Katedra Robotyki i Mechatroniki
Al. Mickiewicza 30, 30 – 059 Kraków fax. 012 634-35-05, andrzej.klepka@agh.edu.pl, tuhl@agh.edu.pl

Streszczenie

W artykule przedstawiono oprogramowanie do śledzenia zmian wartości parametrów modalnych w czasie eksploatacji konstrukcji. Algorytm identyfikacji estymuje parametry modalne, które odpowiedzialne są za zachowanie dynamiczne układu. Na ich podstawie można określić lub przewidzieć np. zjawisko flutteru. Predykcja tego rodzaju zjawisk ma niebagatelne znaczenie dla poprawności działania układu mechanicznego jak również dla celów diagnostycznych. Zastosowany algorytm został stworzony w oparciu o transformatę falkową pozwalającą na rozprzęganie postaci drgań oraz algorytm RLS (Recursive Least Square). Połączenie metody filtracji sygnału z szybkim algorytmem pozwalającym na estymację parametrów modelu pozwoliło na stworzenie narzędzia działającego w czasie rzeczywistym.

Słowa kluczowe: transformata falkowa, algorytm RLS, analiza modalna.

MATLAB® FLUTTER TOOLBOX

Summary

In the paper a software tool for real time modal model tracking has been presented. Identification algorithm estimates modal parameters during system operation. On the basis of this parameters e.g. a flutter phenomena could be tested during a flight. Prediction of this phenomena can be applied for damage detection and system diagnostics. Applied algorithm has been formulated using wavelet transform (for vibration modes decoupling) and RLS (Recursive Least Square) algorithm for model parameters estimation. Proposed solution, due to computational efficiency, can help to identify modal parameters of operating structures in real time.

Keywords: wavelet transform, RLS algorithm, modal analysis.

1. WSTĘP

Identyfikacja parametrów modalnych konstrukcji mechanicznych w warunkach eksploatacyjnych jest zadaniem bardzo trudnym. Brak możliwości wykonania eksperymentu niejednokrotnie zawęża aplikacyjność klasycznych metod analizy. Dodatkowym problemem jest częsta niestacjonarność układów mechanicznych w trakcie pracy oraz brak możliwości zmierzenia wymuszenia działającego na układ. Do tego typu analiz konieczne jest opracowanie metod pozwalających na śledzenie zmian parametrów układu odpowiedzialnych za jego zachowania dynamiczne. Jedną z tych metod jest metoda oparta o rekurencyjny algorytm najmniejszych kwadratów RLS. Pozwala ona na estymację współczynników modelu na podstawie bieżącej odpowiedzi układu. Ograniczeniem tej metody jest skomplikowany proces estymacji parametrów modalnych wymagający wyznaczenia pierwiastków charakterystycznych równania. Dla modeli wyższych rzędów jest to zadanie znacznie obciążające zasoby sprzętowe, co grozi utratą rekurencyjności algorytmu. Rozwiązaniem tego problemu jest redukcja rzędu modelu w taki sposób,

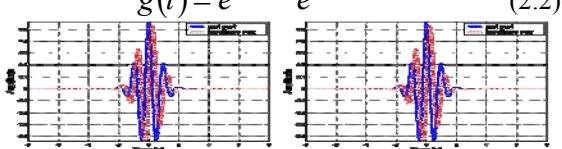
aby wyniki estymat dawały prawidłowy obraz dynamiki układu. Do tego celu użyto filtru falkowego bazującego na ciągłym przekształceniu falkowym. W pracach [5, 6] udowodniono, że transformata falkowa Morleta rozprzęga postacie drgań. Dzięki właściwościom tego rodzaju filtracji rząd modelu znany jest z góry i wynosi dwa, ponieważ śledzona jest jedna rozprzęgnięta postać. Połączenie tych dwóch algorytmów pozwoliło na stworzenie narzędzia do śledzenia wybranych częstości własnych układu oraz odpowiadających im współczynników tłumienia modalnego. Redukcja modelu znacznie obniżyła zapotrzebowanie na moc obliczeniową, co z kolei umożliwia zastosowanie algorytmu do analiz procesów szybkozmiennych, gdzie, określenie parametrów dynamicznych układu ma znaczenie dla bezpieczeństwa pracy urządzenia. Narzędzie FLUTTER TOOLBOX zostało przetestowane przez zespoły badawcze ONERA oraz Airbus w ramach europejskiego projektu badawczego FLITE2.

2. PODSTAWY TEORETYCZNE

W zaproponowanej metodzie wyznaczania parametrów modelu sygnał filtrowany jest przy użyciu transformaty falkowej, którą opisuje równanie:

$$(W_g x)(a, b) = \frac{1}{\sqrt{a}} \int_{-\infty}^{+\infty} x(t) g^* \left(\frac{t-b}{a} \right) dt \quad (2.1)$$

gdzie: a – parametr skali, b – parametr dekompozycji czasowej, $x(t)$ – analizowany sygnał czasowy, g – funkcja falkowa. Transformata falkowa jest metodą dekompozycji sygnału i reprezentuje go na płaszczyźnie czas – częstotliwość. Umożliwia to analizę układów znajdujących się w stanach niestacjonarnych. Pozwala także na rozprzęgnięcie postaci drgań co zostało opisane w pracach [5, 7, 9]. Jako funkcję falkową przyjęto falkę Morleta (rys. 1) opisaną równaniem [11]:

$$g(t) = e^{j2\pi f_0 t} e^{-\frac{|t|^2}{2}} \quad (2.2)$$


Rys. 1. Falka Morleta

Dzięki filtracji falkowej i rozprzęgnięciu postaci drgań, rząd modelu układu reprezentowanego przez sygnał jest znany. Narzuca to sposób estymowania parametrów modalnych. Dla układów drugiego rzędu opisanego równaniem (2.3),

$$A(q)y(t) = C(q)\varepsilon(t) \quad (2.3)$$

gdzie: $A(q) = 1 + a_1 q^{-1} + a_2 q^{-2}$, $C(q) = 1 + c_1 q^{-1} + c_2 q^{-2}$, a a_1, a_2, c_1, c_2 są współczynnikami równania charakterystycznego, proces estymacji częstości własnych i modalnych współczynników tłumienia sprowadza się do wyznaczenia Λ_i przy założeniu, że:

$$\theta^T(k) = [-a_1, -a_2, 1, c_1, c_2], \quad (2.4)$$

Oznacza to, że pierwiastki równania wyznaczone są jako (2.5):

$$\Lambda_i = \frac{-a_1 - \sqrt{\Delta}}{2}, \quad (2.5)$$

gdzie:

$$\Delta = a_1^2 - 4a_2 \quad (2.6)$$

W przypadku tłumienia podkrytycznego pierwiastki te są zespolone i mają postać (2.7):

$$\Lambda = \delta \pm j\omega, \quad (2.7)$$

gdzie: δ – współczynnik tłumienia odniesiony do częstości drgań własnych nietłumionych, ω – częstość drgań własnych tłumionych.

Zależność (2.7) można także zapisać jako:

$$\Lambda = \left(-\xi + j\sqrt{1-\xi^2} \right) \Omega, \quad (2.8)$$

gdzie: ξ jest bezwymiarowym współczynnikiem tłumienia wyrażonym jako:

$$\xi = \frac{\delta}{\sqrt{\omega^2 + \delta^2}}, \quad (2.9)$$

a Ω częstością drgań własnych nietłumionych wyrażona jako:

$$\Omega = \sqrt{\omega^2 + \delta^2}. \quad (2.10)$$

Zagadnienie to nie jest skomplikowane, przez co jego złożoność obliczeniowa jest mała. Wyznaczone z równania (2.5) wartości Λ_i odpowiadają części zdeterminowanej układu, opisującej jego dynamikę w postaci zbioru modalnych współczynników tłumienia oraz częstości drgań własnych.

Metoda wyznaczania współczynników modelu oparta jest o algorytm RLS. Dla systemu komputerowego algorytm ten można przedstawić następująco [2]:

Krok 1: Pobranie bieżącej odpowiedzi systemu $y(i)$ z przetwornika A/C.

Krok 2: Obliczenie estymatora błędu predykcji $\hat{\varepsilon}(i)$ jako różnicy pomiędzy aktualną wartością wyjścia procesu, a wartością „przewidywaną” przez model, bazując na jego oszacowanych parametrach uzyskanych w poprzednich iteracjach:

$$\hat{\varepsilon}(i) = y(i) - \varphi^T(i)\hat{\theta}(i-1) \quad (2.11)$$

gdzie: $\varphi(i)$ - wektor obserwacji wyjściowo-wyjściowej (ang. regressor vector), $\hat{\varepsilon}(i)$ - estymator błędu predykcji, $\theta(i)$ - wektor parametrów modelu

Krok 3: Uaktualnienie wektora wzmocnień:

$$L(i) = \frac{\mathbf{P}(i-1)\varphi(i)}{\lambda + \varphi^T(i)\mathbf{P}(i-1)\varphi(i)} \quad (2.12)$$

gdzie λ - współczynnik zapominania (ang. Forgetting factor)

i aktualizacja macierzy kowariancji $\mathbf{P}(i)$:

$$\mathbf{P}(i) = \frac{1}{\lambda} \left[\mathbf{P}(i-1) - \frac{\mathbf{P}(i-1)\varphi(i)\varphi^T(i)\mathbf{P}(i-1)}{\lambda + \varphi^T(i)\mathbf{P}(i-1)\varphi(i)} \right] \quad (2.13)$$

Krok 4: Aktualizacja wektora estymowanych parametrów modelu $\hat{\theta}(i)$:

$$\hat{\theta}(i) = \hat{\theta}(i-1) + L(i)[y(i) - \varphi^T(i)\hat{\theta}(i-1)] \quad (2.14)$$

oraz wektora obserwacji:

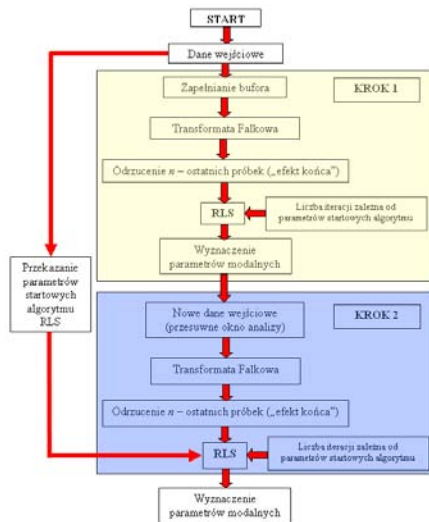
$$\varphi(i) = [y(i), y(i-1), \dots, y(i-n_A)],$$

$$\hat{\varepsilon}(i), \hat{\varepsilon}(i-1), \dots, \hat{\varepsilon}(i-n_C)]$$

Krok 5: Oczekiwanie na następną próbkę i powrót do Kroku 1,

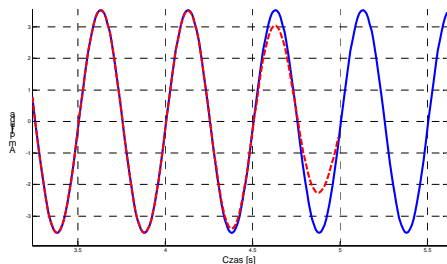
i - oznacza kolejny numer próbki uzyskanej z przetwornika A/C.

Schematycznie działanie algorytmu przedstawia rys. 2.



Rys. 2. Schemat działania algorytmu

Algorytm identyfikacji parametrów modalnych podzielony jest na dwa etapy. W pierwszym gromadzone są dane oraz wyznaczane parametry modalne zawarte w pierwszym odcinku analizowanego sygnału. Podejście takie ma na celu wyznaczenie parametrów algorytmu RLS, które przekazywane są iteracyjnie w dalszej części analizy. Drugą przyczyną takiego podejścia jest tzw. „efekt końca” transformaty falkowej (rys. 3).



Rys. 3. „Efekt końca” transformaty falkowej

Nieuwzględnienie tego zjawiska powoduje, że w kolejnych krokach iteracji algorytm nie ma zapewnionych tych samych warunków początkowych. Może to doprowadzić do błędnych wyników analizy.

Dodatkowo aby przyspieszyć proces estymacji parametrów modalnych zrezygnowano ze standardowych procedur na rzecz zależności analitycznych (2.15, 2.16).

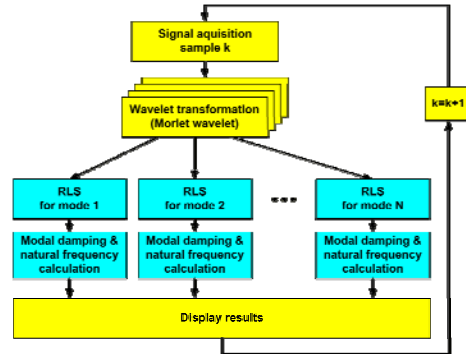
$$\omega := \frac{1}{2} \sqrt{\frac{\ln\left(\frac{\frac{1}{2}\sqrt{a_1^2 + |a_1^2 - 4a_2|}}{Ts^2} + \arctan\left(\frac{\frac{1}{2}\sqrt{|a_1^2 - 4a_2|}, \frac{1}{2}a_1\right)}{Ts^2}\right)^2}{\pi}} \quad (2.15)$$

$$\xi := -\frac{\ln\left(\frac{\frac{1}{2}\sqrt{a_1^2 + |a_1^2 - 4a_2|}}{Ts^2}\right)}{Ts \sqrt{\frac{\ln\left(\frac{\frac{1}{2}\sqrt{a_1^2 + |a_1^2 - 4a_2|}}{Ts^2} + \arctan\left(\frac{\frac{1}{2}\sqrt{|a_1^2 - 4a_2|}, \frac{1}{2}a_1\right)}{Ts^2}\right)^2}} \quad (2.16)$$

gdzie: ω - częstotliwość drgań własnych układu,
 ξ - modalny współczynnik tłumienia,
 Ts - czas próbkowania sygnału. Eliminuje to

potrzebę wyznaczania pierwiastków charakterystycznych równania.

Dzięki redukcji zapotrzebowania na moc obliczeniową proces estymacji parametrów modalnych może być przeprowadzany równolegle dla kilku postaci drgań (rys. 4).



Rys. 4. Schemat zrównoleglenia obliczeń

3. ESTYMACJA PRZEDZIAŁU UFNOŚCI PARAMETRÓW MODALNYCH

Dla metod rekursywnych istnieje możliwość wyznaczania macierzy kowariancji współczynników modelu z zależności:

$$P(i) = \frac{P(i-1) - L * \Psi(i)^T * P(i-1)}{\lambda} \quad (3.1)$$

gdzie: λ jest współczynnikiem zapominania, a Ψ macierzą wektorów własnych.

Wektor wariancji współczynników modelu definiowany jest jako:

$$[\sigma_{a_1}^2, \sigma_{a_2}^2, \dots, \sigma_{a_n}^2, \sigma_{c_1}^2, \sigma_{c_2}^2, \dots, \sigma_{c_n}^2] = \text{diag}(P) \quad (3.2)$$

gdzie $\sigma_{a_i}^2$ jest wariancją i -tego parametru modelu.

Wyznaczenie odchylenia standardowego parametrów modalnych dla zadanego modelu w sposób analityczny jest zagadnieniem skomplikowanym ze względu na nieliniową zależność pomiędzy parametrami modelu a parametrami modalnymi. W celu uproszczenia tego zagadnienia stosuje się metodę rozwinięć Taylora pierwszego rzędu [1].

Przyjmijmy oznaczenia:

$\hat{\kappa}_N = [f_1 \xi_1, f_2 \xi_2, \dots, f_s, \xi_n]$ - wektor wyestymowanych parametrów modalnych, κ_0 - wektor rzeczywistych parametrów modalnych układu.

Wprowadzając macierz kowariancji parametrów modalnych oznaczoną jako $\hat{P}_\kappa(\hat{\kappa}_n)$, odchylenie standardowe parametrów modalnych można estymować według zależności:

$$\hat{P}_\kappa(\hat{\kappa}_n) = E[(\kappa_0 - \hat{\kappa}_N)(\kappa_0 - \hat{\kappa}_N)^T] \quad (3.3)$$

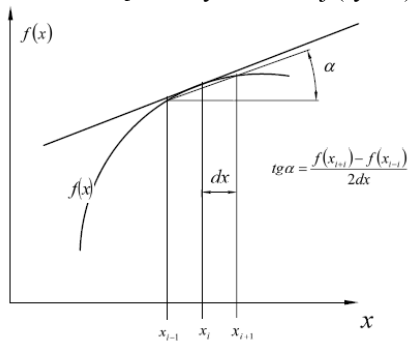
gdzie E jest wartością oczekiwaną. Równanie (3.3) można zapisać jako:

$$\begin{aligned} \hat{P}_\kappa(\hat{\kappa}_n) &= J(\hat{\theta}_N) E[(\theta_0 - \hat{\theta}_N)(\theta_0 - \hat{\theta}_N)^T] J(\hat{\theta}_N)^T \\ &= J(\hat{\theta}_N) P_\theta(\hat{\theta}_n) J(\hat{\theta}_N)^T \end{aligned} \quad (3.4)$$

gdzie: $J(\hat{\theta}_N)$ jest Jakobianem określonym zależnością [1]:

$$J(\theta) = \begin{bmatrix} \frac{\partial f_1(\theta)}{\partial \theta_1} & \frac{\partial f_1(\theta)}{\partial \theta_2} & \dots & \frac{\partial f_1(\theta)}{\partial \theta_n} \\ \frac{\partial f_2(\theta)}{\partial \theta_1} & \frac{\partial f_2(\theta)}{\partial \theta_2} & \dots & \frac{\partial f_2(\theta)}{\partial \theta_n} \\ \vdots & \vdots & \ddots & \vdots \\ \frac{\partial f_m(\theta)}{\partial \theta_1} & \frac{\partial f_m(\theta)}{\partial \theta_2} & \dots & \frac{\partial f_m(\theta)}{\partial \theta_n} \end{bmatrix} \quad (3.5)$$

Macierz ta jest w ogólnym przypadku niemożliwa do wyznaczenia. Konieczne jest więc zastosowanie różniczkowania numerycznego. Dodatkowo elementy macierzy Jakobianu wyznaczone są dla homogenicznej części modelu i w dalszej notacji oznaczone jako $\hat{\theta}_N^H$. Do wyznaczania elementów macierzy Jakobianu zastosowano teorię różnicy centralnej (rys. 5).



Rys. 5. Wyznaczanie wartości pochodnej metodą różnicy centralnej [3]

W metodzie tej zaleca się aby parametr zaburzenia dx był co najmniej o rząd mniejszą niż wymagana dokładność.

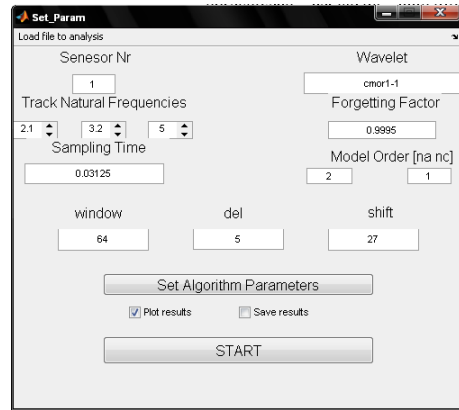
Korzystając z powyższych zależności i – ty element macierzy Jakobianu można zapisać w postaci:

$$J_i(\hat{\theta}_N^H) = \frac{f(\hat{\theta}_N^H + dx_i) - f(\hat{\theta}_N^H - dx_i)}{2dx} \quad (3.6)$$

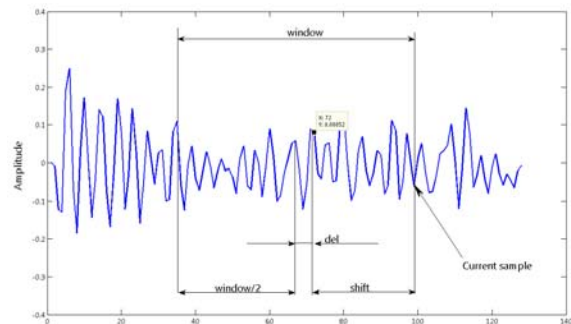
4. FLUTTER TOOLBOX – ANALIZA WYNIKÓW BADAŃ FLATTEROWYCH

Korzystając z powyższych zależności opracowano narzędzie umożliwiające śledzenie wybranej częstości własnej układu w czasie rzeczywistym (rys. 6).

Wszystkie procedury zostały opracowane w środowisku MATLAB/SIMULINK. Narzędzie posiada możliwość ustalenia parametrów tj. rodzaju funkcji falkowej, rzędu modelu, współczynnika zapominania. Parametry oznaczone na rysunku powyżej jako „window”, „del” i „shift” stanowią o opóźnieniu czasowym (rys. 7).



Rys. 6. Flutter toolbox



Rys. 7. Oznaczenia parametrów algorytmu

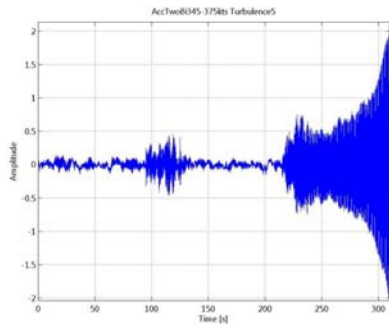
Podejście takie jest konieczne ze względu na „efekt końca”. Powoduje on zmianę amplitudy rozprzęgniętej postaci na końcach przebiegu czasowego (rys. 3). Algorytm estymacji parametrów modelu może interpretować to zjawisko jako zmianę parametrów modelu, co z kolei może prowadzić do błędnych wyników analiz. Według założeń projektu maksymalny czas opóźnienia wynikający z przetwarzania danych nie powinien przekroczyć 1 sekundy. Aby algorytm spełniał wymagania czasowe musi spełniona być zależność:

$$\text{shift}[s] + \text{del}[s] + \text{czas_analizy_del_próbek} \leq \text{max_opóźnienie} \quad (4.1)$$

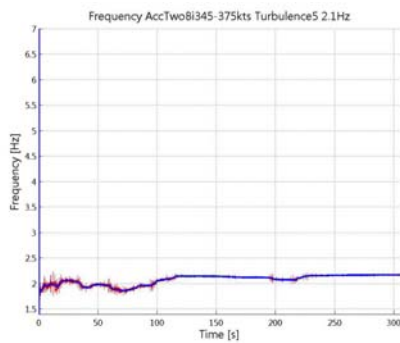
Dla tak przyjętych założeń dokonano licznych analiz sygnałów pochodzących zarówno z symulacji jak i danych rzeczywistych. Dane symulacyjne opracowała firma Airbus w ramach projektu EUREKA. Zawierają one przebiegi czasowe przyspieszeń drgań elementów samolotu w trakcie lotu z różnymi prędkościami, na różnym pułapie oraz przy różnych wymuszeniach (turbulentnym, losowym, sinusoidalnym). Dane rzeczywiste zostały zarejestrowane w trakcie lotu samolotu PZL M28 SkyTruck. Rezultaty wcześniejszych analiz z użyciem filtracji falkowej oraz algorytmu RLS można znaleźć w [4, 8, 9, 10]. Przyjęto przedział ufności na poziomie 95,5% (zaznaczony na rysunkach kolorem czerwonym). Wybrane wyniki analiz danych symulacyjnych przedstawia rys. 8. Jak można zaobserwować algorytm reaguje na zmianę amplitudy sygnału spowodowaną zmianą warunków pracy układu. Szczególnie ważną rolę odgrywa tutaj

współczynnik tłumienia (rys. 8b), którego spadek wartości może świadczyć o możliwości wystąpienia zjawiska flutteru.

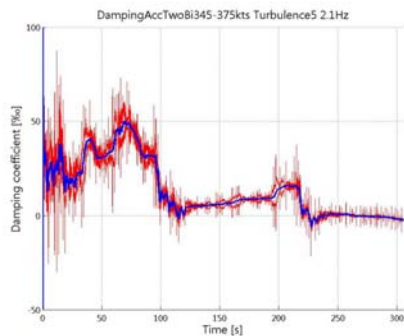
a)



b)



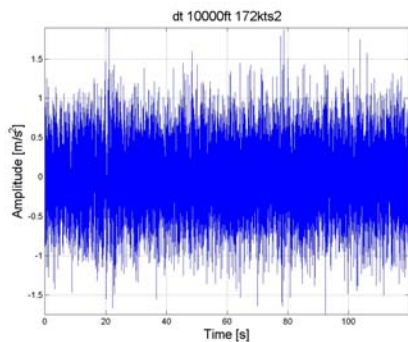
c)



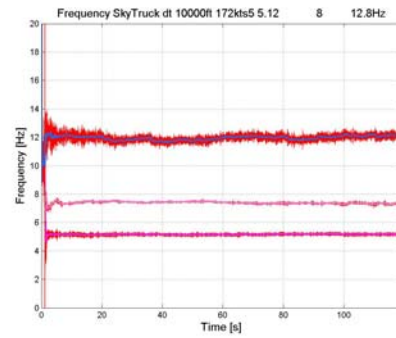
Rys. 8. Przebieg czasowy przyspieszeń drgań (a), częstotliwość drgań (b) oraz tłumienie (c) dla postaci 2.1Hz, prędkość 375 – 390 węzłów, wymuszenie turbulentne

Wybrane wyniki analiz danych rzeczywistych przedstawia rys. 9.

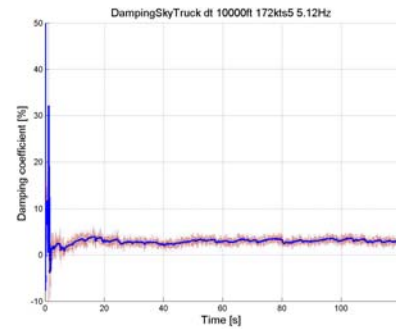
a)



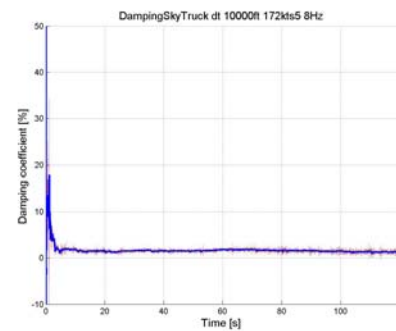
b)



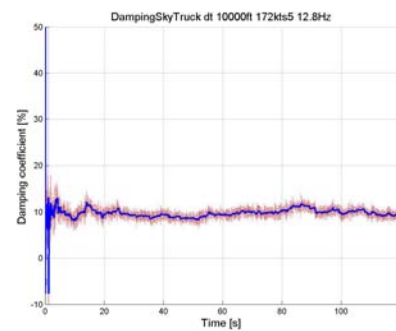
c)



d)



e)



Rys. 9. Przebieg czasowy przyspieszeń drgań (a), częstotliwości drgań (b) oraz tłumienie dla poszczególnych postaci: 5,12Hz (c), 8Hz (d), 12,8Hz (e), prędkość 172 węzły, pułap 10000 stóp

5. PODSUMOWANIE

Metoda filtracji falkowej, używana jako narzędzie wstępnego rozprzegania postaci drgań w sposób znaczący ułatwia i przyspiesza proces estymacji parametrów modalnych przy pomocy algorytmu RLS. Eliminuje się w ten sposób proces filtracji pasmowej sygnału, niezbędny w przypadku stosowania klasycznej metody RLS. Znany i niski

rząd modelu zmniejsza zapotrzebowanie na moc obliczeniową procesora, co daje wymierne korzyści w postaci zmniejszenia wymagań sprzętowych.

Najważniejszą cechą zaproponowanego podejścia jest wyeliminowanie trudności wyznaczania pierwiastków równania charakterystycznego wyższych rzędów w celu podania wartości parametrów modalnych modelu. Proces ten jest krytyczną częścią klasycznego algorytmu RLS działającego w czasie rzeczywistym. W niektórych przypadkach nieodpowiedni dobór rzędu modelu może prowadzić do braku zasobów procesora. Konieczne jest w takich przypadkach tworzenie specjalnych buforów kołowych w celu podtrzymania rekurencyjności klasycznego algorytmu RLS. Zastosowanie transformaty falkowej do rozprzegania postaci drgań zapobiega tym zjawiskom. Dzięki właściwościom falek, rząd modelu znany jest z góry i wynosi dwa, ponieważ śledzona jest jedna rozprzegnięta postać. Narzuca to sposób estymowania parametrów modalnych. Wszystkie wymagania dotyczące czasu obliczeń zostały spełnione. W przypadku bliskich wartości częstotliwości drgań własnych konieczne jest opracowanie metod doboru parametrów funkcji falkowych lub metod pozwalających na wyznaczanie w czasie rzeczywistym parametrów modalnych układów o rzędzie większym niż dwa.

PODZIĘKOWANIE

Prace badawcze zostały wykonane w ramach projektu europejskiego EUREKA E!3341 FLITE 2 i sfinansowana przez Ministerstwo Nauki i Szkolnictwa Wyższego w latach 2004-2007.

LITERATURA

- [1] Andersen P.: *Identification of Civil Engineering Structures using Vector ARMA Models*, Aalborg University, Department of Building Technology and Structural Engineering 1997.
- [2] Bogacz M.: *Analiza modalna konstrukcji w czasie rzeczywistym*, rozprawa doktorska KRiDM, Kraków 2004.
- [3] <http://mathews.ecs.fullerton.edu/n2003/differentiation/NumericalDiffProof.pdf>
- [4] Klepka A., Bogacz M., Uhl T.: *Identyfikacja modalnego współczynnika tłumienia w czasie rzeczywistym przy użyciu transformaty falkowej oraz algorytmu RLS*, XII Symposium Dynamiki Konstrukcji, Zeszyty naukowe Politechniki Rzeszowskiej, Mechanika z. 65, 201 – 208.
- [5] Klepka A.: *Identyfikacja parametrów modalnych układów mechanicznych w warunkach niestacjonarnych*, Praca doktorska KRiM 2006.
- [6] Klepka, T. Uhl: *Zastosowanie transformaty falkowej do rozprzegania postaci drgań oraz do wyznaczania współczynnika tłumienia*, Górnictwo odkrywkowe nr 2 – 3/2003, str. 61 – 64.
- [7] Staszewski W. J.: *Identification of damping in MDOF systems using time – scale decomposition*. Journal of Sound and Vibration (1997) 203(2), 283 – 305.
- [8] Uhl T., Bogacz M., Klepka A.: *In – operational damping identification and its application for flutter detection*, 7th Conference on Dynamical Systems – Theory and Applications, Proceedings, volume 2, Łódź, december 8 – 11, 2003, p. 739 – 746.
- [9] Uhl T., Klepka A.: *Application of wavelet transform for identification of modal parameters of nonstationary systems*, Journal of theoretical and applied mechanics 43,2, pp. 277 – 296, Warszawa 2005.
- [10] Uhl T., Klepka A.: *The use of wavelet transform for in-flight modal analysis*, XII International Conference on Noise and Vibration Engineering, Leuven 2006.
- [11] Young R. K.: *Wavelet theory and its application*, Kluwer Academic Publishers, Boston Hardbound, September 1992.



Prof. dr hab. inż. **Tadeusz UHL** jest kierownikiem Katedry Robotyki i Mechatroniki, Akademii Górniczo - Hutniczej w Krakowie. W swoich pracach zajmuje się zagadnieniami dynamiki konstrukcji, a zwłaszcza ich analizy modalnej. Jego zainteresowania obejmują także układy aktywnej

redukcji drgań, układy sterowania i szeroko pojętą mechatronikę. Jest autorem 15 książek i kilkuset artykułów dotyczących wspomnianych zagadnień.



Dr inż. **Andrzej KLEPKA** jest adiunktem w Katedrze Robotyki i Mechatroniki, Akademii Górniczo – Hutniczej w Krakowie. W swoich pracach zajmuje się zagadnieniami analizy modalnej i diagnostyki, a w szczególności nowymi technikami analizy sygnałów.

APPLICATION OF VIRTUAL POWER PLANT FOR CONDITION MONITORING OF POWER GENERATION UNIT

Tomasz BARSZCZ

Akademia Górniczo-Hutnicza, Wydział Inżynierii Mechanicznej i Robotyki
Al. Mickiewicza 30, 30-059 Kraków, Poland, e-mail: tbarszcz@agh.edu.pl

Summary

The following paper presents the method, called here the Virtual Power Plant (VPP), for the condition monitoring of power generation unit elements. The Virtual Power Plant is the proposal of a group of computers, which model a real power plant unit in the real time. This paper is focused on Virtual Power Plant architecture and procedure to use it for condition monitoring. Such a procedure is based on models of various types tuned to the normal technical state of the plant. Next, this model is used to detect any changes in the behaviour of the plant elements.

The paper present details of the Virtual Power Plant idea: its structure and functionality of key elements. The structure of the model is presented with stress on its modularity and flexibility. Next part of the paper is the case study, where test installation, tuned to a 200MW coal fired unit, was described. Results from operation on the test installation are presented.

Keywords: modeling, condition monitoring, model based diagnostics, power plant.

ZASTOSOWANIE WIRTUALNEJ ELEKTROWNI DO DIAGNOSTYKI BLOKU ENERGETYCZNEGO

Streszczenie

Artykuł przedstawia metodę, nazwaną Wirtualną Elektrownią (VPP, ang. Virtual Power Plant), zastosowaną do oceny stanu elementów bloku energetycznego. VPP jest propozycją zastosowania zespołu komputerów, które będą modelować pracę bloku energetycznego w czasie rzeczywistym. Artykuł koncentruje się na przedstawieniu architektury Wirtualnej Elektrowni oraz na jej zastosowaniu do oceny stanu technicznego. Metoda opiera się na heterogenicznym modelu, dostrojonym do bloku energetycznego w poprawnym stanie technicznym. Następnie model ten jest podstawą wykrywania zmian zachowania elementów bloku.

Artykuł przedstawia szczegóły koncepcji Wirtualnej Elektrowni: jej strukturę oraz główne elementy. Opisano model bloku ze szczególnym naciskiem na modułowość i elastyczność. W kolejnej części artykułu opisano instalację testową, gdzie VPP została dostrojona do rzeczywistego bloku typu 200MW. Zaprezentowano wyniki pracy instalacji.

Słowa kluczowe: modelowanie, ocena stanu, diagnostyka, energetyka.

1. INTRODUCTION

Nowadays, very rapid development of information technologies, especially processing power, enables us to develop innovative methods of condition monitoring of machinery and processes. Among these, power generation equipment is of very significant importance. This significance is the direct consequence of very high construction costs, as well as maintenance and repair costs.

Numerous methods are used to assess the technical state of supervised objects. In general, they are referred to as fault detection and identification (FDI) methods. Comprehensive survey presenting those methods can be found e.g. in [7, 4]. Very successful approach is based on models, either based

on analytical equations, either on parametric models obtained during the process of system identification [8, 6]. On the other hand, feasibility of such an approach is limited when it is applied to large, industrial installations, like power plant units. Key problems can be listed as:

- development of the model; in most cases, even if the underlying physical equations are known, the important obstacle is to obtain correct parameters, and thus – correct model behavior; on the other hand, when the system identification approach is chosen – it is extremely important to acquire sufficient data, covering range of operation of the object;
- flexible work environment; the process of model development and next – diagnostics

requires efficient cooperation of specialists from different fields: power plant staff should deliver data and technical documentation, diagnostic experts are responsible for modeling the process and drawing conclusions, results should be presented in a comprehensible way for the power plant experts and management; in practice, those tasks are executed with a set of heterogeneous tools, making the whole process hard to manage and inefficient.

Following paper presents the proposal of the Virtual Power Plant (VPP) - the innovative work environment for technical state assessment of dynamic objects, here applied to elements of the power plant unit. Such an environment should work with performance close to the real time (when necessary and technically possible). Introduction of such an environment facilitates development of models and next – the process of diagnostics. Such an environment has following benefits:

- flexible structure, enabling multiple configurations;
- import of real data acquired at the object;
- possibility to include models in various formats (though Matlab/ Simulink was chosen as the default);
- possibility to store models in different versions;
- presentation of results in two ways: advanced for experts and simplified for power plant staff.

However, applications of the Virtual Power Plant can be much broader than the diagnostics only. It can be also used to achieve the following goals:

- reply of malfunctions to analyze real cases from the plant;
- modeling of faulty behavior of a plant to improve the knowledge about processes in the real plant;
- simulation of various modifications of the unit and effects it will have, for example in the dynamic state;

- huge resource for search of diagnostic rules, thus it will bring advances in FDI techniques
- testing of existing and the development of new models;
- development of risk management algorithms
- verification of diagnostic systems in operation on a plant;
- testing of equipment behavior, also in abnormal conditions;
- testing of concepts of new equipment elements, using rapid prototyping techniques
- very efficient tool to train operators, also in abnormal conditions;
- improvement of safety of existing plants.

The development of the Virtual Power Plant can also be very interesting option for power plants owners to improve their competitive position on the deregulated market. The possibilities mentioned above will be investigated during future research and development works.

2. VPP ARCHITECTURE

Achieving of the main goals of the Virtual Power Plant depend most on its structure. The key requirement is that it should have a modular structure, similar to that one of a real power plant. Such a structure is presented on the figure 1. The Virtual Power Plant is the group of computers, connected by a fast computer network. Each computer plays a role of a VPP component. The largest part of the system is database, which consists of two cooperating subsystems. The first one is the database as in the typical DCS system. This allows to store the data in the same way they are stored in a real system. On the other hand it will allow to present data in user-friendly way and to interact with the VPP, during training of operators. The second database subsystem is a specialized, fast database which is used to store data generated by

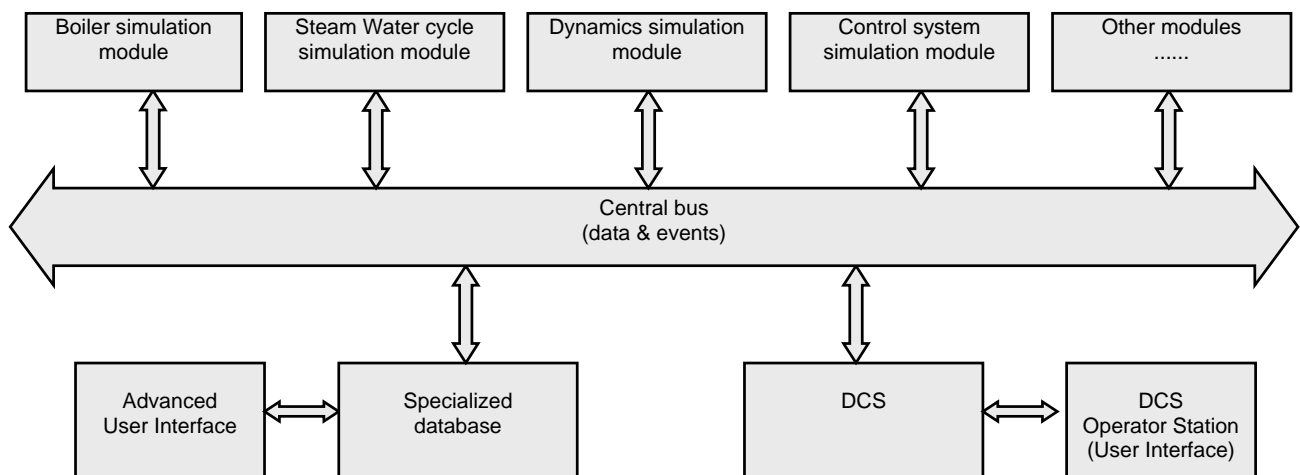


Fig. 1. The structure of the Virtual Power Plant

modules of the VPP. This subsystem is proprietary, efficient database engine, which can also store dynamic data (e.g. vibration waveforms).

The Central Bus is another computer, which is the main data exchange hub in the VPP. It provides common interface for all the modules, which allows to develop each module independent from the others. It is possible to exchange a module, or even to change the structure of the whole system without changes in the software, but only in the configuration. Such an interface is object oriented and thus flexible and very efficient mean of communication. It can exchange not only measurement and dynamic data, but also events. Events are used to inform selected modules about e.g. completion of a task by a module. Events are also used to synchronize the whole system. The Central bus contains several additional components, enhancing it:

- Data Player, which can reply real data acquired on the plant, in order to observe the response of the model and to compare it to the response of the real plant.
- Data Processor, where one can define any calculation, based on other values in the system.
- Limit Checker, which is used to monitor violation of given levels by the chosen variable. It is possible to define several states and to assign limits to states.

The remaining computers are used to run models of the components of the power plant. It is assumed that the model will be developed in the Matlab/Simulink environment [9]. If the speed of calculation is not sufficient to achieve the operation close to the real-time, the Distributed Computing Toolbox (DCT) [9] may be used. Model of the power plant unit will be described later in this paper.

Important novelty of VPP is application of separate computers to implement all modules of VPP. This will allow to mix even different modeling tools as well as exchange of selected ones with data recorded at the real plant and then replayed. Additional benefit is possibility of data processing distribution between several CPUs.

Important part of the Virtual Power Plant are user interfaces, which are closely connected with the databases. The first one is the user interface native to the DCS system. It implements typical mimic screens of the unit control room. Thus, the process can be monitored in the same way as it is done by operators in their daily work. It may be also used in the future to train operators on the VPP. The other user interface access the data in the specialized, fast database. It delivers more advanced plots:

- detailed browsing of data in form of trend plots and waveform plots (for dynamic channels);

- plot of basic dependencies (XY plots);
- export of result data to other systems for in-depth analysis.

Another important feature of the VPP is the remote access, which will increase its usefulness. Experiments can be configured and then monitored remotely. It is also possible to connect e.g. modelling module from a remote location, like a scientific center to the rest of VPP, though fast and reliable network connection is the prerequisite in such a case. Security of processed data and especially model parameters is very sensitive and important factor in VPP. It is thus necessary, that all data exchange with other computers through the Internet is performed via secure channels. VPN (Virtual Private Networks) technology was applied to achieve this goal.

OPC was chosen as the basic communication interface in the Virtual Power Plant. OPC is the international standard [10], developed for exchange of data in industrial applications. Application of such a standard reduces cost and time of integration of various hardware and software system elements, because interfaces between various components need to be only configured, instead of being developed. Matlab/ Simulink as well as virtually all DCS systems are equipped with the OPC interface. Communication over OPC is also used for synchronization of operation of the VPP.

2. MODEL STRUCTURE

The mathematical model used in the Virtual Power Plant is a compromise between the requirements of the accuracy to the real object and available computing and data processing power [5]. There are many available works focusing on modelling of particular elements [2]. The basic requirements towards the model in VPP were, that the model should allow to model the dynamics of key processes and should have potential for the continuous improvement. In other words, it must be possible to develop models by step improvements in such aspects like accuracy, introduction of more advanced or alternative models of subsystems. Therefore, the model must have modular structure. This structure is presented on the figure 2.

The presented model was prepared for 200MW unit. The unit consists of coal fired boiler, reheat steam turbine and generator. One has to mention that the model assumed in VPP does not impose this structure, so it can be modified for some other units. The communication between the model and other parts of VPP is based on items in OPC protocol, which do not require any special model structure.

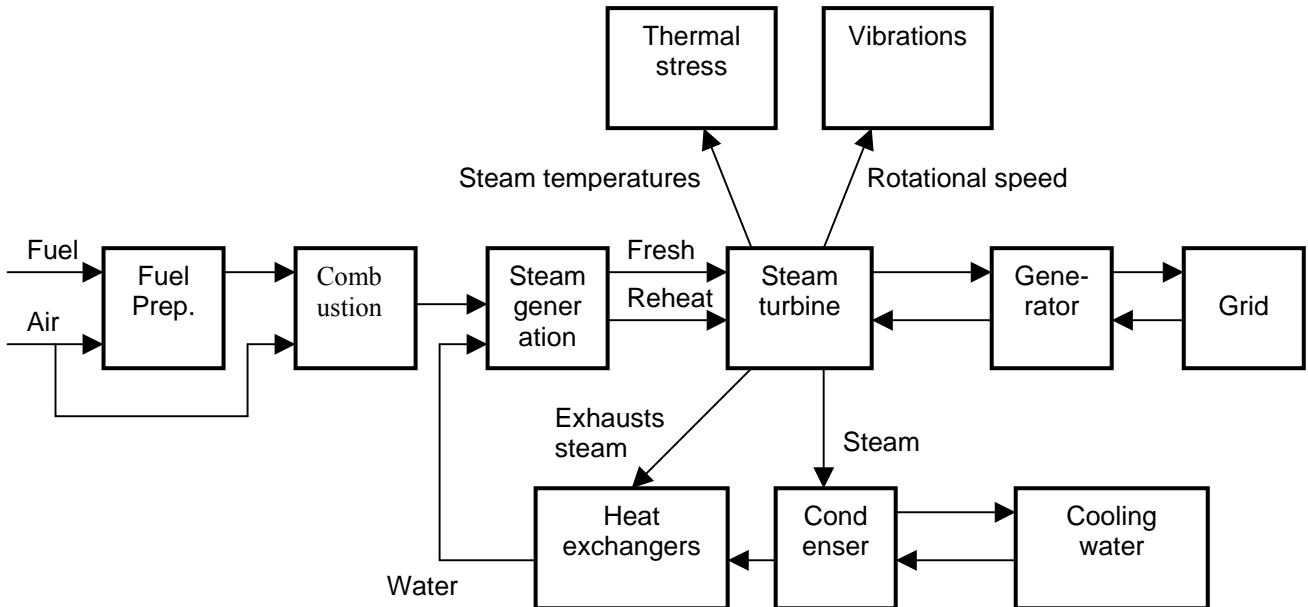


Fig. 2. The structure of the model

The model was focused on main power generation processes, i.e. steam generation in the boiler, steam-water cycle (including steam regeneration in heat exchangers) and generator. Some auxiliary machines were not covered, some processes were only partially implemented. Example of such process is the dynamic state, which depends only on the rotational speed and does not have any feedback to the rest of the model.

Another key requirement to the model in Virtual Power Plant was possibility to keep several variants of model of a given component. It is important, because development of the model is a process, where in the first step independent partial models are developed. Those models have various levels of details, depending on the focus of research. Next, models are interconnected to cover larger part of the power plant processes. The figure 3 presents possible variants of a model in the case of steam control valve.

```

|- Virtual_Power_Plant_Model_V001
|
|- VALVE (steam flow control valve)
|
|   |- V001 (static model, e.g. spring + turbulent flow equation)
|   |   |- model.mdl
|   |   |- model_parameters.m
|   |- V002 (V001 + dynamics, e.g. mass of a head, friction)
|   |   |- model.mdl
|   |   |- model_parameters.m
|   |- V003 (V002 + fluid flow dynamics, e.g. oil/steam acceleration)
|   |   |- model.mdl
|   |   |- model_parameters.m

```

Fig. 3. The structure of variants of sample element model

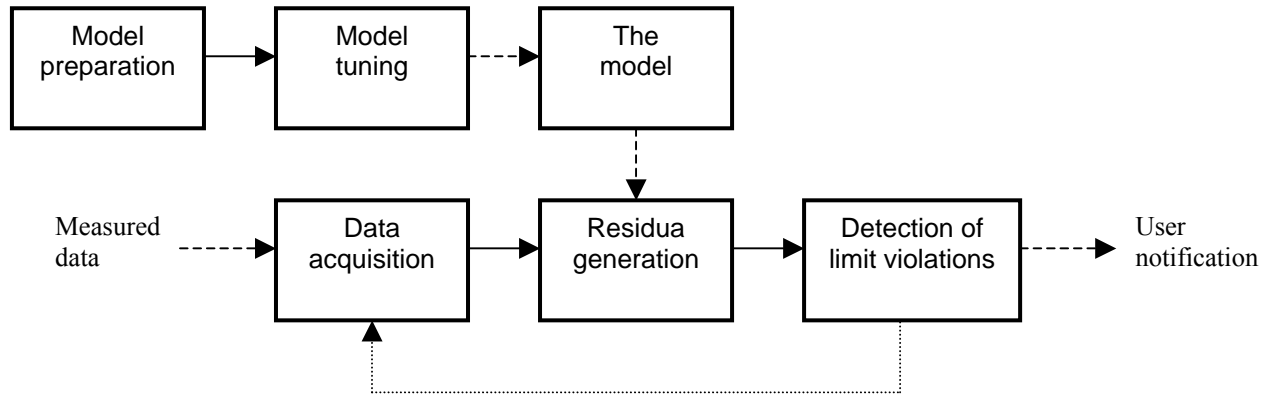


Fig. 4. The process of condition monitoring, based on the mode

All models approximate the same element, namely the steam flow control valve. Each one is another variant, increasing complexity and accuracy. Similar sets of variants are prepared for all modelled components.

As a result of the described process, to create the final unit model, the model of a component can be chosen from a list of available model versions. All such models must have common interface, but they will certainly differ in model parameters. It should be possible to adapt models to the chosen goal of simulation (e.g. response to a load change) by changing model parameters, which in case of Matlab/ Simulink models can be stored in m-files. Preparation of the model should consist of choice of models of subsystems. For each subsystem the model can be chosen out of a library of available ones.

The fundamental distinction is between steady-state and transient models. Whereas the first one can be linearized, the latter is inherently non-linear and thus, is much harder to develop. Therefore, each submodel should have also defined its scope of applications, i.e. valid range of input parameters.

3. APPLICATION FOR CONDITION MONITORING

The application of the Virtual Power Plant, which is presented in this paper is condition monitoring of the power generation unit. The process of condition monitoring, based on the model, is presented on the figure 4.

The process is divided into two subprocesses, shown in the fig.4 as separate levels. The first subprocess is preparation of the tuned model. It starts from choosing the model type and structure. In the next step, the chosen model is tuned to the real object. The tuned model is the input to the second subprocess, which is condition monitoring of the object. It is periodically (which can mean off- or on-line) activated. The approach presented here is based on residua generation, which are next checked against the allowable limits. The presented process

is a typical one, the detailed description can be found e.g. in [3].

There are several advantages, which can be achieved, when the described process will be implemented within the Virtual Power Plant environment. Possible advantages are presented in the table 1.

Tab. 1. Advantages in the process of condition monitoring achieved by application of the VPP

Process	Advantage gained by application of Virtual Power Plant
Model preparation	The model preparation can be much faster, when the library of typical power plant unit elements are used.
Model tuning	The model tuning can be based on the real data from the object, stored in the database of VPP. Sets of parameters can be assigned to particular object operating points (when linearized models are used).
Data acquisition	Data acquisition can be simplified in both off- and on-line modes. In the off-line mode, the possibility of the Central Bus to reply stored data can be used. In the on-line mode, it is possible to acquire the data directly from the Distributed Control System (DCS). In such a case, the VPP can form a part of a monitoring and diagnostic system. Due to complexity of the VPP, it is rather expected, that it will work remotely, acquiring the data via a phone line or network connection.
Residua generation	Another part of the Central Bus – the Data Processor, can be used to calculate any set of chosen mathematical expressions. Every residuum should be configured and will result in creation of new data source (or tag in

	the system). The value of this tags will be updated with every refreshed data input.
Detection of limit violations	Limit Checker, yet another part of the Central Bus, can be directly applied to detect limit violations of residua. Prior to limits configurations, states can be defined. Each state is detected based on values of chosen tag. Limits can be assigned to states, and thus it is easy to achieve residua checking only in certain operational states, e.g. full load, transient.
User notification	For user notification the DCS-like user interface in VPP can be used. One can upgrade the user screens with additional controls, showing the status of particular components.

It is very important that all mentioned functionality can be achieved only by configuration of the VPP, without the need to develop any software.

4. CASE STUDY

The Virtual Power Plant was applied to the real 200MW coal-fired unit in one of Polish power plants. This action was planned as the verification of the concept of the Virtual Power Plant. According to the agreement with the chosen power plant owner, following data were transferred to the research team:

- technical documentation of selected components;
- locations of measurement sensors;
- DCS system configuration;
- DCS screen set with assignments of measurement channels to screen controls;
- data acquired by DCS during the operation of the unit;
- know-how and consulting from power plant experts.

The developed model contained all main elements of the unit, i.e. boiler, steam turbine and generator. The model structure followed the structure shown on fig. 2. The model also contained auxiliary equipment, such as preparation of fuel (coal mills, boiler fans, air heaters), steam water cycle (heat exchangers, condenser, deaerator), cooling water and control systems. The model included submodels of dynamic state and stress, but they had no feedback to the other components. The division of three basic types of model variables is presented in the table 2. Those types are shown as in the DCS system.

Tab. 2. Division of model variables on the sample installation on a 200 MW power generation unit

Variable type	Number of implemented variables
Binary input	81
Analogue input	1072
Binary output	689

The majority of binary output channels had fixed value, since it was sufficient to model only certain states of the power plant. In the user interface system 40 screens from the original DCS were implemented. The figure 5 presents one of implemented screens, presenting overall view of the turbine with steam regeneration and the generator with connection to the grid.

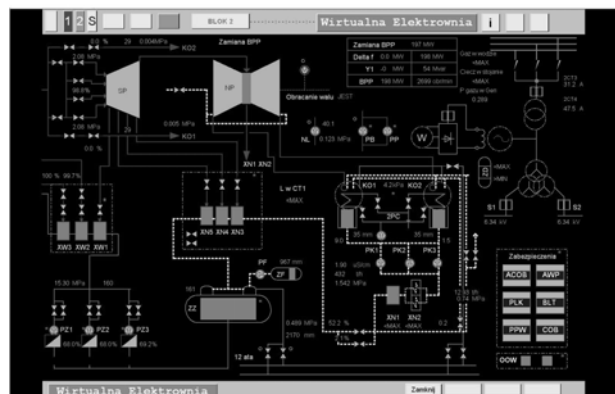


Fig. 5. One of DCS screens implemented in the Virtual Power Plant on a 200 MW unit

In most cases physical equations were used to model the behavior of the plant. However, such an approach resulted in huge CPU consumption and large excession of real-time conditions. Therefore, the hybrid approach was applied [1]. In this step another version of the model was prepared, in which all heat exchangers were implemented as sets of linearized models. Heat exchangers were chosen for linearization, as it was the part of the model, which caused the highest CPU load. This version of the model had worse accuracy, but was much faster, even up to 150% of the real-time in comparison with over 1000% for the analytical model.

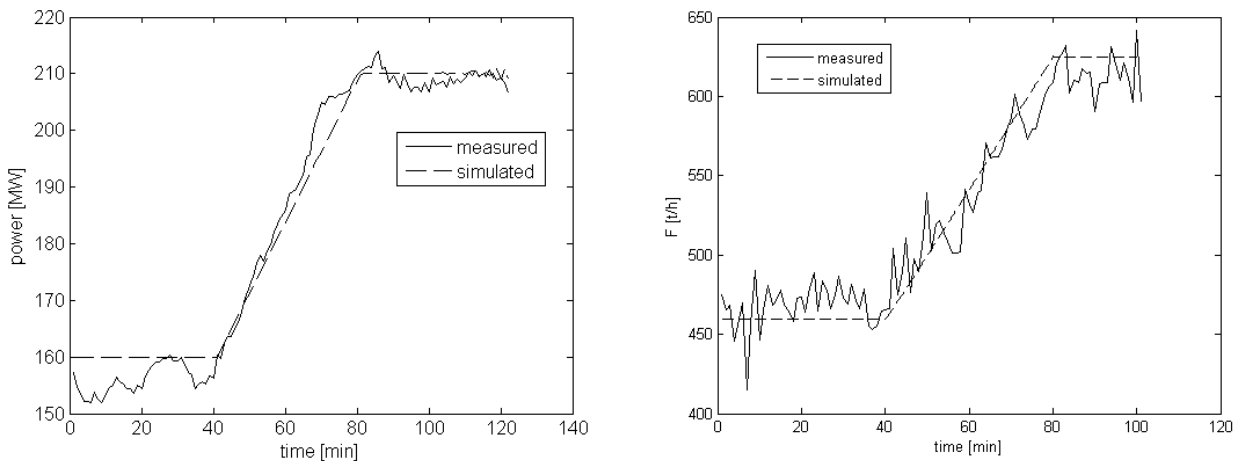


Fig. 6. Comparison of the model output and the real output for load and fresh steam flow

In order to work, the model had to implement several control systems. Following subset of control loops was implemented:

- combustion controller;
- steam pressure controller;
- rotational speed controller load controller;
- water injection controllers;
- heat exchangers controllers (controlled steam exhausts).

Due to very high complexity, only basic functionality of those controllers was implemented. For modelling, large sets of data from real operation of the unit were loaded into the VPP database. For presentation in this paper a part of data as chosen, presenting ramp load change from about 160MW to 210 MW. The fig. 6 presents comparison of the model response to the real data for load and fresh steam flow. It is visible, that only part of the system dynamics was modelled. There were three principal reasons for such a behavior – first, presented results were obtained for the model consisting of set of linearized models. Second, there was no access to the noise acting on the object, so only the basic dynamics was shown by the model. Third, several control systems were implemented with significant simplifications, which again limited the response of the model to only the basic behavior.

Other interesting plots (fig. 7 and fig. 8) present the performance of the model. It shows timeslices required for simulation and the time actually needed for calculation of one step.

One timeslice was 10s of real time and it is shown as the straight horizontal line. As shown above, in the complete model case, VPP required from 15 to 25s to model 10s of the real time a time. The performance was measured during modelling of load change, shown on fig. 6. As expected, during the transient process, CPU load is increased. On the other hand, during steady state operation, the model requires only 50% more time than the real time. In

the second case of linearized model, the performance was much better, requiring 4 to 9s of the real time. Note, that there was some increased load at the start-up, with few periods, where the 10s timeslice was exceeded by approximately 1s.

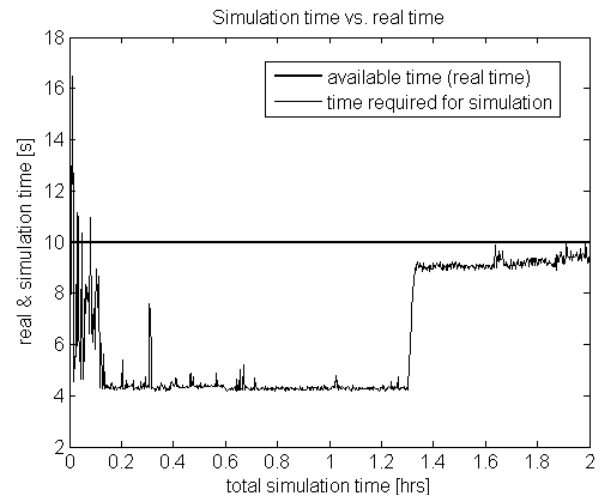


Fig. 7. Performance of model during the simulation of transient process for the complete model

Additionally long term simulation tests were performed. The test duration was 65 hours and the unit was going periodically through states of run-up, steady state, run-down and turning gear. The performance measures were recorded and are presented on the fig. 9.

As shown, the average performance of the model was around 60% of available time, i.e. modeling took only 60% of the real time. This result is very satisfactory.

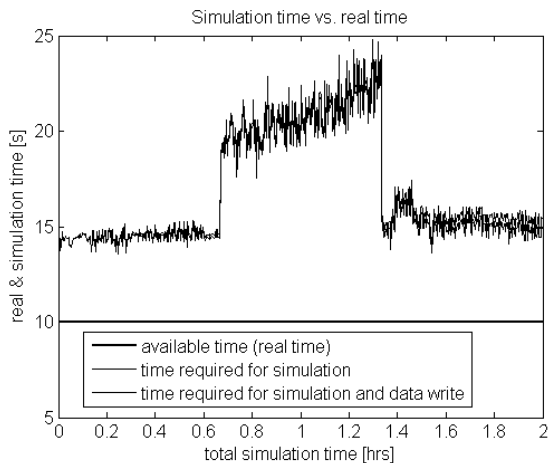


Fig. 8. Performance of model during the simulation of transient process for the linearized model

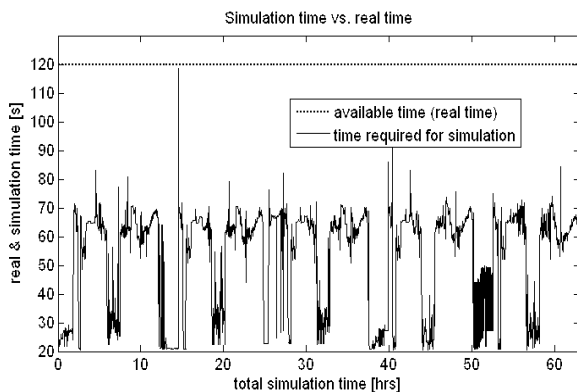


Fig. 9. Performance of model during long term test

SUMMARY

The paper presents the concept of the Virtual Power Plant and its application to the condition monitoring of power plant components. The VPP is a distributed environment, which joins modelling, databases and user interfaces. It is possible to reply the data acquired from a real unit and record the response of the model.

In the next chapter the architecture of the VPP and its main components are described. Two types of databases and their corresponding user interfaces are presented. The condition monitoring algorithm uses the VPP, previously tuned to the power plant unit in good conditions. Next, the data from an unknown conditions are replayed and residua are generated. This classical approach can be facilitated by the use of the VPP.

The following chapter describes structure of models used in the VPP. It is possible to implement several submodel versions to adapt the model to specific need of a modelling task (e.g. transient or steady-state). Example of such an approach for a steam control valve is presented.

The concept was verified on the case of real 200MW power generation unit. The model

generated over 1000 channels and presented the data on 40 mimic screens. There were two models developed: the analytical model, which had good accuracy, but was unacceptable due to very long calculation times and the second one, consisting set of linearized models of most CPU-consuming components. The second model is close to the real time operation. Further research will be performed in the direction to extend applied models to improve accuracy, especially in transient states.

The author gratefully acknowledge the financial support of the research project DIADYN No PBZ-KBN-105/T10/2003, funded by the Polish Ministry of Science (MNiI).

REFERENCES

- [1] Barszcz T., Czop P.: *Hybrid Modeling approach to the diagnosis of a turbine control system, 2004*, Proceedings of the 10th IEEE international conference on Methods and Models in Automation and Robotics MMAR 2004.
- [2] Flynn D. ed.: *Thermal Power Plant Simulation and Control*, Institution of Electrical Engineers, London, 2003.
- [3] Gertler J.: *Fault detection and diagnosis in engineering systems*, Marcel Dekker, New York, 1998.
- [4] Kościelny J. M.: *Diagnostics of industrial processes* (in Polish), EXIT, Warsaw, 2001.
- [5] Kundur P.: *Power System Stability and Control*, Electric Power Research Institute. McGraw Hill, 1993.
- [6] Ljung L.: *System identification – Theory for the User*, Prentice-Hall, 1999.
- [7] Patton R. J., Frank P. M., Clark R. N. (eds.): *Issues of fault diagnosis for dynamic systems*, Springer-Verlag, London, 2000.
- [8] Uhl T., Giergiel J.: *Identification of mechanical systems* (in Polish), PWN, Warsaw, 1990.
- [9] *MATLAB/ SIMULINK documentation*, Mathworks Inc., 2005.
- [10] *OPC. Ole for Process Control. OPC Overview ver.1.0*, OPC Task Force, 1998.



Dr inż. **Tomasz BARSZCZ** pracuje jako adiunkt w Katedrze Robotyki i Mechatroniki Akademii Górniczo – Htnicznej. Obszarem jego zainteresowania jest konstrukcja i zastosowania układów monitorowania stanu maszyn. Jest autorem

monografii o systemach monitorowania i diagnostyki, wielu artykułów o charakterze naukowym oraz wielu wdrożeń w przemyśle.

MECHATRONIC APPROACH TOWARDS FLIGHT FLUTTER TESTING

Grzegorz KARPIEL, Maciej PETKO, Tadeusz UHL

Katedra Robotyki i Mechatroniki
Akademia Górniczo-Hutnicza
al. Mickiewicza 30, 30-059 Kraków
gkarpriel@agh.edu.pl, petko@agh.edu.pl, tuhl@agh.edu.pl

Summary

The paper presents an idea of identification of the flutter phenomena during a flight. The proposed flutter detection algorithm is based on the identification of natural frequencies and modal damping ratio for an airplane structure based on in-flight vibration measurements. The procedure can be realized during a flight using measured actual vibration. The algorithm is based on recursive identification of model parameters and wavelets based signal filtering. The real-time realization is implemented in hardware and tested during a flight. FPGA technology is used for the hardware design. The results of a test of the hardware system prototype are presented.

Keywords: flutter, real-time modal analysis, FPGA.

MECHATRONICZNE PODEJŚCIE DO BADANIA MARGINESU FLATTERU SAMOLOTÓW

Streszczenie

W artykule przedstawiono implementację algorytmu identyfikacji flatteru podczas lotu. Przedstawiony algorytm bazuje na identyfikacji częstotliwości własnych oraz współczynnika tłumienia poprzez pomiar drgań struktury samolotu. Zaprezentowana procedura może być realizowana podczas lotu wykorzystując dostępne sygnały z czujników drgań. Algorytm wykorzystuje transformatę falkową jako filtr częstotliwościowo-czasowy dla izolacji pojedynczych postaci drgań o parametrach zmiennych w czasie. Realizację w czasie rzeczywistym wykonaną w postaci sprzętowej sprawdzono podczas testowego lotu. Do zaprojektowania struktury sprzętowej użyto technologii FPGA. Przedstawiono rezultat działania prototypowego urządzenia.

Słowa kluczowe: flatter, analiza modalna w czasie rzeczywistym, FPGA.

1. INTRODUCTION

Unstable vibrations of airplane can be a reason of a catastrophic failure of an aircraft. Such a case of vibration is commonly defined as a flutter [1]. In the literature [2] [3] many cases of the flutter phenomena are carefully studied. Each aircraft should be tested using numerical simulations and experimental investigation of airplane structure vibrations due to the controlled excitation during a flight. A vibration based experimental flutter test during a flight is very expensive, time consuming and is a critical part of the aircraft certification procedure [4]. The procedure of in-flight flutter testing consists of measurements of structural vibration of an airplane and, based on these measurements, estimation of modal model parameters [5] [6]. Each possible aircraft configuration should be tested separately. There are two cases: first, if an artificial vibration excitation is used during a flight and second, if an ambient excitation (non measured) is a cause of structural vibration. Many papers are focused on the development of operational modal analysis methods,

which can be directly applied for modal parameters estimation during a flight [7] [8]. Some of them are realized iteratively in real-time, with less than 1 second interval between estimations [9]. These methods, applied for flight flutter testing, shorten testing procedure and dramatically decreasing its costs. During the proposed procedure, an aircraft is excited by an operational excitation (turbulences, maneuvers of the airplane) or using dedicated excitation devices, and its vibration responses are measured. Based on the recorded signals, the modal parameters of the structure are estimated using some identification method. These parameters, in particular modal damping and natural frequencies, are useful for flutter boundaries determination. The described procedure should be applied at each test point to determine the Flight Clearance Envelope (FCE) [4]. There are many different modal parameters identification methods that could be used for in-flight flutter testing. They can be categorized to experimental and operational modal analysis methods [8]. The second ones can be applied for an experiment scenario, in which the excitation force is not measured and implemented in the proposed

flutterometer design. The flutterometer is an electronic device that permits estimations of modal parameters during a flight, based on the structure response, focused on tracking of the flutter margin changes with variations of flight conditions. Both time domain and frequency domain methods match requirements of the on-line modal parameters identification [9]. A wide range of methods can be considered for final implementation; many of them have been tested using simulated and real measurement data. The time-domain method, based on a simple recursive RLS algorithm is applied in the proposed solution as efficient enough and relatively easy to implement. The major assumption applied in the procedure is linearity of the isolated system modes that are, however, nonstationary due to changes of flight parameters and variations of aerodynamic feedback. Signal processing procedures should satisfy these assumptions. The wavelet based signal preprocessing is employed in the solution.

2. IMPLEMENTATION OF SIGNAL PROCESSING ALGORITHMS IN FPGA

2.1. Hardware – software partitioning

The flutter monitoring algorithm consists of five steps: data read from analog-to-digital converters (ADC), convolution of a stored wavelet with signals from sensors [10], signals reconstruction, on-line recursive least square (RLS) routine for estimation of parameters of ARMA models [9], and determination of damping coefficients for flutter detection (Fig. 1) [11]. The result of calculation is stored in memory and transmitted to PC by USB interface. The wavelets are generated during system initialization by the processor and stored in buffers in custom hardware. Floating-point operations of software part are accelerated by hardware custom instructions created in the Nios II ALU, namely floating-point addition, multiplication, reciprocal and square root.

The normally most time-consuming part of the algorithm – convolution and signal reconstruction is accelerated by a custom hardware accelerator and executed in fixed-point arithmetic [14]. It is possible because of restricted resolution of input data and fixed size of both the wavelet table and the input buffer. Signal reconstruction is carried out simultaneously with convolution. The hardware accelerator (Fig. 2) is controlled by a single master control unit responsible for signal acquisition from DACs, storing of the samples in a circular buffers, generation of addresses and control signals for memories containing wavelet and signal buffers, and synchronizing data feed with actual calculations performed by multiple identical convolution and signal reconstruction units.

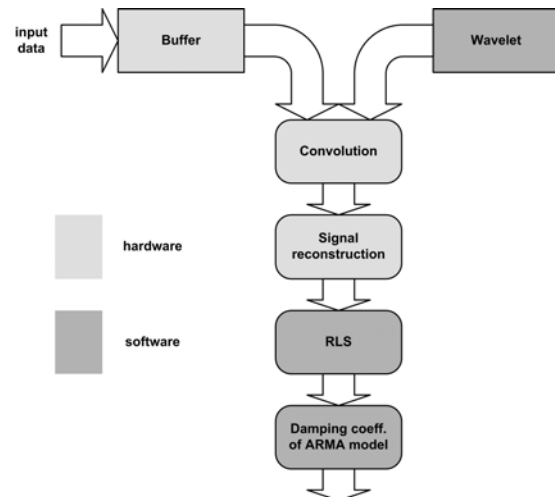


Fig. 1. Hardware-software partitioning of the flutter monitoring algorithm

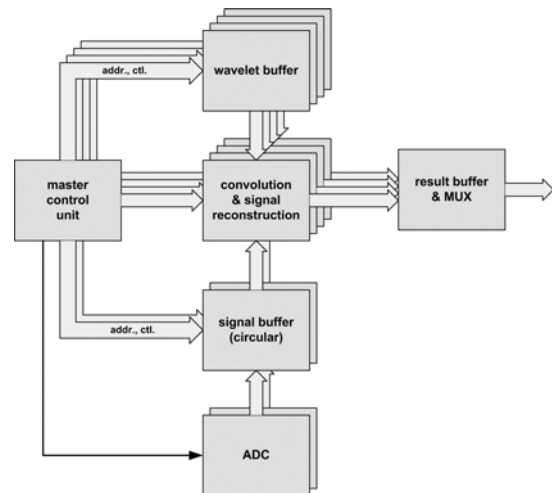


Fig. 2. Architecture of the custom hardware accelerator for multi-channel wavelet transformation

Such an arrangement allows for easy scaling i.e. simultaneously performing variable number of wavelet transformations of each of variable number of input signals without consuming more time, with variable wavelet length in each channel (1024 points maximum) and with signal time window width of 512 samples. In present version, the flutterometer is equipped with hardware accelerator capable of separation of three vibration modes in each of two input signals (six channels altogether).

2.2. Hardware architecture

The processor and the hardware accelerator work in master-slave arrangement with the processor as master. Completion of calculations by the hardware accelerator is registered in status bits and generates a DMA request to transfer the results to software. RLS algorithm and damping coefficients calculations are performed for each wavelet-filtered signal in floating-point arithmetic by the processor

supported by custom instructions. Flutter appearance can be then determined using damping coefficients thresholds table indexed by the actual flight conditions. Fig. 3 shows overall hardware architecture of the flutterometer.

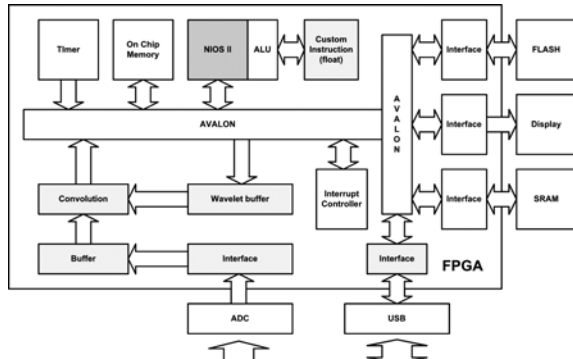


Fig. 3. Internal architecture of the flutterometer FPGA

All calculations are shared between software (dark gray blocks) and hardware (light gray blocks) [15], as shown on Fig. 3, in system created in a Stratix FPGA chip. Software means that parts of the algorithm are written in C and next compiled for Nios II soft-processor [13, 14]. Hardware fragments are realized in the logic of the FPGA and the Avalon Bus is used for data exchange.

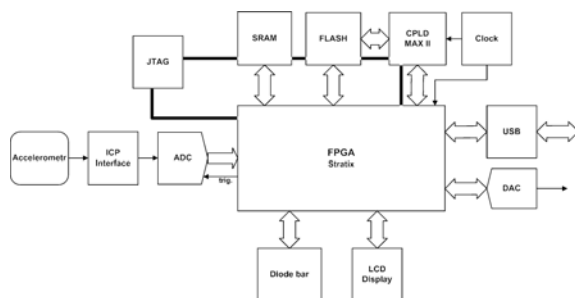


Fig. 4. Block diagram of the flutterometer hardware

The hardware of the flutterometer is based on a Stratix FPGA chip (Fig. 4) that is responsible for algorithm realization. FPGA programming is performed from flash memory by MAX II CPLD chip. Flash can store several configurations for FPGA and can be accessed directly by Nios II microprocessor implemented in FPGA. The latter allows for reading program code and long-term data storage by microprocessor. For temporary data storage, the system is equipped with fast static memory. FPGA, CPLD and both memories are placed in a single JTAG chain for programming and debugging.

The inputs to the flutterometer are signals from ICP piezoelectric accelerometers. After amplification and antialiasing filtering, they are digitized by analog-to-digital converter triggered by FPGA with programmable frequency in the range 10-200 Hz.

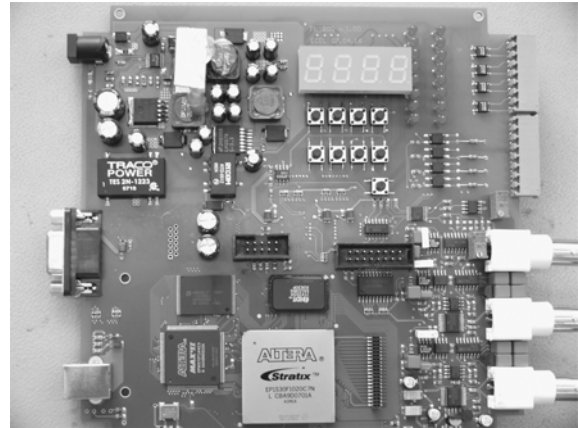


Fig. 5. Prototype of the flutterometer

The system has five outputs:

- analog output, generated by digital-to-analog converter, to enable external recording of changes of damping coefficient;
- serial digital interface for sending results of calculations to external devices;
- 8-segment, 4-digit display and LCD providing the current value of damping coefficient;
- multicolour diode bar indicating current flutter margin;
- digital, optoisolated alarm outputs signalling improper (too small) flutter margin.

The prototype of flutterometer is presented on Fig. 5. All components are placed on single PCB. LCD display is outside of the board and is designed for showing status information.

The whole application occupies 32% of logic elements, 29% DSP blocks and 34% of memory in EP1S30F1020C7 FPGA chip, leaving enough resources for future modifications of algorithm.

2.3. Experimental verification

In the first step of verification a triangle-wave input signal from a generator was used (Fig. 6). The frequency of the signal was 7.48Hz. Because the amplitude of the signal was constant, damping ratio was near zero. The frequency was identified correctly by the RLS algorithm to 7.48Hz.

On the next step, the shape of the input signal was replaced by square-wave. Additionally the amplitude of the signal was variable. For decreasing amplitude, the identified damping ratio was positive and vice-versa (Fig. 7).

Next, the device was tested on signals recorded during a flight of a military jet aircraft when flutter actually appeared [16].

Finally, the performance of the flutterometer has been verified during flight of a "Skytruck" aircraft.

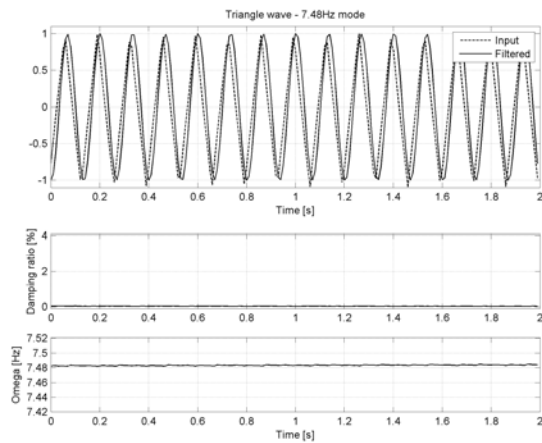


Fig. 6. Laboratory verification: triangle-wave input signal; frequency ca 7.48Hz, sample time 0.01s

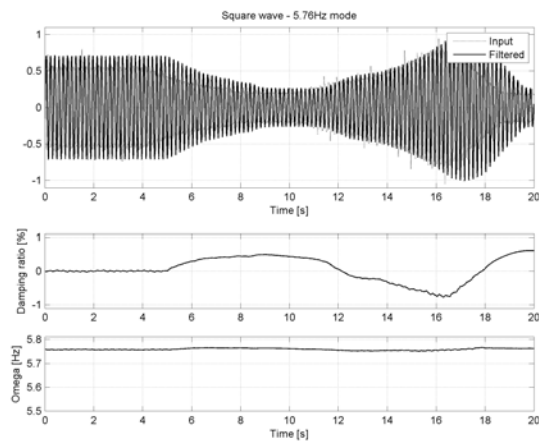


Fig. 7. Laboratory verification: square-wave input signal; frequency ca 5.76Hz, sample time 0.01s

The M28 “SkyTruck” (Fig. 8) is a twin-engined high-wing cantilever monoplane of all-metal structure, with twin vertical tails and a robust tricycle non-retractable landing gear, featuring a steerable nose wheel to provide for operation from short, unprepared runways where hot or high altitude conditions may exist. The M28 is dedicated for passenger or cargo transportation.



Fig. 8. M28 “SkyTruck” aircraft – civil version

During the flutterometer verification experiment, two signals have been used (Fig. 9-a). The first accelerometer was mounted on the right vertical tail.

The second signal came from an accelerometer which was placed on the right plane. Both accelerometers measured vibrations in the vertical direction. Results of the calculations were transmitted to a PC (Fig. 9-b) by the USB interface, and stored on hard disk.

The signals were sampled with frequency of 100Hz during the test flight performed at constant speed of about 172KTS (320km/h). For each channel three modes were estimated. The frequency of the modes and appropriate wavelet parameters had been identified using data from previous flights of the same plane [17]. Results for modes of frequency: 5.2Hz, 7.4Hz and 12.5Hz in the vertical tail sign are presented on the Fig. 10.

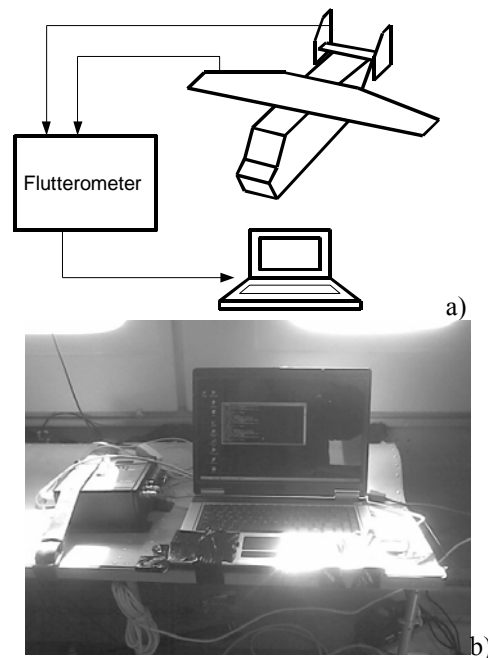
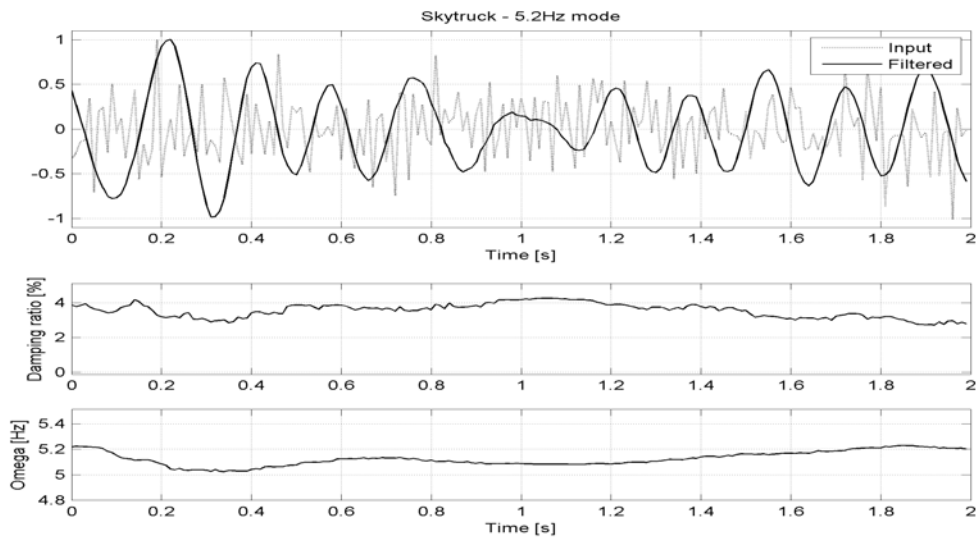


Fig. 9. In-flight experiment: a) diagram of connections, b) picture of equipment; the flutterometer on the left side of the table

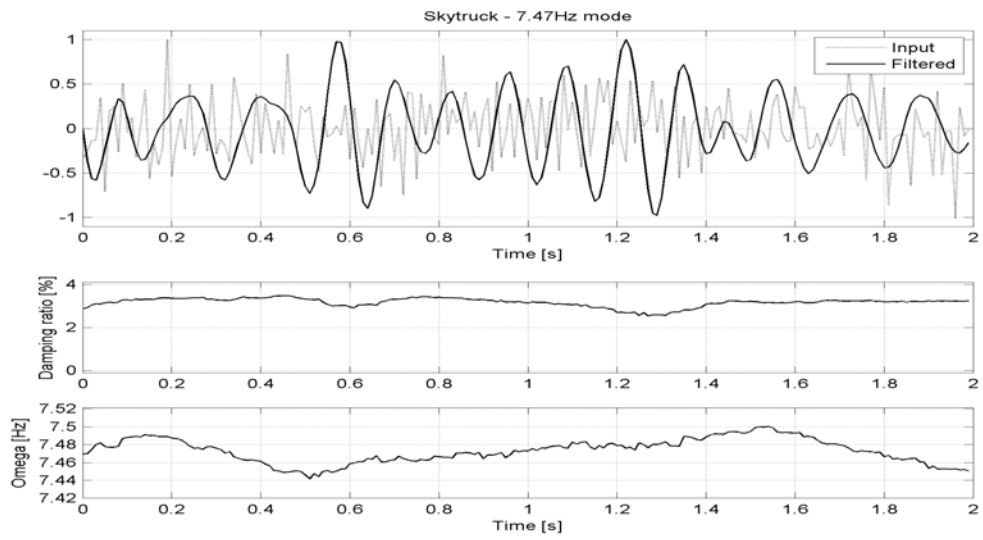
3. CONCLUSIONS

The hardware platform for implementation is based on a modern FPGA chip. Implementation of the flutter monitoring algorithm is proposed with Hardware-Software Co-design approach, i.e. a part of it is realized by hardware and the remaining part by software running on Nios II soft-processor contained in the FPGA. The flutterometer is an example of System-on-Chip, which allows for high level of integration and flexibility – it can be altered, e.g. to optimize for different algorithm, or to add some functionality, by reprogramming the FPGA without modifications of the PCB. The methodology used, lowered costs and the duration time of the development process.

a)



b)



c)

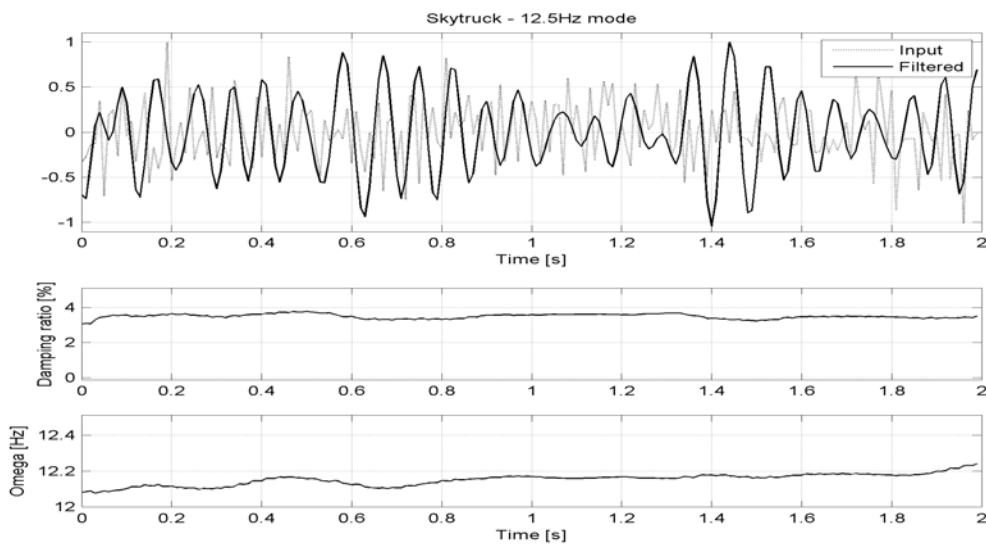


Fig. 10. “SkyTruck” in-flight experiment: $V_{IAS}=172$ KTS, $H_{ST}=10000$ ft. Right vertical tail:
 a) 5.2Hz mode, b) 7.46Hz mode c) 12.5Hz mode

ACKNOWLEDGMENT

The project is financed by the Polish Ministry of Scientific Research in the frame of the EUREKA E13341 FLITE 2 project.

REFERENCES

- [1] Kehoe M. W.: *A historical Preview of flight flutter testing*, AGARD Conference proceedings 566, Advanced Aeroservoelastic Testing and Data Analysis, (1995).
- [2] Garrick I. E. and Reed W. H.: *Historical development of aircraft flutter*, Journal of Aircraft, v.18, (1981), pp. 897-912.
- [3] Brenner M. J., Lind R. C. and Voracek D. F.: *Overview of recent flight flutter testing research at NASA Dryden*, NASA TM/4792, (1997).
- [4] Abbasi A. A. and Cooper J. E.: *Current Status and Challenges for Flight Flutter Testing*, Proceedings of ISMA 2006 Conference, Leuven, (2006), pp. 1523- 1546.
- [5] Nissim E. and Gilyard G.B.: *Methods for experimental determination of flutter speed by parameter identification*, NASA TP-2923, (1989).
- [6] Dimitriadis G. and Cooper J.E.: *Flutter prediction flight flutter test data*, AIAA Journal of Aircraft, vol. 38, (2001), pp. 355-367.
- [7] Hermans L. and Van H. der Auweraer: *Modal testing and analysis of structures under operational conditions: Industrial applications*, Mechanical Systems and Signal Processing, vol. 13(2), (1999), pp. 193-216.
- [8] Uhl T., Lisowski W. and Kurowski P.: *In-operation modal analysis and its application*, AGH, Krakow, (2001).
- [9] Bogacz M. and Uhl T.: *Real time modal model identification and its application for damage detection*, Proceedings of ISMA 2004 Conference, Leuven, (2004), pp. 1065-1075.
- [10] Klepka A. and Uhl T.: *Application of wavelet transform to identification of modal parameters of nonstationary systems*, Journal of Theoretical and Applied Mechanics, Vol. 43, (2005) ,pp. 277-296.
- [11] Klepka A.: *Identification of modal parameters of mechanical structures in nonstationary conditions*, PhD thesis, AGH Univ. of Science and Technology, Krakow, (2005) (in Polish).
- [12] Wegrzyn M., Adamski M. A. and Monteiro J. L.: *The application of reconfigurable logic to controller design*, Control Engineering Practice, Vol. 6, 1998, pp. 879-887.
- [13] Kambe T., Yamada A. and Yamaguchi M.: *Trend of system level design and approach to C-based design*, Microelectronics Journal, Vol. 33, (2002), pp. 875-880.
- [14] Petko M. and Karpiel G.: *Semi-Automatic Implementation of Control Algorithms in ASIC/FPGA*, in 2003 IEEE Conference on Emerging Technologies and Factory Automation: Proceedings, vol. 1,(2003), pp. 427-433.
- [15] Edwards M. D., Forrest J. and Whelan A. E.: *Acceleration of software algorithms using hardware/software co-design techniques*, J. of Systems and Architecture, Vol. 42, (1996/97), pp. 697-707.
- [16] Uhl T., Petko M.: *Real-time flutter detection from in-flight vibration data*, Key Engineering Materials Vol. 347 (2007) pp. 679-684.
- [17] Mendrok K., Lisowski W., Uhl T.: *Sas, Modal analysis of the M28 SkyTruck airplane basing on output only data measured during flight*, Proc. of 10th Int. Congress on Sound and Vibration, Stockholm, (CD) 2003.



dr inż. **Grzegorz KARPIEL** jest adiunktem w Katedrze Robotyki i Mechatroniki, Akademii Górniczo-Hutniczej. Głównie jego zainteresowania skupiają się na mechatronice, zagadnieniach dotyczących robotów równoległych oraz projektowaniu sterowników opartych na układach FPGA.



dr inż. **Maciej PETKO** - adiunkt w Katedrze Robotyki i Mechatroniki AGH. Jego zainteresowania skupiają się na mechatronice, robotyce, zagadnieniach prototypowania i implementacji algorytmów przetwarzania sygnałów, głównie w sterowaniu i diagnostyce technicznej.



Prof. dr hab. inż. **Tadeusz UHL**, jest kierownikiem Katedry Robotyki i Mechatroniki, Akademii Górniczo-Hutniczej w Krakowie. W swoich pracach zajmuje się zagadnieniami dynamiki konstrukcji, a zwłaszcza analizą modalną. Jego zainteresowania obejmują także układy aktywnej redukcji drgań, układy sterowania i szeroko pojętą mechatronikę.

STRUCTURAL CONDITION EVALUATION OF PRESTRESSED CONCRETE STRUCTURES BASED ON VIBROACOUSTIC MONITORING

Stanisław RADKOWSKI, Adam GAŁĘZIA, Jędrzej MACZAK, Krzysztof SZCZUROWSKI

Instytut Podstaw Budowy Maszyn PW
Ul. Narbutta 84, 02-524 Warszawa, ras@simr.pw.edu.pl

Summary

Analysis of the phenomenon of modulation of vibroacoustic signal's parameters, especially the amplitude and the frequency structure of the envelope which is directly associated with the occurrence of group velocity, may prove to be an effective tool for diagnosing the technical condition of pre-stressed structures. This scope of work and the examination of the influence of local defects and of the environmental impact was the main research task during COST Action 534 project duration. An issue that is particularly interesting and that calls for additional analyses and experiments will be the development and adaptation of effective de-modulation algorithms.

Keywords: technical diagnostics, prestressed structures, amplitude modulation.

OCENA STANU TECHNICZNEGO BETONOWYCH KONSTRUKCJI SPRĘŻONYCH NA PODSTAWIE MONITORINGU WIBROAKUSTYCZNEGO

Streszczenie

Analiza zjawiska modulacji wibroakustycznych parametrów sygnału, a w szczególności amplitudy i struktury częstościowej obwiedni, która jest bezpośrednio związana ze zjawiskiem prędkości grupowej, może być efektywnym narzędziem w diagnozowaniu stanu technicznego struktur sprężonych. Ten zakres pracy, jak również badanie wpływu występowania miejscowych wad było głównym zadaniem kończącej się Akcji COST 534. Zadaniem, szczególnie interesującym i wymagającym dalszych analiz i eksperymentów, jest rozwój i adaptacja użytecznych algorytmów demodulacji.

Słowa kluczowe: diagnostyka techniczna, struktury wstępnie sprężone, modulacja amplitudowa.

1. INTRODUCTION, PROJECT AIM AND DESCRIPTION OF PROBLEM

COST Action 534 is UE research project in subject: "New Materials and Systems for Prestressed Concrete Structures". Project started in 2003 and ended in December 2007.

In project were involved 35 participants. Project was divided to 5 Work Groups and each WG had several Group Projects. Author's research project was realized in framework of Work Group 3 – "New assessment methods". WG3 project aimed to evaluate the structural condition of reinforced and prestressed concrete infrastructure facilities by means of acoustic monitoring and by improving the applicability of the dynamic evaluation techniques. Group Project 4 – "Structural condition evaluation of prestressed concrete structures based on acoustic monitoring", whose coordinator was Stanisław Radkowski, was aimed to develop vibroacoustic methods allowing for evaluation of condition of structure. In this Group Project participated researches from: Warsaw University of Technology, KWH Bautechnologen AG, AGH University of Science and Technology, Poznań

University of Technology, Bouwdienst Rijkswaterstaat and Advitam, Budapest University of Technology and Economics, National Technical University of Athens.

In this paper authors would like to present results of their research in framework of COST Action 534 and conclusions related with this subject.

It was intended to achieve the structural evaluation by analysis of the relationships between the distribution of stress in the cross-section and changes of vibroacoustic signal's parameters.

It is generally known that infrastructure facilities (viaducts, bridges, etc.) age over time with an increasing rate due to intensified loads by traffic and aggressive exposure conditions. For concrete structures this process results in cracking in many cases. Consequently, the problem of structural performance regarding to load capacity and user safety becomes of increasing importance. From an owner's perspective condition evaluation by non-destructive techniques could therefore be very helpful in supporting management and maintenance decision's making process.

Basic assumption is that increase and decrease of prestressing forces are accompanied by a change of stress distribution in the cross-section of concrete structure. The parameters of propagation path will change due to this phenomenon.

Using monitoring technique based on the change of their dynamic characteristics to classify structures, it is necessary to determine a numerical relationship between the measurable dynamic characteristics and the degree of deterioration. The availability of several physical models regarding deterioration of prestressing structure makes it possible to establish relationships between defects resulting from degradation of prestressed steel and the stress distribution in the cross section of structure. As the stress level affects the velocity of wave propagation, vibroacoustic is used to provide quantitative information on the general stress. This information is used to evaluate the overall condition with respect to the load-bearing capacity of structures using appropriate numerical modeling tools. It is therefore important to note that the project was aimed at overall condition evaluation of structures rather than provide information on the level of single defects. Based on the development of stress distribution over time predictive evaluation of structure condition to establish the residual service life is performed.

The to-date research, concerning components of machines and especially the shafts, that is the beam-type structures, shows that changes of stress in the outer layer of concrete can be detected by methods of vibroacoustic signal demodulation. Accordingly, the occurrence at the quantitative change of stress distribution leads to the change of distribution of amplitudes around the relevant carrier frequency, usually the natural frequency of structure vibration. Thus, apart from the selection of the relevant model of the modulation phenomenon, the essential task in the proposed project was to define the method and the criteria of selection of modulated bands of diagnostically essential carrier frequencies.

For real-life structures continuous acoustic monitoring using surface applied sensors are a practical way of condition evaluation. The results thus obtained indicate the occurrence and the location of tendon failure. By appropriate filtering techniques the method is capable of providing useful information even in a noisy traffic environment. The data can be used to support decisions regarding management and maintenance of structures.

2. LABORATORY EXPERYMENTS - RESULTS

Examined method of diagnosis relies on the relationship between the parameters of the wave propagation as a function of stress occurring in a given object. This is manifested by changes to the modulation of the vibroacoustic signal's

parameters, which is caused by the disturbance of propagation of the sound wave in the material as a result of changes to the distribution of stress in the cross-section of the pre-stressed structure. Defects appearing in structure leads to the decrease of compressing stress what result in a change in the distribution of stress in the cross-section that is measurable in a degree allowing one to detect the qualitative change of the effect of modulation of the vibroacoustic signal's parameters.

Paper presents method of evaluating the technical condition of a prestressed structure while underscoring the possibilities offered by use of amplitude modulation effects which occur in the observed vibroacoustic signal.

2.1. Description of laboratory tests

In frame work of research project many tests in laboratory conditions were performed. Examined samples were made for purposes of tests. As a result of analysis of signals obtain from measurements, it was possible to define algorithm of failure detection and identification.

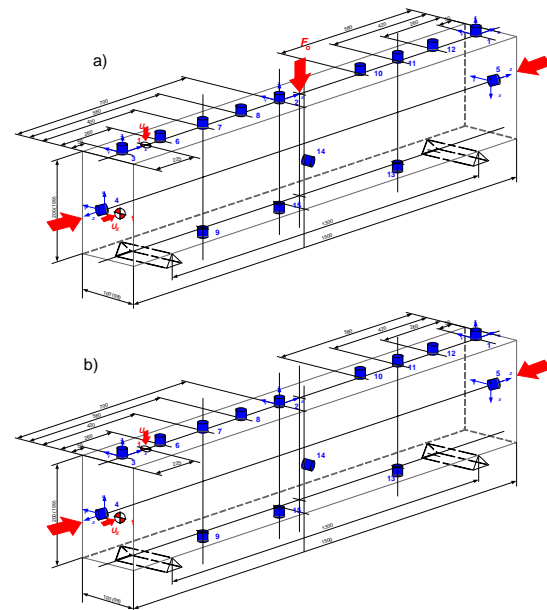


Fig. 1. Location of vibration sensors and directions of vibration-causing forces in the prestressed concrete beam: a) - scheme of measurement made in Kielce and Warsaw (with perpendicular force), b) - scheme of measurement made in Poznań (without perpendicular force)

Tests were aimed for investigation of dynamic response of prestress structure behavior under changeable loading conditions: what is frequency structure of a response pulse and how it depends on technical state and failure evolution.

Preliminary set of tests were carry out in beginning of project and made in Kielce University of Technology. Measurements were carry out on a prestressed concrete beams made of B20 class

concrete with dimensions 1500x100x200mm. The specimen was placed in the strength testing device bed, supported by two symmetrically placed supports and during measurements it was loaded by machine's bending punch with a pre-defined force. Exact description of tests can be found in [5, 6]. The tests were carried out with load changing from 0.5 kN to 70 kN, because loading with force 75 kN resulted in breaking of the beam. The first small cracks usually emerged when the load of 45kN was exerted.

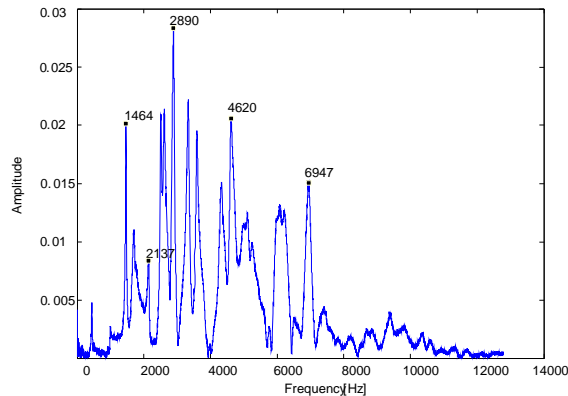


Fig. 2a. Signal spectrum obtained from one of measurements

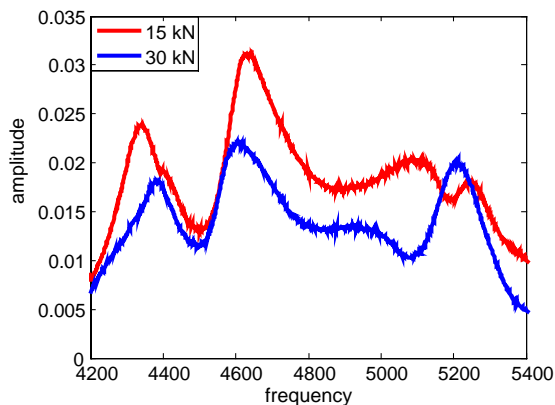


Fig. 2b. Selected frequency band - changes in amplitude modulation resulting from change of load

In order to observe the changes in terms of propagation of the wave through the examined beam vibration sensors were placed on the beam. Their exact locations, locations of impulse excitation force and point of loading are presented in Fig. 1a.

Recorded results of measurements were subjected to analysis in order to define the conditions of propagation of the waves caused by a pulse input. Distinct differences were observed in the values of response delay for the detector located at the opposite side of the beam (see detector no 5).

Figure 2a presents example of signal spectrum obtained from one of measurements. Figure 2b presents sideband of previous spectrum concentrated around 4800 Hz.

First observation was change of natural frequency as a function of crack expansion (figure 3). Changing of loading caused a bending of a specimen. Bending lead to change of stress distribution in beam and change from compressive to tensile. This lead to arise and further expansion of crack under increasing loading. It can be seen that before arise of crack there is no change in natural frequencies and after arise of crack change is significant. Basing on change of natural frequency it is possible to infer about crack appearance and its evolution. This is related with change of mechanical properties of specimen and stress distribution in structure with cracks. However this method gives no information about stress distribution in stage before failure formation so it is impossible to predict how close to failure structure is.

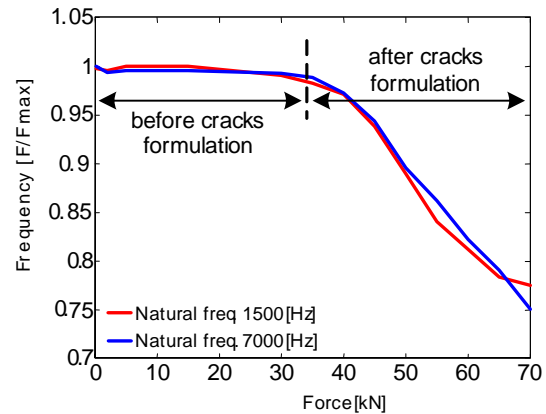


Fig. 3. Change of natural frequency as a function of crack propagation

It was also observed that due to dispersion phenomena in concrete, it is possible to observe not only phase velocity but also the group velocity.

As it was also observed, that around natural frequencies modulation bands are present. These bands are not equivalently distend from carrier frequency, and they are shifting due to change of load.

Next measurements were made in Poznań University of Technology. Set of 11 prestressed concrete beams was tested. Each specimen differs with degree of prestress. Beams had prestressing from 0 kN to 100 kN, with step of 10 kN. Beams dimensions were: 1300x140x110 mm. Specimens were produced in factory with maintaining of production and standard procedures.

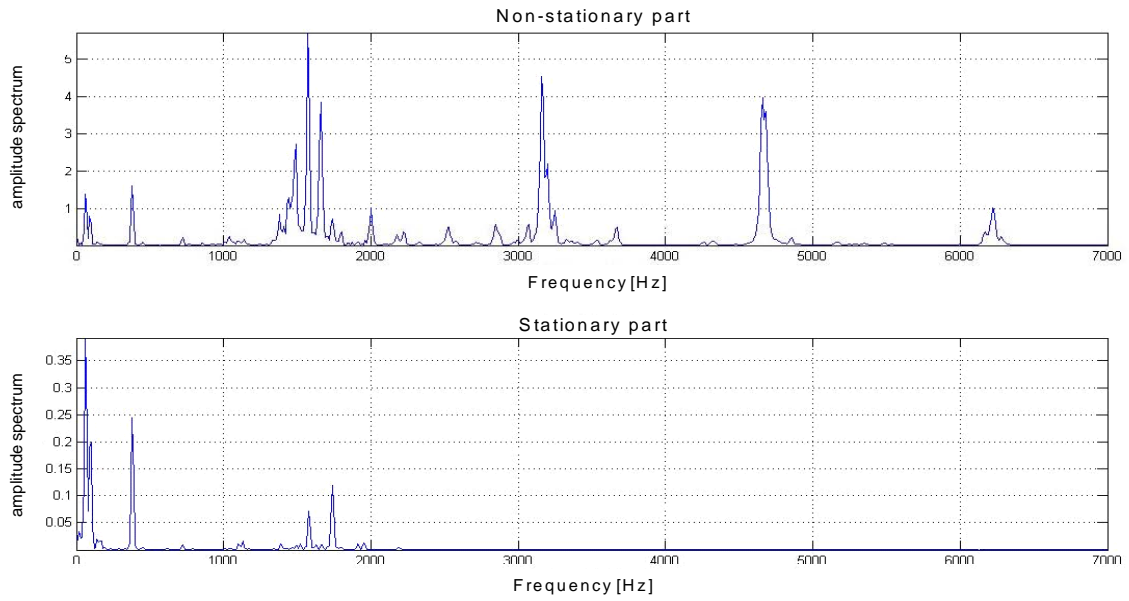


Fig. 4. Spectrum of non-stationary and stationary part of vibroacoustic signal

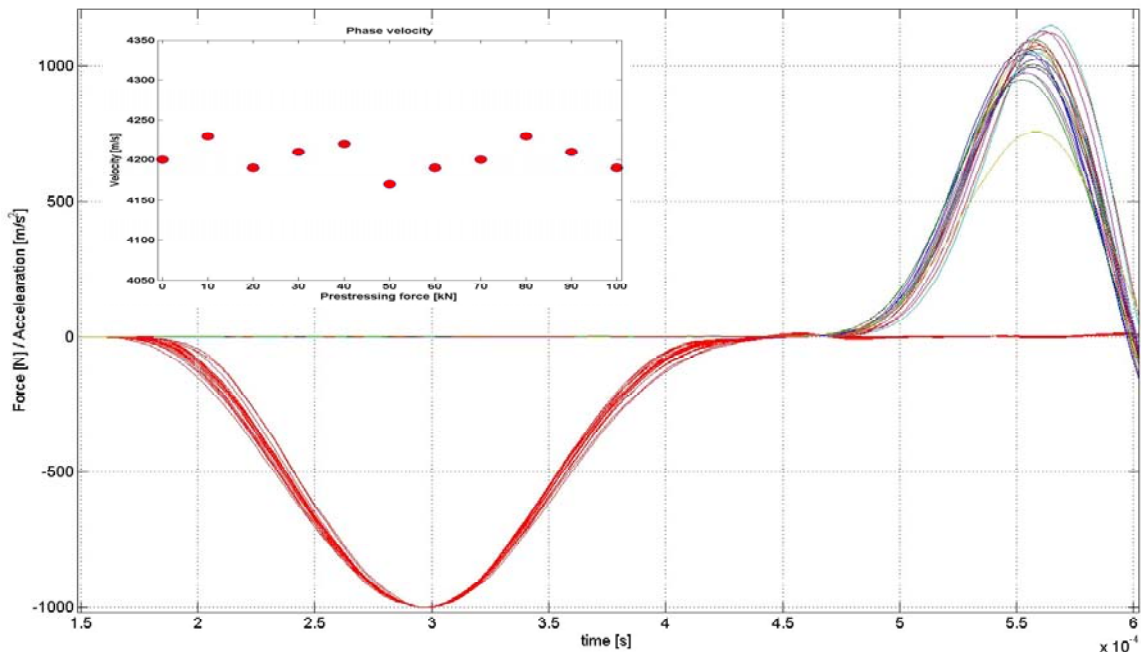


Fig. 5. Changes of phase velocity as a function of prestressing force and waveform of excitation and structure response on opposite end of beam

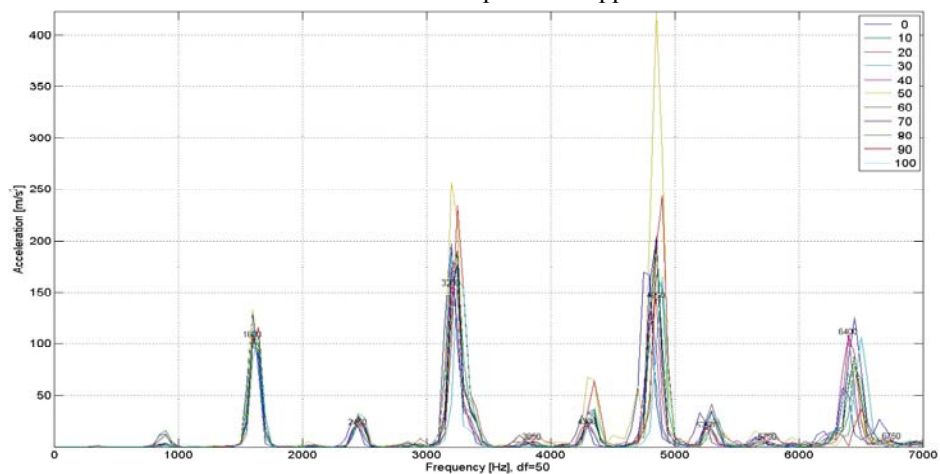


Fig. 6. Spectrum of response signals for different prestressing

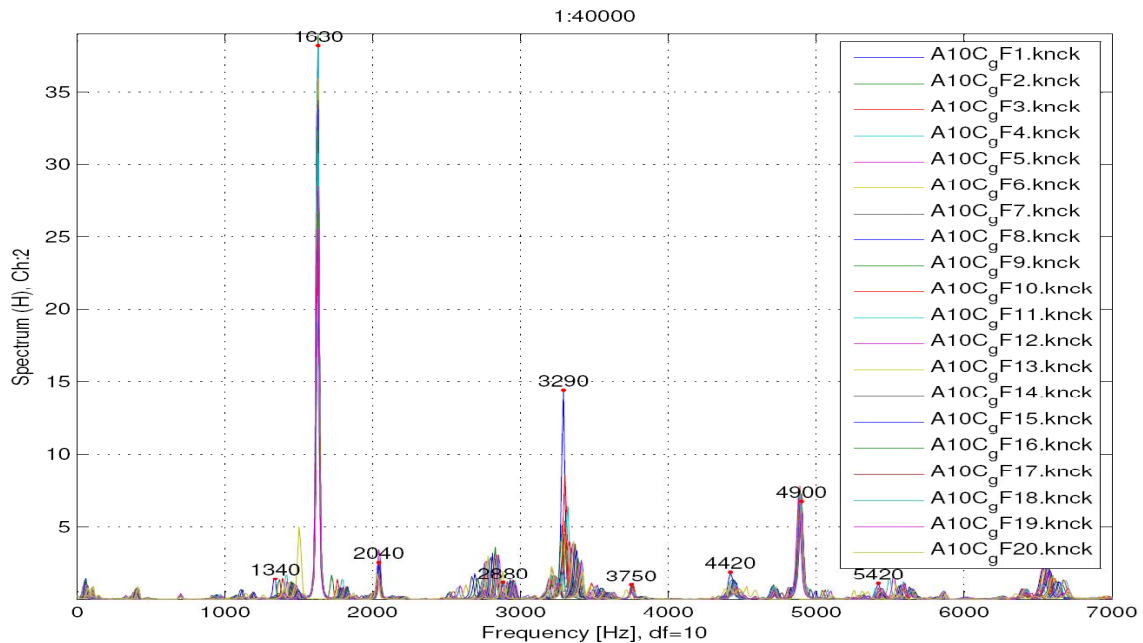


Fig. 7. Signals spectrums for beam with prestressing force 100 kN and different loading

Tested beam was supported on steel prisms and expanders allowing for free vibrations of beam. This was made to verify which support gives more informative results and bring in less disturbances. No additional, external forces were applied to specimen during measurement. Measurements aimed to investigate influence of prestressing force on distribution in spectrum of natural vibrations.

Excitation of vibrations was made by modal hammer and measured by set of vibration sensors attached to surface of specimen. Data acquisition was made using NI equipment with high sampling frequency.

Support on steel prisms introduce less disturbances by damping free low frequency vibrations. For further analysis signals from prisms were examined. An interesting observation is related with frequency structure of response for excitation. From informative point of view, response signal can be divided in to two parts – stationary and non-stationary.

Non-stationary part approximately ends around 0,05 second, from beginning of signal, and its spectrum contains many informative frequencies - higher natural frequencies, modulations around them additional peaks. Problem is duration of this signal, what influence spectrum frequency resolution. Spectrum of stationary part (from 0,05 till ~0,25 sec.) contain peaks of lower frequencies related with free vibrations (fig. 4). Analysis of signal combined from non-stationary and stationary part, in spite of increasing frequency resolution, is not giving improvement in information contained in signal due to decreasing of amplitude of peaks.

A surprising result achieved from analysis of signal was that change of degree of prestress has no influence on phase velocity of wave. Figure 5 presents changes of phase velocity in a function of

prestressing force and waveform of excitation and structure response on opposite end of beam. It can be seen that for unify waveforms of excitation (below 0 line), there is no trend in changes of response waveforms (over 0 line). Such changes were detected in signals coming from measurements made in Kielce.

Also it was discovered that there is no unique and significant changes in signal spectrum for differed prestressings (Fig. 6).

Taking in to consideration that the diagnostic experiment was performed without perpendicular force, it is obvious, that no dispersion phenomenon in prestressed structure was indicated on this way.

It must be remembered that each specimen, having own prestressing, was a different object. This leads that despite of maintaining production procedures difference from assumption can be present. Following conclusions came out after measurements: dynamical behavior of tested structure was very similar, changes of degree of prestress do not influence phase velocity. Phase velocity can not be used as a tool for inferring on stress exiting in structure. Also the measurable change of group velocity was not observed.

Basing on those results additional tests were made in laboratory of Research Institute of Roads and Bridges in Warsaw. Tests were made on selected beams (prestressing force 0 kN, 3 kN, 5kN, 10 kN) from set of specimens tested earlier in Poznań. Thanks to this errors due to different specimen were avoided and could be compared with results from earlier measurements.

During this measurement session, vibration response, to impulse excitation, of each beam, was registered. Specimens were placed in durability machine which implement force on prestressed concrete beams using bending punch. Specimen

dimensions: 1300x100x140 mm, distance between supports in durability machine was 1060 mm. Examined structure was banded until arise of crack. Bending force was changing from 0 kN to 19 kN, with step 1kN.

Analysis of signals gives very interesting results. Similarly to results of measurements made in Poznań, no change in phase velocity has been observed – in both cases - as a function of prestressing and as a function of bending force. Spectrums of signals from beam with prestressing force 10 kN and different loads are presented on figure 7. It can be seen that natural frequencies are not shifting, what is related with stability of phase velocity, in contrast to sidebands around them, what is related with group velocity. This phenomenon is caused by dispersion. It is well visible on side bands around carrier frequency 1630 Hz. (natural frequency).

3. ALGORITHM OF DIAGNOSING

As it was presented in [1-4, 7] dispersion phenomena cause change of group velocity of wave traveling through beam. This change cause as an effect amplitude modulation of carrier frequency. It can be also seen that shift of sidebands has tendency – with increase of stress in cross-section sidebands are shifting in direction of higher frequencies. Main conclusion based on results is that changes of phase velocity carry information about failure development and group velocity may be a very useful tool for estimation of stress distribution in structure.

The analysis of the phenomenon of modulation of a vibroacoustic signal, especially the amplitude and the frequency structure of the envelope which is directly associated with the effect of existence of group and phase velocity, may prove to be an effective tool in the process of diagnosing the technical condition of prestressed structures.

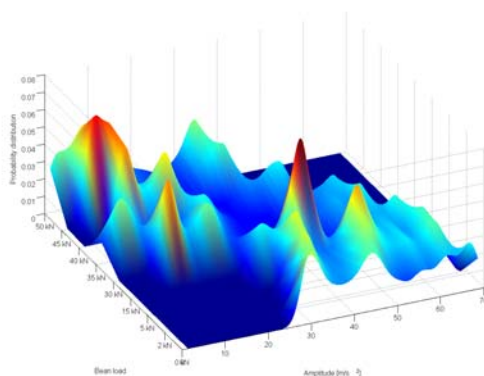


Fig. 8. Probability distribution of acceleration envelope

As an example of usage of probability distribution of acceleration envelope as a diagnostic parameter of technical state of prestressed construction, the quantity change in amplitude due

to formation of structure cracks could be considered (figure 8).

On the one hand there occurs the relationship between phase velocity and frequency while on the other the group velocity changes leads to the phenomenon of amplitude modulation. The existence of direct relation between the stress in the concrete and in the pre-stressing bars on the one hand, and the values of phase and group velocities, on the other, create the possibility of building inverse diagnostic models and thus determining the quantitative changes of such parameters of technical condition as Young's modulus or stress in the concrete and in prestressed steel bars.

The descriptions of the phenomena listed here, the relevant mathematical and diagnostic relations, are presented in [1-6]. They enabled addressing in the present document, the task of developing the algorithm for measuring, analysis, diagnostic inference and estimation of technical condition of a prestressed structure.

Basing on this following algorithm was proposed [7].

In the first step the signal registration and the preliminary analysis of correctness of registered signals are performed. With the use of a signal coming from a force sensor, placed in a modal hammer used for excitation, all the signals are rescaled and averaged (assuming linear relationship with the excitation force). At the stage of research related to prestressed concrete structures we examined the relation between the excitation force and the amplitude of response. Since the amplitude depends on the force in a linear manner, thus its scale can be changed in any way.

In the next step the averaged signals are subjected to a Fourier Transform. At this stage we can observe the changes of own vibration frequency which, as paper [3] demonstrates, are subject to substantial changes along with the emergence of cracks. Defining the values of frequencies of subsequent forms of own vibration enables determination of phase velocity, while its relation to frequency enables initial estimation of stressing forces occurring in the examined structure.

In the further part of the task we determine the bands surrounding own vibration frequency where we can expect the emergence of modulated bandwidths containing relevantly-oriented diagnostic information. After filtering in the bandwidths and demodulating the results, we obtain the information on instantaneous values of the envelope.

At this point attention should be drawn to the need for selecting relevant frequency bands due to the possibility of omitting the information in a situation of its improper selection. Attention should be drawn to the phenomenon of asymmetrical modulation, which was discussed in earlier papers and reports [2, 4].

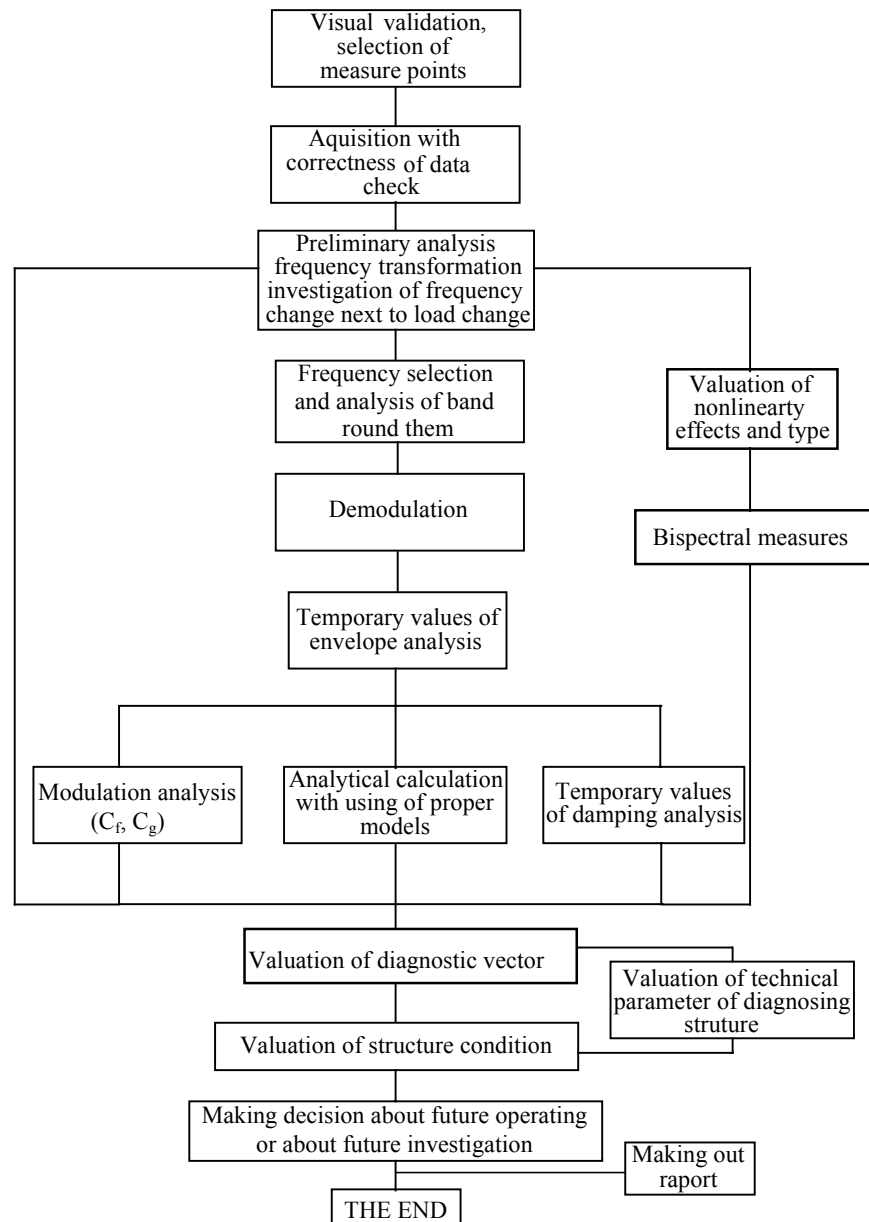


Fig. 9. Algorithm of diagnosing

While observing the changes taking place in the signal's envelope, one can initially define the state of stress: is it in the area of load where stressing or stretching loads occur? It is also possible to initially determine the occurrence of defects in the examined object.

When using demodulation it is possible to examine the phenomena associated with group velocity, which along with phase velocity enables us to define the stress in the cross-section of the examined structure. While relying on the same signal, it becomes possible to define the damping of the examined signal by the structure. In accordance with the examples presented here, while relying on the changes in the damping phenomenon, one can determine the occurrence of unfavorable events, e.g. defects of the prestressing string or significant, local moisture having influence on the strength of a structure.

The algorithm analyzes the tasks resulting from the description in a relevant sequence. What is worth noting is the necessity of maintaining constant control of correctness of measurement results' registration. It is the outcome of extensive requirements related to measurements, in particular the registration at the sampling frequency, which enables determination of instantaneous phase velocity of wave propagation. Respectively, in the next step one should select the parameters of transformation to the frequency domain. The selection of frequency bandwidths should be supported by the analysis of the dynamic model of a structure – in this case a beam, and by the analysis of sensitivity of relevant bandwidths to changes of group velocity as a function of its dependence on the properties of materials and the state of stress or magnitude of prestressing forces.

Signal demodulation, performed as the next step in earlier selected bandwidths, enables estimation of the signal's frequency structure, the frequency structure of the envelope in this case. The demodulation can be performed while using various methods – Hilbert transform was used in this case, which in the task of determining the envelope enables us to obtain results which are satisfactory, correct and precise-enough.

The results obtained this way allow us to define the parameters of the envelope, which are required for further analysis, especially their instantaneous values. Then, based on the relationships developed earlier, the parameters of the envelope obtained this way are in the next algorithm step used for determining the value of phase velocity and group velocity. Similarly, while using a dynamic model which describes transient motion, it becomes possible to determine the damping value. It is worth noting that for the purpose of defining the degree of the influence and type of non-linearity occurring or dominating in a structure, the algorithm provides for the possibility of conducting the relevant bi-spectral analysis.

After conducting the presented activities we have a multi-dimensional vector of diagnostic parameters, which in the next step of the algorithm can be used for calculating the technical parameters of the diagnosed technical structure. As an option the proposed procedure offers the possibility of drafting of reports in a selected format.

REFERENCES

- [1] Radkowski S., Szczurowski K.: *Badanie wpływu stanu naprężeń na proces propagacji naprężeniowej w strukturach sprężonych (Examining the influence of status of stress on the propagation process in prestressed structures)*. Diagnostics Vol. 31 str 89-94.
- [2] Radkowski S. Szczurowski K. et al.: *Report of the Special Research Project, then is our business*, Nr 134/E-365/SPB/COST/T-07/DWM/2004-2007.
- [3] Radkowski S., Szczurowski K.: *The influence of stress in a reinforced and prestressed beam on the natural frequency*, Second Workshop of COST on NTD assessment and new systems in prestressed concrete structures, COST Action 534 New materials and systems for prestressed concrete structures. Kielce 19-21.09.2005, pp. 160-170.
- [4] Radkowski S., Szczurowski K.: *Wykorzystanie demodulacji sygnału wibroakustycznego w diagnozowaniu stanu struktur sprężonych. (Use of vibroacoustic signal demodulation in diagnosis of prestressed structures)*, Diagnostyka Vol. 36. str.25-32.
- [5] Radkowski S., Szczurowski K.: *Hilbert transform of vibroacoustic signal of prestressed structure as the basis of damage detection technique*. Proceedings of the Conference on Bridges, Dubrovnik, Croatia May 21-24 2006, pp.1075-1082.
- [6] Gałęzia A., Radkowski S., Szczurowski K.: *Using shock excitation in condition monitoring of prestressed structures*. The Thirteenth International Congress of Sound and Vibration. Vienna, Austria July 2-6 2006.
- [7] Radkowski S., Szczurowski K.: *Amplitude modulation phenomena as the source of diagnostic information about technical state of prestressed structures*, 6TH International Seminar On Technical System Degradation Problems, Liptowski Mikulasz 11÷14 April 2007.



Stanisław RADKOWSKI the professor of Institute of Machine Design Fundamentals at Warsaw University of Technology, the head of team of Technical Diagnostics and the Analysis of Risk. President of Polish Society of Technical Diagnostics.



Jędrzej MAĆZAK is an assistance in the Institute of Machine Design Fundamentals at WUT. Member of Polish Society of Technical Diagnostics.



Adam GAŁĘZIA is PhD student in the Faculty of Automotive and Construction Machinery Engineering at Warsaw University of Technology.



Krzysztof SZCZUROWSKI is PhD student in the Faculty of Automotive and Construction Machinery Engineering at Warsaw University of Technology. Member of Polish Society of Technical Diagnostics.

THE ROLE OF VIBROISOLATORS IN DAMPING AN RADIAL FAN'S VIBRATIONS

Janusz ZACHWIEJA

Department of Applied Mechanics and Thermal Engineering
University of Technology and Life Sciences in Bydgoszcz
Prof. Sylwester Kaliski street no 7, 85-791 Bydgoszcz

Summary

In this paper there is analyzed an influence of vibroisolators' stiffness and damping qualities on vibrations level of centrifugal fan. The results obtained from numerical simulations confirmed the regularity that a limitation of force affecting the fan's foundation can cause an increase of its own vibrations' amplitude.

Keywords: springy vibroisolators, rubber vibroisolator, resonance response.

ROLA WIBROIZOLATORÓW W TŁUMIENIU DRGAŃ WENTYLATORA PROMIENIOWEGO

Streszczenie

W pracy analizowany jest wpływ sztywności i własności tłumiących wibroizolatorów na poziom drgań wentylatora promieniowego. Wyniki symulacji numerycznych potwierdziły prawidłowość, że ograniczenie wielkości siły działającej na posadowienie wentylatora może powodować wzrost amplitudy jego drgań.

Słowa kluczowe. wibroizolator sprężynowy, wibroizolator gumowy, odpowiedź rezonansowa.

1. INTRODUCTION

Fans are commonly applied in turbomachinery industry. Main mediums in these devices are: air, air mixture with particles of solids or other gases depending on the system character. Fans are devices with not complicated designs. Its principal element is a rotor with blades and typical streamlined profile whose diameter may reach a few meters. The width depends on the rotor function. Machines with great volume flow rate have wide rotors while fans with high pressure differences have narrow rotors. Rotating rotor transmits kinetic energy to the medium flowing in chambers between blades. This kinetic energy is changed into dynamic pressure of gas. In a helical chamber the medium is compressed which causes static pressure increase[1].

The fan rotors bases are fixed usually either directly to the foundation using anchors, or on steel frames after being placed in armored concrete. Frequently between the frame and the body vibroisolator is mounted, in which springy-damping element is spring or rubber pad. Using vibroisolators is not always necessary and desirable because their influence on the system dynamic properties. Generally, the principle is suggested, according to which vibroisolators should be used in case when there is a necessity to limit the action of forces on the foundation. Using element with lower stiffness than stiffness of direct connection of the fan body

with the frame or the foundation results in decrease in device free vibration frequency. Small damping in the system is factor which favors growing of vibrations parameters amplitude. Sometimes stiffness and body damping are so small, that vibration amplitudes in frequencies both excitation frequency and free frequencies reach values higher than permitted by the norm [2-3].

2. FAN MOUNTING ON VIBROISOLATORS

For the needs of vibroisolation two kinds of vibroisolators are commonly used: springy Fig. 1 and rubber ones. The basic difference between these kinds of vibroisolators lies in their characteristic



Fig. 1. An example of springy vibroisolator

The static characteristics of springy vibroisolators W2-434, W2-435, W2-482 and rubber vibroisolator W100/55 determined by first of the author, have been presented in Fig. 2.

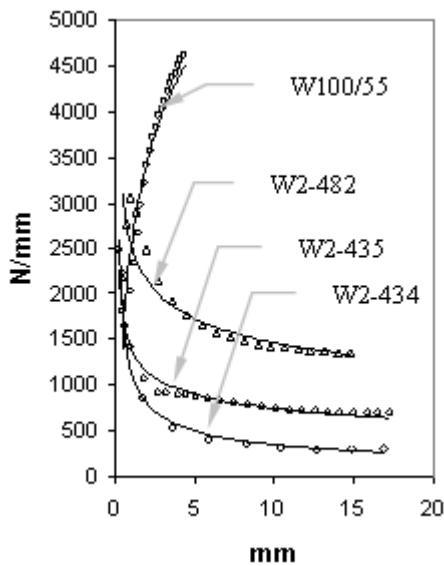


Fig. 2. Static characteristics of springy vibroisolator stiffness and rubber vibroisolator

Comparison of forced frequency function changes of vibroisolators dynamic properties can be evaluated through determination of their resonance response. For this purpose an exciter with controlled forced frequency can be used (Fig. 3)



Fig. 3. Determination of the vibroisolator resonance response

In this way the resonance point shift for vibroisolators (W2-435, W2-482) and has been defined. Resonance area of vibroisolator W2-482 is shifted in the direction to the higher frequencies (Fig. 4) due to their higher stiffness (Fig. 2).

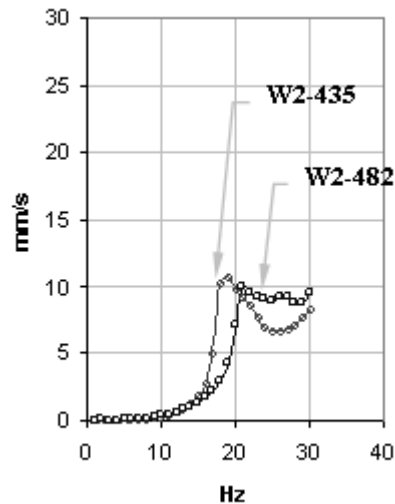


Fig. 4. Resonance point shift for vibroisolators (W2-435, W2-482)

3. GENERAL PRINCIPLES OF VIBRO-ISOLATION

The ratio of maximal force transmitted to the foundation in time of vibrations to static force is called transmission coefficient. It is expressed by the following dependence:

$$\varepsilon = \frac{\sqrt{1 + 4 \frac{h^2}{\omega^2} \frac{v^2}{\omega^2}}}{\sqrt{\left(1 - \frac{v^2}{\omega^2}\right)^2 + 4 \frac{h^2}{\omega^2} \frac{v^2}{\omega^2}}} \quad (1)$$

Maximal value of force transmitted from the ventilator to the foundation is:

$$P_{\max} = kx_{st} \varepsilon \quad (2)$$

whereas:

v - forcing frequency,

ω - free vibration frequency,

$h = \frac{1}{2} \frac{c}{m}$ - vibroisolator damping constant,

k - vibroisolator spring stiffness,

x_{st} - vibroisolator spring static deflection,

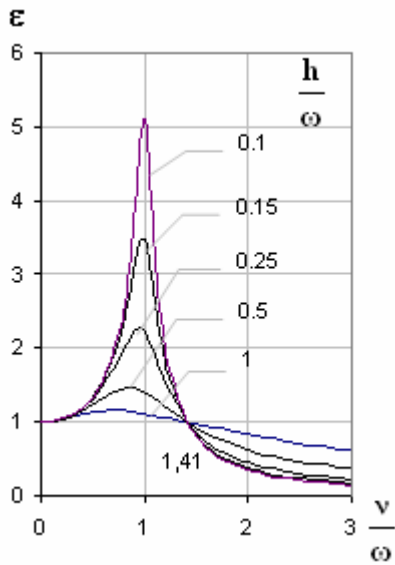


Fig. 5. Dependence of transmission coefficient from forced frequency and free vibration frequency

From Fig. 5 we can read that effectiveness of amortization is correct, when:

$$\frac{\nu}{\omega} > \sqrt{2} \quad (3)$$

Advisability of this condition will be analyzed on a simple example of vibrations of a mass mounted on a vibroisolator affected by forcing with frequency $f=6\text{Hz}$ (Fig. 6).

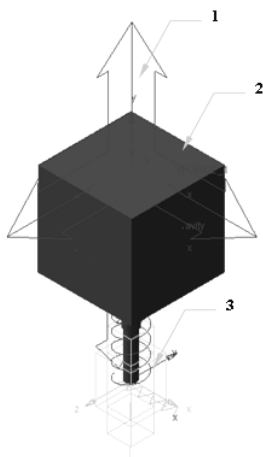


Fig. 6. Idea scheme of vibroisolator operation
1 – harmonic forcings with 10N amplitude and 6Hz frequency, 2 – system mass 7.8kg 3-vibroisolator

For vibroisolators with $k=10\text{N/mm}$ stiffness the system free vibration frequency is 5.7Hz. For harmonic forcing with frequency 6Hz we can talk about near rezonans vibrations of the system. Thus, the values of the force transmitted onto the foundation (Fig. 7a) and and the vibration high velocity are significant (Fig. 7b). If we assume that the forced frequency can not be moved out of the resonance area it should be recognized that the

choice of the vibroisolator has not been proper. Improvement of vibration isolation effectiveness defined by the value of force transmitted onto the foundation, according to condition (3) needs application of a less stiff vibroisolator.

$$k < 5.54 \frac{N}{mm} \quad (4)$$

Vibroisolator with stiffness 3N/mm can really decrease the force value diametrically, almost to a value resulting from static loading (Fig. 9a.).

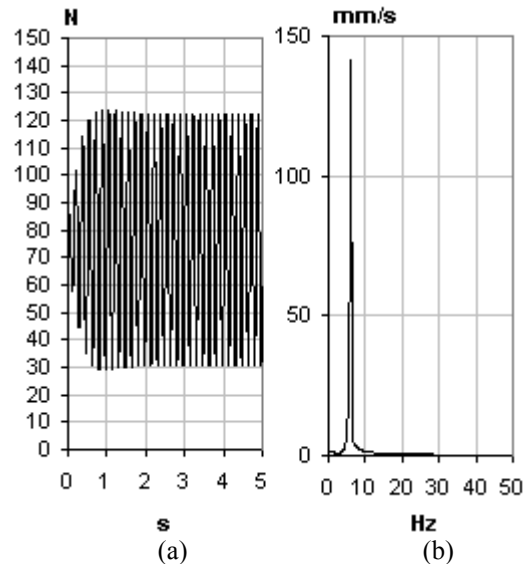


Fig. 7. Changes in time of force acting on the foundation with vibroisolator frequency 10N/mm (a) and amplitude-frequency characteristic of the system vibration velocity with vibroisolator stiffness 10N/mm (b)

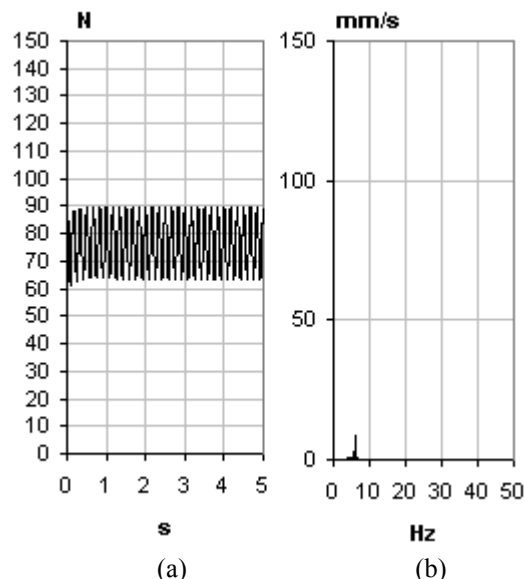


Fig. 8. Changes in time of force acting on the foundation with vibroisolator frequency 50N/mm and amplitude-frequency characteristic of the system vibration velocity with vibroisolator stiffness 50N/mm

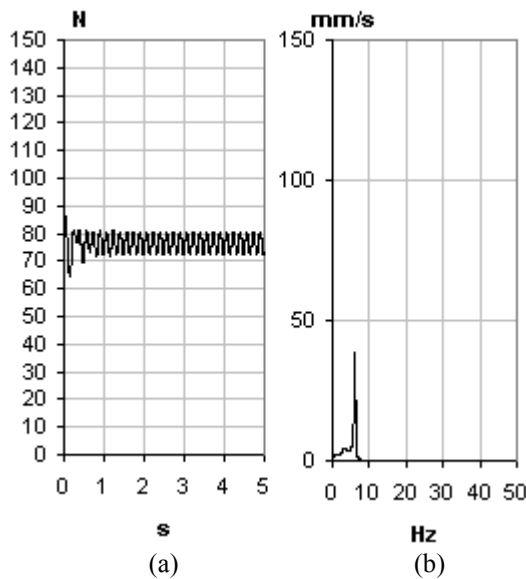


Fig. 9. Changes in time of force acting on the foundation with vibroisolator frequency 3N/mm and amplitude-frequency characteristic of the system vibration velocity with vibroisolator stiffness 3N/mm

The velocity of system vibrations is still very high (Fig. 9b). In real conditions such a situation could be considered as unsatisfactory. It must be noted that increasing the spring stiffness up to value 50N/mm causes that effectiveness of vibroisolation is related to decrease in (Fig. 8a) the system force action on the foundation, however vibration velocity amplitude value reaches the accepted level. (Fig. 8b).

3. VIBROISOLATION IN CASE OF INERTIAL FORCING

For the rotor rotation centrifugal force appears caused by its unbalancing.

$$F_b(\omega) = m_n \cdot \omega^2 \cdot r \quad (2)$$

m_n – mass unbalanced,

ω - angular velocity,

r – radius of rotor,

Because of the fact that the amplitude of the forcing force depends on the forcing frequency, we can not talk here about a transmission coefficient in the same terms as we do in the case of the amplitude constant value. The ventilator rotor is an example of this kind of forcing.

An analysis of a radial ventilator vibrations is easy to be performed with the use of the method of multi body systems(MBS). The calculation model is used for simulation, and is presented in Fig. 10.

Depending on the degree of complexity of the model the dynamic properties of the system can be considered taking into consideration an array of

factors affecting them. In Table 1 the physical features of a radial ventilator of medium size with a hung rotor have been set up. Also the influence of vibroisolators damping features on the rotor operation stability and in relation to the fact that while being started it undergoes through the resonance area for vibrations in the horizontal direction, vertical and twisting vibrations has been analyzed.

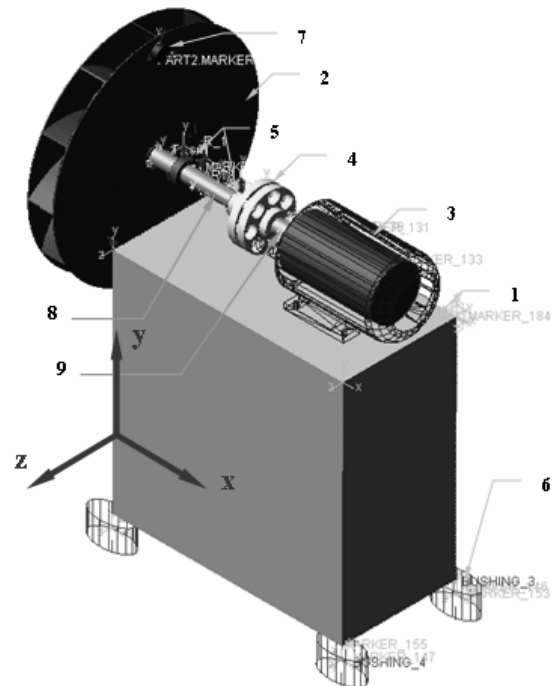


Fig. 10. Computational model of a radial ventilator
1. body, 2. rotor, 3. motor, 4. coupling,
5. bearing, 6. vibroisolator, 7. unbalancing of rotor,
8. rotor shaft, 9. engine shaft

Table 1.
Computational parameters of a ventilator model

	Mass kg	I_{xx} kg mm ²	I_{yy} kg mm ²	I_{zz} kg mm ²
1.	304	$7.26 \cdot 10^7$	$4.94 \cdot 10^7$	$4.75 \cdot 10^7$
2.	181	$1.42 \cdot 10^7$	$7.67 \cdot 10^6$	$7.67 \cdot 10^6$
3.	151	$3.51 \cdot 10^6$	$3.47 \cdot 10^6$	$1.80 \cdot 10^6$
	119	$1.94 \cdot 10^6$	$1.94 \cdot 10^6$	$7.18 \cdot 10^5$
4.	8.3	$4.37 \cdot 10^4$	$2.38 \cdot 10^4$	$2.38 \cdot 10^4$
5.	1.18	2000	1088	1088
7.				
8.	8.8	$1.2 \cdot 10^5$	$1.2 \cdot 10^5$	3970
9.	2	1786	1786	893

Table 2 contains a setting up of stiffness and damping of vibroisolators.

Table 2.
Springy-damping properties of vibroisolators have been accepted in the following way

	k_{xx} kN/m	k_{yy} kN/m	k_{zz} kN/m	c_{xx} kNs/m	c_{yy} kNs/m	c_{zz} kNs/m
6	5000	5000	4000	10	10	10
				2	2	2

For damping value 10Ns/mm the system response expressed in decibels that is Bode's characteristics is presented in Fig. 11 and Fig. 12. The first left represents vibrations in the horizontal direction, and the right is connected with the vertical direction.

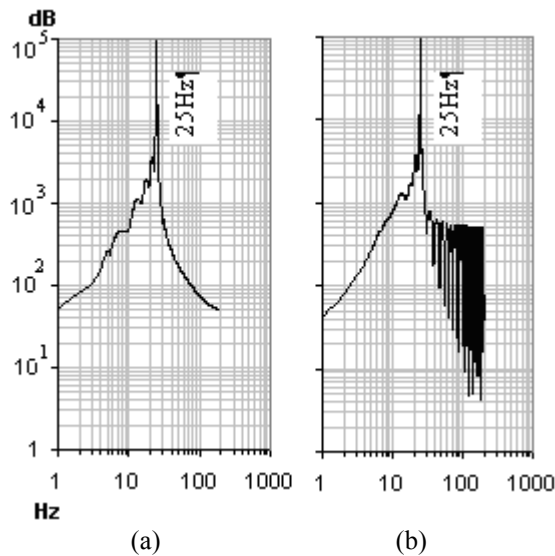


Fig. 11. Bode's diagram for the system vibrations in the horizontal (a) and vertical (b) direction (damping 10Ns/mm)

The rotor operation stability for such damping is not threatened. Vibrations both horizontal and vertical ones undergo strong damping (Figs. 12-13).

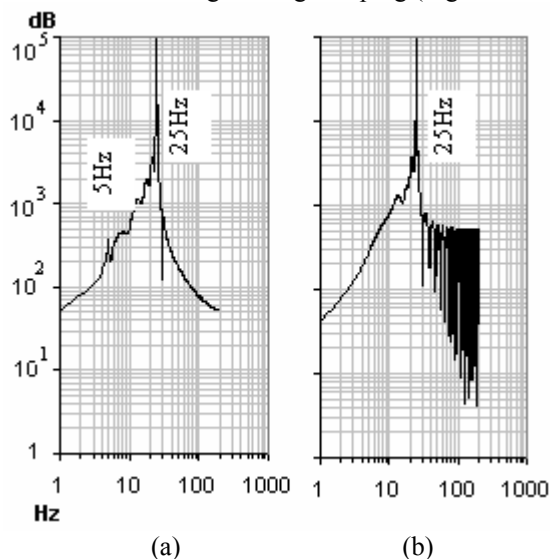


Fig. 12. Bode's diagram for the system vibrations in the horizontal (a) and vertical (b) direction (damping 2Ns/mm)

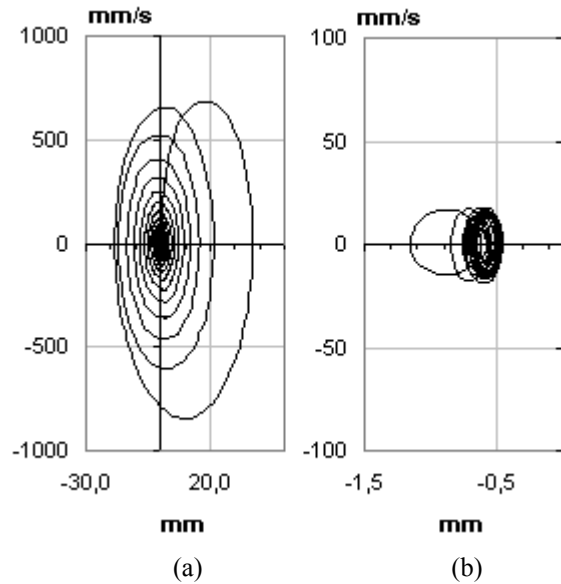


Fig. 13. The system vibration phase plane in the horizontal (a) and vertical (b) direction (damping 10Ns/mm)

The movement of the body of a ventilator mounted on vibroisolators is of chaotic character, especially while going through the resonance area

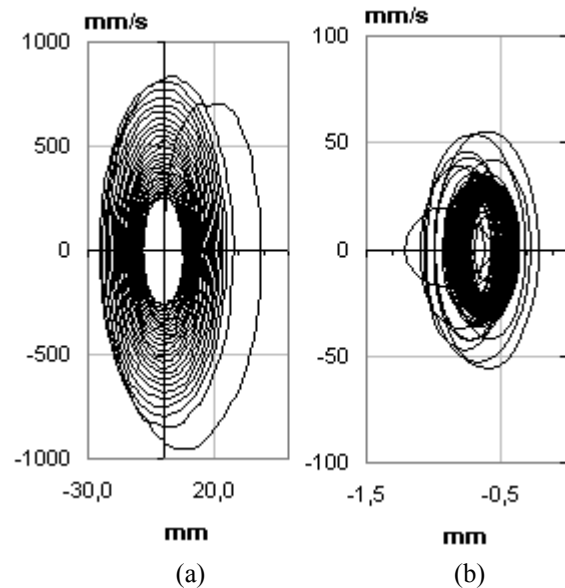


Fig. 14. The system vibration phase plane in the horizontal (a) and vertical (b) direction (damping 2Ns/mm)

In connection with this it is natural to present a picture of this movement on Poincare diagram.

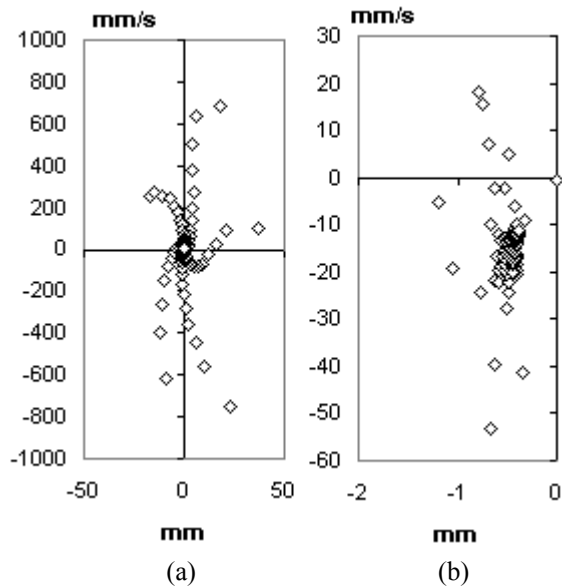


Fig. 15. Poincaré diagram for the system vibrations in the horizontal (a) and vertical (b) direction (damping 10Ns/mm)

An analysis of the damping quantity influence on the rotor movement stability makes it possible to conclude that for a fan with mass similar to the one that was accepted for the model and similar inertial excitement, vibroisolators with viscotic damping and damping properties -10Ns/mm will provide sufficient damping.

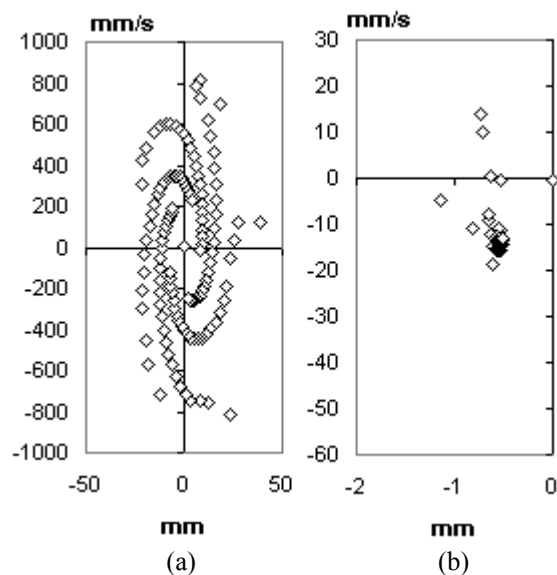


Fig. 16. Poincaré diagram for the system vibrations in the horizontal (a) and vertical (b) direction (damping 2Ns/mm)

4. CONCLUSIONS

The author of the paper presents the fact that issues connected with an application of vibroisolators in industry are not simple ones. A radial ventilator has been chosen as an object of consideration because it is widely used as a turbo machine in many branches of industry. Being an

element of a technological line it is often placed in halls' ceilings that is where dynamic excitement with significant amplitude affecting the construction is undesirable. Thus, it is necessary to limit values of the forces transmitted to the machine foundation. The right choice of vibroisolators' damping and stiffness requires deep analyses with the use of knowledge on the machine dynamics and calculation methods allowing to use this method[4-5].

LITERATURA.

- [1] Zachwieja J., Peszyński K.: *Experimental test of flow parameters influence on ventilators system vibrations*, International Conference Experimental Fluid Mechanics, Liberec (Czech Republic) 2007.
- [2] Zachwieja J.: *Diagnostic of two-stream ventilators*, Diagnostyka 29/2003, 35-40.
- [3] Zachwieja J.: *Diagnosis of horizontal ventilator rotor with small support stiffness*, Diagnostyka 35, 2005, 63-70.
- [4] Zachwieja J., Gawda M.: *Dynamic Properties of Pipe-Pump System Diagnosis from Point of View Damping Vibrations* Diagnostyka 4(40)/2006, 27-31.
- [5] Zachwieja J., Ligier K.: *Numerical analysis of vertical rotor dynamics of ACWW1000 centrifuge*, Journal of Theoretical and Applied Mechanics, 43(2), 2005, 257-275.



Janusz ZACHWIEJA - Phd. eng. is an assistant professor in the Department of Applied Mechanics and Thermal Engineering in University of Technology and Life Sciences in Bydgoszcz.

AN APPLICATION OF SPLINES IN SYNCHRONOUS ANALYSIS OF NONSTATIONARY MACHINE RUN

Tomasz KORBIEL, Piotr KRZYWORZEKA
Institute of Mechanics and Vibroacoustics
AGH Cracow, krzyworz@agh.edu.pl

Summary

As an addition to the order analysis procedures is an approximation of a discrete measurement result by a cubic splines which allows further signal analysis also by analytical means without preliminary large oversampling of a vibration signal. The proposed simple algorithm of conversion from dynamic time scale to momentary cycle time scale of a machine proved itself practically useful by supporting the diagnosis of gearboxes and bearing with use of amplitude spectrum also during the exploitational variations of rotation speed.

Keywords: vibroacoustics, diagnostics, order analysis.

WYKORZYSTANIE FUNKCJI SKLEJANYCH W ANALIZIE SYNCHRONICZNEJ NIESTACJONARNEGO BIEGU MASZYN

Streszczenie

Uzupełnieniem dotychczasowych procedur analizy rzędów jest tu aproksymacja dyskretnego rezultatu pomiaru sklejanymi wielomianami stopnia 3- co umożliwia dalsze badanie sygnału także na drodze analitycznej i pozwala uniknąć wstępnego znacznego nadpróbkowania sygnału drgań. Proponowany, stosunkowo prosty algorytm konwersji skali czasu dynamicznego na skale czasu cyklu chwilowego maszyny sprawdził się w praktyce analizy rzędów wspomagając diagnozowanie przekładni zębatych i łożysk tocznych z wykorzystaniem widm amplitudowych także podczas eksploatacyjnych zmian prędkości obrotowej.

Słowa kluczowe: wibroakustyka, diagnostyka, analiza rzędów.

1. INTRODUCTION

Let us consider objects where repeated interactions of elements or moving medias exist. The sequence of chosen event series of main target completion [4, 6] repeats in time intervals defined as momentary cycle Θ_k . The following appearances Θ_k are not identical even in good technical state and settled conditions of machine run (hence the cyclic movement is not a synonym for periodical movement). The diagnosis of cyclic machines in variable work conditions causes spectrum load which in turn causes the lack of selectivity of stems corresponding to particular harmonics of rotation speed.

As an example the Fig. 1 shows amplitude spectrum of offset vibration of shaft with a disc with speed increase of 0.6% per cycle. The spectrum blur could be seen.

Only one harmonic independent from the rotation speed could be clearly seen (of frequency 100Hz), in a diagnostic sense it is disturbance

related to the supply voltage of the drive system. From that example one can state that diagnostics of machines in run-up or run-down state can not be held by means relevant to stationary signals. Nonstationarity causes spectrum load and it seizes to be a state symptom. Even small changes in speed cause the lack of stem selectivity for primary harmonic which impairs making unequivocal diagnostic decisions. The research presented in [3] shows that relative change in run cycle in the range of 0.1% have a negative effect on the diagnosis outcome.

The remedial mean is search for signal changeability definition in another time scale such that:

- changeability definition simplifies
 - significant features of informational changeability are preserved
 - non-informational changeability reduces
- One of them is the order analysis.

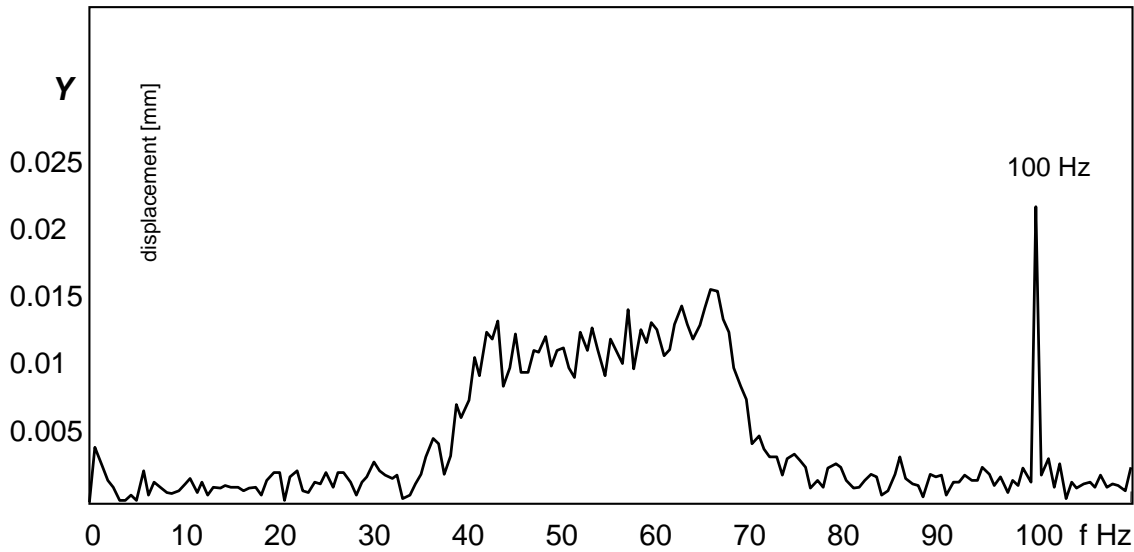


Fig. 1. Amplitude spectrum of offset vibration of shaft with a disc.
Blur of kinematic lobes due to rpm growth

2. TIME SCALE CONVERSION

If assumed [3], that the valuable information transfer is organized through cycle, then its length might be a conditional time unit η . Let us assume that:

- the run η , timed by cycle is uniform and in real-time scale 't' it is not (see fig. 2b), since the cycles are not of equal length.
- The scale 'η' might be recreated by non-uniform sampling – such that not only the number of samples per cycle was uniform, but also their distribution throughout of the cycle was similar in each cycle and related to similar events in the range of scale transformation. The number of momentary cycles should be equal in both scales.

For rotating machines the cycle time is conditioned by an rotational movement. The most used tachometric measurement allows simple presentation (see Fig. 2b) and formalizes the rule of dynamic time scale 't' transformation into cycle time scale 'η'.

Let m be the number of position markers per 1 rotation a , $\Delta\varphi$ be the rotation angle increase – thence:

$$m\Delta\varphi = 2\pi = 2\pi \sum_{k=1}^m \frac{\Delta t_{tk}}{\Theta_{tk}}$$

$$\Delta\varphi = \text{const}, \Delta t_k = \text{var} \quad (1)$$

where Θ_{tk} = momentary values of the cycles in moments t_k ,

The set of reference events $\{z_k\}$ is defined by moment t_k of the angle detection markers (Fig. 2b).

Those moments are the reference for the clock counting momentary cycle count Θ ,

$$\{z_k\} \Rightarrow \{\eta_k\} = \{k\}$$

$$\Delta\varphi \Rightarrow \Delta\eta \quad \{t_k\} \Rightarrow k\Delta\eta \quad (2)$$

timed uniformly, as $\Delta\varphi = \text{const}$ for $\Delta\eta = \text{const}$.

For the range T including $1 \dots n \dots M$ cycles:

$\eta \in [0, mM]$, $t \in [0, T]$, the number of distinguishable moments η from the beginning of counting defines 'now' according to:

$$\eta_{\text{now}} = m(n-1) + k \quad k = 0, m-1$$

$\Delta\eta$ – unitary range

In case of persistent cycle change $\Theta(t)$ the transformation formula takes the form (3)

$$\frac{d\eta}{dt} = \frac{1}{\Psi[\Theta(t)]} \quad (3)$$

$\Psi_k(\Theta)$ – characteristic of momentary cycle. The choice of operation Ψ – decides of reference event set of clock η , the practical usefulness of that new scale in diagnostics and of completion method and complexity of the transformation procedure [3 4 5].

It is worth to notice that the number of observed moments η is in practice finite. The value of $m/2$ denotes the expected range of order spectrum [1, 2]). Its increase not always is justified by a need, hinders the measurement and the result processing.

In practice, as the authors research shows, consideration of continuous nature of η by means of interpolation might be advisable, of which we speak later.

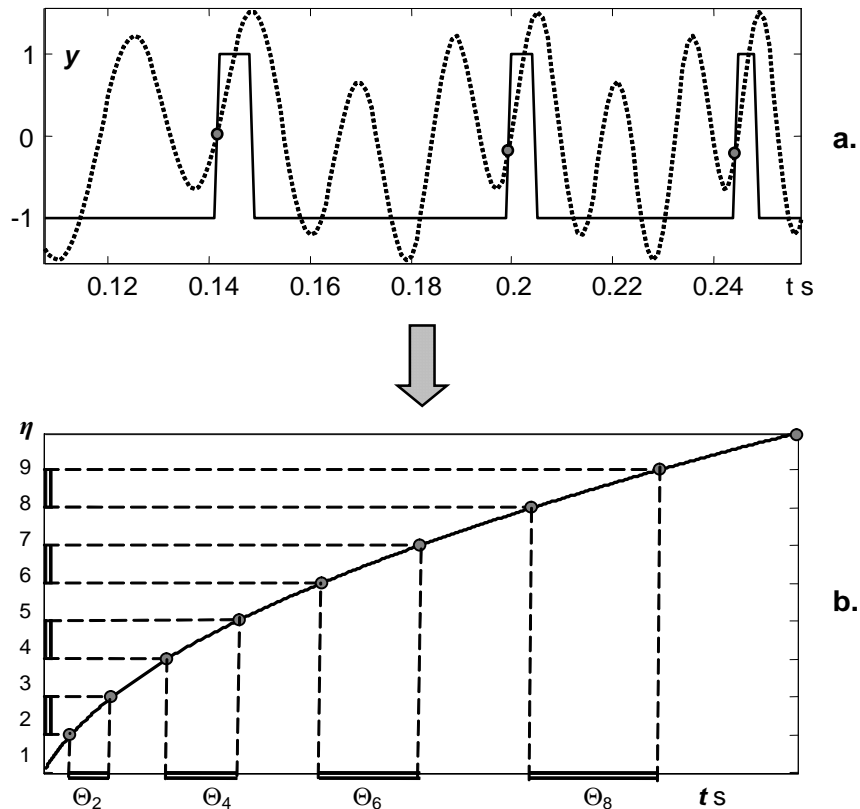


Fig. 2. The principle of order time clock synchronization

a) synchronizing impulse series b) curve ψ of time scale conversion ' $t \Rightarrow \eta$ '

3. ORDER TRANSFORMATION

In the fig. 3a the set m of rotation angle markers defines the set of reference events (moments) of order time clock, synchronized by momentary cycles. In a new time scale the subsequent synchronizing cycles are of equal length and the description of signal changeability simplifies. Then the trend and the work cycle fluctuations might be reduced to allow usage of analysis methods relevant to stationary signals [2, 4].

Simultaneous ranges Θ_k of dynamic time t correspond to non-uniform sampling in the scale ' t ', since $\Delta t_k = \text{var}$. But the measured signal is sampled uniformly and the demand of constant number of samples per cycle is not met.

How to handle this?

Large preliminary oversampling of the signal y allows improvement of synchronization through choice of samples proportional to linear approximation of work cycle changes – that is how linear decimation procedure PLD works [3]. Such an estimation well recreates the spectrum of rotation harmonics and the angle modulation in the range of monotonic cycle changes. In case of standard measurement equipment the demand of 50-100 fold oversampling might be impossible to be met.

For such conditions it is possible to resample the signal by means of cubic splines interpolation.

The method described below uses splines for inter-sample approximation of signal y . The stages of such an order analysis are presented by Fig. 3. and following is the short description:

- normalized synchronizing pulses of phase marker signal (Fig. 3b) split the analyzed signal y to particular cycles Θ_k corresponding to rotation angle $\varphi = 2\pi$;
- by synchronization with m under-multiplicity of the 2π angle the sample subsets correspond to equal values of $\Delta\varphi_k = \Delta\varphi$, but not equal to $\Delta\Theta_k$ (Fig. 3b);
- for such subset in ranges of Θ_k (or $\Delta\Theta_k$) interpolated continuous function is created. In presented algorithm such function is build from cubic splines [2] (Fig. 3c)
- resulting continuous function is split into equal time sections $\Delta\eta$. A mean value is calculated for each section creating data vectors \mathbf{u}_k of the same length corresponding to subsequent $\Delta\varphi$ (Fig. 3c);
- the resulting data vector $\mathbf{u} = [\mathbf{u}_k]$ describes the signal y changeability in scale ' η ' of order time.

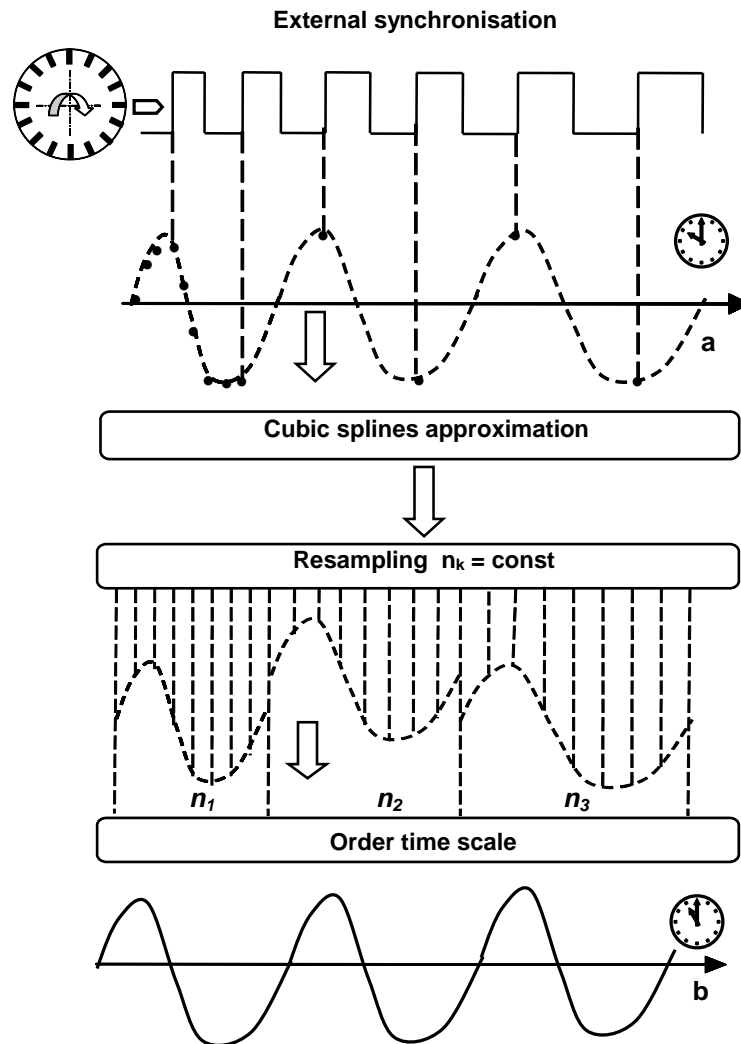


Fig. 3. Order transformation using splines approximation
a) real-time clock, b) order-time clock

5. NOTES ON PRACTICAL USE

Apart from procedure programming the correct synchronization is important which is conditioned by:

The synchronizing cycle choice - the procedure filters the rotation harmonic corresponding to synchronizing cycle transforming it to the stationary signal whereas stationary parts of the signal become nonstationary in order time scale and corresponding spectra diffused and heavily loaded

Synchronizing signal forming - mean square error of order spectrum component and its number depends on the resolution and measurement accuracy of encoder disc

Normalization - the aim of this operation is precise definition of beginnings of subsequent $\Delta\varphi_k$ (see Fig. 2a). In given case normalization means the calculation of i -th derivative of phase marker signal

and zeros detection with considerations of function monotonicity and signal level variation hysteresis.

Scaling - necessary for whole measurement and processing channel of y, u if the values of spectrum stem have the diagnostic interpretation. It is also important to define the conversion range ' $t \Rightarrow \eta$ ' considered as satisfying.

An example

Here the result presentation as RMS spectra of a gearbox in the range of rotation harmonic serves only as a mean to compare the effects of order transformation to the original signal spectrum, thence the scaling is omitted with the scale similarity kept. Both simulated (Fig. 4) and real signal spectra (Fig. 5) has been compared. It's seen that spline approximation provides more details in low frequency domain of kinematic spectra.

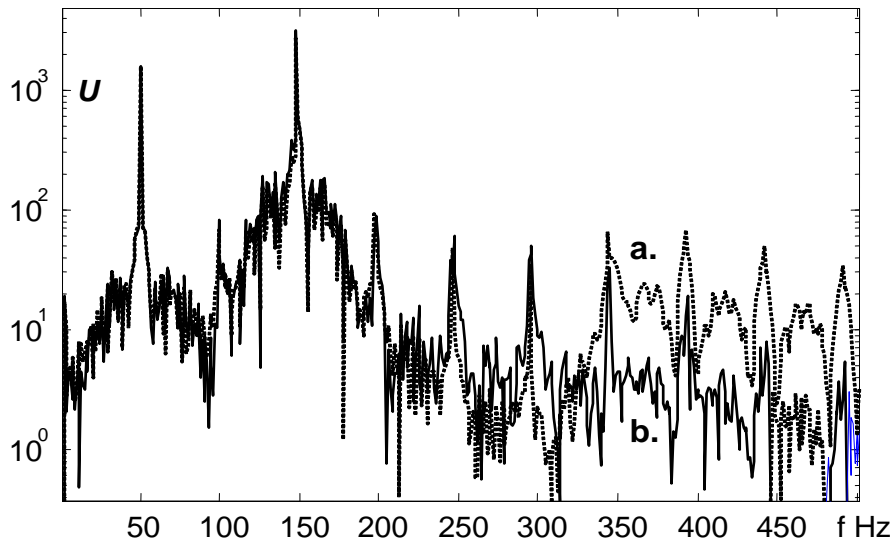


Fig. 4. Order spectra of simulated signals: a) linear approximation, b) 3-rd order spline approximation

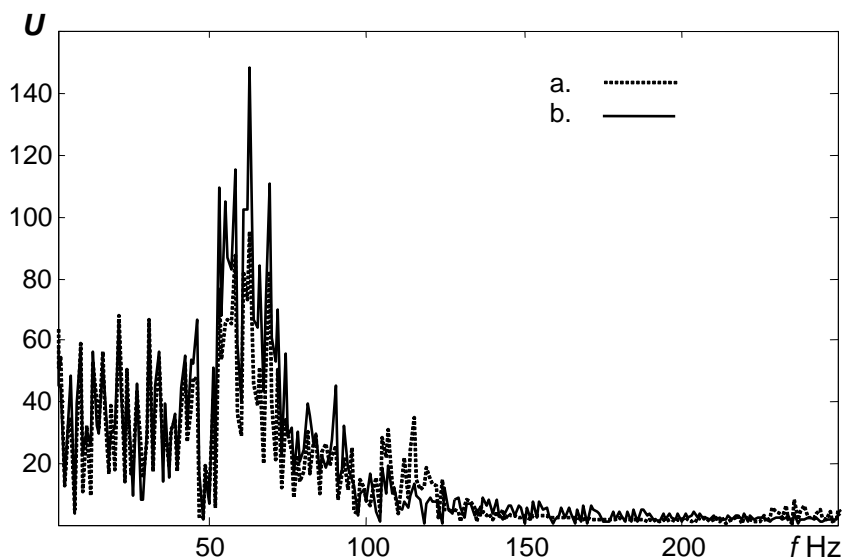


Fig. 5. Order spectra of bevel gear vibrations: a) linear approximation, b) 3-rd order spline approximation

6. CONCLUSION

In recent applications the described method proved to be fairly effective in analysis of vibration of gearboxes and bearing of rotating machines with the exploitative variations of rotation speed.

Calibration with non-stationary modeling signals showed its superiority (at least in the tested range) over the popular algorithm of order analysis using resampling and low-pass filtering.

Main advantages are:

- Harmonic spectrum dynamics < -40dB.
- Square mean error < 5%.
- Possibility of application for classic data analysis methods.
- Fast and simple algorithm.

REFERENCES

- [1]. Batko W., Dąbrowski Z., Engel Z., Kiciński J., Weyna S.: *Nowoczesne metody badania procesów wibroakustycznych*. PIB, Radom 2005
- [2]. Batko W., Korbiel T.: *Przetwarzanie sygnałów diagnostycznych wygładzanych algorytmami krzywych sklepanych*, XXIV Ogólnopolskie Sympozjum Diagnostyki Maszyn, Węgierska Górka, 1997
- [3]. Krzyworzecka P.: *Wspomaganie synchroniczne w diagnozowaniu maszyn*: Kraków-Radom. BPE, Wyd. ITE . 2004
- [4]. LabView: *Order analysis toolset* User manual. National Instrument 2003.

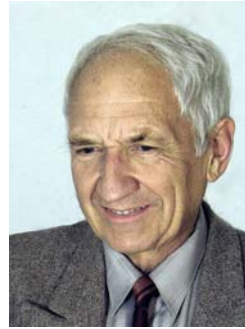
- [5].Piotrowski A., Stankiewicz A., Balunowski J., Solbut A.: *Diagnostics symptoms forming in the rotating machine monitoring based on the order tracking analysis*. II International Congress of Technical Diagnostics, Diagnostika'2000, Poland, Warsaw 19-22 September 2000.

8. GLOSSARY OF SYMBOLS

DPR	–	dynamic residual process;
MVS	–	machine vibration signal;
OT	–	Order transform;
PDI	–	Diagnostic identification procedure;
PLD	–	linear decimation procedure;
TSC	–	Time scale conversion;
$\psi(\Theta)$	–	synchronizing cycle characteristic;
$\Delta\varphi$	–	angular step of synchronization;
Θ	–	characteristic cycle;
Θ_0	–	Duty cycle;
y	–	original measured signal;
u	–	final signal after TSC;
η'	–	order time scale;
t'	–	real time scale;
s_F	–	characteristic signal;
T	–	przedział obserwacji sygnału;
η	–	cycle time;
z_k	–	referential event;



Dr inż. **Tomasz KORBIEL** jest adiunktem w Katedrze Mechaniki i Wibroakustyki AGH. Jego zainteresowania związane są z diagnostyką techniczną, analizą sygnałów oraz nowoczesnymi systemami pomiarowymi.



Dr hab. inż. **Piotr KRZYWORZEKA**, prof. AGH pracuje na tej uczelni od ukończenia studiów. Wykładał kilka lat w Algierii. Jest autorem ok. 90 publikacji, głównie o tematyce diagnostycznej, rzeczoznawcą SEP w zakresie elektroakustyki, a także członkiem PTDT od momentu jego powstania. W pracy badawczej preferuje podejście sygnałowe. Interesuje się także psychologią i filozofią. Jako środek transportu preferuje rower.

VIBRATION ANALYSIS OF RUNNING-UP TURBINE ENGINE GTD-350

Witold CIOCH, Piotr KRZYWORZEKA
Department of Mechanics and Vibroacoustics
Akademia Górniczo-Hutnicza - University of Science and Technology
Al. Mickiewicza 30, 30-059 Kraków
email: cioch@agh.edu.pl

Summary

The article contains the example of practical application of the procedure for non-stationary signals processing developed at Department of Mechanics and Vibroacoustics University of Science and Technology (AGH). The developed method – Procedure of Linear Decimation (PLD) was applied for signal analysis of vibrations of GTD–350 turbine engine in unstable operating conditions. As a reference signal the rotational speed of driving shaft was adapted. The results were enclosed for turbine running-up and coasting state.

Keywords: diagnostics, turbine engine, unstable state.

BADANIE DRGAŃ ROZRUCHOWYCH SILNIKA TURBINOWEGO GTD-350

Streszczenie

W artykule przedstawiono przykład praktycznego zastosowania opracowanej w Katedrze Mechaniki i Wibroakustyki Akademii Górniczo-Hutniczej procedury przetwarzania sygnałów niestacjonarnych. Opracowaną metodę – Procedurę Liniowej Decymacji (PLD) zastosowano do analizy sygnałów drgań silnika turbinowego GTD–350 w nieustalonych stanach pracy. Jako sygnał referencyjny przyjęto prędkość obrotową wału napędowego. Wyniki przedstawiono dla stanu rozbiegu i wybiegu turbiny.

Słowa kluczowe: diagnostyka, silnik turbinowy, stan nieustalony.

1. INTRODUCTION

Many rotary machines are rated among crucial devices. Energetic turbines, and particularly aviation turbine engines, belong to this group. For safety reasons, specification of their technical state is vital in their exploitation period [3]. As they are required to feature very high reliability, the scheduled maintenance service is not sufficient nowadays – monitoring systems are more and more often applied. These systems enable real-time evaluation of technical state during the operation of an object. Technical state changes most often occur when operating conditions change. Unstable operating conditions, apart from creating a threat of emergency state or even distress, they can hamper the diagnosis process.

One of the methods assisting the specification of technical state in non-stationary conditions is a procedure for processing non-stationary measuring signals developed by the authors. Intended for cyclical machines, it enables converting signals recorded at variable rotation speeds into the form corresponding with stabilized operating states. It is known as Procedure of Linear Decimation (PLD) [2]. This method was oft-cited by the authors, and its theoretical bases were explained in many

publications [11, 13, 10]. It involves oversampling of significantly oversampled signal with variable increment corresponding to the changes in reference cycle. It assumes linear increase of cycle tend in an observation window, which also results in its certain limitations [1]. Widening application range of the PLD method can be obtained through more accurate approximation of trend of cycle change.

At present it is also implemented on the basis of FPGA programmable systems in the hardware form. Implemented in a portable measuring device referred to as Programmable Unit for Diagnostic (PUD), it is successfully put into practice. The manufactured device with applied programmable systems enabled to significantly oversample signals (10 MS/s) creating vast capabilities of examining new PLD implementations. This solution allows for increasing decimation coefficient D_c even up to 1000 and signal analysis in high-frequency bands, e.g. gear meshing or turbine blades operating, without the necessity of applying interpolating filters. Furthermore, this implementation enables the realization of the method in real-time conditions. Results of the device implementation in former PLD method researches along with specification of its ranges are enclosed in publications [7, 8, 12].

2. SHORT-TIME PROCEDURE OF LINEAR DECIMATION

Developed method was meticulously tested on non-stationary signals recorded on various types of rotary machines. Simple in implementing, yielding positive results, it is also used for shock absorbers subject to cyclical excitation – the research was conducted at Silesian University of Technology.

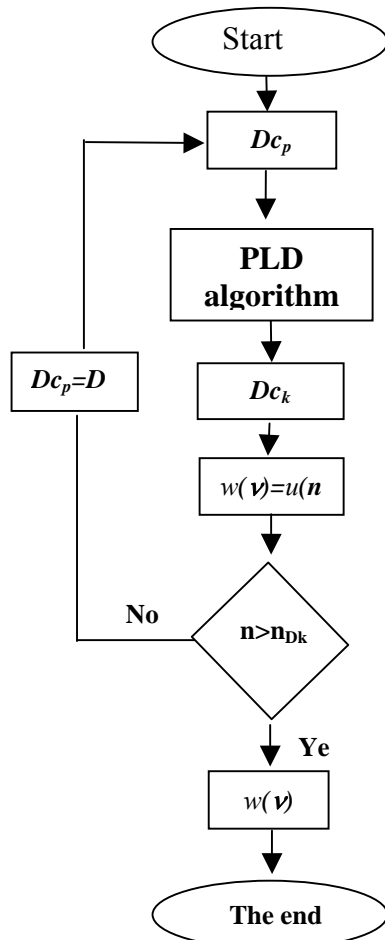


Fig. 1. Algorithm of Short-time Procedure of Linear Decimation STPLD

- $v(n)$ – primary vector
- $w(v)$ – secondary vector
- Dc_p – initial decimation coefficient,
- Dc_k – final decimation coefficient,
- n – number of the sample of primal vector
- n_{Dk} – sample number enabling PLD ending on primary vector stage

Having manufactured device that enables to record diagnostical signals the purpose was to increase c_p decimation coefficient up to greatest possible value to obtain the most linear approximation function. Without the application of interpolation, it was the only way to preserve the highest linearity of approximating function.

However, it turned out not to be suitable approach since it brought good results only with cycle trends being close to linear ones. As for rotary machines at the stage of run-up, particularly machines of dynamic changes of rotation speed, preserving linearity did not significantly improve spectral selectivity, especially in high-frequency band. This prompted developing modified algorithm of the method enabling adjustment to cycle change in short time-periods of an observation window. The new method of analyzing signals in narrow time-periods was referred to as Short-time Procedure of Linear Decimation STPLD. It is explained in the article [9]. Its algorithm is enclosed in fig. 1, and fig. 2 presents schematically the adjustment of linear approximation to cycle changes in observation window.

STPLD method was tested in high-frequency bands. Results obtained during examining signals in gear-meshing frequency band were very satisfactory, as presented in papers [9].

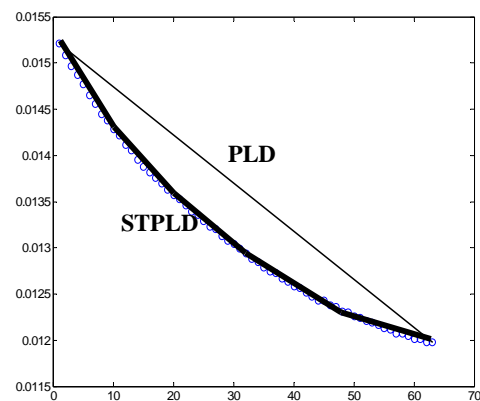


Fig. 2. Approximation of cycle change in observation window with STPLD

3. RESEARCH OBJECT

After successful laboratory tests on rotary machines in full frequency-band range, it was decided to test the method on a device of much greater rotation speed and featuring several reference speeds.

For those tests a GTD-350 turbine was selected [4]. This turbine normally works as an engine of MI-2 helicopter. It has two independent shafts [5]. High-pressure turbine rotates at maximum speed of 43 200 rpm, and propulsion turbine - 24 000 rpm. Rotation speed of output shaft is reduced to one fourth in relation to propelling turbine speed.

Cross section of the tested engine is enclosed in fig. 3 along with the descriptions of its individual elements. Photographs taken during the experiment at laboratory test bed at Navy Academy in Gdynia are presented in fig. 4 and fig. 5.

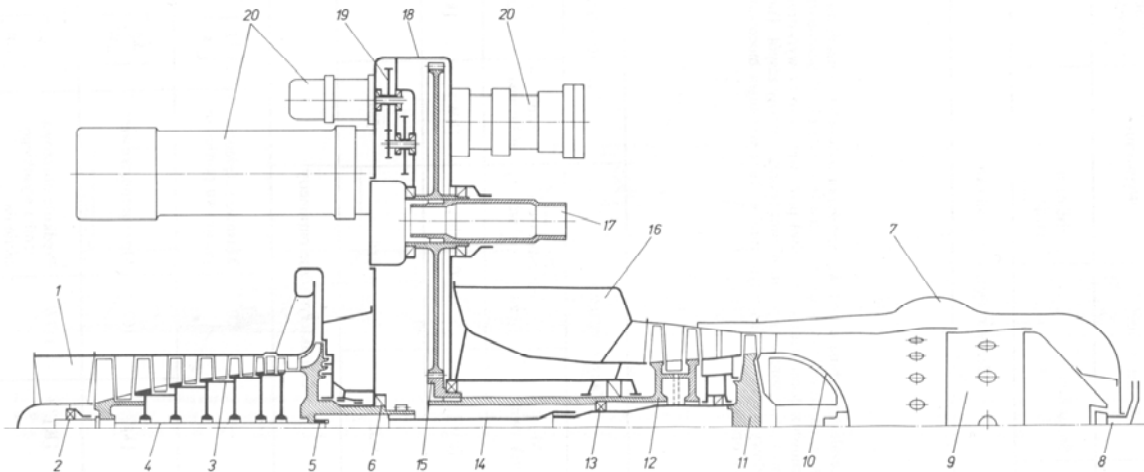


Fig. 3. GTD-350 turbine engine scheme (source [14]):

1 – intake stator blades, 2 – roller bearing, 3 – compressor rotor, 4 – screw attaching compressor rotor plates, 5 – nut, 6 – ball bearing, 7 – air duct leading to combustion chamber, 8 – fuel injector, 9 – fire pipe, 10 – turbine plate cap, 11 – generator turbine, 12 – propelling turbine, 13 – middle (roller) bearing, 14 – middle shaft, 15 – reducer driving wheel, 16 – exhaust manifold, 17 – engine output shaft, 18 – reducer casing, 19 – aggregate-drive gear box for, 20 – engine aggregates.

First of the photographs presents the attachment of laser sensor of reference speed with beam directed at output engine shaft. Rotation speed of the shaft was a reference speed of the executed decimation procedure algorithm. On the second photograph we can see attachment point of triple-axis ICP accelerometer.

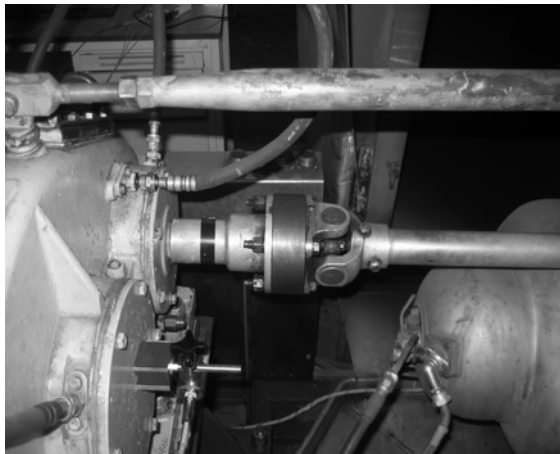


Fig. 4. Laser measurement of rotation-speed changes on output shaft

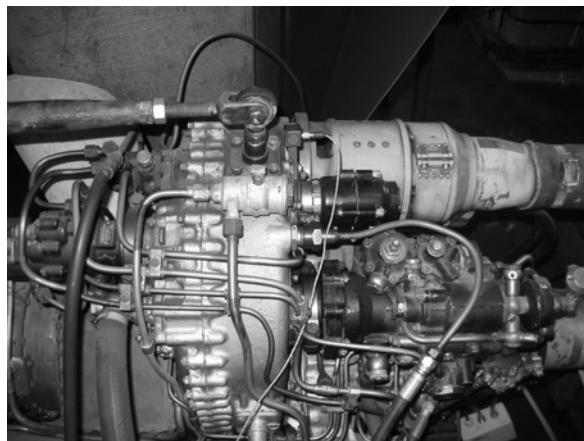


Fig. 5. Location of attachment point of triple-axis ICP acceleration sensor on GTD – 350 engine

4. PLD CAPABILITIES

Experiment was conducted in stabilized turbine operating conditions, during its run-up and coasting.

It also included variable work loading of tested GTD-350 engine.

Fig. 6 presents amplitude spectrum of vibration acceleration for stable working conditions in rotation frequency band. Three dominant frequencies are clearly visible. The first represents basic frequency of output shaft, the second, four times as great - basic frequency of propelling turbine shaft and the third, independent, being frequency of the turbine propelling engine compressor [6].

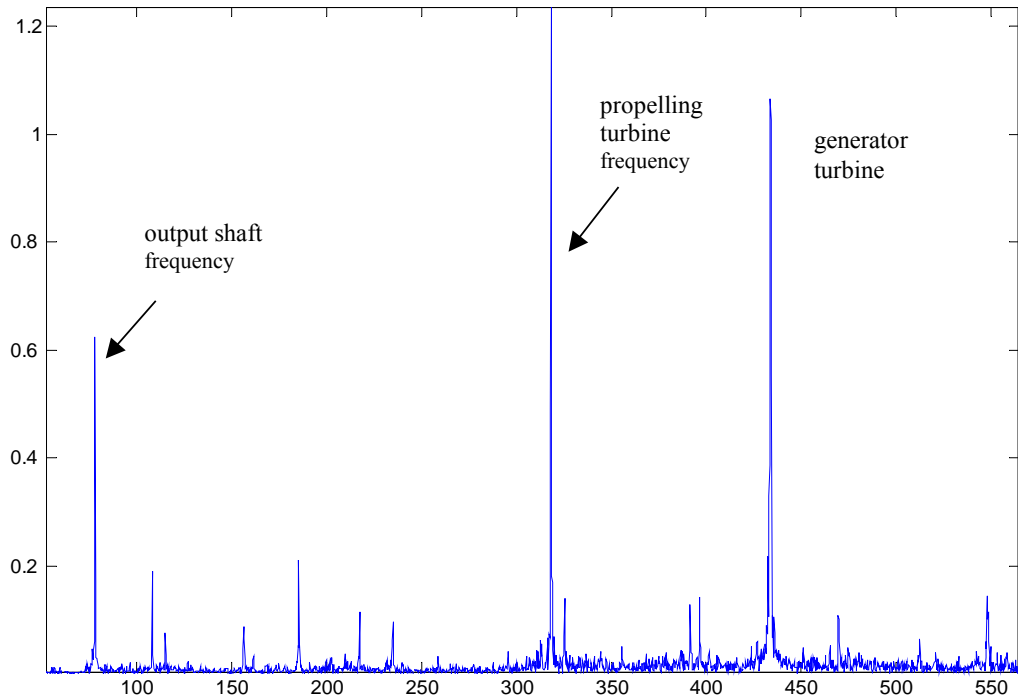


Fig. 6. Amplitude spectrum of GTD-350 engine in rotational frequency band in nominal operational conditions

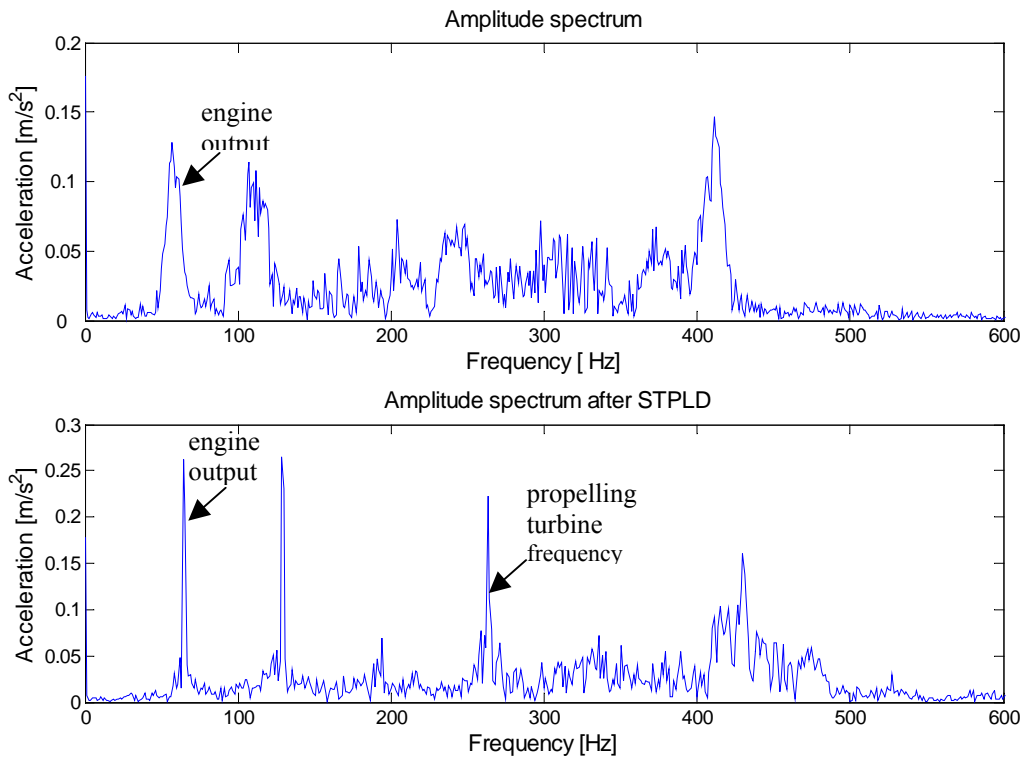


Fig. 7. Vibration-acceleration signal of running-up turbine.

Fig. 7 contains amplitude spectrum of vibration acceleration during run-up: a – spectral analysis, b - spectral analysis after applying procedure of linear decimation. Enhancement of spectral selectivity occurs at shaft frequencies corresponding with reference speed. The last of presented experiments introduces a situation of vibration interference of diagnostical signal by the components of voltage signals of aggregates.

Fig. 8 contains vibration acceleration spectra during turbine coasting: a - amplitude spectrum and b – spectrum after applying STPLD. After applying decimation procedure, components not synchronized formerly with reference speed become fuzzy and the components representing vibrations of propelling shafts, earlier fuzzy, now become distinct.

- newly developed method of Short-time Procedure of Linear Decimation based on the approximation in short time-spans reflects cycle-trend changes with sufficient accuracy
- with significant 10 MS/s oversampling it is possible to narrow decimation analysis to a single cycle period
- Short-time Procedure of Linear Decimation can be competitive for row analysis in terms of simplicity of calculations executed in real-time
- in terms of accuracy STPLD is based on actual samples without the application of filters interpolating signals
- further research will be directed to more accurate adjustment of approximation and cycle trend through the application of higher-level functions

5. CONCLUSIONS

Experiments conducted on GTD-350 engine brought positive assessment of the effects of applying innovative method of processing non-stationary signals – Procedure of Linear Decimation. Those results though, were not accepted uncritically. Recapitulating, we can state that:

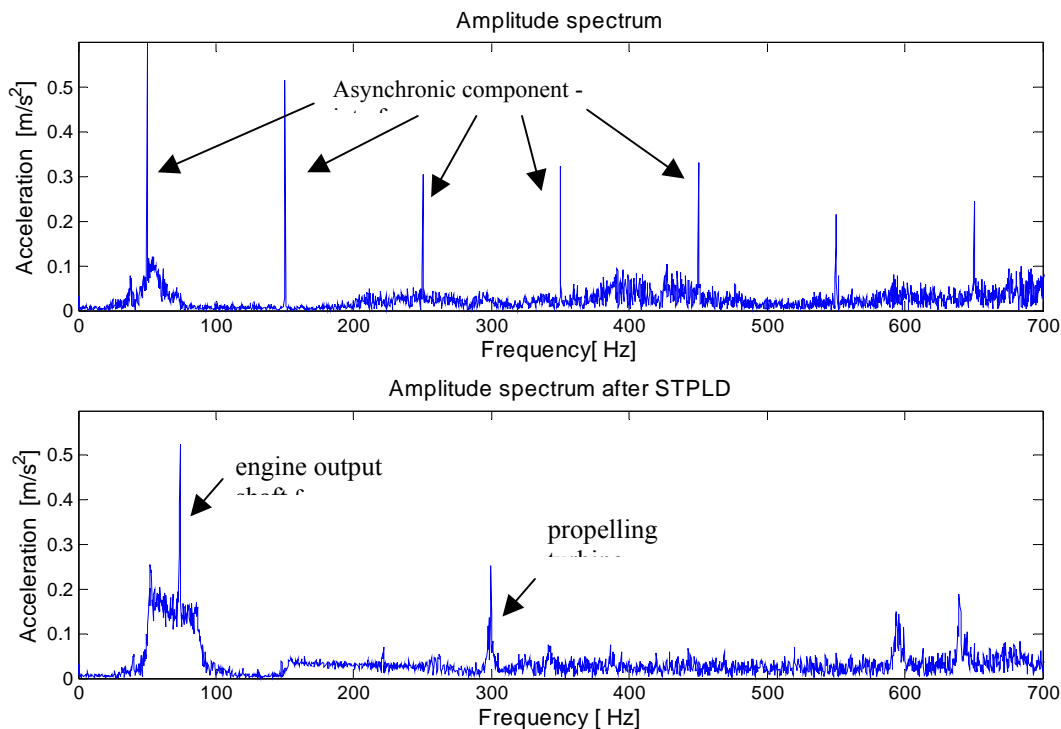


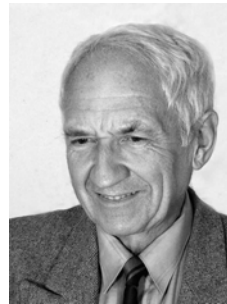
Fig. 8. Amplitude spectrum of vibration accelerations of engine during run-up with interfering frequencies coming from electric devices

6. REFERENCES

- [1]. Adamczyk J., Cioch W., Krzyworzecka P.: *Wpływ interpolacji na procedurę liniowej decymacji*. Diagnostyka, vol. 27, 2002.
- [2]. Adamczyk J., Cioch W., Krzyworzecka P.: *Inżynieria Diagnostyki Maszyn. Elementy teorii diagnostyki technicznej – praca zbiorowa*, Roz. 14: Metody synchroniczne w diagnozowaniu maszyn, s. 264–278, Radom 2004.
- [3]. Cempel Cz.: *Diagnostyka wibroakustyczna maszyn*, Wydawnictwo Politechniki Poznańskiej. Poznań, 1985.
- [4]. Dzierżanowski P., Kordziński W., Otyś J., Szczeciński S., Wiatrek R.: *Turbinowe silniki śmigłowe i śmigłowcowe*. WKŁ. Warszawa, 1985.
- [5]. Dzygadlo Z., Łyżwiński M., Otyś J., Szczeciński S., Wiatrek R.: *Zespoły wirnikowe silników turbinowych*. WKŁ, Warszawa, 1982.
- [6]. Grządziela A.: *Ocena stanu technicznego układu wirnikowego okrętowych turbinowych silników spalinowych*. Mat XXVII Sympozjum Diagnostyka Maszyn, z. 1, Z.N. Pol. Śl., Katowice, 2000.
- [7]. Jamro E., Adamczyk A., Krzyworzecka P., Cioch W.: *Programowalne urządzenie diagnostyczne stanów niestacjonarnych pracujące w czasie rzeczywistym*. XXXIII Ogólnopolskie Sympozjum Diagnostyka Maszyn, Węgierska Górka, 8.-11.03. 2006 r.
- [8]. Krzyworzecka P., Adamczyk J., Cioch W., Jamro E.: *Monitoring of nonstationary states in rotating machinery*. Instytut Technologii i Eksploatacji, Radom 2006.
- [9]. Krzyworzecka P., Cioch W., Jamro E.: *Hardware abilities of Linear Decimation Procedure in practical applications*. Journal of POLISH CIMAC, Diagnosis, Reliability and Safety, vol. 2, No 2, Gdańsk, 2007.
- [10]. Krzyworzecka P., Cioch W.: *Machine diagnostics in cycle-time scale using linear decimation procedure*. 1st Int. Conf. on Experiments/Process/System/Modelling/Simulation /Optimization, Univ. of Patras. LFME Athens 6–9 July 2005, Greece.
- [11]. Krzyworzecka P., Cioch W.: *Dynamiczna kompensacja wpływu zmian długości cyklu na sygnał drganiowy*. Mat XXVII Sympozjum Diagnostyka Maszyn, z. 1, Z.N. Pol. Śl. Katowice 2000.
- [12]. Krzyworzecka P., Cioch W., Jamro E.: *Dokładność przybliżonej analizy drgań maszyn w stanach niestacjonarnych*. Diagnostyka, vol. 4, 2006.
- [13]. Krzyworzecka P.: *Wspomaganie synchroniczne w diagnozowaniu maszyn*. Instytut Technologii i Eksploatacji, Radom 2004.
- [14]. Szczeciński St., Bielecki J., Glass A., Grzegorzczak H., Konieczny J., Sobieraj W.: *Ilustrowany leksykon lotniczy*. Napędy. WKŁ, Warszawa, 1993.



Ph.D. (Eng.) **Witold CIOCH** is a graduate of Aviation and Machine Construction Department of Technical University in Rzeszów, aviation-propulsion specialization, and a graduate of Mechanical Engineering and Robotics Department of AGH Technical University of Science & Technology, specialization in vibroacoustics. He obtained a Ph.D. degree at ME&R Dept. and is currently in the position of the assistant professor at Mechanics and Vibroacoustics Department of AGH-UST. Member of Polish Society of Technical Diagnostics. Author of 48 publications from the realm of technical diagnostics and vibroacoustics.



Piotr KRZYWORZEKA D.Sc. received a M.Sc. degree in electrical engineering as well as Ph.D. and D.Sc. degrees from AGH Technical University of Science & Technology, Cracow Poland. He also works at AGH, recently as a professor in Dept. of Mechanical Engineering & Robotics. His

research encompasses both electrical and mechanical systems with a strong emphasis on technical diagnostics including signal processing and hardware design. He is a member of the AES, Polish Association of Electrical Engineers and a founding member of Polish Society of Technical Diagnostics. Author and coauthor of more than 100 research papers – some of which were concerning spontaneous synchronism in rotating machinery.

MONITORING SYSTEM FOR DIAGNOSING MACHINES IN NON-STATIONARY STATES

Wojciech BATKO*, Witold CIOCH*, Ernest JAMRO**
Department of Mechanics and Vibroacoustics*
Department of Electronics**
Akademia Górniczo-Hutnicza – University of Science and Technology,
Al. Mickiewicza 30, 30-059 Kraków
email: cioch@agh.edu.pl

Summary

Monitoring the operation of machine tools, such as grinders used for jet-engine turbine blades is vital for demanded product quality and economic expenses associated with defected products and production stoppages. In the technological process of grinding, even wear of tools does not always occur, and machine tools definitely work in non-stationary conditions. Self-induced vibrations are often observed. Therefore monitoring system of module structure was designed, dedicated to non-stationary signal processing. The system is composed of modules for recording and preliminary hardware signal processing, database servers and user's terminals.

Keywords: monitoring, diagnostics, grinding machine.

SYSTEM MONITORINGU MASZYN W NIESTACJONARNYCH STANACH PRACY

Streszczenie

Monitorowanie obrabiarek takich jak szlifierki łopatek silników lotniczych ma szczególne znaczenie ze względu na wymaganą jakość produktu, jak również koszty ekonomiczne związane z wytwarzaniem braków oraz przestojów produkcyjnych. Podczas procesu technologicznego szlifowania następuje nie zawsze równomierne zużycie narzędzi, a obrabiarki pracują w warunkach niestacjonarnych. Często występują również drgania samowzbudne. Dlatego stworzono system monitorowania, dedykowany przetwarzaniu sygnałów niestacjonarnych o modułowej budowie. Składa się on z urządzeń do rejestracji i wstępnego sprzętowego przetwarzania sygnałów pomiarowych, serwerów bazy danych i terminali użytkowników.

Słowa kluczowe: monitoring, diagnostyka, szlifierka.

1. INTRODUCTION

Despite varied production technologies, machining is still commonly applied nowadays. It is the result of the fact that it provides a very high accuracy, high efficiency and could be easily automated. Perfect examples of devices carrying out machining process are grinding machines for aviation turbine blades.

Problems regarding grinders operations can have various causes. They can be associated with machine-tool defect, tool wear processes or self-induced vibrations [3]. Hence it is advisable to diagnose machine-tool condition not only before machining process but also during the actual process. The condition of machine tool is vital for the product quality and for continuity of production process, the stoppage of which would bring significant economic losses.

Monitoring systems enable to detect changes in condition or operation parameters of machine tools [2]. Based on data collected, it is also possible to

project the technical condition, which is important for production-process planning. It is of great significance in aviation industry, where manufactured elements are of high quality and precision. Therefore their production is expensive and loss of the whole batch of product is not acceptable.

Machine tool condition and machining process characteristics are vitally affected by dynamic phenomena. Hence vibration is a basic quantity measured in a monitoring process. Vibration is also measurement quantity bringing the most valuable diagnostical information [5]. Monitoring tool condition and self-induced vibrations is still an unsolved problem.

The most significant features, determining functional properties of monitoring systems are according to [4]:

- purpose (machine tool, machining type),
- type of selected diagnostical signals and their measurement manner,
- signal transformation methods,

- method of determining boundary values,
- diagnostical inference methods,
- maintenance characteristics, interfaces.

Having those items in mind, an innovative monitoring system for grinder machine of aviation turbine blades has been designed.

2. THE STRUCTURE OF THE DURATIVE MONITORING SYSTEM

The monitoring system for grinding machine includes methods and algorithms for signals acquisition, pre-processing; data transmission, processing and storage.

Consequently, the whole system consists of the following modules:

- Programmable Unit for Diagnostic (PUD)
- Dedicated server for data collection and processing
- Dedicated server for data storage with limited users' access.
- External user terminals for diagnostic signals analysis.

The block diagram of whole system is presented in Fig. 1.

3. PROGRAMMABLE UNIT FOR DIAGNOSTIC (PUD)

Programmable Unit for Diagnostic (PUD) is an electronic device which core is an FPGA chip [6]. The block diagram of the PUD is shown in Fig. 2 and it incorporates the following parts:

- Four independent analog / digital modules on separate PCB
- Two independent SDRAM memory banks, 64MB each, employed to store acquired data from analogue / digital modules and other temporal data,
- CPLD (Xilinx XC95144XL device) – module employed to configure FPGA and to control the PUD in power stand-by mode,
- Flash memory (4MB) to store FPGA configuration, MicroBlaze program and other non-volatile data,
- Hard Disk Drive (HDD) to store high volume data,
- LCD display employed to visualise the state of the device and results for acquired data,
- Keyboard – allows user to control the PUD and to start / stop data acquisition,
- PC computer communication by Ethernet, Parallel or Serial Ports.

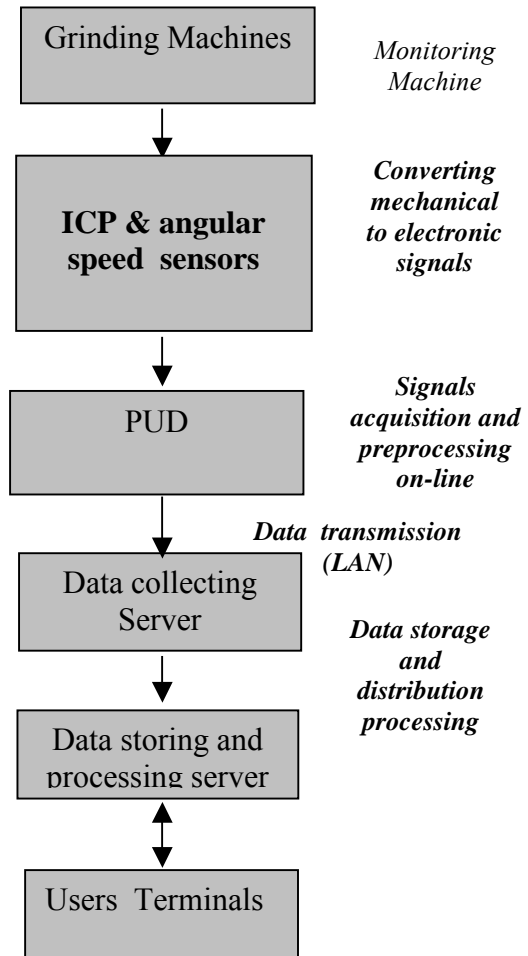


Fig. 1. The monitoring system block diagram

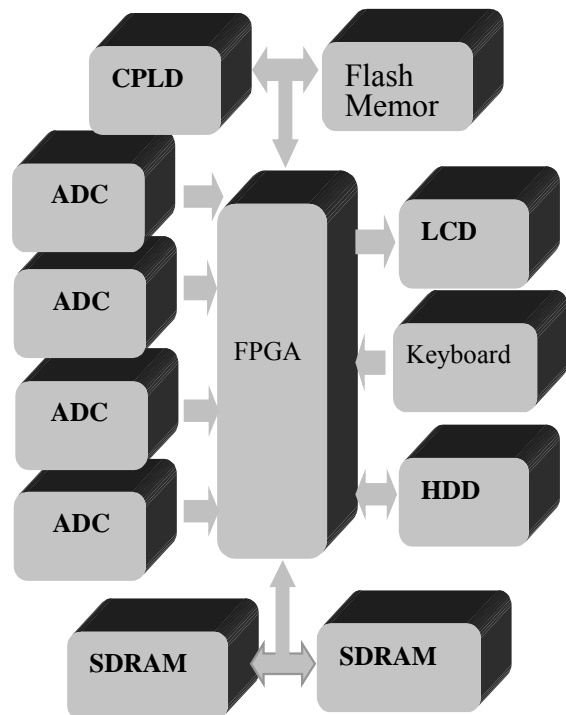


Fig. 2. Block diagram of the Programmable Unit for Diagnostic (PUD)

Besides, the PUD incorporates some optional devices: Compact Flash memory, VGA display, PC keyboard, and Ethernet and Radio Communication modules.

The PUD incorporates four independent analog/digital boards. These boards include Analog Digital Converters (ADC), input signal amplifiers with digitally controlled level of amplification and ICP sensor interface. Each analog board incorporates 2 channels 16-bit 500kS/s each or 4 channels 16-bit 250kS/s each, consequently up to 8 (16-channels) can be acquired by the PUD. It should be noted that changing analog / digital board requires FPGA configuration to be changed. Fortunately modular design in EDK significantly reduces the design time.

One of the most significant feather of the PUD is hardware implementation of selected signal processing procedures. Consequently these procedures calculation time is significantly reduced. Besides Xilinx Embedded Development Kit (EDK) design software was employed to reduce design time. The EDK supports modular design and incorporates a great number of pre-design modules such as external memory interface and the MicroBlaze soft-processor. The MicroBlaze is a master micoprocessor which configures and controls all other hardware modules.

One of the most important digital processing procedure adapted on the PUD is the Procedure of Linear Decimation (PLD) [8]. Therefore this procedure was implemented directly in hardware. This implementation can be divided into three separate tasks:

- Marker logic detection – rotation period indicator,
- Anti-aliasing filter,
- Linear decimation.

4. PC - PUD COMMUNICATION

The PUD devices can run in two different modes:

- 1) Portable standalone system
- 2) PC-controlled signal acquisition and processing unit.

In the standalone mode, the PUD acquires, processes and stores signals without any communication with PC. The PUD incorporates its own menu which controls the device: allows to set e.g. signal acquisition parameters: acquisition time, sampling frequency, invokes signal processing procedures e.g. PLD etc. The sequence of the commands can be grouped in a macro – the macro can be programmed directly in the PUD or on a PC. The final results can be stored on the local HDD and then transferred to the PC.



Fig. 3. PCB board and electronic devices view of the PUD

In the PC-controlled mode, the PUD is connected with the PC Fig. 4 and can be fully controlled remotely by a PC. Signal processing can be still completed in the PUD and then only final results transferred to the PC. Alternatively, raw data (signals acquired by the ADC) can be transferred to the PC where they are processed, e.g. in MATLAB.

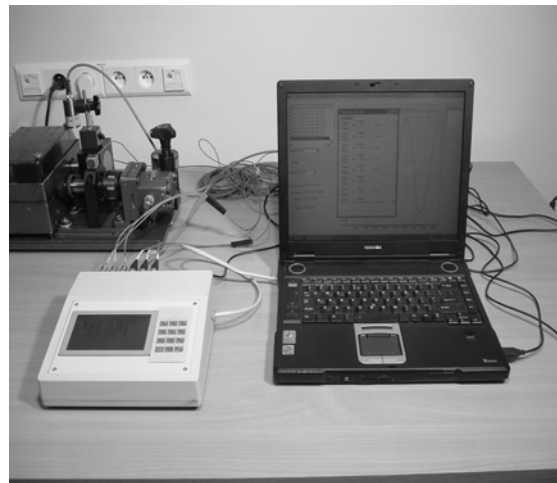


Fig. 4. The PUD device connected to PC

In the PUD signal records, apart from acquired signals some additional information, as acquisition time, sampling frequency and amplifier settings are stored. The PUD allows also to store some additional information as channel number and name, kind of signal processing procedure carried out on the signal, etc. In these records every channel can be processed independly, or a signals processing procedure can be carried out on a group of selected channels. Monitoring system used for laboratory tests is shown in Fig. 5.



Fig. 5. Monitoring system used for laboratory tests

5. DATA SERVERS

The signals acquired and processed on the PUD can be then transmitted to a computer where the database program allows to edit these signals and add additional information such as grinding machine distribution and user comments. The database allows to group selected signals as a result of acquisition time, data processing type, etc [1]. It also allows to process recorded signals by external programs such as MATLAB.

To increase data security and to improve data visualization data are stored on two independent servers. On the first server, data transmitted directly from the signal acquisition unit (PUD) are collected. Then they may be preprocessed in order to decrease the data volume and to select only important diagnostic estimates. Then preprocessed data are stored in a local database and are transferred to the second server. The main task of the second server is data backup and data distribution as a database or by HTTP protocols on WWW. As a result, end users can access data by users terminals which need not advance diagnostic programs. This solution allows controlling data access to a limited number of users.

6. SIGNAL ANALYSIS

Hardware realisation of linear decimation procedure based on FPGA programmable systems gives the possibility of diagnosing cyclical machines at variable operating conditions in real time. Besides a novel Short-Time PLD method was developed, enabling to adapt the approximation to the cycle changes [8]. This method solves the problem of non-linear trend change and minimized the error resulted from the original PLD assumption of linear cycle trend in the observation window. This solution has brought the method nearer to the order analysis without the necessity of applying interpolation filters.

To prediction technical state of a monitoring machine, sophisticated methods including time-frequency analysis was adopted employing MATLAB. This is possible as a history of a great number of records is stored in the database.

The described system may check production process in order to reduce production defects by monitoring vibration parameters. Fig. 6 shows where vibration sensors are located on the grinders of aviation-turbine blades.

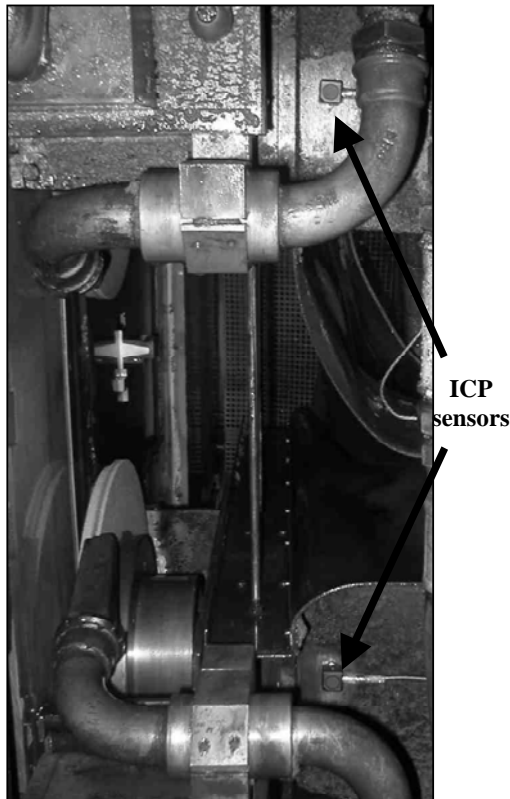


Fig. 6. ICP sensor location on the grinder machine

Examples of diagnosing non-balanced grinder disc during working state is shown in Fig. 7.

7. CONCLUSIONS

Application of the Programmable Unit for Diagnostic (PUD) into preliminary signal processing system enable to record data with high frequency and data hardware processing [7]. Using programmable FPGAs brought the possibility of non-stationary signal analysis in real time. The applied PUD module enabled, apart from measuring diagnostical signals, to record parameter signals, especially rotation speeds of spindles.

In the database part, employing two servers for data collecting and for data distribution separately improved the safety of database. It also gave the vast possibilities of processing (implementing Matlab suite) and surveying of collected signals by authorised users. Thanks to this solution, classifying grinding-machine condition and diagnosing operational process can be carried out by means of:

- numeral measures,
- functional measures,
- neural networks,
- parametrical models.

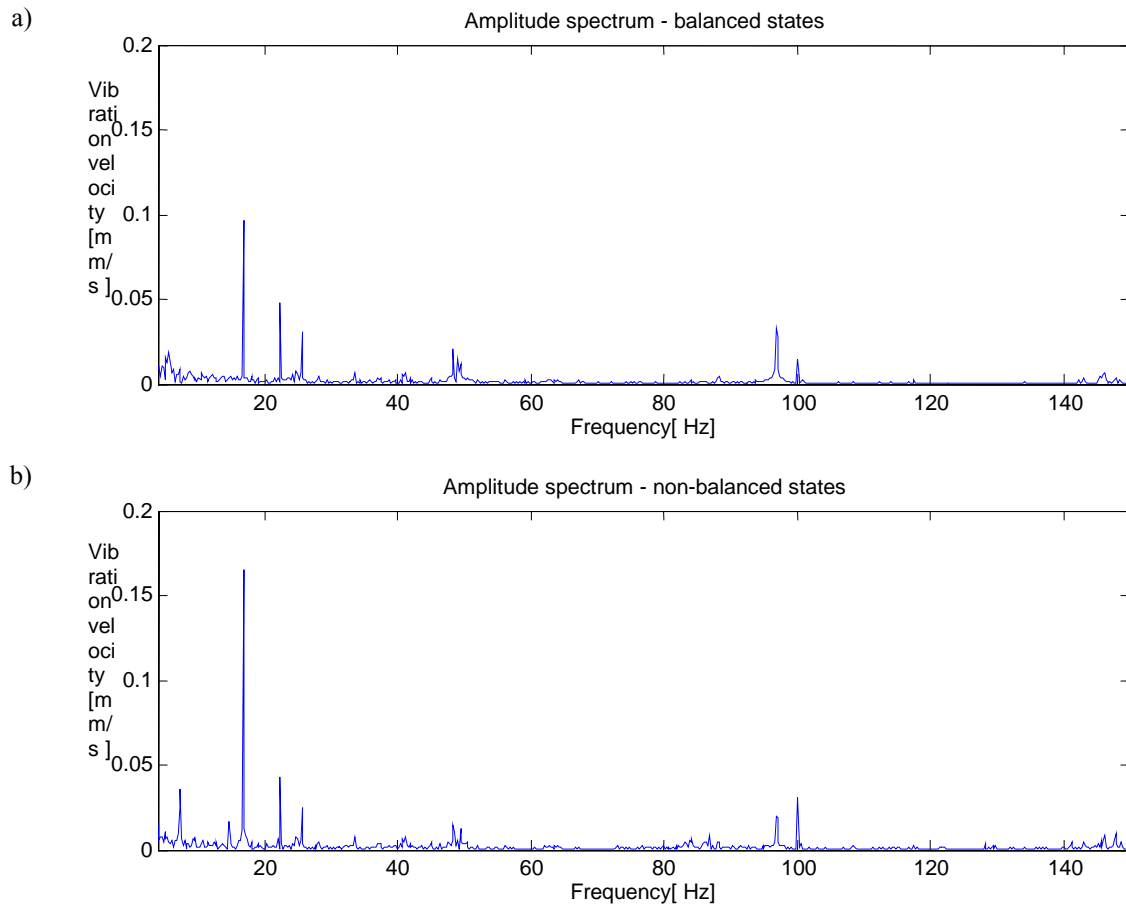


Fig. 7. Vibration velocity of grinder spindle: a) balanced states, b) non-balanced states

The modular construction of the monitoring system allows the whole system to be easily extended or modified to new grinding machines and acquisition points.

6. REFERENCES

- [1]. Batko W., Głocki K., Borkowski B.: Application of database systems in diagnostic machine monitoring, *Eksploatacja i Niezawodność*, No 4, 2007.
- [2]. Batko W., Korbiel T.: *System monitoringu diagnostycznego przekładni planetarnej pracującej w warunkach zmiennego obciążenia*, *Diagnostyka* nr 1(37)/2006.
- [3]. Bodnar A.: *Vibration Monitoring on a Milling Machine Using the Analysis of Stochastic Features of Generated Noise*, Ninth World Congress on the Theory of Machines and Mechanisms, 1995, Milano, Vol. 4, s. 2910-2914.
- [4]. Bodnar A.: *Diagnostyka i nadzorowanie drgań obrabiarek*. Materiały Sekcji Podstaw Technologii Komitetu Budowy Maszyn PAN z 50 posiedzenia w dniu 24.06.93 w Szczecinie, *Prace Inst. Technologii Mechanicznej Politechniki Szczecińskiej*, 1993, s. 5-16.
- [5]. Cempel Cz.: *Diagnostyka wibroakustyczna maszyn*, Wydawnictwo Politechniki Poznańskiej. Poznań, 1985.
- [6]. Jamro E., Adamczyk, A. Krzyworzeka P., Cioch W.: *Programowalne urządzenie diagnostyczne stanów niestacjonarnych pracujące w czasie rzeczywistym*, XXXIII Ogólnopolskie Sympozjum Diagnostyka Maszyn, Węgierska Górka, 2006 r.
- [7]. Krzyworzeka P., Adamczyk J., Cioch W., Jamro, E.: *Monitoring of nonstationary states in rotating machinery*. Instytut Technologii i Eksploatacji, Radom 2006.
- [8]. Krzyworzeka P., Cioch W., Jamro E.: *Hardware abilities of Linear Decimation Procedure in practical applications*. Journal of POLISH CIMAC, Diagnosis, Reliability and Safety, vol. 2, No 2, Gdańsk, 2007.

This work has been executed as part of research project at KBN no 6T0720005C/06545



Wojciech BATKO – a professor and a head of Mechanics and Vibroacoustics Department of AGH-University of Science and Technology (AGH-UST). He is an author of over 230 publications including 12 books. His subject of interest is machines dynamics and vibroacoustics, and technical diagnostics.



Ph. D. (Eng.) **Witold CIOCH** obtained a Ph. D. degree at Mechanical Engineering and Robotics Department of AGH – University of Science and Technology and is currently in the position of the assistant professor at Mechanics and Vibroacoustics Department of AGH-UST. Member of Polish Society of Technical Diagnostics. Author of 48 publications from the realm of technical diagnostics and vibroacoustics.



Ernest JAMRO – received M.Sc. degree in electronic engineering from the AGH University of Science and Technology (AGH-UST), Cracow Poland in 1996; M.Phil. degree from the University of Huddersfield (U.K.) in 1997; Ph.D. degree from the AGH-UST in 2001. He is currently a professor assistant in the Department of Electronics AGH-UST. His research interest include reconfigurable hardware (esp. Field Programmable Gate Arrays – FPGAs), reconfigurable computing systems, system on chip design.



W Jachrance, w dniach 29-30 listopada 2007 r. odbyła się XIII Konferencja Naukowa Wibroakustyki i Wibracji oraz VIII Ogólnopolskie Seminarium Wibroakustyki w Systemach Technicznych – **WibroTech 2007**.

Organizatorami konferencji były Politechnika Warszawska (Wydział Samochodów i Maszyn Roboczych – Instytut Podstaw Budowy Maszyn) oraz Akademia Górniczo-Hutnicza w Krakowie (Wydział Inżynierii Mechanicznej i Robotyki – Katedra Mechaniki i Wibroakustyki).

Celem konferencji była wymiana doświadczeń i osiągnięć naukowo – badawczych, różnych ośrodków w kraju, z zakresu wibroakustyki i wibracji z uwzględnieniem zagadnień związanych z występowaniem procesów wibroakustycznych w technice i przyrodzie oraz analizy, modelowania i identyfikacji ich oddziaływań dynamicznych i związanych z nimi oddziaływań wibroakustycznych, a także oceny ich wartości informacyjnej dla celów diagnostyki technicznej i kształtowania ich pożądanych charakterystyk.

Program konferencji obejmował trzy rodzaje sesji: jubileuszową poświęconą prof. Zbigniewowi DĄBROWSKIEMU, plenarną oraz plakatową.



W pierwszej z wymienionych sesji, Jubilat wygłosił referat nt.: *Drgania nieliniowe - problem nadal otwarty* oraz uczestnicy wysłuchali wystąpienia prof. Wojciecha BATKO pt.: *35 lat pracy naukowej i 60 urodziny Profesora Zbigniewa Dąbrowskiego*.

W czasie obrad plenarnych wygłoszono następujące referaty:

Zbigniew ENGEL: *Analiza porównawcza metod wzajemnościowych i inwersyjnych stosowanych w wibroakustyce*.

Czesław CEMPEL, Maciej TABASZEWSKI: *Teoria szarych systemów w zastosowaniu do modelowania i prognozowania w diagnostyce maszyn*.

Jan KICIŃSKI, Paweł PIETKIEWICZ: *Próba uwzględnienia stochastycznej zmienności danych wejściowych w modelowaniu heurystycznym wirników*.

Wojciech BATKO: *Nowe idee w budowie systemów monitorujących*.

Wiktor ZAWIESKA: *Modelowanie transformatora energetycznego jako źródła hałasu*.

Andrzej GRZĄDZIELA: *Analiza możliwości wykorzystania metod drganiowych w diagnozowaniu okrętowej linii wałów*.

Iwona KOMORSKA: *Poszukiwania modelu wibroakustycznego silnika spalinowego*.

Wojciech HOMIK: *Analiza porównawcza drgań skrętnych wału korbowego silnika z tłumikiem wiskotycznym i gumowym*.

Grzegorz KLEKOT: *Ocena wpływu elementów nieliniowych na propagację energii wibroakustycznej*.

Wojciech SKÓRSKI: *O ruchu jachtu liniowo czy nieliniowo?*

Walter BARTELMUS, Radosław ZIMROZ: *Nieliniowe zjawiska w dynamice przekładni zębatych*.

Marian W. DOBRY, Roman BARCZEWSKI: *Wpływ obciążenia i stanu technicznego belki strunobetonowej na przepływ energii w czasie testu impulsowego*.

Henryk MADEJ: *Diagnozowanie uszkodzeń mechanicznych silników spalinowych metodami wibroakustycznymi*.

Piotr TADZIK: *Prezentacja firmy Brüel&Kjær*.

Krzysztof KOSAŁA: *Możliwości zastosowania rozkładu względem wartości szczególnych do analizy właściwości akustycznych obiektów sakralnych*.

Bartosz STANKIEWICZ: *Aktywny układ tłumienia hałasu w samochodzie osobowym*.



Na sesji plakatowej przedstawiono następujące prace:

Renata BAL, Wojciech BATKO: *Analiza uwarunkowań estymacyjnych poziomu hałasu w środowisku*.

- Roman BARCZEWSKI: *Ocena stanu naprężeń i spójności belek strunobetonowych na podstawie parametryzacji charakterystyk czasowo-modalnych.*
- Wojciech BATKO, Bartłomiej STEPIEŃ: *Wykorzystanie symulacji komputerowej do estymacji funkcji gęstości prawdopodobieństwa wskaźników hałasu.*
- Wojciech. BATKO, Józef FELIS, Artur FLACH, Tadeusz KALISIŃSKI: *Opracowanie projektu koncepcyjnego manipulatora do pomiarów akustycznych w komorze bezdechowej.*
- Mirosław BOLKA, Roman BARCZEWSKI: *Oddziaływanie drgań na rowerzystę w przypadku rekreacyjnej jazdy terenowej.*
- Andrzej BUCHACZ, Andrzej WRÓBEL: *Badanie zjawiska piezoelektrycznego bimorficznego układu i jego praktyczne zastosowanie w czujnikach poziomu.*
- Grzegorz CIEPŁOK: *Krzywe utknięcia nadrezonansowej maszyny wibracyjnej.*
- Piotr CZECH, Bogusław ŁAZARZ, Henryk MADEJ: *Diagnostyka uszkodzeń zębów kół walcowych przekładni zębatych przy użyciu radialnych sieci neuronowych oraz selekcji widmowej.*
- Włodzimierz FIGIEL, Jerzy TARNOWSKI: *Analiza wpływu wymuszonych drgań gruntu górniczo odkształcalnego na gazociąg stalowy.*
- Piotr DEUSZKIEWICZ: *Uwagi o dynamice wałów maszynowych wykonanych z kompozytu węglowego.*
- Jacek Dziurdź: *Identyfikacja modelu na potrzeby diagnostyki technicznej.*
- Tomasz FIGŁUS: *Propozycja metody obliczania drgań kadłuba silnika spalinowego.*
- Tomasz FIGŁUS, Andrzej WILK, Henryk MADEJ, Piotr FOLGA: *Badania wibroaktywności uzębrowanego korpusu przekładni zębatej.*
- Andrzej GOŁAŚ, Ryszard OLSZEWSKI: *Zagadnienie dostrajania akustycznych modeli obliczeniowych opartych na metodzie elementów skończonych i brzegowych.*
- Marian JABŁOŃSKI, Agnieszka OZGA: *Statystyczne cechy drgań struny z tłumieniem, drgań wymuszonych stochastycznymi silami.*
- Tomasz KORBIEL: *Zastosowanie Autonomicznego Czujnika Drgań do określenia wibracji elementów rotacyjnych.*
- Tomasz KORBIEL, Krzysztof NIEMIEC: *System diagnostyki turbozespołu w środowisku LabVIEW.*
- Tomasz KUCHARSKI, Piotr JAKUBOWSKI: *Mikroprocesorowa technika niezależnego sterowania amplitudą i częstotliwością drgań przenośnika wibracyjnego.*
- Henryk MADEJ, Marek FLEKIEWICZ, Grzegorz WOJNAR: *Różne aspekty diagnostyki WA silników spalinowych z wykorzystaniem analiz w dziedzinie czasu i skali.*
- Damian MARKUSZEWSKI: *Laboratoryjne stanowisko do badań drgań własnych masztów kompozytowych.*
- Jerzy MICHALCZYK, Łukasz BEDNARSKI: *Rezonans parametryczny w ruchu względnym wibratora maszyny wibracyjnej.*
- Marianna MIROWSKA, Marek NIEMAS: *Badania hałasu w mieszkaniach od przejeżdżających pociągów Metra.*
- Leszek MORZYŃSKI: *Badania modelu systemu aktywnej redukcji hałasu wykorzystującego materiał inteligentny jako przetwornik wykonawczy.*
- Radosław PAKOWSKI: *Badania stanów krytycznych wałów kompozytowych i stalowych spajanych metodami niekonwencjonalnymi.*
- Przemysław PIENIECKI, Jerzy Z. SOBOLEWSKI: *Analiza wybranych przyczyn powstawania hałasu w mechanizmie śrubowym tocznym.*
- Jacek Polechoński: *Oddziaływanie szumu i aplauzu kibiców na charakterystykę wychwiania spontanicznych postawy stojącej.*
- Marek PRASZKIEWICZ, Jacek RYSIŃSKI: *Komputerowy system do akustycznej diagnostyki przekładni.*
- Lesław STRYCNIEWICZ, Janusz PIECHOWICZ: *Model pola akustycznego w pomieszczeniu przemysłowym.*
- Mariusz WĄDOŁOWSKI: *Maskowanie uszkodzeń elementów rozrządu przez nowoczesne systemy sterowania silnikiem.*
- Renata WALCZAK, Rafał ŻÓŁTOWSKI, Krzysztof JASIŃSKI, Antoni KORYTKOWSKI, Jacek GUTKOWSKI: *Ustalenie przyczyn nadmiernych drgań agregatu pompowego cyrkulacyjnej wody chłodzącej instalacji produkcji płatków woskowych.*
- Jerzy WICIAK: *Obliczenia izolacyjności akustycznej metodą hybrydową.*
- Wiesław WSZOŁEK, Maciej KŁACZYŃSKI: *Wibroakustyczne metody pomiaru drgań fałdów głosowych.*
- Tadeusz WSZOŁEK: *Badania wibracji przewodów powodowanych zjawiskiem ulotu w liniach wysokiego napięcia.*
- Janusz ZALEWSKI, Andrzej GANCARZEWICZ: *Problemy ograniczenia hałasu upustu pary wodnej z urządzeń technologicznych.*
- Michał ŻEBROWSKI-KOZIOŁ, Wojciech TARNOWSKI: *Wstępne badania dynamiczne luzu sworzni przednich zwrotnic samochodów osobowych.*
- Sławomir ŻÓŁKIEWSKI: *Analiza charakterystyk dynamicznych drgających układów podatnych z uwzględnieniem ruchu unoszenia.*

Recenzenci publikowanych prac:

prof. dr hab. inż. Jan ADAMCZYK
prof. dr hab. inż. Wojciech BATKO
prof. dr hab. inż. Adam CHARCHALIS
dr inż. Marcin JASIŃSKI
dr hab. inż. Piotr KRZYWORZEKA, prof. AGH
dr hab. inż. Henryk MADEJ, prof. PŚ
prof. dr hab. inż. Andrzej NIEWCZAS
prof. dr hab. inż. Stanisław NIZIŃSKI

prof. dr hab. inż. Stanisław RADKOWSKI
dr hab. inż. Bożena SKOŁUD
prof. dr hab. Aleksander ŚLADKOWSKI
prof. dr hab. inż. Tadeusz UHL
prof. dr hab. inż. Andrzej WILK
prof. dr hab. inż. Maciej WOROPAY
dr inż. Maciej ZAWISZA

Druk:

Centrum Graficzne „GRYF”, ul. Pieniężnego 13/2, 10-003 Olsztyn, tel. / fax: 089-527-24-30

Oprawa:

Zakład Poligraficzny, UWM Olsztyn, ul. Heweliusza 3, 10-724 Olsztyn
tel. 089-523-45-06, fax: 089-523-47-37



Uniwersytet Warmiński – Mazurski
w Olsztynie
Wydział Nauk Technicznych
Katedra Budowy, Eksploatacji
Pojazdów i Maszyn



Polskie Towarzystwo Diagnostyki
Technicznej

Zespół Diagnostyki SE KBM PAN



Instytut Maszyn Przepływowych
PAN Gdańsk



Akademia Marynarki Wojennej
w Gdyni
Wydział Mechaniczno-Elektryczny
Instytut Konstrukcji i Eksploatacji
Okrętów

IV MIĘDZYNARODOWY KONGRES DIAGNOSTYKI TECHNICZNEJ



09–12 WRZEŚNIA 2008
OLSZTYN – POLSKA
Komunikat nr 2

www.uwm.edu.pl/wnt/kongres

Wszystkie opublikowane w czasopiśmie artykuły uzyskały pozytywne recenzje, wykonane przez niezależnych recenzentów.

Redakcja zastrzega sobie prawo korekty nadesłanych artykułów.

Kolejność umieszczenia prac w czasopiśmie zależy od terminu ich nadesłania i otrzymania ostatecznej, pozytywnej recenzji.

Wytyczne do publikowania w DIAGNOSTYCE można znaleźć na stronie internetowej:

<http://www.uwm.edu.pl/wnt/diagnostyka>

Redakcja informuje, że istnieje możliwość zamieszczania w DIAGNOSTYCE ogłoszeń i reklam.

Jednocześnie prosimy czytelników o nadsyłanie uwag i propozycji dotyczących formy i treści naszego czasopisma.

Zachęcamy również wszystkich do czynnego udziału w jego kształtowaniu poprzez nadsyłanie własnych opracowań związanych z problematyką diagnostyki technicznej. Zwracamy się z prośbą o nadsyłanie informacji o wydanych własnych pracach nt. diagnostyki technicznej oraz innych pracach wartych przeczytania, dostępnych zarówno w kraju jak i zagranicą.